

ASSESSMENT OF ADHESIVE BONDING FOR STRUCTURAL DESIGN WITH THICK ADHERENDS

by

Safa A Hashim, B Sc, M Sc

**Dissertation submitted to the Faculty of Engineering,
University of Glasgow, for the degree of
Doctor of Philosophy**

August, 1992

**Department of Mechanical Engineering
University of Glasgow
Glasgow G12 8QQ**

© S A Hashim 1992

ProQuest Number: 13815421

All rights reserved

INFORMATION TO ALL USERS

The quality of this reproduction is dependent upon the quality of the copy submitted.

In the unlikely event that the author did not send a complete manuscript and there are missing pages, these will be noted. Also, if material had to be removed, a note will indicate the deletion.



ProQuest 13815421

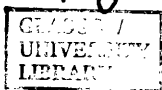
Published by ProQuest LLC (2018). Copyright of the Dissertation is held by the Author.

All rights reserved.

This work is protected against unauthorized copying under Title 17, United States Code
Microform Edition © ProQuest LLC.

ProQuest LLC.
789 East Eisenhower Parkway
P.O. Box 1346
Ann Arbor, MI 48106 – 1346

Thesis
9332
copy 1



*To my parents,
brothers and
sisters*

SUMMARY

The research programme reported herein explores high performance engineering adhesives in joining relatively thick adherends for lightly loaded structures, particularly those in ships and marine construction. With the original design requirements for conventional structures in mind, the assessment approach for bonded connections is based on experimental and theoretical techniques.

The design engineer has very little understanding of adhesives and adhesion. A necessary review to this subject is therefore presented. The behaviour and design of adhesive joints and bonded structures are reviewed and areas of particular concern in adhesive and adhesive joints are highlighted.

Twelve types of structural epoxy adhesives were used in this investigation to select a hot curing adhesive for bonding steel to steel adherends and another for bonding steel to glass reinforced plastic (GRP) adherends and also to evaluate bonding processes. The selection processes were aided by specially formulated experiments for small mechanical test specimens. The experiments included strength, durability in a wet environment and thermal creep aspects.

A series of experiments for larger specimens has been developed around representative elements of skin/stiffener joints to establish a design basis for replacing fillet weld and bolted connection in steel and hybrid steel/GRP constructions respectively. These experiments included the static and impact performances and the fire resistance of thermally insulated hybrid steel/GRP panel. Meanwhile, development of prototype bonding process was established for large steel and steel/GRP panels using standard fabrication equipment for surface preparation, clamping and heat curing.

Finite element methods were used to assess the failure in bonded joints due to cleavage tensile stresses and to correlate between small and larger joints in order to assess the local failure in bonded structure. The overall behaviour of bonded structures under lateral loading was also studied using a theory modified from composite beam and plate theory. These theoretical techniques proved to be effective in predicting the failure and behaviour of bonded structures which form a useful basis for design. Visual examination of failure surfaces of bonded joints was used to support the analyses.

Significant results of this work include: (i) epoxy structural adhesives can provide effective structural connections in thick adherend applications, replacing welding and fasteners in some configurations, (ii) adherend type, stiffness and surface preparation significantly affect the strength of adhesively bonded joints and (iii) a bonded structure can be markedly different in behaviour (stiffness and strength) from its welded equivalent.

CONTENTS

SUMMARY	i
LIST OF TABLES	vi
LIST OF FIGURES	vii
NOMENCLATURE	xi
ACKNOWLEDGEMENTS	xiv
1. INTRODUCTION	1
2. LITERATURE REVIEW AND BACKGROUND	8
2.1. STRUCTURAL ADHESIVES	8
2.1.2. ADHESION MECHANISIMS	10
2.1.3. BONDING PROCESSES	12
2.1.3.1. SURFACE PREPARATION	12
2.1.3.2. ADHESIVE APPLICATION	14
2.1.3.3. BONDING PRESSURE (CLAMPING)	14
2.1.3.4. HEAT CURING	15
2.1.4. STRUCTURAL APPLICATIONS	16
2.2. ADHESIVE JOINTS	17
2.2.1. DESIGN AND BEHAVIOUR	18
2.2.2. STRUCTURAL INTEGRITY	19
2.2.3. MECHANICAL TESTING	21
2.3. FAILURE MECHANISIMS	23
2.3.1. ANALYTICAL METHODS	25
2.3.3. NUMERICAL METHODS	27
3. ADHESIVE SELECTION AND PROPERTIES	49
3.1. EXPERIMENTAL JIGS AND FIXTURES	50

3.2. PRODUCTION OF SPECIMENS	50
3.3. TESTS FOR ALL ADHESIVES	52
3.3.1. COMPARITIVE RESULTS	53
3.3.2. EFFECT OF SPEW FILLET	54
3.3.3. EFFECT OF ADHESIVE THICKNESS	55
3.3.4. RELIABILITY OF BONDING PROCESSES	55
3.4. PROPERTIES OF THE CANDIDATE ADHESIVES	56
3.4.1. MODULUS OF ELASTICITY	56
3.4.2. LONGER TERM DURABILITY IN SEAWATER ENVIRONMENT	57
3.4.3. BONDING PROCESSES FOR STEEL/GRP JOINTS	58
3.4.4. SHORT TERM ELEVATED TEMPERATURE STRENGTH	59
3.4.5. CREEP RESISTANCE AT ELEVATED TEMPERATURES	59
4. ELEMENTARY STRUCTURAL JOINT TESTING	86
4.1. EXPERIMENTAL JIGS AND FIXTURE	86
4.2. BONDING PROCESS FOR STRUCTURAL ELEMENTS	87
4.2.1. BONDING OF STEEL/STEEL	87
4.2.2. BONDING OF STEEL/GRP	88
4.2.3. GENERAL CONSIDERATIONS	88
4.3. STIFFENED STEEL/STEEL JOINT TESTING	89
4.3.1. EXPERIMENTAL RESULTS	90
4.4. LATERAL LOADING OF STIFFENED PANELS	91
4.4.1. TEST RESULTS	91
4.5. STEEL/GRP STIFFENED CONNECTIONS	92
4.5.1. EXPERIMENTAL RESULTS	93

5. STRESS ANALYSES	114
5.1. STEEL/STEEL JOINTS	115
5.1.1. MODEL IDEALISATION	115
5.1.2. EXPERIMENTS AND RESULTS	115
5.1.3. NUMERICAL ANALYSIS	117
5.1.4. ANALYTICAL SOLUTION	120
5.2. STEEL/GRP TENSION JOINT	121
5.2.1. MODEL IDEALISATION	121
5.2.2. EXPERIMENTS AND RESULTS	121
5.2.3. NUMERICAL ANALYSIS	122
5.3. FLEXURAL BEAM LOADING	123
5.3.1. MODEL IDEALISATION	123
5.3.2. EXPERIMENTS AND RESULTS	124
5.3.3. ANALYTICAL THEORY	125
5.3.4. NUMERICAL ANALYSIS	127
6. DESIGN LIMITATIONS	152
6.1. LATERAL IMPACT RESISTANCE	152
6.1.1. DEVELOPMENT OF TEST RIG	153
6.1.2. TEST PROCEDURES	153
6.1.3. TEST RESULTS	154
6.2. FIRE RESISTANCE	155
6.2.1. SMALL SCALE EXPERIMENTS AND RESULTS	156
6.2.2. LARGE SCALE TEST AND RESULTS	157
7. GENERAL DISCUSSION	175
7.1. ADHESIVE SELECTION	175

7.2. BONDING PROCESS /FABRICATION	176
7.3. EXPERIMENTAL EVALUATION METHODS	181
7.4. THEORETICAL EVALUATION METHODS	183
7.5. DESIGN LIMITATIONS	185
7.6. LOCI OF FAILURE	188
7.6.1. STEEL/STEEL LAP SHEAR JOINT	188
7.6.2. STEEL/GRP LAP SHEAR JOINT	189
7.6.3. STEEL/STEEL STIFFENED JOINTS	190
7.6.4. STEEL/GRP TENSILE CLEAVAGE JOINT	191
7.7. DESIGN IMPLICATIONS	192
8. CONCLUSIONS AND RECOMMENDATIONS	208
REFERENCES	211
APPENDICES	220-257

LIST OF TABLES

TABLE 1.1	PROPERTIES OF GLASS REINFORCED PLASTIC (POLYESTER) LAMINATE
TABLE 2.1	PROPERTIES OF VARIOUS STRUCTURAL MATERIALS
TABLE 2.2	PROPERTIES OF ACRYLIC STRUCTURAL ADHESIVES
TABLE 2.3	COMPARATIVE PROPERTIES OF ACRYLIC VERSES EPOXY STRUCTURAL ADHESIVES
TABLE 2.4	APPLICATIONS FOR STRUCTURAL ADHESIVES
TABLE 2.5	TEST RESULTS AND PREDICTION: FRACTURE LOAD PER mm JOINT WIDTH
TABLE 3.1	PROCESSING PROPERTIES OF ADHESIVES FOR BONDING STEEL TO STEEL
TABLE 3.2	PROPERTIES OF ADHESIVES FOR BONDING STEEL TO STEEL
TABLE 3.3	COMPARATIVE PERFORMANCES OF TWO PART EPOXY ADHESIVES
TABLE 3.4	STRENGTH PROPERTIES FOR ARA LDITE -2004 EPOXY ADHESIVE
TABLE 3.6	TEST RESULTS OF TENSILE BUTT SPECIMENS
TABLE 3.5	IMPACT RESISTANCE FOR VARIOUS ADHESIVE THICKNESSES (ARALDITE 2007)
TABLE 3.7	SHORT TERM FAILURE SHEAR STRESS AT ELEVATED TEMPERATURES (ARALDITE 2007)
TABLE 3.8	CREEP RESISTANCE OF LAP SHEAR JOINTS AT ELEVATED TEMPERATURES
TABLE 4.1	EFFECT OF BASE PLATE THICKNESS AND FLANGE WIDTH ON THE CLEAVAGE STRENGTH
TABLE 4.2	EFFECT OF JOINT'S SHAPE AND WIDTH ON CLEAVAGE STRENGTH
TABLE 4.3	RESULTS OF FOUR POINT BENDING OF LARGE PANELS (STEEL / STEEL)
TABLE 4.4	RESULTS OF LOCAL LOADING ON FULL SCALE STEEL / GRP SPECIMENS (TYPE 4 FOR COMPRESSION AND TYPE 5 FOR TENSION-FIGURE 4.21)
TABLE 5.1	COMPARISONS OF ADHESIVE STRESS ANALYSES IN LARGE STEEL/STEEL CLEAVAGE JOINTS
TABLE 6.1	IMPACT TEST RESULTS
TABLE 6.2	SUMMARY FROM CONE CALORIMETER TEST RESULTS AT 60kW/m^2 HEAT FLUX
TABLE 7.1	ADHEREND STRESS FROM EXPERIMENT AND THEORY AT ADHESIVE FAILURE

LIST OF FIGURES

FIGURE 1.1	MICROSTRUCTURE AND MECHANISM OF TOUGHENED ADHESIVES
FIGURE 1.2	POSSIBLE BONDED STIFFENER FOR STRUCTURAL PANEL
FIGURE 2.1	TIME-TEMPERATURE-TRANSFORMATION (TTT) CURE DIAGRAM FOR THERMO-SETTING POLYMER
FIGURE 2.2	LAYERS THROUGH A BONDED JOINT
FIGURE 2.3	A CONCEPT FOR ADHESION MECHANISM
FIGURE 2.4	COMPARISON BETWEEN TWO DESIGN CONCEPTS OF GRILLAGE PANELS
FIGURE 2.5	LOADINGS IN ADHESIVE JOINTS
FIGURE 2.6	AN OPTIMISATION OF THIN METALLIC LAP SHEAR JOINT
FIGURE 2.7	EFFECT OF ADHEREND THICKNESS ON STRENGTH AND STIFFNESS FOR LAP SHEAR JOINT
FIGURE 2.8	FAILURE MECHANISMS OF STIFFENED PANELS
FIGURE 2.9	POSSIBLE FAILURE MECHANISM IN BONDED BEAM
FIGURE 2.10	FIRE TEST CURVES
FIGURE 2.11	IDEALISED CREEP CURVE OF ADHESIVE IN A LAP SHEAR JOINT
FIGURE 2.12	DURABILITY OF ADHESIVE BONDED BUTT JOINTS AFTER SEAWATER IMMERSION
FIGURE 2.13	SENSITIVITY OF THE TEST RESULTS FOR ADHESIVE AND ADHESIVE JOINT
FIGURE 2.14	STRESS-STRAIN CURVES FOR ADHESIVES
FIGURE 2.15	TESTING OF PANELS AND JOINTS IN THE AEROSPACE INDUSTRY
FIGURE 2.16	VARIOUS FAILURE MECHANISMS OF BONDED JOINTS
FIGURE 2.17	POSSIBLE LOCATIONS OF FAILURE INITIATION IN LAP SHEAR JOINTS
FIGURE 2.18	ADHESIVE STRAIN MEASUREMENTS ALONG A LAP SHEAR JOINT
FIGURE 2.19	SINGULAR EIGENVALUES OF BIMATERIAL WEDGE
FIGURE 2.20	REPRESENTATIONS OF FRACTURE FAILURE IN BONDED STRUCTURES
FIGURE 2.21	SOLID AND LAYERED SECTIONS OF A RECTANGULAR BEAM
FIGURE 2.22	PRINCIPAL ADHESIVE STRESSES AROUND THE END OF LAP SHEAR JOINT
FIGURE 3.1	ASSEMBLY JIG FOR LAP SHEAR SPECIMENS
FIGURE 3.2	ASSEMBLY JIG FOR STANDARD IMPACT SPECIMENS
FIGURE 3.3	ASSEMBLY JIG FOR SMALL STEEL/GRP SPECIMENS
FIGURE 3.4	LOADING YOKES FOR TENSILE CLEAVAGE SPECIMEN
FIGURE 3.5	HOLDER FOR SHEAR IMPACT SPECIMEN
FIGURE 3.6	SMALL STEEL/STEEL TEST SPECIMENS
FIGURE 3.7	SMALL STEEL/GRP TEST SPECIMENS
FIGURE 3.8	SMALL TEST SPECIMENS - VARIOUS MATERIALS COMBINATIONS
FIGURE 3.9	HEAT CURING CYCLE OF A SMALL ADHESIVE JOINT (ARALDITE 2007)
FIGURE 3.10	TESTING OF TENSILE LAP SHEAR SPECIMEN (TYPE 1)
FIGURE 3.11	BOLT LOADED TENSILE CLEAVAGE SPECIMEN (TYPE 4)
FIGURE 3.12	INFLUENCE OF SPEW FILLET ON JOINT STRENGTH (TYPE 1)
FIGURE 3.13	INFLUENCE OF ADHESIVE THICKNESS ON JOINT STRENGTH (TYPE 5)

- FIGURE 3.14 LOAD- DISPLACEMENT FOR TENSILE BUTT SPECIMEN (TYPE 2)
- FIGURE 3.15 DURABILITY OF STEEL/STEEL SPECIMENS AFTER 28 MONTHS CONTINUOUS IMMERSION IN SALT WATER (TREATED WITH SILANE)
- FIGURE 3.16 DURABILITY OF DOUBLE STRAP LAP SHEAR STEEL/GRP SPECIMENS AFTER 18 MONTHS IMMERSION IN SALT WATER (TYPE 6-ARALDITE 2004)
- FIGURE 3.17 FAILURE SURFACE OF DOUBLE STRAP LAP SHEAR SPECIMEN AFTER 18 MONTHS CONTINUOUS IMMERSION IN WATER (TYPE 6-ARALDITE 2004)
- FIGURE 3.18 DURABILITY TEST OF CHAINED LAP SHEAR SPECIMENS UNDER WEIGHT LOADING
- FIGURE 3.19 CONDITION OF A LAP SHEAR SPECIMEN BEFORE AND AFTER CLEANING FOLLOWING TWO YEARS IMMERSION IN SEAWATER (UNDER LOAD)
- FIGURE 3.20 INFLUENCE OF PEEL PLY AND MACHINE ADHESIVE MIXING ON THE STRENGTH OF LAP STEEL/GRP SPECIMENS (ARALDITE 2004)
- FIGURE 3.21 STRENGTH OF ADHESIVE IN LAP SHEAR JOINT AT ELEVATED TEMPERATURES (ARALDITE 2007)
- FIGURE 3.22 DETAILS OF LAP SHEAR SPECIMENS USED FOR THERMAL CREEP TESTING
- FIGURE 3.23 THERMAL CREEP OF LAP SHEAR SPECIMEN AT A TEMPERATURE OF 130°C/3% OF ROOM TEMPERATURE FAILURE LOAD (ARALDITE 2007)
- FIGURE 3.24 THERMAL CREEP PROFILE OF LAP SHEAR SPECIMEN AT A TEMPERATURE OF 80°C/25% OF ROOM TEMPERATURE FAILURE LOAD (ARALDITE 2007)
- FIGURE 4.1 PNEUMATIC ABRASIVE WHEEL FOR SURFACE ROUGHENING
- FIGURE 4.2 LOW VOLTAGE HEAT CURING EQUIPMENT (60V)
- FIGURE 4.3 CERAMIC HEATING ELEMENT (3kW)
- FIGURE 4.4 ADHESIVE MIXING MACHINE
- FIGURE 4.5 SUPPORTS AND MANDERLS FOR PANEL TESTING
- FIGURE 4.6 BONDED STIFFENER/PLATE CONNECTIONS
- FIGURE 4.7 CLAMPED STEEL/STEEL SPECIMEN (SHOWING HEATING ELEMENT)
- FIGURE 4.8 SCHEMATIC DIAGRAM OF THE HEAT CURING PROCESS
- FIGURE 4.9 STEEL/GRP JOINT UNDER DEAD WEIGHT CLAMPING DURING CURING
- FIGURE 4.10 MACHINED STEEL STIFFENERS (SQUARE AND SHAPED ENDS)
- FIGURE 4.11 STEEL/STEEL CLEAVAGE SPECIMENS
- FIGURE 4.13 LOAD-DEFLECTION FOR STEEL/STEEL CLEAVAGE SPECIMENS
- FIGURE 4.12 TESTING OF STEEL/STEEL CLEAVAGE SPECIMENS
- FIGURE 4.14 STRENGTH PERFORMANCE OF STEEL/STEEL CLEAVAGE SPECIMENS
- FIGURE 4.15 DEFORMED STEEL/STEEL CLEAVAGE SPECIMENS (AFTER TESTING)
- FIGURE 4.16 TEST ARRANGEMENT AND DETAILS OF PANEL TESTING
- FIGURE 4.17 LARGE STEEL/STEEL PANEL DURING TESTING
- FIGURE 4.18 LOAD-DEFLECTION FOR PANEL TESTING
- FIGURE 4.19 DEFORMED PANEL SPECIMENS AFTER TESTING (TABLE 4.4)
- FIGURE 4.20 STEEL/GRP CLEAVAGE SPECIMENS
- FIGURE 4.21 PRESSURE LOADING ON GRP SKIN BETWEEN STEEL STIFFENERS
- FIGURE 4.22 PRESSURE LOADING TEST ON STEEL/GRP TENSION SPECIMEN (TYPE 5)
- FIGURE 4.23 LOAD (PRESSURE)-DEFLECTION OF STEEL/GRP TENSION SPECIMEN UNTIL FAILURE

- FIGURE 3.14 LOAD- DISPLACEMENT FOR TENSILE BUTT SPECIMEN (TYPE 2)
- FIGURE 3.15 DURABILITY OF STEEL/STEEL SPECIMENS AFTER 28 MONTHS CONTINUOUS IMMERSION IN SALT WATER (TREATED WITH SILANE)
- FIGURE 3.16 DURABILITY OF DOUBLE STRAP LAP SHEAR STEEL/GRP SPECIMENS AFTER 18 MONTHS IMMERSION IN SALT WATER (TYPE 6-ARALDITE 2004)
- FIGURE 3.17 FAILURE SURFACE OF DOUBLE STRAP LAP SHEAR SPECIMEN AFTER 18 MONTHS CONTINUOUS IMMERSION IN WATER (TYPE 6-ARALDITE 2004)
- FIGURE 3.18 DURABILITY TEST OF CHAINED LAP SHEAR SPECIMENS UNDER WEIGHT LOADING
- FIGURE 3.19 CONDITION OF A LAP SHEAR SPECIMEN BEFORE AND AFTER CLEANING FOLLOWING TWO YEARS IMMERSION IN SEAWATER (UNDER LOAD)
- FIGURE 3.20 INFLUENCE OF PEEL PLY AND MACHINE ADHESIVE MIXING ON THE STRENGTH OF LAP STEEL/GRP SPECIMENS (ARALDITE 2004)
- FIGURE 3.21 STRENGTH OF ADHESIVE IN LAP SHEAR JOINT AT ELEVATED TEMPERATURES (ARALDITE 2007)
- FIGURE 3.22 DETAILS OF LAP SHEAR SPECIMENS USED FOR THERMAL CREEP TESTING
- FIGURE 3.23 THERMAL CREEP OF LAP SHEAR SPECIMEN AT A TEMPERATURE OF 130°C/3% OF ROOM TEMPERATURE FAILURE LOAD (ARALDITE 2007)
- FIGURE 3.24 THERMAL CREEP PROFILE OF LAP SHEAR SPECIMEN AT A TEMPERATURE OF 80°C/25% OF ROOM TEMPERATURE FAILURE LOAD (ARALDITE 2007)
- FIGURE 4.1 PNEUMATIC ABRASIVE WHEEL FOR SURFACE ROUGHENING
- FIGURE 4.2 LOW VOLTAGE HEAT CURING EQUIPMENT (60V)
- FIGURE 4.3 CERAMIC HEATING ELEMENT (3kW)
- FIGURE 4.4 ADHESIVE MIXING MACHINE
- FIGURE 4.5 SUPPORTS AND MANDERLS FOR PANEL TESTING
- FIGURE 4.6 BONDED STIFFENER/PLATE CONNECTIONS
- FIGURE 4.7 CLAMPED STEEL/STEEL SPECIMEN (SHOWING HEATING ELEMENT)
- FIGURE 4.8 SCHEMATIC DIAGRAM OF THE HEAT CURING PROCESS
- FIGURE 4.9 STEEL/GRP JOINT UNDER DEAD WEIGHT CLAMPING DURING CURING
- FIGURE 4.10 MACHINED STEEL STIFFENERS (SQUARE AND SHAPED ENDS)
- FIGURE 4.11 STEEL/STEEL CLEAVAGE SPECIMENS
- FIGURE 4.13 LOAD-DEFLECTION FOR STEEL/STEEL CLEAVAGE SPECIMENS
- FIGURE 4.12 TESTING OF STEEL/STEEL CLEAVAGE SPECIMENS
- FIGURE 4.14 STRENGTH PERFORMANCE OF STEEL/STEEL CLEAVAGE SPECIMENS
- FIGURE 4.15 DEFORMED STEEL/STEEL CLEAVAGE SPECIMENS (AFTER TESTING)
- FIGURE 4.16 TEST ARRANGEMENT AND DETAILS OF PANEL TESTING
- FIGURE 4.17 LARGE STEEL/STEEL PANEL DURING TESTING
- FIGURE 4.18 LOAD-DEFLECTION FOR PANEL TESTING
- FIGURE 4.19 DEFORMED PANEL SPECIMENS AFTER TESTING (TABLE 4.4)
- FIGURE 4.20 STEEL/GRP CLEAVAGE SPECIMENS
- FIGURE 4.21 PRESSURE LOADING ON GRP SKIN BETWEEN STEEL STIFFENERS
- FIGURE 4.22 PRESSURE LOADING TEST ON STEEL/GRP TENSION SPECIMEN (TYPE 5)
- FIGURE 4.23 LOAD (PRESSURE)-DEFLECTION OF STEEL/GRP TENSION SPECIMEN UNTIL FAILURE

FIGURE 6.12	TEMPERATURE PROFILES FOR TEST FURNACE AND HYDROCARBON FIRE
FIGURE 5.13	TEMPERATURE PROFILE OF STAINLESS STEEL SURFACE (T/C 2)
FIGURE 5.14	TEMPERATURE PROFILE OF ADHESIVE LINE AT STEEL/GRP JOINT (T/C 3)
FIGURE 6.15	TEMPERATURE PROFILES FOR GRP REAR SURFACE
FIGURE 6.16	THERMAL GRADIENT THROUGH MULTI-LAYERED INSULATION OF GRP PANEL
FIGURE 6.17	PANEL AFTER TESTING (STAINLESS STEEL AND INSULATION LAYERS ARE REMOVED)
FIGURE 6.18	ADHESIVE JOINT OF PANEL AFTER TESTING
TABLE 7.1	ADHEREND (STEEL) STRESS FROM EXPERIMENT AND FINITE ELEMENT ANALYSIS AT ADHESIVE FAILURE
FIGURE 7.1	GAP FILLING DEFICIENCY OF ADHESIVE IN LARGE PANEL JOINT
FIGURE 7.2	FRACTURED SURFACES OF STANDARD STEEL/STEEL SPECIMENS AFTER 28 MONTHS CONTINUOUS IMMERSION IN SALTWATER
FIGURE 7.3	LOCUS OF FAILURE OF TENSILE LAP SHEAR SPECIMEN
FIGURE 7.4	POSSIBLE MECHANISM OF STEPS FORMATION IN STEEL/STEEL STANDARD TENSILE LAP SHEAR SPECIMEN AS A RESULT OF JOINT INITIAL FAILURE
FIGURE 7.5	SEM MICROGRAPHS COMPARING TWO STEEL SURFACES
FIGURE 7.6	FRACTURED SURFACES OF LAP SHEAR SPECIMEN (WITH SPEW FILLET)
FIGURE 7.7	FRACTURED SURFACES OF TENSILE CLEAVAGE SPECIMEN (STEEL/STEEL)
FIGURE 7.8	FRACTURED SURFACES OF LAP SHEAR SPECIMEN (STEEL/GRP)
FIGURE 7.9	FRACTURED SURFACES OF TENSILE CLEAVAGE SPECIMEN (STEEL/GRP)
FIGURE 7.10	LOCUS OF FAILURE OF STEEL/STEEL JOINT
FIGURE 7.11	SEM MICROGRAPHS COMPARING TWO STEEL SURFACES
FIGURE 7.12	SEM MICROGRAPH OF ADHESIVE SURFACE INDICATING ADHESIVE FAILURE
FIGURE 7.13	FRACTURED SURFACES COMPARING TWO CLEAVAGE SPECIMENS
FIGURE 7.14	FRACTURE STIFFENER SURFACE OF CLEAVAGE SPECIMEN (TYPE 2)
FIGURE 7.15	DELAMINATION OF GRP SKIN IN STEEL/GRP TENSION SPECIMEN PRIOR TO ADHESIVE JOINT FAILURE
FIGURE 7.16	FRACTURED SURFACE OF STEEL/GRP TENSION SPECIMEN AFTER SEPARATING ADHERENDS
FIGURE 7.17	BEAM SPECIMENS TESTED IN THREE POINT BENDING

NOMENCLATURE

a : length of crack in material

b : width (or breadth)

A, B, C, D : constants

A_{ij}, B_{ij}, D_{ij} : inverse matrices

E : modulus of elasticity of isotropic material

E_o : modulus of elasticity of resin matrix

E_c : modulus of elasticity of composite material

E_1, E_2 : modulus of elasticity of adherends

E_3 : modulus of elasticity of adhesive

E_p : modulus of elasticity of toughening particles

E_k : kinetic energy

f_1 : coefficient or factor for interface condition between bonded adherends

F, P : applied forces

g : acceleration due to gravity

G : shear modulus of elasticity

R_a, H_a, R_b, H_b : reaction forces

h_r : rebound height

h : height or depth

I : second moment of area

K : creep gradient

k : number of laminated layers

k_s : spring stiffness

k_f : fracture constant

L_1, L_2 : beam lengths

L_g : gauge length

m : striking mass

M : bending moment

N : number of specimens

P_p : work of peel strength

q : shear flow in beam

Q : first moment of area

Q_{ij} : reduced stiffness term

S : statistical distribution function

t : time

t_d : creep delay time

T_1, T_2 : adherend thickness

T_3 : adhesive thickness

V_z : transverse shear force

v_f : volume fraction of a material in a mixture

V_s : striking velocity of a falling mass

V_r : return velocity of a bouncing mass

W_a : work of adhesion

W_c : work of cohesion

w_a : width of adhesive joint

X : measure for average test values

x, y, z : co-ordinates

ν_1, ν_2 : Poisson's ratio of adherend materials

ν_3 : Poisson's ratio of adhesive

σ_x, σ_y : tensile bending stress of the adherends

σ_y : tensile cleavage stress of the adhesive

$\bar{\sigma}_y$: average cleavage stress of the adhesive

σ_x^k : bending stress in the surface of the k th layer of a laminated beam section

τ_{xz} : transverse shear stress in a beam

σ_f : fracture stress of material

$\bar{\sigma}$: average tensile stress of the adhesive

τ : average shear stress of the adhesive

$\Psi_{v/e}$: viscoelastic work losses in a strained polymer

Ψ_{plas} : plastic work losses in a strained polymer

ζ : total work per unit crack extension

δ_z : vertical deflection

δ_z^k : vertical deflection of a beam with kth number of laminated layers

α : constant of stiffness deference between two adherends

γ : shear strain

χ : measure represents a test value

ϵ : elastic strain

λ : singularity constant

w : beam deflection

β : angle

ACKNOWLEDGEMENTS

The author wishes to express his most sincere gratitude to Professor M J Cowling, of the Department of Mechanical Engineering and Director of the Glasgow Marine Technology Centre for his active supervision, guidance and encouragement throughout the study. Equal thanks are also due to Mr I E Winkle, of the Department of Naval Architecture and Ocean Engineering for his invaluable discussions and effective contribution in the supervision.

The author is grateful for financial and "in kind" support from:- Science and Engineering Research Council, their agent the Marine Technology Directorate, Ministry of Defence (Navy), adhesives manufacturers (Bostik, Ciba Geigy, Evode, Permabond and 3M) and fabrication and oil industry sponsors.

The author also thanks colleague Esther Smith, technicians Alex Tory and Neil Flaherty and secretary Lynn Cullen for their assistance and friendship.

Finally, the author wishes to thank his wife Helen for her constant support and encouragement throughout this study.

1. INTRODUCTION

Adhesive bonding has emerged as a structurally efficient and cost-effective fabrication process for aerospace vehicles. The process was originally used to bond name plates and decorative surfaces in non-critical applications. Nowadays adhesive bonding has grown to include fabrication of primary aerospace structural components without mechanical fasteners. This successful experience has inspired other developments in the non-aerospace applications including the automotive, domestic, locomotive and marine industries^{6,15,23,24,25,26}. However, few applications have been investigated in the fields of large steel and composite structures which are the subject of this thesis.

High performance toughened epoxy adhesives, which were not available until the 70's, now appear to offer relative ease of application together with high joint strength and good resistance to aggressive environments¹¹⁸. The mechanism of toughening the base adhesive is illustrated in Figure 1.1 where small spherical particles of elastomeric materials acting as crack stoppers are dispersed throughout the resin matrix^{11,38}.

Adhesive bonding, just as welding and fastening, has specific requirements and successful application depends upon establishing specific conditions. Therefore it may not be simply a replacement for other joining methods but in many cases offers a complementary technique⁴². The major advantages of adhesive bonding for structural applications^{1,9,26,38,42,49} are as follows:

- absence of residual stress and distortion associated with welding
- reduction of corrosion due to the absence of weld defects (metallurgical notches and undercut) and the additional benefit of the adhesive acting as a sealant within a joint.
- ability to create complex joints
- ability to join dissimilar materials and inhibit galvanic corrosion at biometallic joints
- in joining composites where fire resistance is required, it can eliminate the problem of heat bridges produced by metallic bolts or rivets
- potential for production cost saving through the use of relatively unskilled labour
- potential for good fatigue strength

The main disadvantages of the use of adhesives are as follows:

- some surface pre-treatment is required to obtain strong and durable joints
- it is difficult to combine in a single adhesive maximum impact resistance and maximum elevated temperature resistance
- long term durability under severe service conditions is uncertain due to a shortage of design data at present
- load bearing joints require new design skills and may require modified standard sections
- high temperature sensitivity
- it may take some time after processing before full joint strength is achieved

In view of the above characteristics of the structural adhesives, this study concentrates on two areas of stiffened skin structural applications featured in Figure 1.2. The first is related to adhesive bonding of stiffeners to relatively thin (6-10mm) plating in configurations typical to ship-like structures which may include a variety of marine and land-based fabrications. The main motivation in this case was to avoid the thermal distortion associated with fillet welded stiffeners and the costly rectification often required.

The second application is related to structurally supporting (by adhesive bonding) glass reinforced plastic (GRP) panels with a steel frame forming fire/blast barriers for offshore platforms or similar structures where the fire risk is a dominating design criterion. The GRP was made of hand laid laminate of polyester resin and E glass fibres (woven roving). The GRP skin for consideration was up to 20mm thick. Typical mechanical properties of this laminate⁴ are shown in Table 1.1. The steel used for stiffeners and plates was mild steel to BS4360 Grade 43A.

In each application the adhesive bonding was evaluated with reference to the original design criteria required from the equivalent conventional designs.

This thesis essentially deals with the feasibility of using the adhesive on its own for joining steel to steel and steel to GRP for relatively thick gauge adherends. These form reference point applications from which to establish a general evaluation technique for use with structural adhesives. The majority of the research work represented here is concerned with steel/steel joints bonded with single part epoxy adhesive. This is because the steel/GRP joints studied were rather a special case in which the adhesive used was somewhat brittle.

The aim of this thesis is to assess the viability of using adhesive bonding for structural joints in aggressive environments, particularly in marine applications, and

therefore the overall objectives are as follows:

- to establish practical bonding processes
- to formulate a technique suitable for selecting candidate adhesives.
- to assess the static strength performance and limitations of adhesively bonded structural joints
- to assess the problem of long term durability in wet environments
- to investigate numerical and analytical methods for the prediction of failure strength in structural joint configurations
- to determine the behaviour of adhesively bonded beam elements in comparison with the welded equivalent and therefore to compare the strength of such configurations
- to investigate the potential of adhesive bonding in fire resistant structures
- to establish areas of further research which are necessary to apply structural adhesives successfully in new designs for marine applications

The next chapter (Chapter 2) contains the necessary background to adhesives, adhesion and bonding processes and thus provides the basis from which to tackle the objectives listed above.

Chapter 3 describes a comprehensive experimental study spanning seven single part epoxy adhesives and seven two part epoxy adhesives in order to select prime candidate adhesives and to establish a data base for the properties and bonding variables of structural adhesives. The two adhesives chosen for the remainder of the research programme were a single, hot curing, toughened epoxy, (Araldite 2007) and a two part, cold curing, slightly toughened epoxy, (Araldite 2004). Both adhesives are manufactured by Ciba-Giegy Plastics.

Carefully formulated large scale experiments in which the behaviour and design parameters of load bearing joints have been investigated, are presented with their results in Chapter 4. During this exercise suitable bonding processes for large panel elements were established.

In Chapter 5 two areas of stress analysis were examined with reference to the experimental work carried out in Chapters 3 and 4. One relates to local cleavage stress levels and their prediction in a structural joint and the the second area considers the overall behaviour of bonded panels as that of a "composite" steel/adhesive/steel structure. Both numerical and analytical methods are considered and results are discussed.

Chapter 6 explains two essential design limitations for adhesives. The first is associated with the effect of high strain impact loading and the second is with adhesive resistance to a hydrocarbon fire. Each of these two experimental investigations has been carried out with reference to one type from each of the two main classes of adhesives. In the impact loading experiments (steel/steel joints) Araldite 2007 epoxy adhesive was used due to its high toughness and therefore its impact resistance. In the fire resistance experiments (steel/GRP joints) the slightly toughened Araldite 2004 epoxy adhesive was used due to its suitability for the GRP as well as its relative high glass transition temperature as two part adhesive.

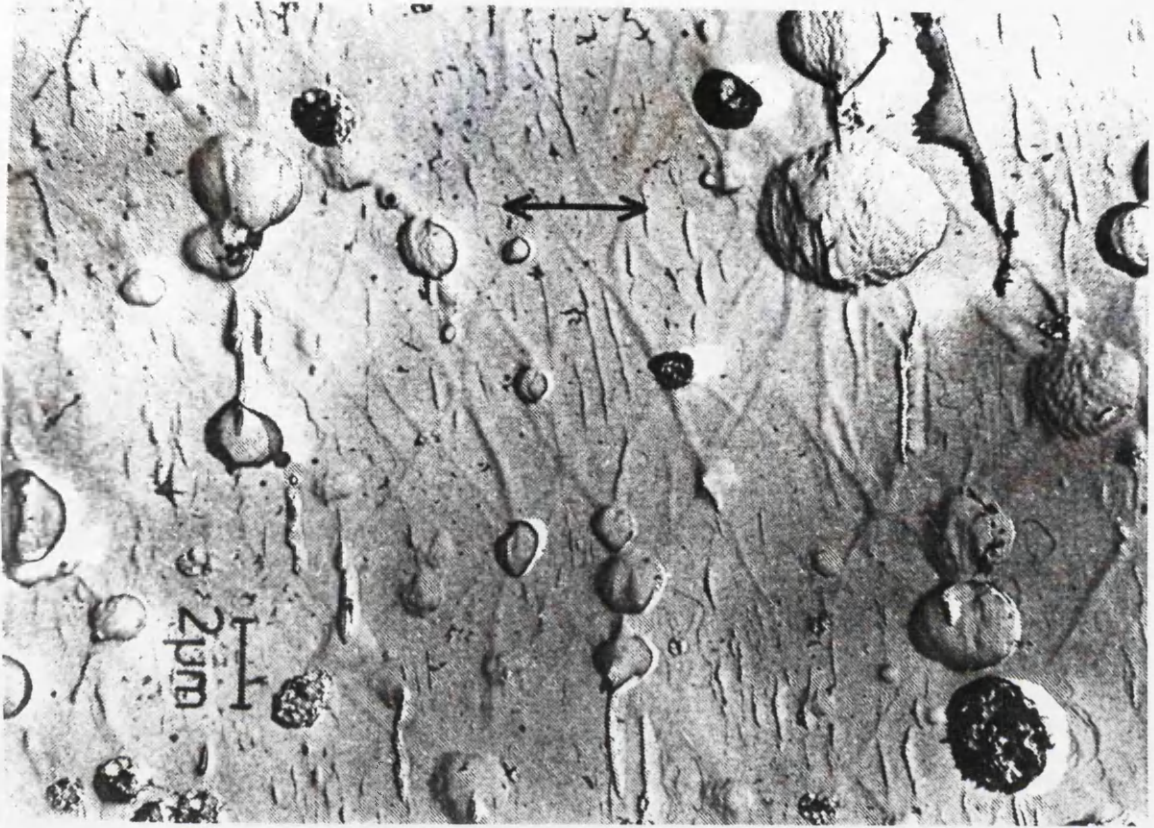
Discussion relating to the above six chapters is detailed in Chapter 7 with subheadings relating the discussion to the most important findings of the thesis. An attempt to understand the failure mechanisms and mode of failures is included with illustrations from an electron microscope.

Chapter 8 presents the conclusions and recommendations for future work.

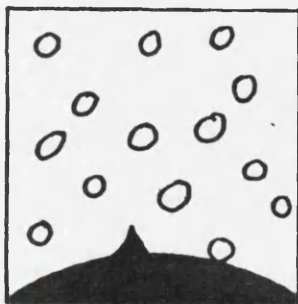
Finally, It should be mentioned here that while the topics studied in this research programme may seem diverse, they are all closely related to the knowledge base required for design of adhesive bonded structures. The specific topics studied were necessarily influenced by the fact that the research reported here relates to three independent funded projects¹²⁷ (part industry - part government) and the individual interests of the sponsors.

Glass content [%]	50 ± 2
U.T.S. [N/mm ²]	207
U.C.S. [N/mm ²]	172
In-plane Shear Strength [N/mm ²]	62.1
Interlaminar Shear Strength [N/mm ²]	13.8
Shear Modulus [N/mm ²]	3.09×10^3
Young's Modulus [N/mm ²]	14.7×10^3 (warp)
	13.1×10^3 (weft)
Poisson's Ratio	0.123(warp)
	0.139(weft)

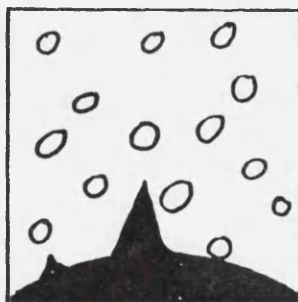
TABLE 1.1 PROPERTIES OF GLASS REINFORCED PLASTIC (POLYESTER) LAMINATE⁴



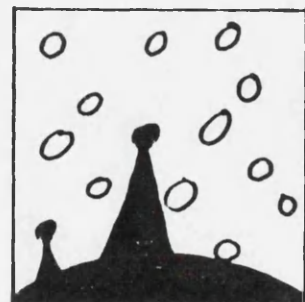
SEM micrograph of cured adhesive (showing particles and loading direction)



Crack initiation



Crack propagation



Crack arrest

FIGURE 1.1 MICROSTRUCTURE AND MECHANISM OF TOUGHENED ADHESIVES^{11,38}

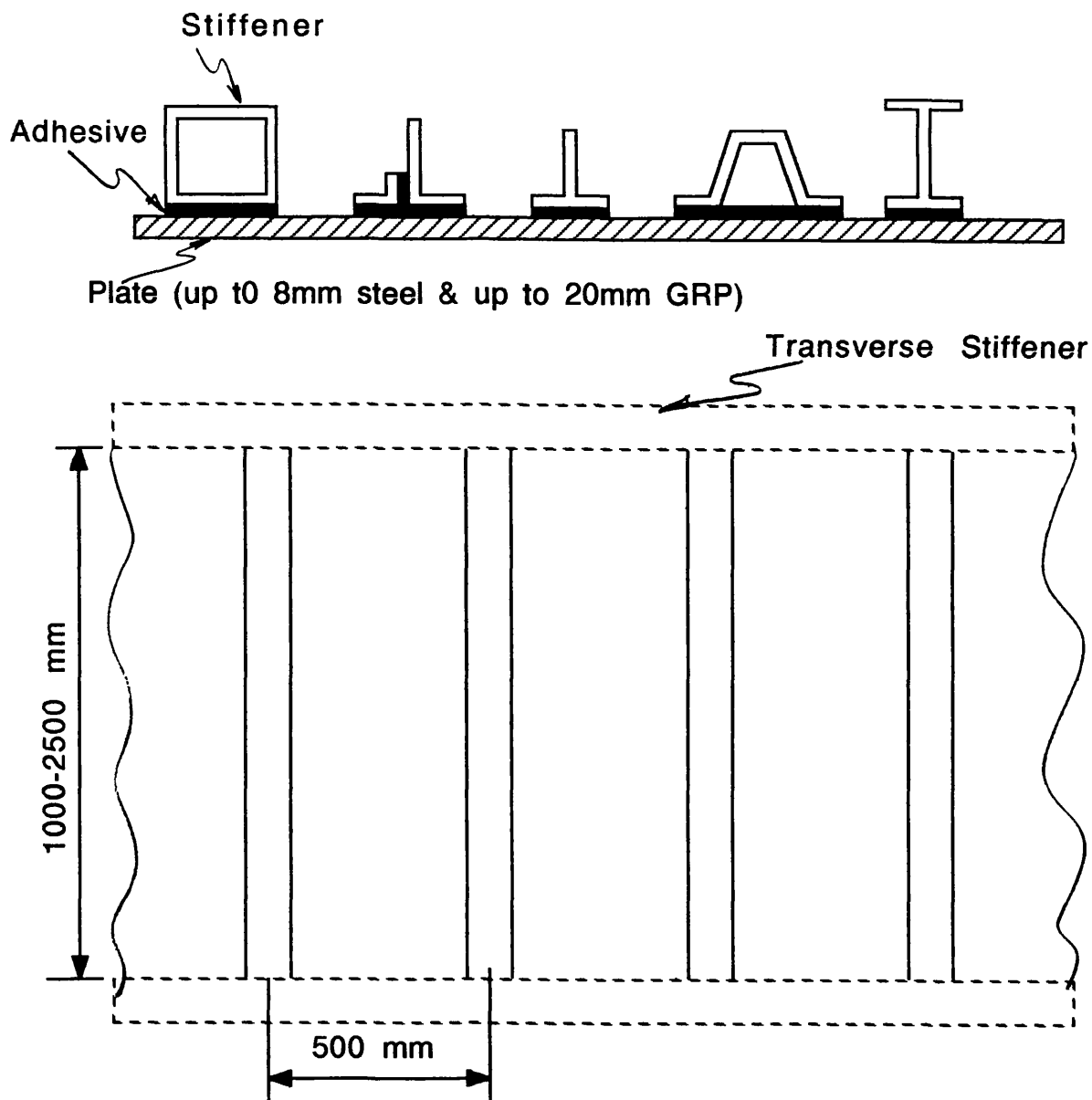


FIGURE 1.2 POSSIBLE BONDED STIFFENER FOR STRUCTURAL PANEL

2. LITERATURE REVIEW AND BACKGROUND

The following review provides a survey of a significant part of the technical literature available on joining of structural engineering components with structural adhesives. This study is mainly concerned with relatively thick substrates (up to 10mm steel and up to 20mm GRP adherends-Chapter 1). Since there is little published literature which is specific to this area it was felt important to introduce and review the background to adhesive bonding, joint design, stress analyses limitations and evaluation techniques relating to joining of thin substrates. While there is more emphasis on the bonding of steel adherends in comparison with glass reinforced plastics (GRP), the views presented are, in many cases, applicable to both types of adherend.

In the following sections the approach relates to the aims and objectives which were outlined in Chapter 1.

2.1. STRUCTURAL ADHESIVES

Modern engineering adhesives permit joining of metals to themselves as well as to thermosetting reinforced plastics in many non-aerospace applications. They may also be incorporated in production and manufacturing systems to provide cost effective products

Polymeric (organic) adhesives - proteins, dextrans, resins, elastomers and plastics are synthetic materials which are melted, dissolved and emulsified to produce the necessary liquid phase, or else used in low-molecular form and polymerised in situ (to set as a strong solid or viscous gel)¹. A time-temperature-transformation (T-T-T) curve diagram, which may be used to provide an intellectual framework to understand the cure stage and physical properties of an adhesive system², is shown in Figure 2.1. The diagram shows the different states encountered during isothermal reaction which include liquid, gel, glass and char, as well as the range of the glass transition temperatures (T_g). The diagram also shows the phase separation which occurs for example between the toughening rubber phase and the resin during cure.

Modern adhesives can be divided into two classes³ -those which set by chemical reaction(thermosets) and those which set by a physical change such as loss of solvent or solidification (thermoplastics). Both classes are important industrially, but generally only thermosets are able to withstand sustained loading. However, recent developments

have introduced high strength thermoplastics such as polyetheretherlecion (PEEK), but these are extremely expensive and also very difficult to bond^{4,5}.

Thermoset adhesives can be classified in many ways including, the type of adherends to be joined, the form of adhesive, the bonding requirements and the chemical types. The former way may be more relevant from an engineering point of view. Table 2.1 shows relations between adhesive, adherend and load bearing capacity⁶.

Developments in the fields of epoxide and acrylic resin technology have led to the introduction of toughened adhesive formulations. Toughening reduces the potential for crack propagation in an adhesive through the incorporation of a rubber phase with the cured resin (Figure 1.1). This concept has so far not been successfully applied to other types of structural adhesives⁷. This development appear to have made epoxies and acrylics the two most important structural adhesives at the present time.

Acrylic adhesives derive their bonding properties from their ability to wet the substrates to be bonded, then polymerise rapidly in the bond line to form a strong joint. This class of adhesive includes cyanoacrylates, anaerobics and modified acrylics, however, these differ in formulation and polymerisation^{7,8}. Cyanoacrylate adhesives are relatively low viscosity fluids based on acrylic monomers and are characterised by extremely fast rates of cure. Anaerobic adhesives are based on acrylic polyester resins. The modified acrylic adhesives have become more important for structural applications recently due to the introduction of a suitable toughening mechanism⁸ by using polyisoprene and polyacrylate elastomers. This development enables bonding through the oil film on steel sheets as well as the addition of substantial impact resistance to structural joints. Table 2.2 summarises some key properties of these adhesives. Bondline thickness up to 2mm can be accommodated^{8,9}.

A range of different types of epoxy adhesives is available: liquids and pastes in a wide range of viscosities, solids in a wide range of melting points, as well as supported and unsupported films, in either one or two part systems. They may be cured over a wide range of temperatures through proper selection of the curing agent¹⁰. In heat curing systems the curing agent is incorporated by the manufacturer beforehand. Two part types consist of a base binder and a separate liquid curing agent, which is mixed prior to application. Epoxy adhesives cure without releasing by-products in vapour or liquid form. For this reason, only contact or little pressure is required during curing and shrinkage is negligible^{4,2}.

In comparing general properties and performance of both epoxies and acrylics for

steel and/or polyester -GRP adherend materials it can be noticed that epoxies are preferable as shown in Table 2.3^{7,8,9,10}.

Three mechanisms for the toughening of epoxy adhesives have been developed. One is based on rubbery dispersed particles¹¹ and the second based on rigid dispersed particles¹². Although the addition of brittle particles tends to cause a reduction in the fracture strength of the materials, crack propagation becomes more difficult in such materials. This is because the addition of rigid particles tends to impede a propagating crack.

The addition of rubber particles to a polymeric system tends to reduce the modulus of elasticity of the product. In rigid systems the result is an opposite one. The simple "rule of mixture" equal strain Voigt model predicts that the modulus of composite E_c is given by¹¹:

$$E_c = E_p V_f + E_o (1 - V_f)$$

Where E_p is Young's modulus of particles, E_o Young's modulus of matrix and V_f the volume fraction of the particles. The properties of the product will also depend on particle size and distribution and the adhesion strength between particles and polymer. An important recent development in this area is concerned with the preparation of hybrid particulate composites¹³ in which there are both rubbery and rigid particles and it is claimed that very impressive mechanical properties can be obtained.

2.1.2. ADHESION MECHANISMS

The term "adhesion" is defined¹⁴ as the state in which two surfaces are held together by interfacial forces which may consist of valence forces, interlocking forces or both. This simply means the sticking together of two similar or dissimilar materials. In addition, basic adhesion is associated with surface chemistry and physics as it depends directly on interatomic and intermolecular forces¹⁵. An adhesively bonded joint represents in itself a complex system in which at least five layers can be described¹⁶ as shown in Figure 2.2. Each of these layers has a distinct physical size and will possess a set of unique properties.

There are various theories or mechanisms of adhesion^{17,18,19} but there is no single theory or mechanism which can explain all adhesion behaviour. All these mechanisms are valid to varying degrees, however, and their relative importance depends on the adhesive/adherend system in question. In an adhering system, adhesion can be expressed

in terms of forces or work of attachment. If expressed in the former manner, then the correct description should be "fundamental adhesion" or "interfacial adhesion". On the other hand, adhesion is measured experimentally in terms of forces or the work of detachment or separation of the adhering phases. The separation may take place at the interface, or in the interfacial region, or in the bulk of the weaker adhering phase. Separation in the bulk adhesive is termed cohesive failure and is related to the cohesive strength of that bulk phase. The cohesive failure of a thin adhesive layer however, is unlikely to be the same as cohesive failure of the same material in bulk. Mechanical constraints imposed by the adherends or differences in chemical composition or morphology due to the conditions of coating, deposition or joint formation are two possible causes.

The forces required to disrupt the interface can be applied in various forms (tensile, peel, shear etc.) and practical adhesion is expressed in terms of "strength" as a numerical measure of level of adhesion. This measure does not depend on the form of loading only, but also on the dimensions of the test pieces. Forces of adhesion and the work or energy of adhesion can be related only if assumptions are made about the changes in forces with distance of separation. Thus the peel strength for example²⁰ can be expressed as the sum of the energy dissipation processes which occur under particular circumstances of these tests. This sum will include the thermodynamic work of adhesion W_A or cohesion W_C (depending on whether failure is interfacial or cohesive), viscoelastic losses $\psi_{v/e}$ in any strained polymer (plastic losses ψ_{plast}) and according to the detailed circumstances other losses. Thus the peel strength P_p is given by:

$$P_p = W_A(\text{or } W_C) + \psi_{v/e} + \psi_{plast} + \dots$$

Of course, in an actual peel test the adhesive is not uniformly stressed and other energy dissipation processes may be important, but this model does serve to illustrate how the strength of the interfacial bonds can influence the energy dissipated in deforming the adhesive.

Some theoretical and experimental research which includes the butt joint concept¹⁶ has concluded that failure could never occur at the interface. It is claimed that failure only occurs in the weaker phase, often in a weak boundary layer (WBL) close to the interface. These theoretical arguments have been challenged¹⁸ however and many workers now accept the possibility of interfacial failure. It is considered that stress concentrations near the interface during many types of adhesion tests make it likely that

failure will be close to the interface irrespective of the presence of a layer of intrinsically lower strength²¹.

The modification of the Griffith theory of fracture has been developed^{18,20} and may have an important role in explaining the adhesion mechanism. The application of the theory which expresses the fracture stress σ_f (in plane stress) of a body of modulus E containing a crack of length of a as:

$$\sigma_f = k_f \frac{E\zeta}{\sqrt{a}}$$

Where k_f is a constant and ζ is the total work per unit of crack extension. It is assumed here that failure of an adhesive joint will occur where $\frac{E\zeta}{\sqrt{a}}$ is lowest. As it is difficult to generalise the variation of crack length a in term of position within an adhesive joint, attention is concentrated on the product $E\zeta$ which will depend on joint type and conditions. In the case of adhesive/metal contact the variation of fracture work ζ will depend largely on the strength or weakness of interfacial bonding^{20,22} which is illustrated in Figure 2.3. For a weak interface (Figure 2.3b) there will be a minimum product $E\zeta$ at or close to the interface (Figure 2.3c). The above equation does not quantify the relationship between factors relate to effectiveness of wetting, residual stresses, and environmental effects.

2.1.3. BONDING PROCESSES

When two parts or materials are connected by a third material, unlike the base materials, the process is called bonding. Thus brazing, soldering, cementing and the use of an adhesive, are all means of bonding parts together¹¹⁹. Successful bonding depends on surface preparation, adhesive type and method of application, correct alignment of the parts to be bonded and finally curing. Details in this section are extracted from various literature sources^{6,15,23,24,25,26,30,120}. Four basic requirements are developed below.

2.1.3.1. SURFACE PREPARATION

The first step is to ensure the removal of loose deposits such as dirt, scale, flaking, paint and any foreign matter that may impede the wetting of the base material as well as roughening of the surface to increase the bond surface area exposing a fresh, high

surface energy, adherend surface and also to provide a physical keying system. Several mechanical pre-treatment methods can be used including, shot blasting, abrading, machining and scouring with abrasive paper²³. It is claimed that surface roughness of 5 - 10 μm for steel adherends provides the ideal base for a strong joint²⁷.

Any metal surface, exposed to normal atmospheric conditions, is soon covered by a water film, along with different gases and vapours which are bound due to adsorption. Thus, such surfaces are soon covered by a layer which reduces the potential for adhesion²⁴. Furthermore greasy layers are formed and contaminants are deposited on the surface of materials during transport and storage. Organic solvents (acetone, methylene chloride, trichlorethylene) are commonly employed for degreasing bonding areas^{15,25}. However, it is desirable that degreasing is not simply carried out by wiping, since dissolved grease collects in the solvent, as well as on the cloth or brush used. The degreasing in a vapour bath is normally recommended for mild steel²⁵. But this is not practical for larger joint components. In general mild steel surface preparation is less complicated compared with titanium, aluminium and stainless steel⁴².

In the case of GRP with a polyester resin matrix, the surface requires light abrasion, followed by a solvent wipe^{26,30}. An alternative method involves use of the peel plies on the GRP surface. In this technique the final layer, instead of being the glass fibre, is a knitted nylon impregnated with a lower proportion of resin to ensure relatively good surface flatness. When the composite is to be bonded, the peel ply is stripped off to leave a clean roughened surface⁶. This is followed by solvent wipe to reduce the possible presence of any release agent associated with the peel ply layers. In many cases the solvent application can be eliminated and peel plied adherend surface is bonded directly¹²⁰.

In addition surface preparation may include the use of bonding primers which are typically 2.5-10 μm thick¹²¹. The control of thickness depends highly on the skill of the operator. Adhesive primers comprise low solid content solution of polymers, which in some cases contain chromates as a bondline corrosion inhibitor. One frequently used is a silane primer which combines both chemical and physical protection mechanisms to provide corrosion inhibition as well as hydrophobic characteristics to displace water at the adhesive/adherend interface⁶. The use of primers will not of itself convert an unsuitable highly moisture sensitive adhesive into an environmentally stable system, but they contribute to improving surface wetting and adhesion and bondline durability in

wet environments¹²¹.

2.1.3.2. ADHESIVE APPLICATION

Paste adhesives must generally be applied either in uniform film thickness or in continuous bead patterns so that no air bubbles are trapped when the adherends are brought together^{38,57}. Voids or air pockets in the bond line introduce defects and weaknesses that endanger the integrity of the bond. Suitable methods of adhesive application distribute the material as a uniform film of the correct thickness. The requirement is met by a number of methods, depending on physical properties of the adhesive, the shape and dimension of the bonding surface and the existing production facilities^{23,57}. These methods include flowing, brushing, spraying, roll coating and knife coating. For the two part adhesives there will be need for metering and mixing equipment. This can provide a cost effective method for production and has the added advantage that air is not incorporated into the mixed adhesive as is common when hand mixing and application are employed^{23,42,57}.

Those parts that are not to be bonded should be covered before applying the adhesive with greasy paper, polyamide foil, or other parting agents²⁹. It is advisable to bond the freshly cleaned steel surfaces immediately or within eight hours of surface preparation²⁹.

2.1.3.3. BONDING PRESSURE (CLAMPING)

Pressure on the adhesive in the bond line can have a positive effect on durability in several ways. It can promote better wetting and spreading of the adhesive when applied in conjunction with heating. It can be the physical factor for forcing adhesive into surface of marked roughness or porosity. It can help reduce interfacial imperfections like air bubbles or voids and increase uniformity in the bond line⁴². A great variety of means are available for the pressing of joints that are being bonded⁴². These include dead weights, spring clamps, hydraulic clamps, threaded clamps, solenoid clamps, hydraulic or pneumatic presses, enclosed pressure vessel (autoclave) and vacuum bag arrangements. An alternative method of clamping involving permanent clamping of the adherend surfaces is that of "weld-bonding" in which a combination of spot welds and adhesive is used³¹. It is often expedient to design equipment for a specific assembly

problem.

The pressure applied during the cure should never exceed that specified for the adhesive^{23,42}. Too much pressure produces internal stresses in a joint and results in either a decrease in its bond strength or early failure. Film adhesive generally requires pressure several times higher than that for paste forms. Epoxy paste adhesives for example may be bonded with contact pressure only⁴². In the curing of adhesives whose polymers can form volatile products, the use of relatively high, constant pressure on the bond line is highly recommended. Vinyl-phenolic adhesives for example, can suffer significant reductions in what would otherwise be good durability performance if the recommended curing pressure is not maintained.

2.1.3.4. HEAT CURING

The performance of bonded joints can be positively affected in several ways by a hot cure. At elevated temperatures, the lowered adhesive viscosity can more readily lead to better surface wetting^{38,42}. Adhesive manufacturers are usually able to specify the curing schedule to give optimum adhesion. Faster production generally results from heat curing procedures²³. A number of methods are used to apply heat and pressure either separately or together to bonded assemblies. Cure time depends upon the cure temperature, methods of heat application, production limitations and the bond properties required. Heat curing can be carried out by the use of conventional infrared, electrical resistance, heating blankets or tapes, autoclaves, laminating platen press and ovens. With low voltage electric heating tapes and blankets approximately 1kW is required to heat 0.3-0.4 m² with plate temperature varying between 70 and 200°C. Temperature uniformity with large panels can sometimes be a problem²³. Single part epoxy is not normally used for bonding GRP-polyester adherend because the higher curing temperature required. If single part epoxies are used then care should be taken over the release of absorbed water during the heat curing process¹²².

A recent development for the aerospace industry is rapid adhesive bonding (RAB)²⁸ for hybrid metallic/composite joints which can be used for local areas as well as whole structural joints efficiently. In this method high resistance electrical conductive elements are placed in the bond line with energy consumption for curing of 1.2-2kW/m².

It is important that certain rules concerning safety precautions for working

personnel are observed. These relate to skin protection, ventilation and flammability of solvents⁴². Successful bonding processes are largely dependent on proper bonding procedures and often have potential for automation. The cost of installing plant for bonding will probably be the strongest factor restraining expansion of adhesive bonding, but this effect may be counterbalanced by the desire, once new equipment has been installed, to see it fully utilized²⁹. These influences will operate alongside recent developments of adhesive technology which are rapidly increasing the ability to produce specific adhesives that are "tailored" to the technical and economic requirements of a practical application.

2.1.4. STRUCTURAL APPLICATIONS

The first successful demonstration of metal bonding with adhesives²⁹ was given at the RAE at Farnborough in 1941. A bonded skin/stringer panel tested in compression was shown to have greater strength than the conventionally riveted counterpart. Since then there are many applications covering most of the aerospace industry including satellites and space vehicles. Westland Lynx helicopter blades, for example, are in fact almost wholly dependent on epoxy adhesives. The main motivation is weight reduction and this industry is enjoying a good economical return from the adhesive bonding technology.

The adoption of adhesive bonding for primary structural assembly by other engineering industries has not yet been as dramatic as in the aerospace industry. Nevertheless, adhesive bonding is being used in many applications which involve a stress carrying function, but with specific motivation behind the application. Table 2.4 shows some applications with assembly description, adhesive type and main motivation extracted from several references^{30,31,32,33,34,35}. Other applications are reported¹⁰ for GRP materials including vehicle doors, tailgates, body panels of vans, buses and coaches and refrigerated containers.

Any comparison between engineering practices in the aerospace and aerospace-influenced industries and that in other engineering industries reveals one fundamental difference: aerospace engineering is vitally concerned with minimizing the weight of structures and therefore makes widespread use of light alloys and other lightweight materials, whereas the most commonly used materials in other industries are the ferrous metals which provide a good compromise between structural weight and cost²⁹.

Related to this difference in practice is the level of stress to which materials are

expected to work. Designing a structure in which weight is minimized by making materials work at very high stress levels is a very costly exercise²⁹. It is very much cheaper to design with generous safety factors at all points of complex stress, and accept the resultant of weight penalty. If this design philosophy is acceptable, many of the more striking technical advantages that can be gained by bonding are largely neutralized. Bonding will then be considered only if it offers economic or other advantages on the shop floor. Even when bonding is seriously considered, the cost of installing jigs or other plant for applying the heat and pressure may provide an argument in support of conservatism.

Cost optimization also raises the basic problem of assigning realistic costs to the various unit operations involved in structural fabrication and assembly. Studies^{36,37} using data from shipyard workstations have related work content, man-hours and labour costs to the structural design variables, so that weight, costs and structural response to load can all be expressed independently as function of the design variables. In this way it has been shown that production costs should not be regarded as proportional to the weight of the structure. Figure 2.4 shows the sections of two panels designed for the same lateral pressure loading - one to minimize weight, the other production costs. The implication of this approach for the use of adhesives requires a reconsideration of joint design and an evaluation of the costs associated with adhesion in similar terms to those applied to welding.

2.2. ADHESIVE JOINTS

There are four basic types of loading in adhesive joints^{6,23}: tensile, shear, peel and cleavage, which are illustrated in Figure 2.5. The strength of a bond is expressed by load per unit area of joint. By comparison with the poor performance in peel and cleavage, adhesives can support shear and compression loads extremely well. Indeed the stronger³⁸ materials are destroyed only under compression loading exceeding 350 N/mm². Thus wherever possible a structural joint should always be designed to distribute imposed loads within the adhesive layer as a combination of shear and compression forces which is the case of the current design concept for carrying bending shear under lateral loading.

Well designed adhesively bonded joints are normally stronger than surrounding structures. Thus no-one would seriously consider adhesively bonding 6mm mild steel

plates together with a single lap joint as a structural connection, because the adhesive bond would obviously be too weak in comparison with adherends.

Nearly all load bearing structures involving bonded joints, however complex, can be reduced to two basic types L's and T's^{38,39}. These two configurations include nearly all situations encountered in stiffened panel shapes. The effectiveness of various joint configurations has to be demonstrated by failure of the stiffener rather than the adhesive in a shear panel test. It is possible that more than one configuration will prove acceptable with the final choice depending on application and fabrication preference.

Having a symmetric foot on both sides of a stiffener web reduces the cleavage/peel stresses far below the stresses that would develop under abrupt heel of Z or L type stiffeners⁴⁰. Also, tapered and reduced ends in lap shear joints was shown to be superior in their strength compared with square or inversely tapered joint ends⁴¹. In addition, the selection of joint configuration should include both manufacturing and engineering aspects of the design.

In the dimensioning of a joint, such as a simple lap joint, there is no benefit in using an overlap longer than those just able to initiate adherend yield on the grounds that the joint will then in any case not be able to transmit higher loads⁴². Figure 2.6 illustrates a definition of optimum design in a lap joint based on yield strength of adherends⁴². However, this apparently attractive method may, on closer inspection, not be very reliable. No fail-safe behaviour can be expected from joints designed on this basis. It is rather difficult to give definite recommendations for minimum bonded flange width, for stiffened compression panels. Normal design procedures dictate wide flange width to minimize peel, particularly in thin gauge plating to enhance fatigue strength⁴³.

Another factor in optimising a joint design is the stiffness of the joint. When one adherend is stiffer than the other both adherend bending moments and peak cleavage/peel stress are intensified at the ends of the joint from which the thinner (less stiff) adherend extends⁴⁴. Figure 2.7 shows how stiffness imbalance reduces the adherend bending strength of a single lap joint. This would consequently increase the peak peel stresses causing adhesive failure at an average adherend stress much lower than the allowable/maximum stress ratio of the adherends.

2.2.1. DESIGN AND BEHAVIOUR

In general, stiffened panels should be designed such that stiffener collapse occurs

before gross panel collapse. For longitudinally stiffened panels, there are three basic types of loads⁴⁵ as follows:

- Lateral load causing negative bending of the panel
- Lateral load causing positive bending of the panel
- In-plane compression

The behaviour of these collapse mechanisms is summarised in Figure 2.8. The failure modes are recognised and usually failure starts with the stiffener because the neutral axis position is near to the base plate. In the case of lightly loaded structures such as minor ship bulkheads, machinery casings and containers, the most likely failure mechanism would be related to the case of lateral loading.

In aircraft structures, the peeling/cleavage effects are present in flanges attached to sheets, either primarily due to service load conditions, with given bending moments along the edge or secondarily due to buckling in compression or shear of the metal skin adjacent to the joint edges in extreme conditions⁴³.

The behaviour of the adhesive line in a deformed stiffened panel is idealised by the author in Figure 2.9 based on early experiments⁴⁶. In addition to the shear stress between the surfaces of the stiffener and plate, in case of ultimate loading, there are cleavage stresses in both the longitudinal and the transverse directions due to stiffener rotation which are illustrated in the figure. Tensile cleavage stress (due to tripping component-Figure 2.9) and transverse shear (bending shear) stress will be examined in Chapters 4 and 5.

In the topside structures for offshore platforms and ships, which may be made of hybrid GRP/steel constructions using adhesive bonding, the local loading can be brought up by air blast associated with explosion pressure exerted on the GRP plate between the stiffeners (frame). This can produce cleavage stresses which causes failure in these attachments⁴⁷. The service loading requirements in many secondary topside structures in the offshore application is very small and therefore will not produce significant stresses⁴⁸

2.2.2. STRUCTURAL INTEGRITY

Four major limiting factors will govern structural integrity: impact loading, fire conditions, thermal creep and wet environments. Understanding these factors is crucial to design and in service performance⁴⁹.

The most important factor is thought to be impact loading although in practice, it is rarely allowed for at the design stage⁴⁹. In spite of considerable research efforts applied to the impact tolerance of adhesively bonded structures⁵⁰, insufficient published data is available and in most cases this is applicable only to specific situations and not relevant to the larger scale applications being considered in this thesis. However there is one feature common to all applications, in that most adhesives are less sensitive to strain rate than steel^{51,52}. Thus the effect of high loading rate on adhesively bonded steel joints makes their behaviour different from welded or bolted ones. Investigation of single lap joints bonded with epoxy adhesive⁵² shows that when high strength adherends are used, there will be an increase in joint impact strength (and a significant reduction in energy absorption) when compared with a joint of low adherend strength. Thus it would appear that adhesives may be suitable for joining elements of steel structures subject to accidental impact.

The second obvious limitation is elevated temperature associated with fire conditions. The strength of most structural adhesives is limited by their glass transition temperatures. The hot curing adhesives offer a range of glass transition temperature, usually higher for those products requiring high cure temperatures¹⁰. Epoxy adhesives can have glass transition temperature greater than 160°C (cold curing is limited to 100°C). Above this (200-250 °C), they decompose to carbonaceous charring. This char may enable a joint to sustain a very small load for a limited period⁶. In the case of intensive fire it is highly unlikely that structural adhesives would enable exposed joints to survive with any degree of strength retention.

There has been growing awareness of fire testing for structural applications and the need for sufficient insulation of structures, particularly to resist hydrocarbon fires⁵³. The temperature and rate of heating from these fires is well above those based on the standard furnace test to BS 476:part 8⁵⁴. Figure 2.10 shows typical temperature/time curves for such fire conditions. While the temperature on the front (hot) face of a structure (whatever joining method is applied) can be as high as 1150°C (as shown), the requirement for the rear face should not generally exceed 150°C. This suggests that there may be a role for using adhesives in joining thermally insulated structures of steel and steel/GRP materials. The latter may incorporate the GRP into the insulation due to its low thermal conductivity.

Creep at elevated temperatures may arise from service conditions. Creep in polymers is one manifestation of their viscoelastic behaviour and is a characteristic feature of the macroscopic deformation behaviour of polymeric materials in general. Creep has been defined as time dependent flow under constant load irrespective of whether any component is recoverable on removal of the load. Previous work^{55,56} on the subject of adhesive creep has shown that there is usually a characteristic delay time, t_0 , after the application of load but before any strain creep is discernable. Once creep has been established it is essentially logarithmic and can be described by drawing the estimated best strength line through the creep section with gradient, k_c , as is indicated in Figure 2.11. In general, brittle materials exhibit less strain creep than ductile or plastic materials and require longer time to fracture⁵⁷.

The fourth limiting factor which governs the integrity of bonded steel structures is durability in wet environments. Much of the existing durability data concerns aluminium adherends which are widely used in the aerospace industry⁵⁸. When an adhesively bonded steel joint is exposed to conditions of high relative humidity, water may enter and alter the properties of the joint by one or a combination of processes⁵⁹. These include : diffusion of water through the adhesive and transport along the adhesive adherend interface. However the most destructive mode is believed to be the interface attack and this is a function of both the surface condition and the resistance of the adhesive itself to plasticisation^{60,61}. The initial strength properties exhibited by hot curing adhesives are generally superior to the cold curing types because of their greater crosslinking density and superior wetting abilities³³. These same reasons also suggest that hot curing adhesives should be more durable to wet environments. However recent developments for cold curing epoxy adhesives in steel joints for underwater repair applications⁶² show good durability, but for unstressed joints as shown in Figure 2.12. Major improvements in the durability for steel sheet joints have also been reported⁶³ using primer pretreatments such as a silane coupling agent.

2.2.3. MECHANICAL TESTING

Testing is important in all aspects of materials science and engineering and it is particularly important in the case of adhesives. There is no substantial database of material properties and the inherent non-linear behaviour of the adhesives in bonded joints⁶⁹. An extensive review of the testing methods can be found elsewhere⁶⁴.

The requirement for strength of an adhesive bonded joint, for an airframe structural member for example⁶⁵, is that the average ultimate shear stress of an adhesive bonded single lap joint should be greater than 35N/mm^2 and the adhesive bonded T type peel strength should be greater than 9N/mm . Further test methods including cleavage under bending loads (e.g a rectangular butt joint in three point bending) are being formulated but not yet fully established. Joint strength under tension is usually expressed as an average stress from load divided by bond area. Under bending load, strength is defined as ultimate bending moment or load divided by width. Failure in these joints is normally related to cleavage stresses generated by the bending moments. The relation between both ultimate tensile strength of an adhesively bonded joint under bending load and ultimate bending moment needed to produce failure has not been established⁶⁵.

The problems in trying to relate the performance of structural bonded joints to results from a test coupon are significant. It has been stated that there is almost a complete lack of any one-to-one correlation even though certain test data are obviously needed as the basis for design⁶⁶.

Most standard test procedures^{67,68} for adhesive properties utilise a joint in which the adhesive stresses are far from uniform⁶⁹. Nevertheless, the strength is presented as a nominal value of the ratio of failure load to bond area. Therefore the nominal stress for joints such as in cleavage, tensile and shear test specimens will not closely relate to the failure stress in a full scale load bearing connections.

Furthermore adhesive properties in tension are sensitive to joint parameters and test equipment and therefore the failure load can be a misleading parameter with significant scatter. This is particularly true for the case of tensile butt joint testing in which the scatter may be as much as 60%^{70,71} due to difficulties in producing a perfect joint and lack of control over boundary conditions⁷². In addition there is scatter in the determination of both Young's modulus and Poisson's ratio for an adhesive when bulk adhesive is being used in a comparison with a joint test⁷³ as shown in Figure 2.13. This provides an insight into the sensitivity of the methods to scatter in the different test results.

Many studies^{66,73} have dealt with measurement of shear deformation in thin adhesive layers. These measurements have been based on methods including the use of 'napkin ring' and thick lap shear adherent specimens. Typical stress-strain curves which define elastic and elasto-plastic behaviour for brittle and ductile adhesive respectively are shown in Figure 2.14. In general, for linear elastic analysis there is a

need to determine the Young's modulus, E , and Poisson's ratio, ν , as well as shear modulus of elasticity, G .

In the aircraft industry adhesive testing can generally be classified into two categories⁷⁴. The coupon scale, using single specimens to characterise adhesive materials and bonding processes and the structural scale in which the total design of full size or the detailed design of intermediate size components are evaluated. Element structural testing is usually performed on intermediate size test components. At this scale of testing bonded joints are tested in such a way as to simulate the expected aircraft service conditions. These scale test specimens are usually small enough to fit into environment chambers, but large enough to represent the complicated load paths of aircraft structures. A good example of the testing of these joints is shown in Figure 2.15. The panel test is used to determine the behaviour of structural elements under ultimate loading conditions (buckling capacity of panel). The T-joints tests can be used to determine the required flange width and flange type and to assess their behaviour

Mechanical testing will remain the most important technique to examine the viability of the bonding processes as well as the quality of the bond due to lack of a reliable non-destructive testing (NDT) technique^{75,76,77}. The performance of the available inspection processes is very limited. Practical inspection capability is seen to be in need of improvement but the target inspection performance should be determined as a result of structural integrity requirements.

2.3. FAILURE MECHANISMS

One of the most common and useful types of test on which the study of adhesive joint mechanisms has been based is the single lap shear test⁶. It is not only simple and economical to conduct but it also closely duplicates the type of loading to which standard adhesives are often subjected in service. Figure 2.16 provides representation to the mechanics of these joints and possible location of failure initiation under peel stresses which are relevant to thin sheet metal bonded joints⁶⁶. The bending of the adherends caused by the eccentricity of the applied tension produces significant tensile stresses particularly at the joint ends, where their effect is to tear the composite type adherends or, in the case of metal adherends may lead to plastic deformation⁶⁶.

There are a number of possibilities for different fracture pattern, size and location that may be initiated at the "terminus" of an adhesively bonded joint with spew

fillet^{78,79}. These possibilities are illustrated in Figure 2.17 and depend on type of adhesive as well as the stiffness of the adherend.

Many studies, based on single lap joint have investigated the influence of joint design parameters in relation to level of stress concentration and failure^{80,81,82} but in many cases there is a lack of correlation between theoretical and experimental results. One example is that the effect of increasing adhesive line thickness in lap shear joints decreases the ultimate joint strength while the theoretical analysis shows significant reduction in stress concentrations at joint ends.

Even with knowledge of the detailed stress distribution, the appropriate failure criterion and failure mode are not fully understood. The options for failure criteria include at least the following:

- the attainment of an absolute critical level of stress or strain¹¹⁰
- a fracture process involving defects inherent in the joint such that the failure may be modelled using fracture mechanics⁸⁸
- a criterion taking account of non-linear stress/strain behaviour of the adhesive and employing global yielding⁸³
- a criterion associated with yielding in the adherends^{9,42}

The above options can depend on material properties, local geometry, adhesive line thickness and joint rotation. The question of how to interpret stress distributions for strength prediction remains unsolved and no universal criterion has gained acceptance⁸⁴. While a maximum stress to failure criterion is found applicable for brittle adhesives, maximum strain is often more appropriate for ductile materials⁷⁸. The use of photoelastic experimental analysis¹¹² can give a very good picture of the level of stress concentration across and along an adhesive line. Figure 2.18 shows a typical strain distribution in a thick lap shear joint loaded within the elastic limit for the adhesive. It clearly indicates the high stress concentration towards the end of the joint, near to or at the adhesive/adherend interface.

Many studies^{85,86} examined the stress levels at bimaterial wedge geometries, such as an adhesively bonded joint, in order to assess the presence, strength and oscillatory behaviour of singular points (singularities). The strength of singularity (if it exists) depends upon material properties and boundary conditions. Figure 2.19 shows singularity level for homogenous and bimaterial joints with varying wedge angle. This in practice suggests that any non-filletted bond line or with a fillet less than 63° has a singularity point and the application of a strain and stress failure criteria may be

questioned when linear elastic analysis is used. Even filleted joints may have singularity points where the calculation for stress concentration seems complicated⁸⁷.

Because of the singularity and other problems associated with stress criteria of failure, several studies have applied the principle of fracture mechanics to adhesive joints⁶⁹. Of particular interest to load bearing structural applications is the attempt to apply linear elastic fracture mechanics (LEFM) to predict joint failure^{88,89,90} based on the calculation of stress intensity factors and energy release rate methods. Most studies claim some agreement with experimental data and note an apparent dependency of the adhesive fracture energy on the mode (fracture mode) of applied stress at crack tip. Figure 2.20 shows typical representations of mixed mode test specimens. The conclusion from using thick type adherends in studying fracture mechanics⁸⁹ is that failure criteria can be based on fracture energy for the opening mode and shear stress for the shearing components. The main difficulty in using fracture mechanics is the need to define an initial flaw size in a joint, its location and the cause for its presence due to a manufacturing defect or local damage. There is, however no clear reason for trying to correlate failure mechanisms based on the designed model with an assumed crack-like defect. Initial studies for adhesive failure in thick adherend joints^{89,90,91} based on LEFM including static, fatigue and impact loadings have indicated both difficulties in and the importance of producing a sharp notch in the test specimens used. Work relating to fracture and fatigue based on compact tension specimens of bulk adhesives appears to offer a good model for studying the fracture aspect of such structural materials⁹⁴.

Analysis of surface failure of bonded specimens is an important part of any bond evaluation test, but is frequently disregarded, resulting in gross misinterpretation⁷⁴. Sophisticated techniques may be needed to determine precise cleavage planes for research work, however for routine testing visual or low power optical microscopy are sufficient⁷⁴. In the case of both adhesive and cohesive failure surfaces, a fracture may be due to normal tensile stresses even in the case of shear loading⁹⁵

The difficulties in assessing failure in bonded joints increase when environmental and variable bonding criteria are also to be considered. In either case there is a greater need for reliable numerical and analytical methods.

2.3.1. ANALYTICAL METHODS

The early work on joint mechanics by Vollkersen and Goland and Reissner laid the

foundation for a closed form solution of the stresses in bonded joints⁹⁷. Their analysis of single lap shear joints, based on classical theory of structures, was supported by mathematical solutions, assuming only linear material properties. Many contributions have followed their approach to attempt to avoid conservative (underestimated) stress distribution in a lap shear joint⁶. Perhaps the most recent modelling which accounts for bending, shear and normal stresses has been produced by the Allman theory⁹⁸. In this theory the adhesive stresses have been set to zero at the overlap ends and allowed for a linear variation of the normal stresses across the adhesive thickness. This analysis is also based on a single lap joint but, unlike the previous theories⁹⁷, it accounts for dissimilar materials and different adherend thicknesses and is therefore regarded as less conservative. Recent study⁹⁹ has stated that Allman's theory for elastic stresses in a lap shear joint is suitable for linear, rigorous analysis and can be modified for non-linear adhesive behaviour. This study⁹⁹ shows a comparison between Allman's analysis and the finite element method with the difference in peak strain level as little as 5%.

The main problem with such theories is that they are limited to the simple lap shear joints. To enable designers to obtain a good qualitative stress distribution for the normal tensile stresses associated with the peel effect for a variety of practical configurations attempts were developed for general solutions¹⁰⁰. Good correlation, from such general solutions with average stress distributions obtained from finite element analysis is claimed¹⁰⁰ with reference bonded joints between thin gauge metal skins and T or L shape stiffeners. Suitability of such technique will be investigated in Chapter 5 with reference to thick adherends.

There seems no analytical technique which can assess the stress level in a long continuous bonded joint (e.g. beam structure). The shear stresses which are developed in elastic beams of solid cross section due to lateral transverse shear loads which induce bending are examined in most 'strength of materials' text books¹⁰¹ and described in Appendix I. The importance of the transverse shear stress component (generated by the transverse shear force) along a beam, τ_{zx} (Appendix I), subject to a flexural loading is in reducing bending stresses and bending deflections of the beam. This can be seen from the comparison of a beam of a solid rectangular section with its equivalent laminated leaf-spring beam¹⁰³ as illustrated in Figure 2.21. With the assumption that there is no friction between the layers, the maximum bending stress deflection for a given section depth depends on a number of layers (leaves) k and can be written as follows:

$$\sigma_x^k = k \sigma_x$$

$$\delta_z^k = k^2 \delta_z$$

Where:

σ_x^k is the maximum bending stress of the multi-layered beam section

k is the number of stacked layers in a given section

σ_x is the maximum bending stress of solid beam section (Appendix I)

δ_z^k is the maximum vertical deflection of multi layered beam section

δ_z is the maximum vertical deflection of solid beam section

If such an approach is used to determine the structural parameter for bonded joints, then it would ignore the shear generated along the adhesive line. This would be as a very crude assumption. These interfacial shearing forces depend on the type of adhesive and increase with increasing adhesive modulus leading in turn to an increase in flexural rigidity of adhesively bonded structure^{104,105}.

An attempt¹⁰⁶ to evaluate the system mechanics a metal/adhesive/ bulk adhesive beam using fluxer beam theory based on longitudinal strain and equilibrium, using three point bending model failed to determine the adhesive adherend interface force coefficients. It was concluded that a suitable analytical approach to this problem has yet to be established and the finite element methods are required in order to account for such a problem. The current study attempts (Chapter 5) to apply analysis developed for laminated materials in which classical beam theory is modified to account for interface conditions¹⁰⁷

2.3.3. NUMERICAL METHODS

Finite element methods are based on sub-dividing the structure into a number of finite elements. The displacement at discrete point on the element boundaries called nodes are the problem solving variables. By defining the displacement within the element in terms of nodal displacement, it is possible to obtain expressions for strain and stress¹⁰⁸. The accuracy of the solution from finite element analysis depends upon sufficient mesh refinement as well as proper assumption for boundary conditions. The majority of finite element analysis for metal-metal bonded joints are based on single or double lap shear joints using a two dimensional model. One of the first attempts¹⁰⁹ in the 1970's used constant strain quadrilateral elements which has shown close agreement

with some aspects of the Goland and Reissner analysis, even though they did not account for the non-linear effect of joint rotation. Furthermore, this early analysis did not refine the joint mesh at the ends and it was therefore necessary to extrapolate results to obtain stresses at the ends of the joint. A later analysis¹¹⁰ used linear strain elements and allowed for rotation of the joint. The stresses quoted from these analyses are at the centre of the elements rather than the nodes.

Several parametric studies have investigated stress concentration and distribution in lap shear joints^{81,109,110} based on elastic analysis. Figure 2.22 shows two mesh models as examples showing the effect of stress distribution in a joint, with and without spew fillet of adhesive⁶. Investigations have recently considered elasto-plastic behaviour for both adhesive and adherends, together with edge geometries for the adherend⁸¹. However, it appears that despite the considerable research into the numerical analysis of the single lap shear joints^{78,79,80,81,84,87} the prediction/evaluation of the stresses is far from certain. Prediction of stress in lap shear joints with different overlap lengths⁸⁷ is shown in Table 2.5. While these may be one of the best published data in this respect they lack consistency (Table 2.5).

Conventional finite elements are based on an assumed strain field and hence only satisfy equilibrium in the overall sense. This means that the method will not satisfy conditions at a stress free boundary. In the same way, finite elements developed from the equilibrium model lead to continuous stress but discontinuous displacement¹¹¹. These arguments are true not just for the free edge of a joint but also within the interface between adhesive and adherends¹¹.

Various special mixed finite elements for the static analysis of adhesive joints have recently been developed to take into consideration the continuity conditions at the interface, including displacement and transverse stresses for the two dimensional elastic analysis¹¹². This method claims possible determination of shear stress distribution along the interface of a butt joint which is not possible to obtain using conventional finite element techniques. Other attempts for solving the interface problems include the concept of boundary element method for adhesive joints^{113,114}. In these each material in a bonded joint is treated as a separate zone. Elements are placed around zone boundaries only. The aspect ratio of a rectangular zone is limited to 10:1. Thus the typical adhesive layer has to be split into several zones. These techniques, however cannot be applied in the case of adhesive interface with composite adherend¹¹⁵.

Many finite element codes, using special material discontinuity elements, are being

developed for fracture mechanics analysis⁷¹. These are modified to allow positioning of the node in isoparametric elements which produce singularity, using frontal element techniques for the stiffness matrix.

It is very difficult and inefficient to model small detailed changes in the joint design on a model of an automobile structural component because of the geometrical nature of having a thin adhesive line within a large joint. The alternative is therefore to make a detailed generalised model of the joint and investigate the influence of design parameters^{116,117}. This would be even more difficult in modelling the adhesive joints of marine structural components such as interframe panels. The finite element analysis for this study (Chapter 5), therefore will be restricted to joints which represents elements within the structures

Material	Relative density	Young's modulus (GN.m ⁻²)	Specific modulus (GN.m ⁻²)	Shear modulus (GN.m ⁻²)	Specific shear modulus (GN.m ⁻²)	Tensile strength (MN.m ⁻²)	Specific strength (MN.m ⁻²)
Mild steel	7.5	210	26.7	80	10.7	400	53.3
Brass	8.3	100	12.0	40	4.8	300	36.1
Aluminium	2.6	70	26.9	26	10.0	550	212
						(max for alloys)	
Wood (spruce along the grain)	0.7	14	20	—	—	100	143
Epoxy adhesive	1.2	4	3.3	1.4	1.2	50	42

TABLE 2.1 PROPERTIES OF VARIOUS STRUCTURAL MATERIALS⁶

Property	Nominal bond line thickness	
	0 mm	2 mm
Speed of cure		
Time to fixture		
Room temperature	5 min	30 min
Spot-heat ^b	5 s	3 min
Strength		
Tensile shear (N/mm ²) (ASTM D1002-64)	11	9
T-peel (N/mm) (ASTM D1876-69T)	7	15
Environmental resistance		
Strength (%) retained after 1000 h at		
40°C/95% RH	95	95
150°C/air	80	80

TABLE 2.2 PROPERTIES OF ACRYLIC STRUCTURAL ADHESIVES^{8,9}

Property/ Performance	<u>Acrylic</u>	<u>Epoxy</u>
Shear strength	2	3
Modulus of elasticity	1-2	2-3
Cleavage strength	3	2-3
Impact resistance	3	2-3
General durability	2-3	3
Heat resistance	2-3	3
Solvent resistance	2-3	3
Toxicity	1-2	1
Capital cost	1	1
Material cost	2-3	2-3
Bonding process complexity	1-2	1

KEY 1 = Low, 2 = Medium and 3 = High

TABLE 2.3 COMPARATIVE PROPERTIES OF ACRYLIC VERSES EPOXY STRUCTURAL ADHESIVES^{7,8,9,10}

Industry	Structural Components	Joint Description	Adhesives	Motivations	Remarks
Automotive	roof, bonnet, pillar crossmember, siderail	aluminium to steel or aluminium to themselves and steel to themselves in thin stiffened panels using top-hat and box beams	cold curing epoxy or acrylic with or without other mechanical joining methods	weight reduction and corrosion elimination	acrylics adhesives are favoured due to their oily surfaces and rapid curing properties
Civil	bridge decks	steel plate or stiffeners to steel or concrete at intermediate joints	cold curing epoxy	reinforcement to meet requirements for increases in designated loading	the durability for cold curing epoxy adhesives are limited to meet 120 years design requirements
	lamp posts and flag poles	tubular and triangular thin sections with overlap of steel and aluminium	hot and cold curing	reduction of weight and simplify assembly	limited to thin metal parts
Marine	for hovercraft buoyancy tank superstructure and bulkhead	stiffened aluminium panels and honeycomb covered sandwich panels	phenolic and epoxy adhesives	reduction of production time compared with riveting	the biggest user of structural adhesives outside the aerospace industry b. production environment more related to aerospace industry (clean room operations)
	small ships, bulkhead watertight doors, casing and ducting	steel, aluminium and composite sheets up to 3mm and stiffened panels	cold curing epoxy adhesive or weld bonding	elimination of distortion	a. both bonded and bond-welded stiffened joints have shown good fatigue performance when compared with spot-welded ones b. bonded joints have been reported after 5 years in service to be in very good conditions c. adhesives used are considerably weaker than modern adhesives
	ship repair super-structures	cracked aluminium decks and bulkheads batched with steel and FRP sheets	cold cured epoxy adhesive	to avoid fracture fatigue which may be caused by welding aluminium	it is started with novel applications for emergency reasons and now adopted for passenger ships
	offshore structure repair - steel jacket (underwater)	damaged tubular bracings cased with steel sleeve segments	cold cured modified epoxy	avoid high cost of underwater welding	a. adhesive should possess good wetting characteristics under water
Manufacturing	picard's bathscaph	three forged steel parts bonded together	warm cured two parts epoxy	ideal application for bonded joints subject to compression	it has been tested in water depth of 11,500m
	horizontal milling machine	steel and cast iron parts	cold cured epoxy adhesives	to reduce the size of frame parts casts and reduce vibrations	
Railway	rail joint	screwed and bonded joint between lashes and the rails with isolating materials	cold cured adhesive	to obtain electrically insulated joints	a. superior to bolted joint only specially at lower temperatures b. some environmental attack observed from laboratory tests

TABLE 2.4 APPLICATIONS FOR STRUCTURAL ADHESIVES^{30,31,32,33,34,35}

Overlap length (mm)	From testing (N mm ⁻¹)	Predictions	
		Linear elastic only (N mm ⁻¹)	Non-linear geometry added (N mm ⁻¹)
6.2	336.0	492.3	432.9
12	447.6	516.0	485.1
17	537.2	537.2	537.2
25	587.5	572.5	571.0

110 INT.J.ADHESION AND ADHESIVES APRIL 1988

TABLE 2.5 TEST RESULTS AND PRIDITION: FRACTURE LOAD PER mm JOINT WIDTH⁸⁷

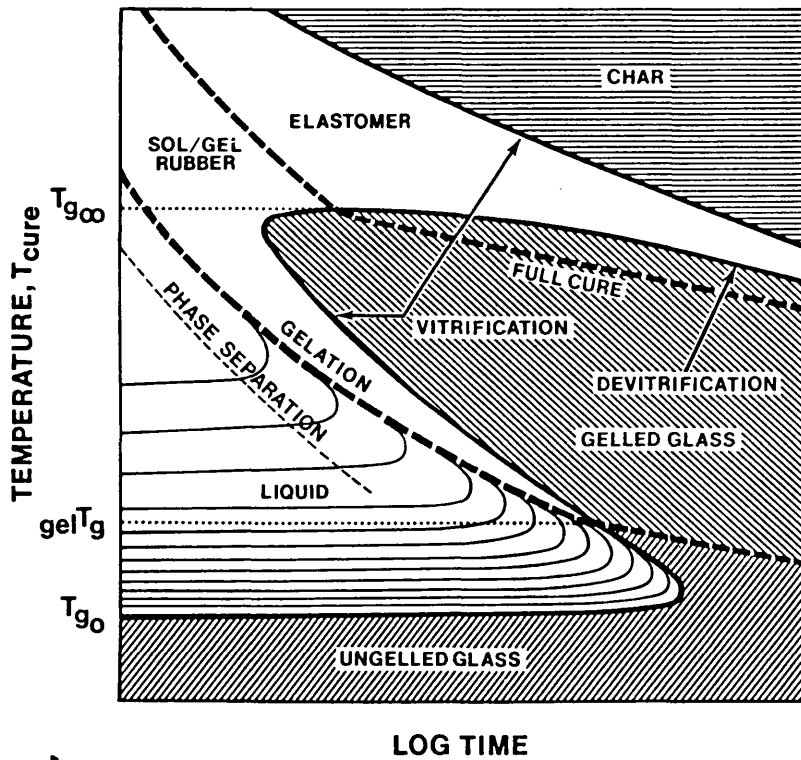


FIGURE 2.1 TIME-TEMPERATURE-TRANSFORMATION (TTT) CURE DIAGRAM FOR THERMO-SETTING POLYMER SHOWING THE DIFFERENT STATES DURING ISOTHERMAL REACTION (T_{g0} , $\text{gel}T_g$ AND $T_{g\infty}$ ARE THE GLASS TRANSITION TEMPERATURE OF THE REACTANT, THE TEMPERATURE AT WHICH THE TIMES TO GELATION AND VITRIFICATION ARE THE SAME, AND THE GLASS TRANSITION TEMPERATURE OF THE FULLY REACTED SYSTEM RESPECTIVELY)²

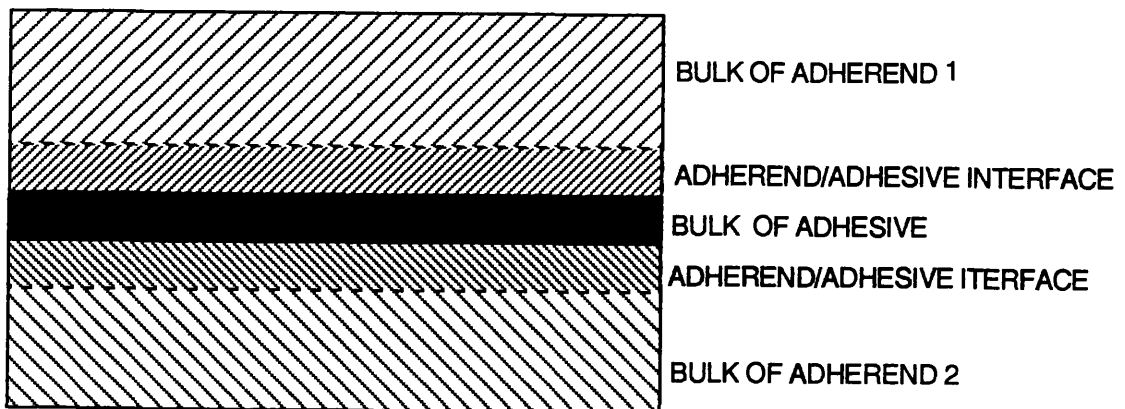
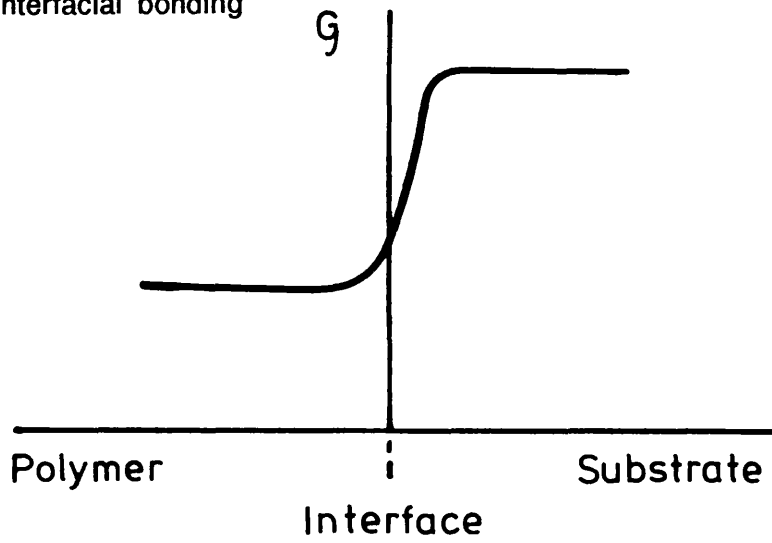
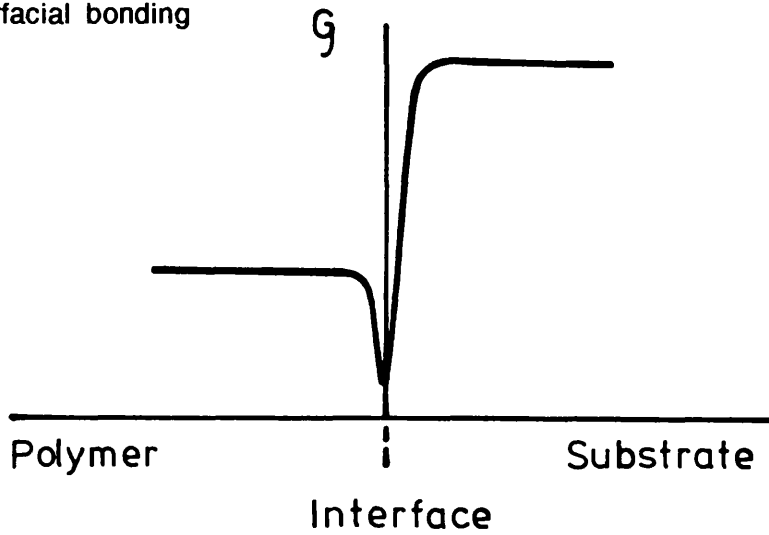


FIGURE 2.2 LAYERS THROUGH A BONDED JOINT¹⁶

a-Strong interfacial bonding



b-Weak interfacial bonding



c-Variation of product of effective local modulus (E) and fracture work (ζ)

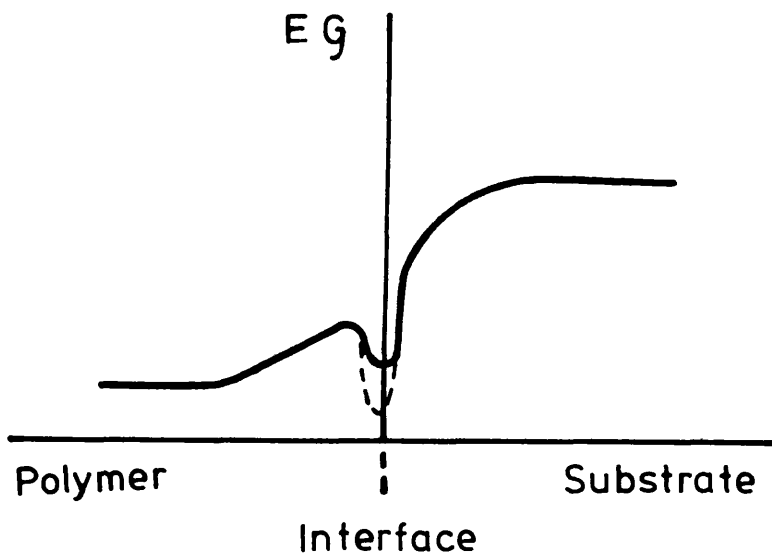


FIGURE 2.3 A CONCEPT FOR ADHESION MECHANISM²⁰

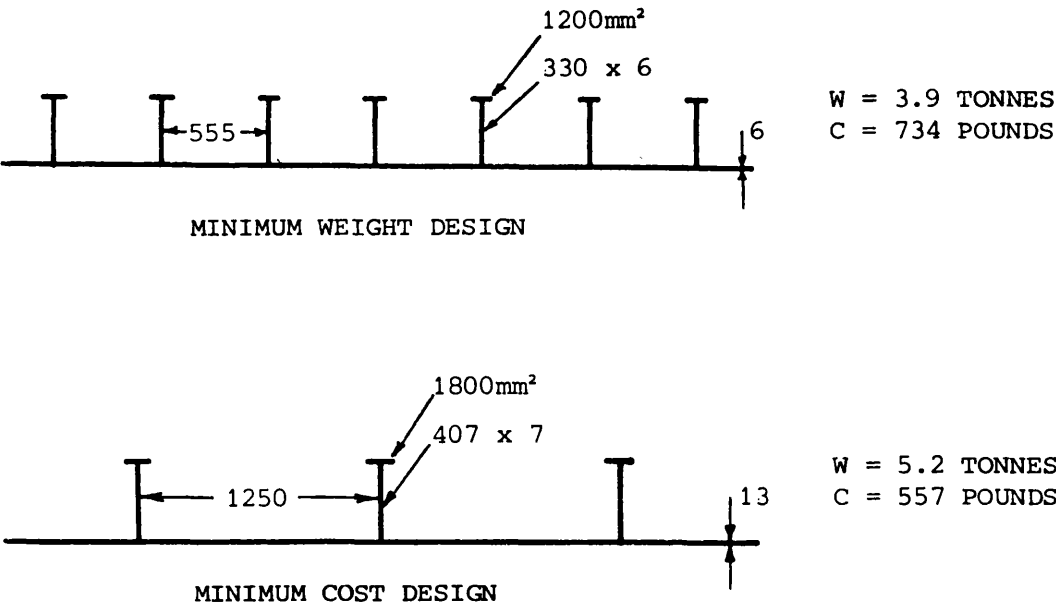


FIGURE 2.4 COMPARISON BETWEEN TWO DESIGN CONCEPTS OF GRILLAGE PANELS³⁶
(C: COST AND W: WEIGHT)

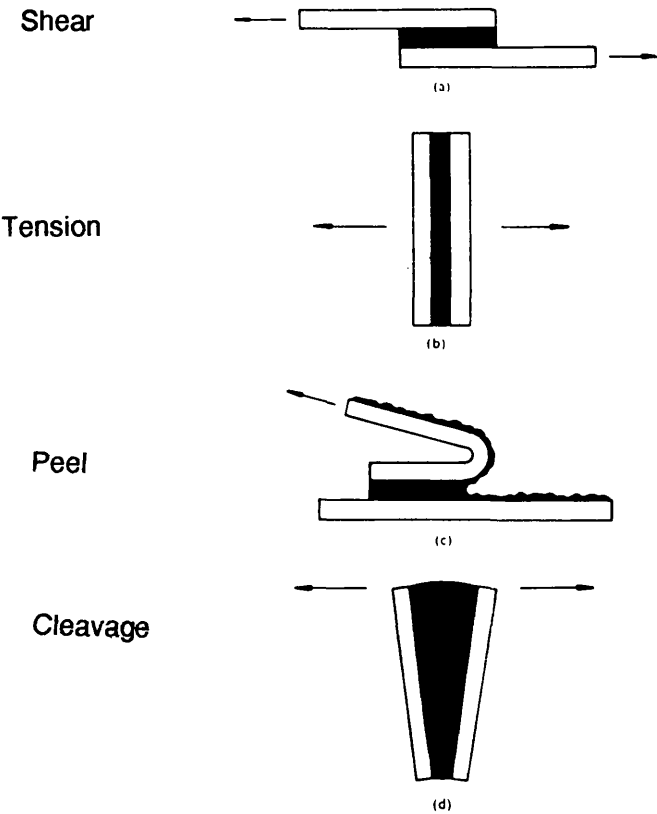


FIGURE 2.5 LOADINGS IN ADHESIVE JOINTS²³

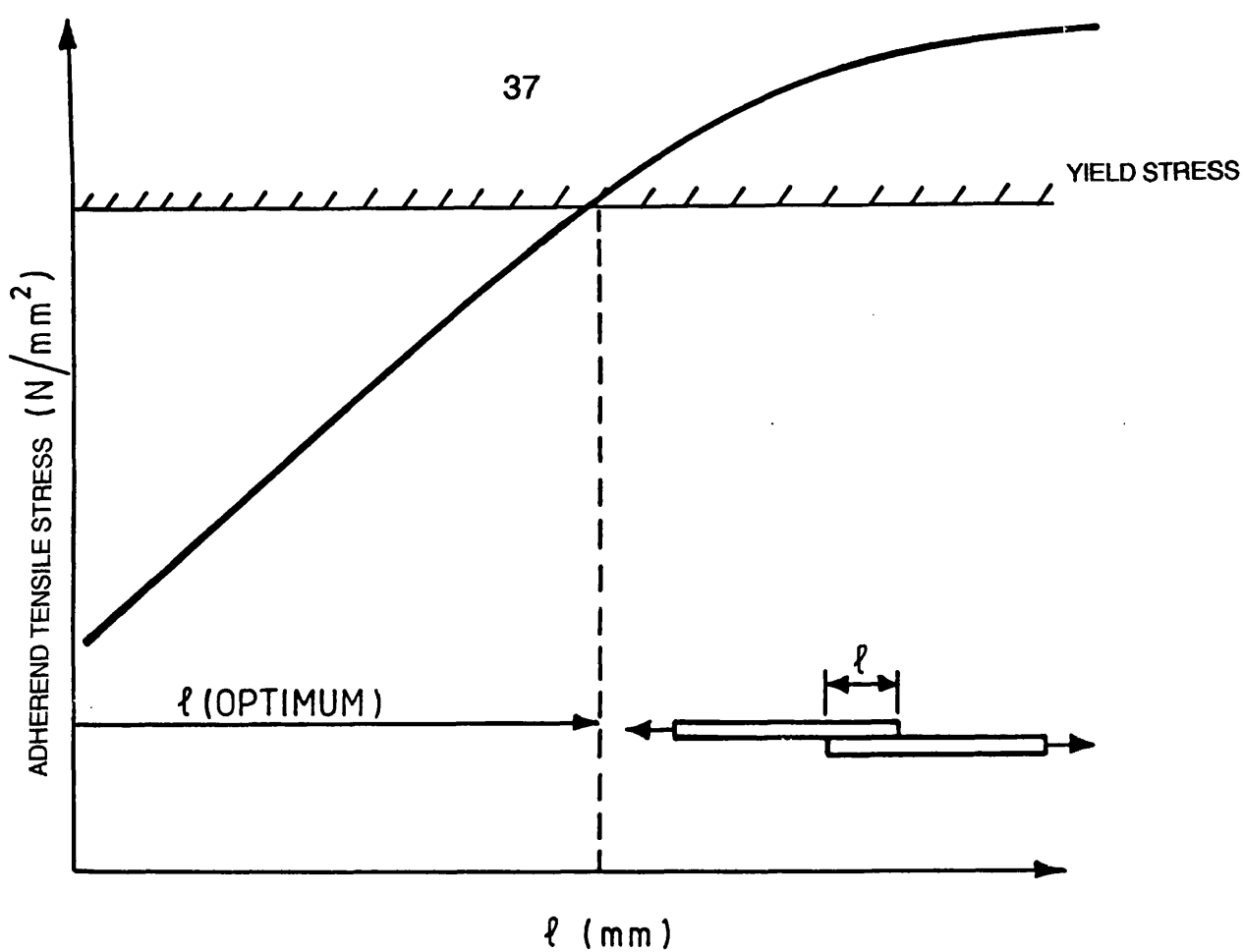


FIGURE 2.6 AN OPTIMISATION OF THIN METALLIC LAP SHEAR JOINT⁴²

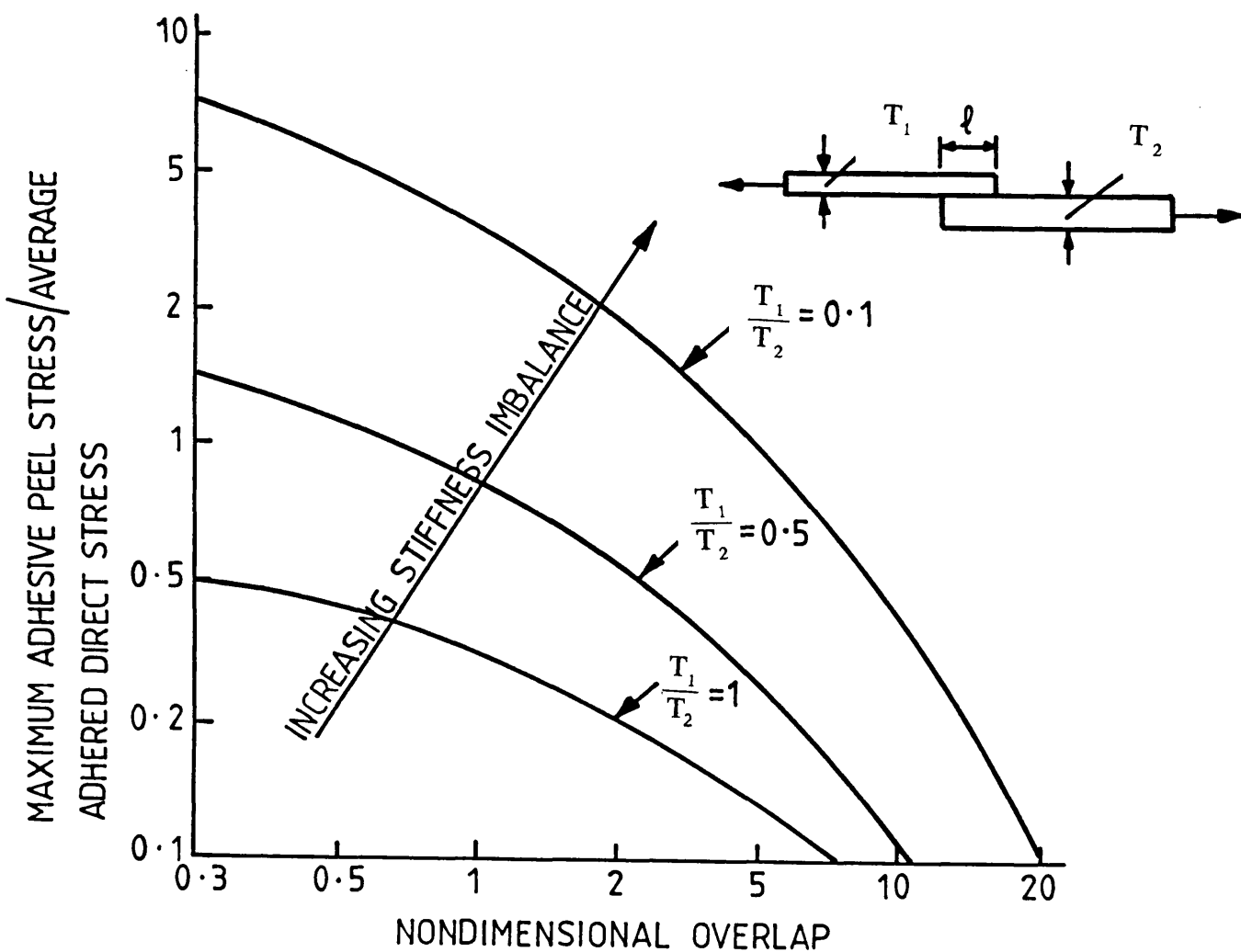


FIGURE 2.7 EFFECT OF ADHEREND THICKNESS ON STRENGTH AND STIFFNESS FOR LAP SHEAR JOINT⁴⁴

I: COMPRESSION YIELD OF STIFFENERS

II: COMPRESSION FAILURE OF PLATING

III: COMBINED FAILURE OF STIFFENERS AND PLATING

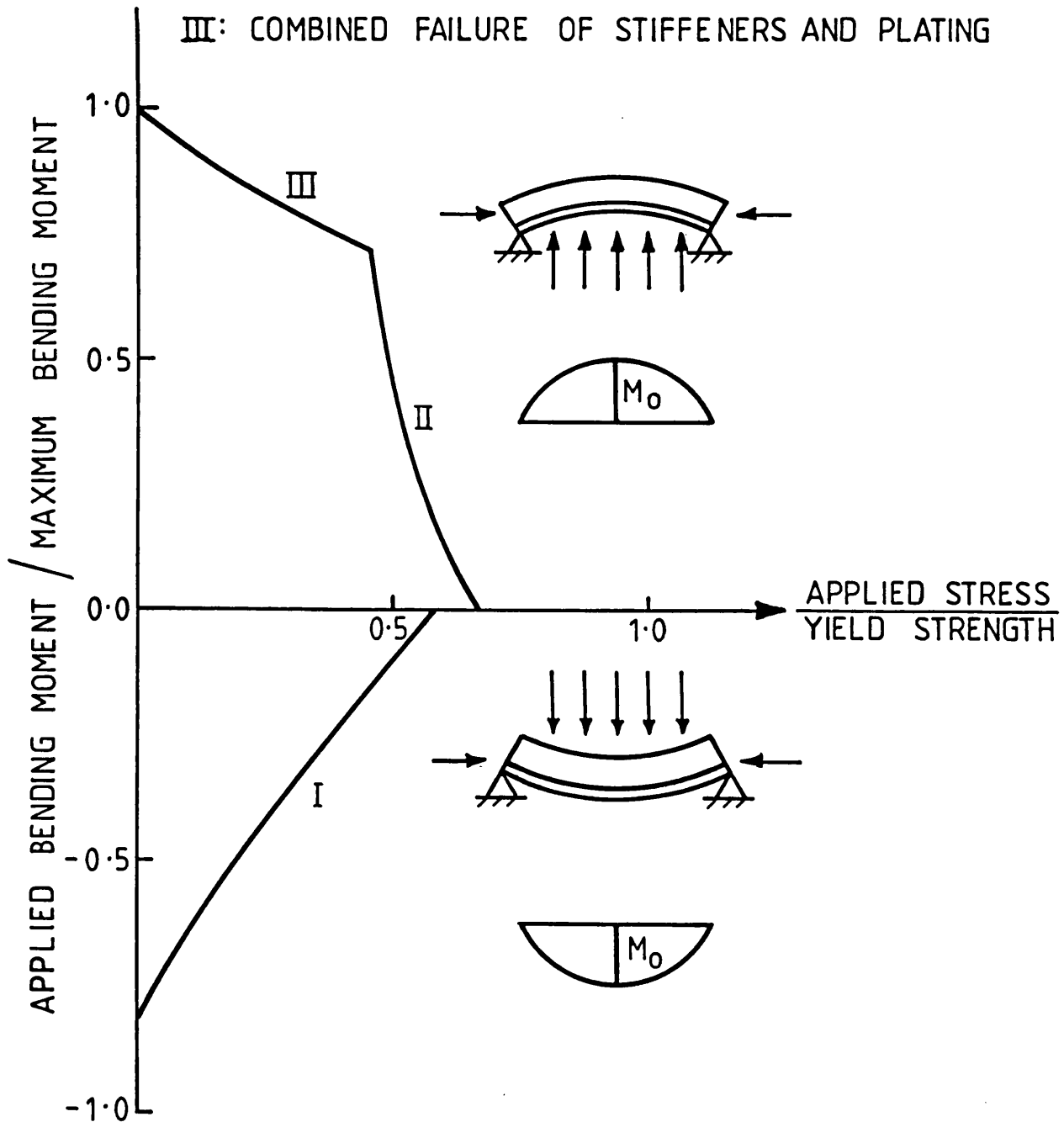


FIGURE 2.8 FAILURE MECHANISMS OF STIFFENED PANELS⁴⁵

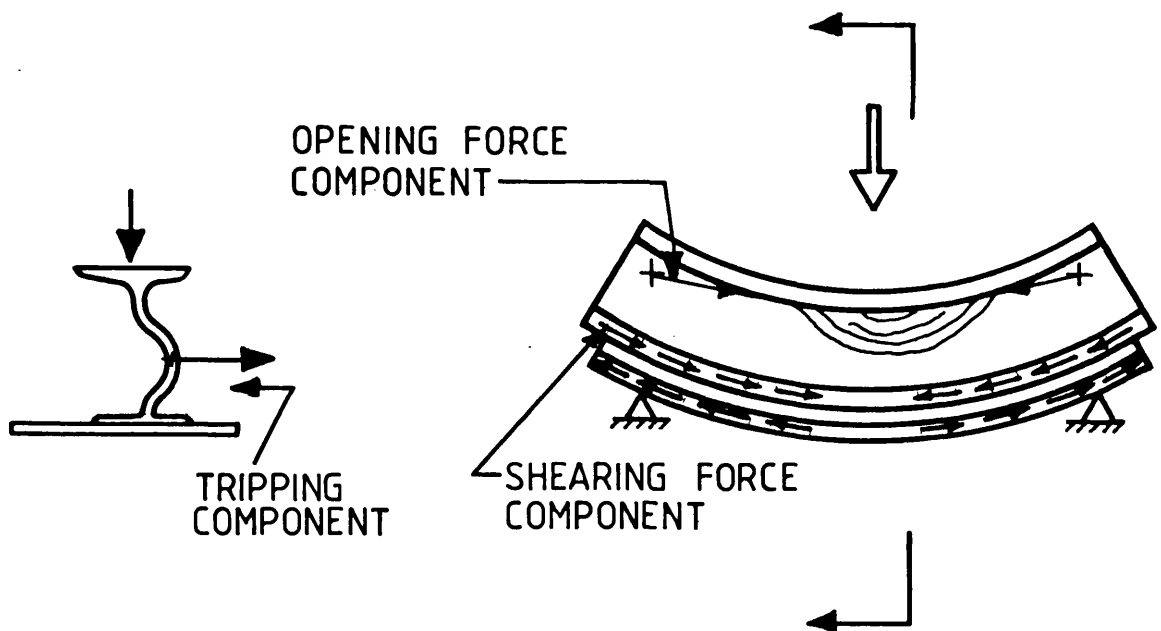


FIGURE 2.9 POSSIBLE FAILURE MECHANISM IN BONDED BEAM

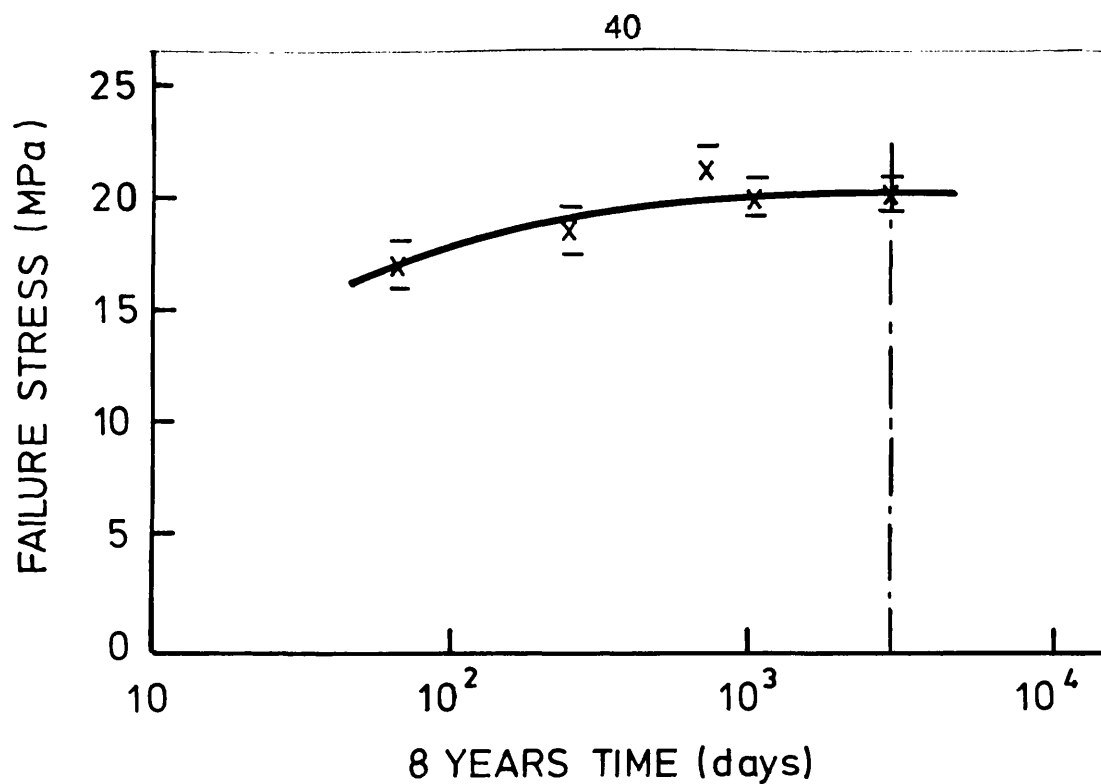


FIGURE 2.12 DURABILITY OF ADHESIVE BONDED BUTT JOINTS AFTER SEAWATER IMMERSION⁶² (UNSTRESSED)

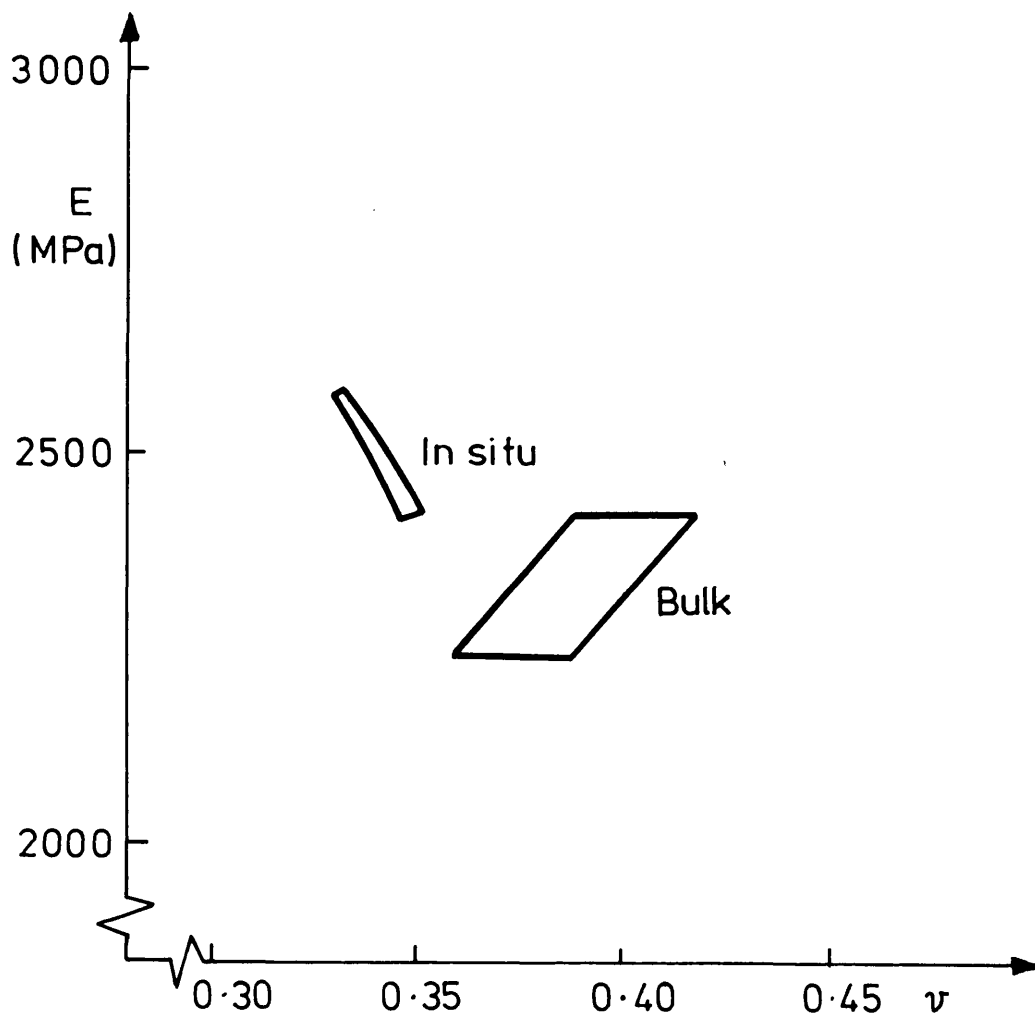


FIGURE 2.13 SENSITIVITY OF THE TEST RESULTS FOR ADHESIVE AND ADHESIVE JOINT⁷³

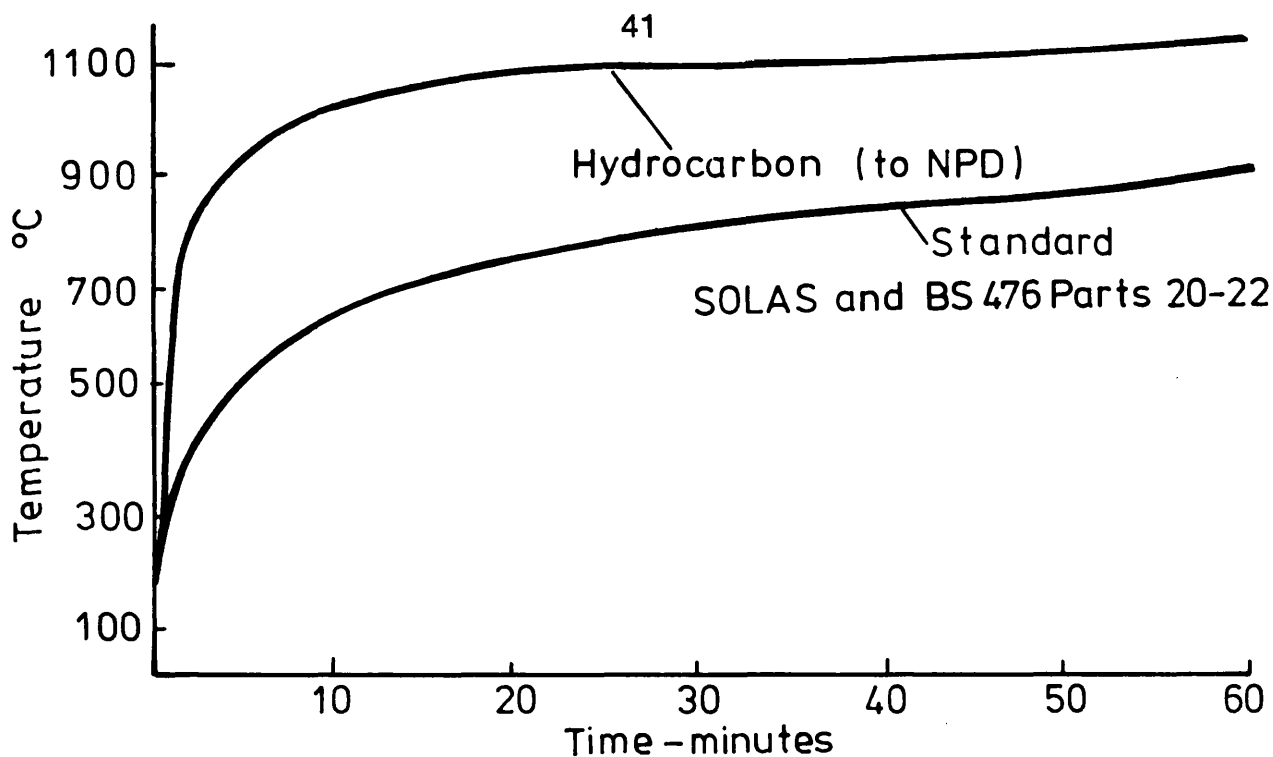


FIGURE 2.10 FIRE TEST CURVES⁵³

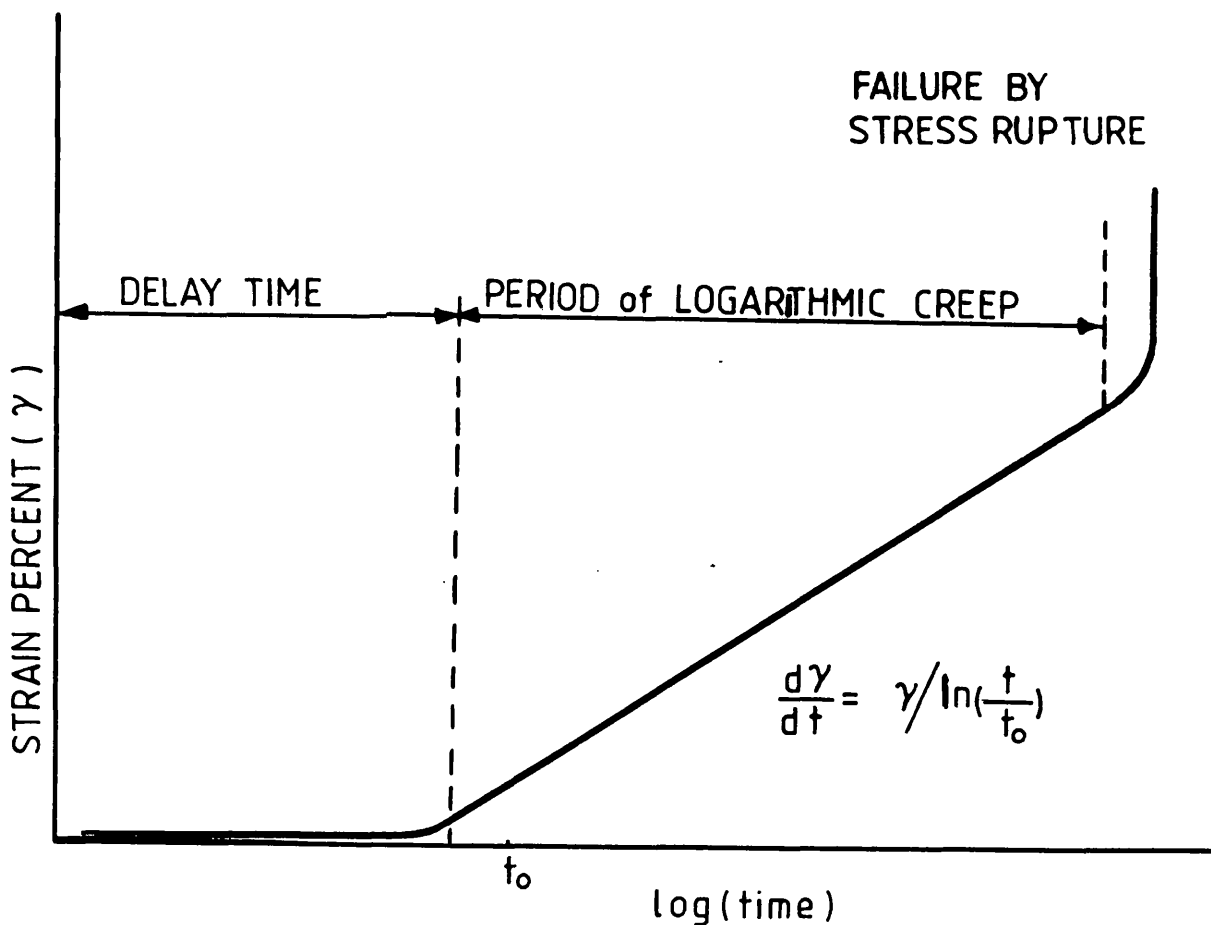


FIGURE 2.11 IDEALISED CREEP CURVE OF ADHESIVE IN A LAP SHEAR JOINT⁵⁵

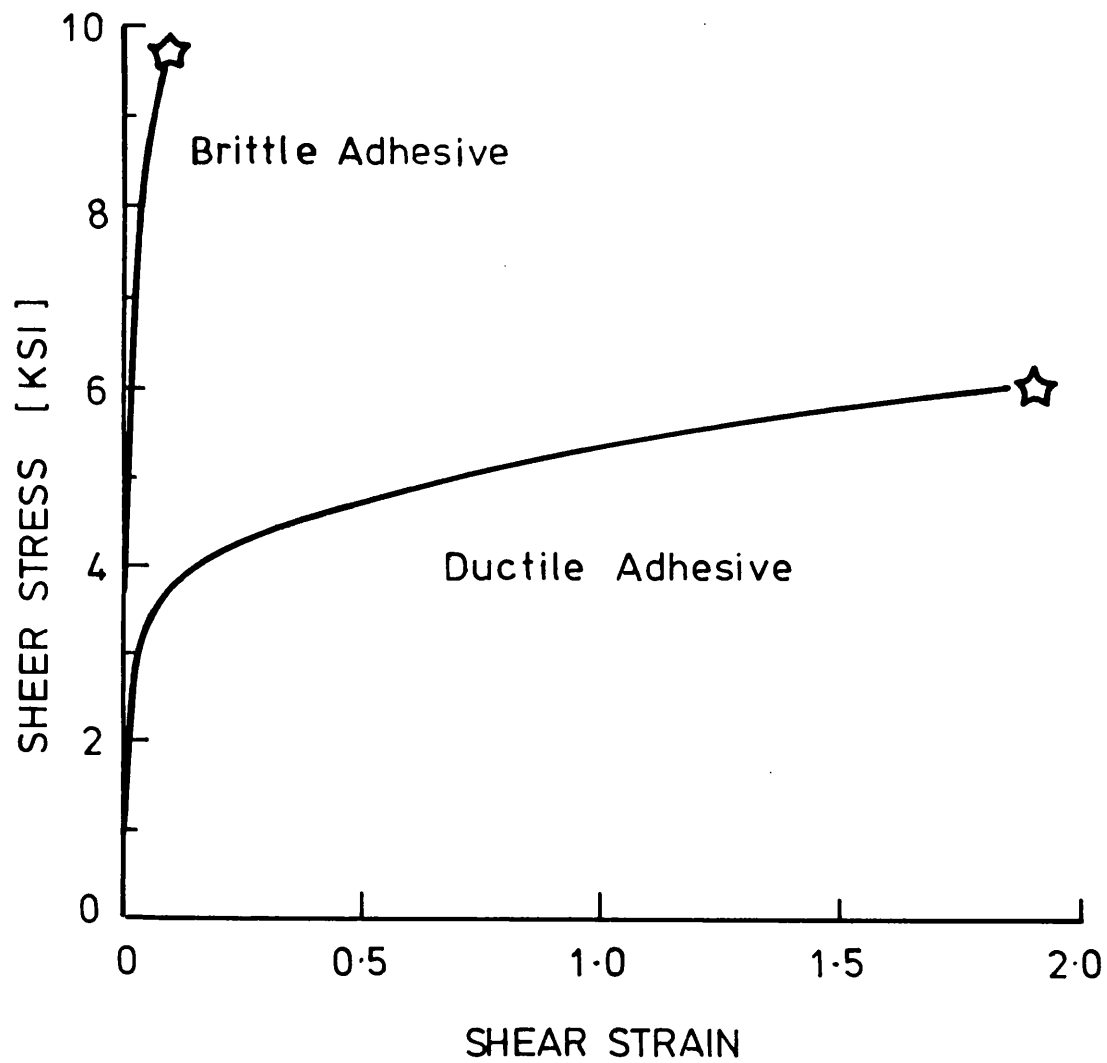
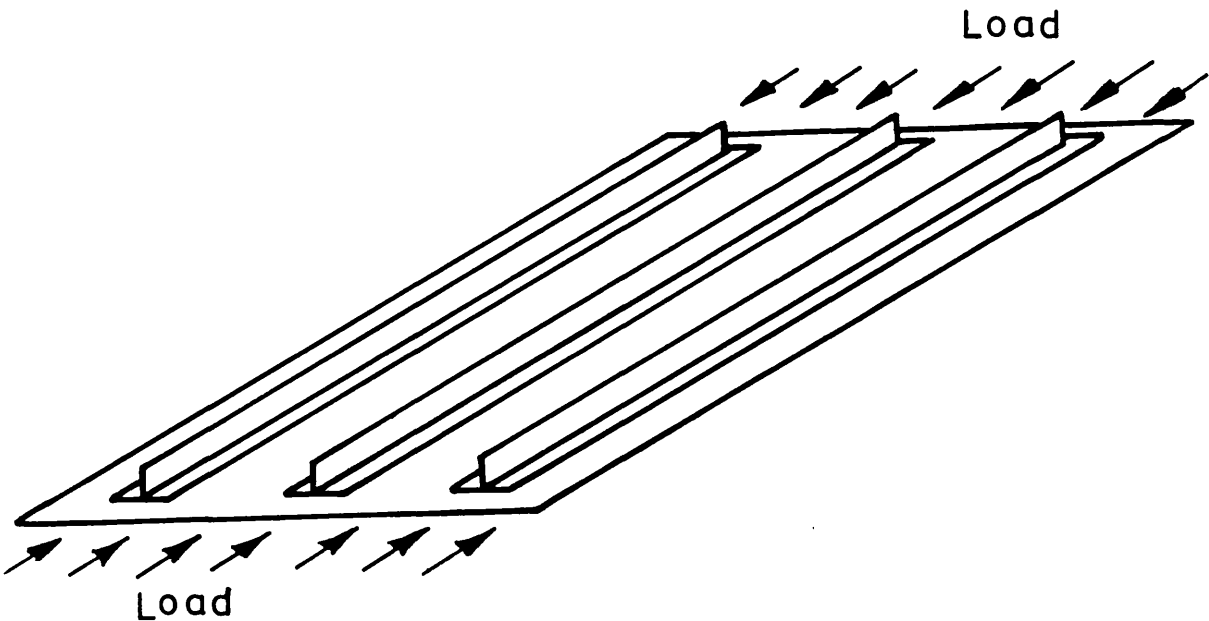


FIGURE 2.14 STRESS-STRAIN CURVES FOR ADHESIVES⁷³



END LOADED COMPRESSION PANEL.

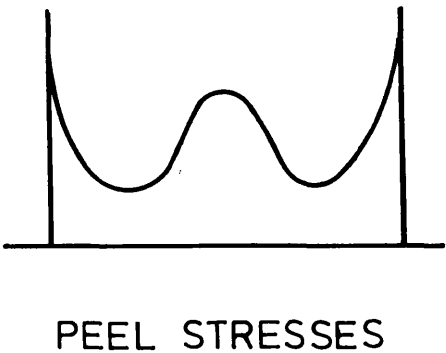
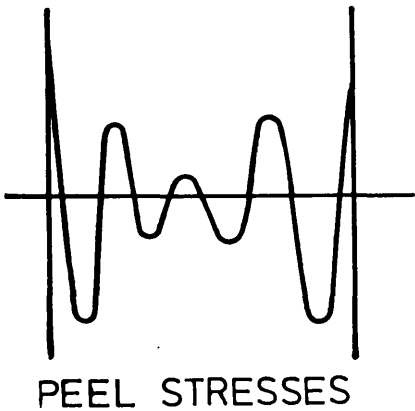
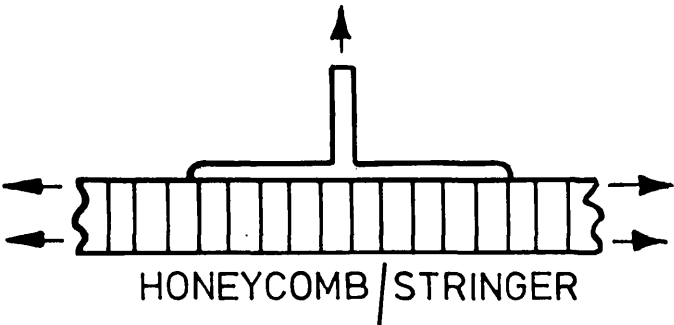
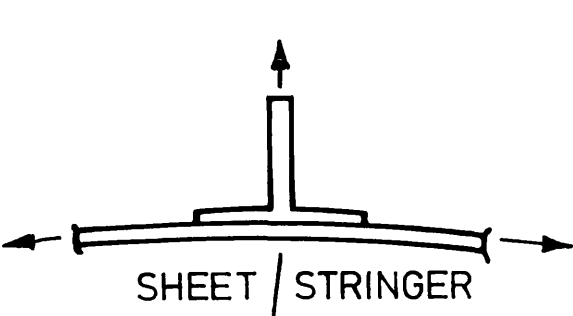


FIGURE 2.15 TESTING OF PANELS AND JOINTS IN THE AEROSPACE INDUSTRY⁷⁴

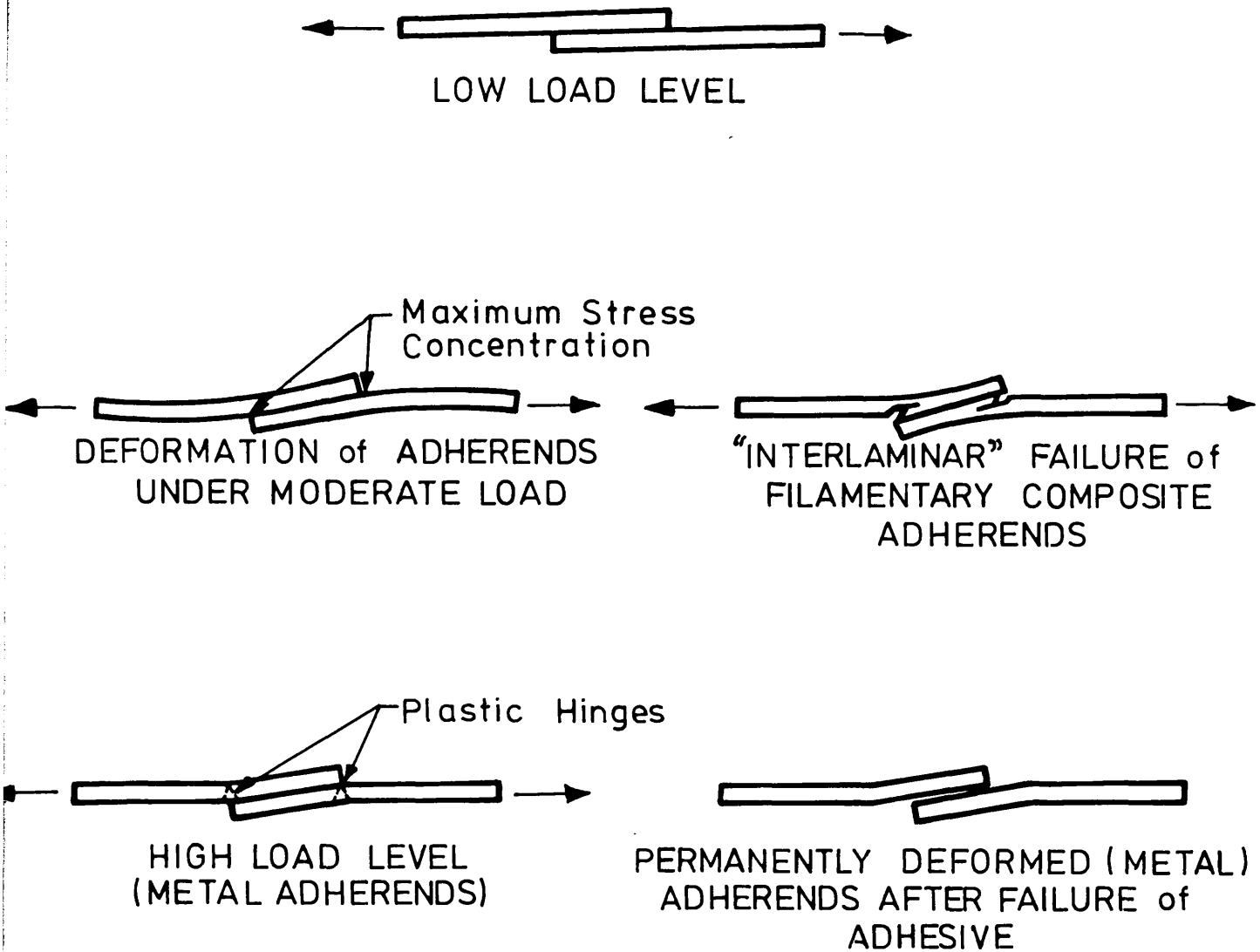


FIGURE 2.16 VARIOUS FAILURE MECHANISMS OF BONDED JOINTS⁶⁶

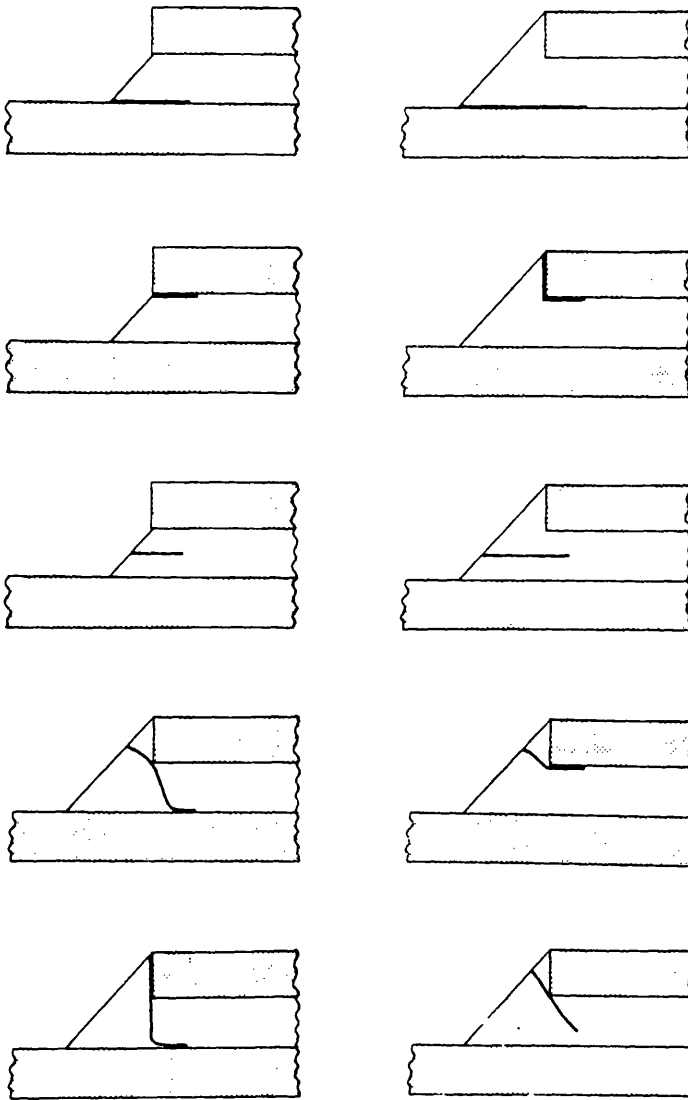


FIGURE 2.17 POSSIBLE LOCATIONS OF FAILURE INITIATION IN LAP SHEAR JOINTS⁷⁹

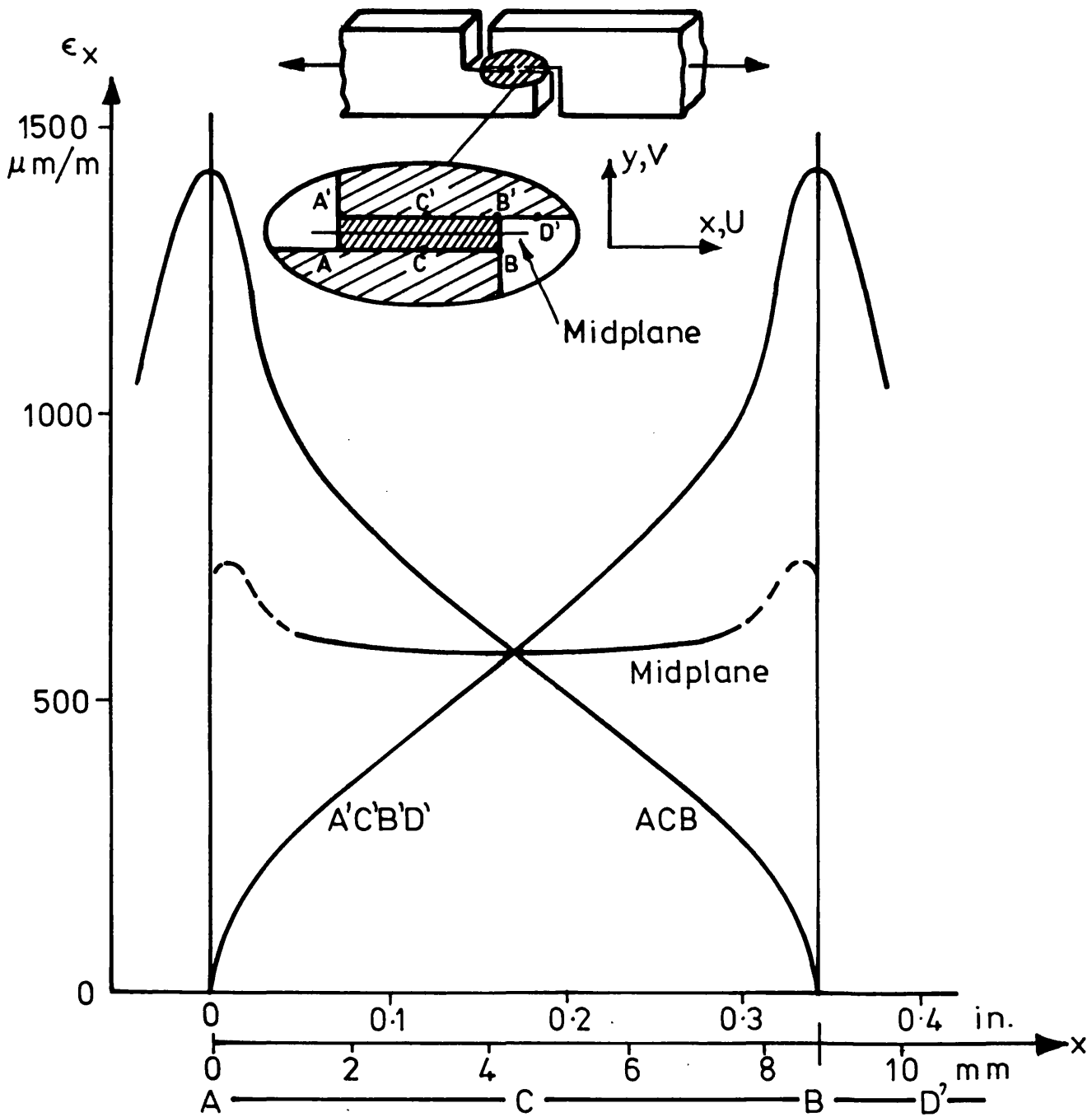


FIGURE 2.18 ADHESIVE STRAIN MEASUREMENTS ALONG A LAP SHEAR JOINT¹¹²

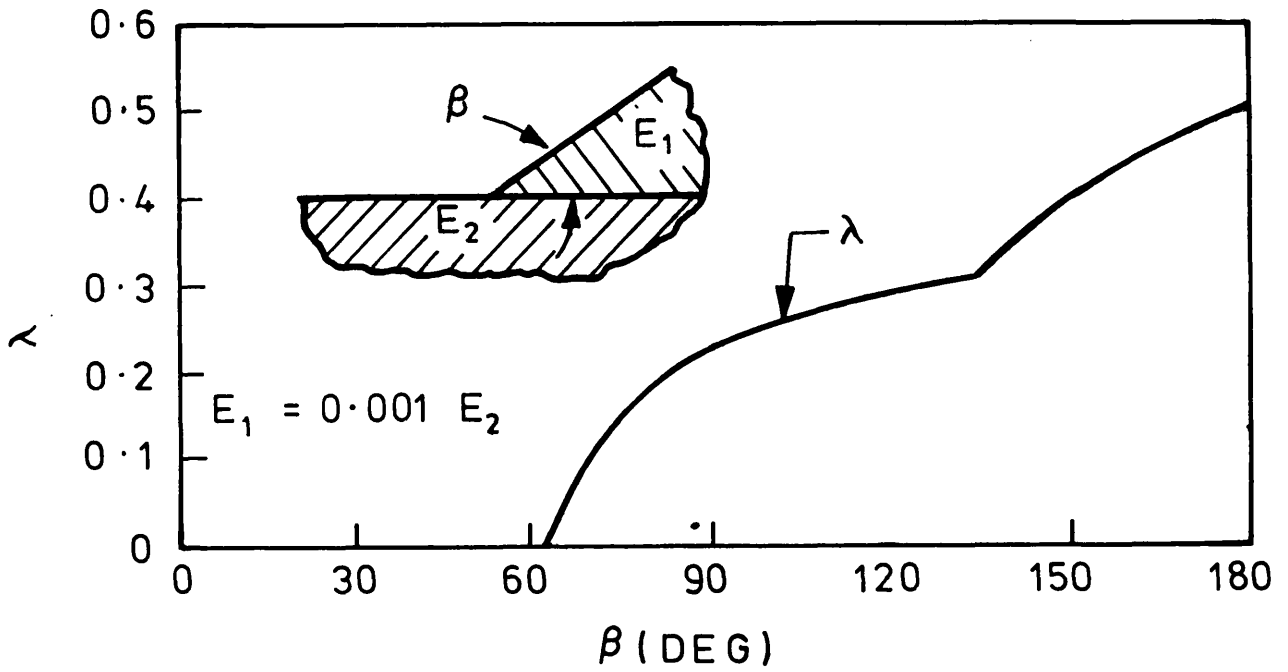
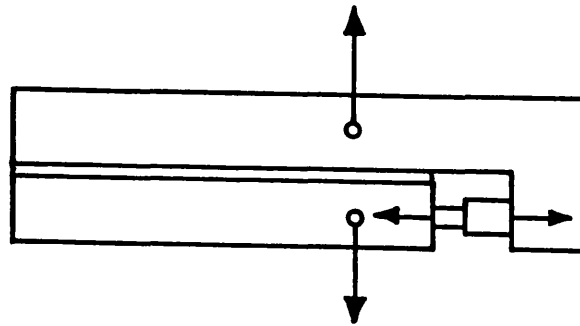
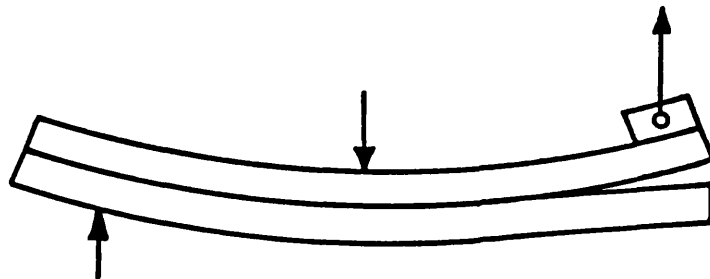


FIGURE 2.19 SINGULAR EIGENVALUES OF BIMATERIAL WEDGE⁸⁵



(a). INDEPENDENTLY LOADED MIXED-MODE SPECIMEN



(b). MIXED MODE FLEXURAL SPECIMEN

FIGURE 2.20 REPRESENTATIONS OF FRACTURE FAILURE IN BONDED STRUCTURES^{89,90}

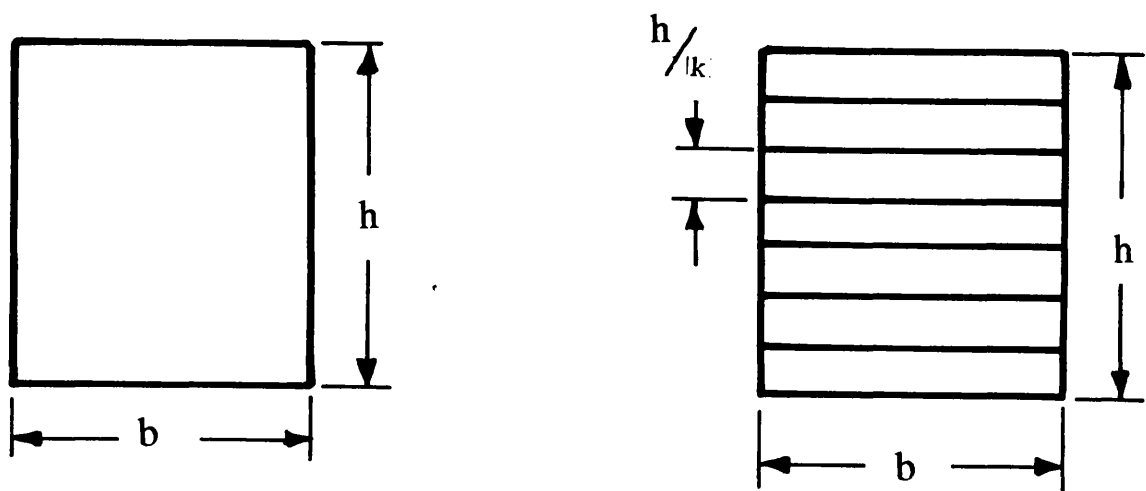


FIGURE 2.21 SOLID AND LAYERED SECTOINS OF A RECTANGULAR BEAM

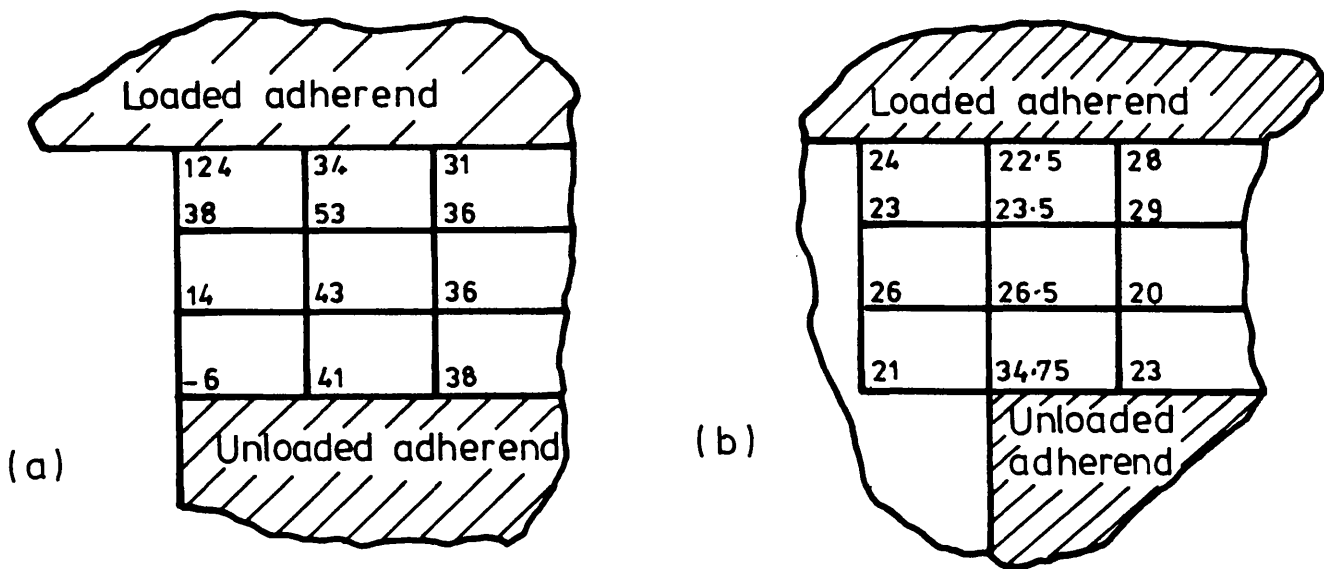


FIGURE 2.22 PRINCIPAL ADHESIVE STRESSES AROUND THE END OF LAP SHEAR JOINT⁶

- (a) Square -edge joint
- (b) Joint with full depth spew fillet

3. ADHESIVE SELECTION AND PROPERTIES

The adhesives tested were structural adhesives which are used in the aircraft and automotive industries. In these applications they are typically used for bonded structures, i.e. for skin-stringer bonds, sheet to sheet doubling and core-bonded (sandwich) components. Thus they are used for a wide range of metal and nonmetallic applications. Some of the adhesives examined in the current study are recent developments not yet applied in routine production. The following list shows the modified epoxy adhesives studied for bonding steel, listed according to their manufacturers' and trade name:-

Bostik Ltd	E5238
Ciba Geigy Plastics	Araldite 2007
Ciba Geigy Plastics	ALDS 748
Ciba Geigy Plastics	Redux 338A
Evode Ltd	Epoxy Weld 7168
Evode Ltd	Evo-Stick
Permabond Adhesives Ltd	ESP110

In addition the following two part cold curing epoxy adhesives were studied for bonding of the GRP to steel;

Ciba Geigy Plastics	Araldite 2005
Ciba Geigy Plastics	Araldite 2004
Permabond Adhesives Ltd	E32
Permabond Adhesives Ltd	E34
3M (UK) Ltd	9323
3M (UK) Ltd	1838

The adhesives were delivered by supplier as partially processed, in the form of adhesive paste. Film forms of 0.2mm thickness, for the steel to steel bonding were also considered. Table 3.1 shows characteristic adhesive data, manufacturers, and processing data.

The selection of a suitable candidate adhesive was based on an experimental programme using a laboratory technique for producing and testing adhesive bonds between mild steel components. The initial selection was based on short term destructive testing using small test specimens. For the bonding of steel/steel joints the initial selection criterion was the strength of the adhesive. In the case of the steel/GRP

joints, the strength was not the dominating factor due to the nature of the application in mind (Chapter 1). Following the short term selection procedures, a longer term test programme was used to verify the initial choice and evaluate the candidate adhesive further. The experimental programme and results are described and discussed below.

3.1. EXPERIMENTAL JIGS AND FIXTURES

Standardized techniques have been used to ensure adequate control and reliability for adhesive application and mixing, bonding, heat curing and testing methods. Many jigs and fixtures have been developed to suit the available testing machines and tests. Several assembly jigs and clamps were also designed to hold the adherends during the bonding process. These components were selected or manufactured from mild steel and include the following:

- Assembly jig for clamping tensile lap shear and butt test specimens as shown in Figure 3.1.
- Assembly jig for clamping shear impact test specimens as shown in Figure 3.2. This jig can also control adhesive thicknesses to 0.2, 0.5, 1.0 or 1.5mm in these specimens.
- A universal assembly jig for clamping various types steel/GRP specimens as shown in Figure 3.3.
- Loading yokes for axial cleavage test specimens, for use with the Instron testing machine as shown in Figure 3.4.
- Holder for shear impact test specimen for use with the Izod impact testing machine as shown in Figure 3.5.
- Stainless steel shackles, chains and dead weights to apply tension along a series of lap shear test specimens for site exposure.

3.2. PRODUCTION OF SPECIMENS

The steel adherends were cut from mild steel to BS 4360-43A grade and the GRP were produced from woven roving glass/polyester laminates (produced by Vosper Thornycroft Ltd to MoD standards) by milling and grinding to the correct dimensions. Several configurations of steel/steel test specimens were produced with modifications from ASTM and BSI standards. Figure 3.6 illustrates and categorizes the different test

specimens with their dimensions. For the steel/GRP specimens two groups of test specimens were formulated for testing. The first, which is shown in Figure 3.7, were used to select a candidate adhesive. The second group, which is shown in Figure 3.8, were used to study the properties and the bonding processes for the chosen candidate adhesive.

Steel and GRP surfaces were prepared by solvent (acetone) degreasing, grit blasting and further degreasing. Specimens were then placed under a stream of warm air for drying and then bonded within 2 hours. For long term wet environment testing, some steel specimens were additionally coated with a silane primer (SIP from Permabond Adhesives Ltd)). This primer coating was cured at room temperature for 7 hours before adhesive application (manufacturer's instructions).

Paste adhesives were applied to one surface using a dispensing gun and/or spatula with care to prevent air entrapment when closing the joints. In the case of the GRP specimens the two part adhesives were mixed to the proper ratio (Table 3.1) and applied to the GRP adherend to ensure good wetting of the GRP. Film form adhesives were cut to dimensions and placed on one surface. For the initial short term testing a thickness of 0.2 mm was applied. In further short term and longer term testing on candidate adhesives a thickness range of 0.05-1.50mm was considered. Thickness control was carried out by means of shims, spacers or wires.

The specimens were clamped in their assembly jigs with the required approximate clamping pressure. With paste form adhesives, only contact pressure was applied and for film form adhesives pressure up to 30 N/cm^2 were necessary for good wetting during the polymerisation process. The clamped assembly was then placed in an oven in the case of hot curing adhesives, according to the manufacturer's recommendations (Table 3.1). A typical heating and cooling cycle for a bonded joint is shown in Figure 3.9. Most hot cured adhesives require a temperature of approximately 180°C for 20-30 minutes. The temperature was measured by a thermocouple attached to the adherend. The curing time for the cold curing two part adhesive was for a maximum of 48 hours at room temperature (which can generally be reduced to 1 to 2 hours by warm curing at 60°C).

After curing of the joint excess adhesive was then removed from around the bonded joints by using cutting tools and/or files. Some lap shear test specimens however have their adhesive squeeze-out (spew) machined carefully to produce a 45° fillet with a

1.5mm leg at both ends of the joint.

3.3. TESTS FOR ALL ADHESIVES

The initial test programme included seven types of adhesives for steel/steel bonding in order to select a candidate adhesive(s) for further testing and also to examine some bonding process variables such as the effect of spew fillets, reliability of bonding in laboratory conditions and the effect of adhesive thickness.

Initially, for each type of adhesive used, three tensile lap shear, tensile butt and tensile cleavage specimens (Types 1, 2 and 3 respectively-Figure 3.6) were considered for testing on a 250kN Instron testing machine at room temperature, with a crosshead speed of 0.5mm/min (quasi-static). Figure 3.10 shows a lap shear joint installed on the testing machine. The maximum applied load at joint failure was recorded. The average strength was calculated by dividing the maximum applied load by the bonded joint area.

Type 5 shear impact test specimens were tested on an Avery impact testing machine utilising the Izod set-up at room temperature. Energy absorption/resistance at joint failure was recorded and the average resistance to impact has been calculated by dividing energy absorbed by the bonded area.

Type 5 test specimens were also used to examine adhesive gap filling capabilities. In this, predetermined gaps up to 1.5mm could be obtained in the joint by using a specially designed jig (Figure 3.2). The adhesive had to be able to retain thixotropy during the hot curing time inside the oven, otherwise it would flow out leaving a thinner adhesive line. Adhesive line thickness was measured by an optical microscopic measurement after cleaning of the joint.

Type 4 cleavage test specimens were also loaded on the Instron testing machine to about 70% of the failure load obtained from testing Type 3 cleavage test specimens. The crosshead of the testing machine was then stopped and the brass bolt within the joint was tightened to lock the joint under the sustained load. The self loaded specimens were then removed from the testing machine and continuously immersed in salt water for 1000 hours at room temperature. Figure 3.11 shows features of self loaded cleavage specimen with the preloading bolt. The specimens were subsequently retested to failure in air to measure the residual strength/strength degradation as a result of the immersion.

For the steel/GRP bonding seven cold-curing, structural epoxy adhesives were selected for the preliminary series of small scale mechanical tests. These were double

strap shear, three point bending cleavage and shear impact (steel/GRP) specimens (Types 6, 7 and 5 respectively-as shown in Figure 3.7). Two specimens for each type were used to test each of the seven adhesives. The testing was carried out on the Instron and Avery testing machines, in the same manner and conditions described for the previous types of steel/steel specimens (Types 1, 2, 3,4 and 5). This series of tests was then followed by a second series based on the joint configurations which are shown in Figure 3.8. These included steel/steel joints of shear, butt and cleavage specimens (Types 1,2 and 3). In addition, these types have the combinations of steel/GRP and GRP/GRP test specimens. This second series were used to test only one type of cold curing adhesive (Araldite 2004) as will be discussed, in the light of the tests results in the following section.

3.3.1. COMPARATIVE RESULTS

Table 3.2 contains the basic experimental results for the bonding of steel/steel specimens with hot curing structural adhesives. It should be noticed that some particular tests on some adhesives were omitted. This is due the relatively low initial strength results which rendered further experimental work of little value. Among the seven types of adhesives tested initially it is clear that both ESP110 and Araldite 2007 exhibited good static strength properties, shear impact resistance and short term durability in a corrosive environment.

Significant differences in shear strength values were observed and the maximum average difference when comparing Araldite 2007 and ALDS 748 is about 186% in the favour of the former. This result may be due to poor wetting in the film adhesive. The minimum average difference when comparing Araldite 2007 and ESP 110 was about 8% in favour of the former.

The average tensile test strength in butt joints (Type 2) was approximately 5.1, 4.4 and 3.4 times the average strength in the cleavage joints (Type 3) for ESP110, Araldite 2007 and E5238 adhesives respectively. This appears to be due to significant differences in the value of Young's modulus, which consequently influences the stress concentration factors in the edge loading joint (cleavage specimen).

There was a scatter in the symmetric tensile strength values from a maximum of 96 N/mm² to 7N/mm². This may due to the high sensitivity of the butt joint to the inherent misalignment of most standard tensile machines (referred to in Chapter 2).

The change of surface topography of the reusable specimens can lead to adhesive thickness variation and therefore this would further, contribute to the problem of the misalignment of the butt joints.

Table 3.2 shows that some shear strength values are higher than those specified by the adhesive manufacturers. This may be because a thicker adherend has been used compared to the one usually specified for standard adhesive testing (1mm sheet thickness). However higher results are not observed for film form adhesives since it appears to be difficult to obtain good wetting on the relatively rough steel surface.

From the results of these initial tests, as well as its good gap filling capabilities (to 1.5mm adhesive thickness), Araldite 2007 epoxy adhesive was selected for a further and more extensive test programme .

The comparative results for the performances of Types 5, 6 and 7 steel/GRP test specimens are presented in Table 3.3. Although all the candidates performed well, Araldite 2004 was selected for the remainder of the steel/GRP experimental programme because it provides a satisfactory combination of strength and temperature resistance (this will be discussed in relation to the fire testing results in Chapter 6) with potentially significant durability in the wet environment (from communication with the adhesive manufacturer). Also, results comparing the average strength properties for Types 1,2 and 3 specimens with three adherends combinations (steel/steel, steel/GRP and GRP/GRP-Figure 3.8) bonded with Araldite adhesive 2004 are presented in Table 3.4. It is clear from these results that the GRP/GRP bond is substantially weaker than steel/GRP which is itself significantly weaker than the equivalent steel/steel joint. Further discussion on this topic will be presented in Chapter 7.

It should be noted here that the strength of a steel/steel joint bonded with a hot curing adhesive (Araldite 2007) is considerably higher than that obtained with a cold curing adhesive (Araldite 2004). This may be due to the good wetting of adhesive to the adherends(lower viscosity at elevated temperature)and high density of the cross linking (polymerisation) resulted from the hot curing process.

3.3.2. EFFECT OF SPOW FILLETS

Spew fillets produced from the squeeze-out of an adhesive in joints provide additional strength, as well as environmental sealing advantage. The strength advantage depends on the size of the specimen as well as the type of adhesive. To investigate this

five filleted lap shear specimens were compared with non-filleted samples from a strength point of view. All these specimens were bonded at the same time using Araldite 2007 with an adhesive line thickness of 0.5 mm. The fillet leg length of 1.5 mm was achieved by machining the fillet after bonding. The results from the static loading tests are shown in Figure 3.12. From these results it may be seen that an increase of approximately 10% in the failure strength was observed in the filleted joints. This increase may be explained by an effective increase in the joint length of the same order. A similar effect was obtained on the strength of steel/GRP lap shear joints from spew fillets of Araldite 2004.

3.3.3. EFFECT OF ADHESIVE THICKNESS

To examine the implications of adhesive thickness on joint strength, Type 5 shear impact specimens were used. In this case the adhesive thickness was controlled in the range from 0.05 to 1.5mm. The results of these tests are shown in Figure 3.13 and Table 3.5. From these tests, the effect of thickness is clearly visible as a progressive decline in impact strength with increasing thickness approximately 25% reduction in the strength across the thickness range was observed. It was however difficult to obtain reliable thickness control on the lowest range.

3.3.4. RELIABILITY OF BONDING PROCESSES

In order to measure the coefficient of variation (COV) which represents a percentage measure of the scatter in the data of failure load of the non-filleted lap shear specimens, the following statistical equation may be used⁵⁷:-

$$COV = 100 \frac{S}{\bar{X}}$$

$$S = \left[\frac{\sum (X - \bar{X})^2}{n - 1} \right]^{\frac{1}{2}}$$

$$\bar{X} = \frac{\sum X}{n}$$

Where:

X is a non-dimensional measure which represents the failure load of each specimen

\bar{X} is a nondimensional measure representing the average failure load of all tested specimens

S represents a statistical distribution function

n is the number of specimens

Therefore from load values of non-filletted specimens Figure 3.12) the following results are obtained:-

$$\chi = 17.07$$

$$S = 0.5413$$

Thus

$$COV = 3.2\%$$

In the case of the tests on the 5 steel/GRP lap shear specimens bonded with Araldite 2004 the COV was found to be 6.8%.

3.4. PROPERTIES OF THE CANDIDATE ADHESIVES

The choice of epoxy adhesive Araldite 2007 and Araldite 2004 for bonding steel/steel and steel/GRP respectively, necessitated further small scale experiments to obtain average elastic properties and to examine durability aspects order to asses some design requirements which for the relevant bonded constructions in mind. These experiments, their results and discussions are presented in the following sub-sections.

3.4.1. MODULUS OF ELASTICITY

Elastic strain was measured in a butt joint adhesive line thickness of 0.45 mm. A displacement transducer placed across the tensile butt joint allowed load as a function of elongation to be deduced. A typical plot is shown in Figure 3.14. Results from three tests are shown in Table 3.6 for total axial elongation at a load of 25 kN. From consideration of equilibrium and Hook's law based on testing a butt joint in which the the gauge length (29mm) includes both steel and adhesive parts, the following equation may be used:-

$$\delta_z = \frac{\sigma}{E_1} L_g + \frac{\sigma}{E_3} \cdot T_3$$

Where

δ_z is the total elongation of the joint within the gauge length

L_g is the gauge length of the joint

T_3 is the thickness of the adhesive

σ is the axial tensile stress along the joint

E_1 is the modulus of elasticity of the adherend

E_3 is the modulus of elasticity (apparent) of the adhesive

Given $\delta_z = 0.0092$ mm (Table 3.6), $L_g = 28.5$ mm, $T_3 = 0.45$ mm, $\sigma = 45$ N/mm²

and $E_1 = 210 \times 10^3$ N/mm²

Thus $E_3 = 4700$ N/mm²

The modulus values used for analysis purposes obtained from experiment and above equation were approximately 5000 N/mm² for Araldite 2007 (average from three tests) and 4000 N/mm² for Araldite 2004.

3.4.2. LONGER TERM DURABILITY IN SEAWATER ENVIRONMENT

Three test specimens for each of type (a total of 12 specimens-Types 1, 3, 4 and 5- Figure 3.6) were prepared having their bond surfaces initially primed with a silane. In all cases the spew fillets were left in place. These specimens were then immersed without any further protection in a bath of synthetic seawater at room temperature for 28 months. These specimens were then tested in the same manner as the earlier batch of dry specimens discussed in Section 3.3. In this latter case, all specimens were tested in the wet condition. The result of each group of three specimen tests are compared in Figure 3.15 with those of the three original dry specimens for each type of loading. In all cases a small loss of strength can be observed. Strength losses of 15-17% were found for the tensile lap shear and unloaded cleavage specimens while only 8-10% losses were observed in the preloaded cleavage and shear impact specimens.

In the case of the steel/GRP bond with Araldite 2004, three double strap lap shear specimens (Type 6- Figure 3.7) were continuously immersed in seawater without surface protection. After 18 months these specimens were tested in wet conditions under static loading. The results from these experiments are compared in Figure 3.16 with those of three original dry specimens. A loss in strength of 12% may be observed from the figure. Examination of failure surfaces of the specimen (double strap lap shear joint), shown in Figure 3.17, indicated no sign of corrosion to the naked eye (the surfaces were wet at the boundaries due to contact with contaminated water during handling).

In addition, in August 1989, eight tensile lap shear specimens were modified so that they could be strung together with stainless steel shackles to form a chain tensioned

by a heavy weight to approximately 10% of failure static load, as shown in Figure 3.18. This chain was designed so that failure of any one bonded 'link' will not influence the remaining individual specimens. Four specimens were bonded with silane while the remainder did not receive the silane treatment. All samples were fully coated with an epoxy paint system to eliminate metal corrosion of the adherends. The chain was suspended from a pier in the inter tidal range of the lower Clyde estuary where it is subject to the additional loads of wave and currents. Twenty months later, the specimens were retrieved from the water for inspection. The retrieved specimens are shown in Figure 3.19. It was found that none of the eight specimens suffered any visible bond failure, however there were limited signs of external metal corrosion for all the specimens. Two specimens were removed out of the chain and replaced by identical ones. The removed specimens then, were tested to destruction in the laboratory, one was in the wet condition and the other in the dry condition. The drop in the strength of these joints again, was limited to approximately 10%. In addition there was no noticeable difference in the failure strength between the dry and wet test conditions. The chain of samples has been deployed for further continuous immersion and future assessments.

3.4.3. BONDING PROCESSES FOR STEEL/GRP JOINTS

The use of a peel ply to provide an alternative to surface roughening of the GRP by abrasion or gritblasting was investigated using Type 1 lap shear specimens. The results of these tests are shown in Figure 3.20. The strength of joints (average from three specimens) with the peel ply application is approximately 15% higher than joints with mechanically roughened GRP surfaces. This may be due to the absence of fibre damage as well as a more uniform surface topography.

The inherent problems of voids included within adhesive joints and the limited pot-life of the two-part adhesive can produce reliability problems, even in laboratory environments, when manual metering and mixing is involved. These problems are significantly greater in a production environment. The effect of using automated dispensing equipment has been examined therefore using a dispensing machine comprising two component meters and static mixture facility. Three lap shear joints were used for this investigation and the results of failure load are included on Figure 3.20 for comparison. The results indicate an increase in joint strength, (about 15%) reflecting a more consistent adhesive mixture with fewer voids and presumably a more uniform cure.

3.4.4. SHORT TERM ELEVATED TEMPERATURE STRENGTH

For this study several tensile lap shear specimens were bonded using Araldite 2007 with an adhesive thickness of 0.5 mm. The specimens were loaded on the Instron testing machine equipped with a heating chamber. Prior to loading, thermal equilibrium was ensured by enclosing the joint assembly within the oven for 30 minutes at the required temperature. The loading was then applied at a crosshead speed of 0.5 mm/min. Table 3.7 shows test results and the average shear strength values derived are also plotted as a function of temperature in Figure 3.21. These results indicate the dramatic overall reduction in strength that occurs as the temperature increases towards the glass transition temperature (T_g), which is approximately 120°C for this adhesive. Beyond 160°C only marginal strength remains until the char temperature of 250°C is reached, at which point the adhesive starts to carbonise.

3.4.5. CREEP RESISTANCE AT ELEVATED TEMPERATURES

Specially designed thick adherend lap shear joints, with steel/steel and steel/GRP adherends were produced to suit an existing creep testing rig used for this investigation. Figure 3.22 shows details of these lap shear specimens. In this test the resistance to application of sustained tensile shear force was measured over a wide range of temperatures. The creep testing rig was equipped with thermostatically controlled heating furnace and timer. The sustained forces were applied by suspended weights through lever mechanisms. Thermal equilibrium for each test specimen was first ensured inside the heating furnace before the force application. Total time to specimen failure was recorded. Table 3.8 shows test results for the epoxy adhesives Araldite 2007 (steel/steel) and Araldite 2004 (steel/steel and steel/GRP). From Tables 3.7 and 3.8 it can be noted that for a given elevated temperature and load, resistance to long term stress (sustained force) is significantly lower than that for short term stress. For example, at a temperature of 100°C the lap shear joint can fail at a stress which is one fourth the short term strength of the same joint, after 3 hours of load application. This degradation in strength is due to the viscoelastic behaviour of polymeric materials and their time dependent components when subject to continuous stress. It can be noted that at a temperature of 200°C, the time to joint failure in the case of the Araldite 2004 -

(steel/steel) is higher than that in the case of Araldite 2007 despite the opposite trend in their relative strengths at lower temperatures. This in turn suggests that the decomposition/char temperature for the Araldite 2004 is higher than that for Araldite 2007. This is a desirable characteristic in fire related applications for adhesives.

Examination of failure surfaces indicates that failure appears to initiate at the interface between the adhesive and steel for both steel/steel and steel/GRP specimens .

In addition to time to failure measurement, deflection was also measured against time in some cases. The temperature/loading for these samples were 130°C at 3% of maximum shear stress and 80°C at 25% of maximum shear stress. For this purpose linear transducers with a data acquisition/logging system for creep deflection measurement were used. Creep deflection measured the shear deformation of the adhesive line with a nominal thickness of 1.0mm and overlap length of 15mm. Figures 3.23 and 3.24 illustrate the creep deflection curves for these cases (above and below T_g respectively). In the case of the specimen maintained at 130°C (Figure 3.23) it is clear that at even very low stress levels failure will occur in a matter of hours (Table 3.8). However, in the 80°C case the specimen continued to creep at a slow, but in approximately linear logarithmic rate (secondary creep) for the first 500 hours, following 1.5 hours of delay (primary creep) period.

Prediction of creep deflection within the logarithmic stage of the creep deflection-time curve for 80°C (Figure 2.12) may be performed by applying a theory based on a linear secondary creep relationship⁵⁵. The assumptions are that the applied load L and the delay time t_d is approximately linear, and that, the gradient K_c is related linearly to the applied load F . Thus this theoretical relationship may be written as follows:-

$$K = \frac{\gamma}{\ln t - \ln t_d}$$

and also

$$F = A \ln K$$

$$B = F \ln t_d$$

Where A and B are constants which may be assumed proportional to the level of the applied load. Thus, for example, for a load level of 20% of maximum ambient temperature failure load (stress), the time, t , to reach specific deflection may be calculated as follows;

From the idealised line indicated on Figure 3.24 at, the linear creep deflection of 400 micron (Actual creep deflection of 300 micron) the values of $t_d = 1.5$ hour and $t = 400$ hour. Constants of A and B are the same for the two cases of loading and the

predicted delay time for the case of 20% loading will be

$$\ln t_d = (25/20) \ln 1.5$$

$$= 0.507 \text{ (ie delay time of 1.7 hours)}$$

and

$$\ln t - 0.507 = (25/20) \ln 300$$

Thus

$$\ln t = 7.637 \text{ and}$$

$$t = \underline{2073} \text{ hours}$$

From these theoretical results it can be seen that a significant improvement in exposure life (eight times) can be achieved by small load reduction (5%) for a given temperature. The above results require large number of experiments in order to be regarded as conclusive. There were considerable difficulties in carrying out such experimental work due to sensitive parameters of temperature control and very small deflection measurements.

MANUFACTURER	TRADE NAME	GLASS TRANS.			RECOMMENDED CURING CONDITIONS		
		FORM	TEMPERATURE	1 OR 2 PART	CURE TEMP.	PRESSURE	TIME
			[oC]		[oC]	[N/cm2]	[Hour]
Permabond	ESP110	Paste	150	1	180	5	0.5
Adhesives Ltd	E32	Paste	50	2	20	5	48
	E34	Paste	90	2	20	5	24
Ciba Geigy	Araldite 2007	Paste	120	1	180	5	0.5
Plastics	ALDS 746	Film	80	1	180	30	0.5
	Redux 338A	Film	80	1	170	30	1
	Araldite 2004	Paste	80	2	20	5	24
	Araldite 2005	Paste	50	2	20	5	48
Bostik Ltd	E5238	Paste	120	1	190	5	0.5
Evode Ltd	Epoxyweld 7168	Paste	120	1	160	5	0.5
	Evo-stick	Paste	50	2	20	5	48
3M(UK) Ltd	9323	Paste	50	2	20	5	48
	1838	Paste	50	2	20	5	48

TABLE 3.1 PROCESSING PROPERTIES OF ADHESIVES FOR BONDING STEEL TO STEEL

Adhesive	Specimen No.	Shear (Type 1)		Butt (Type 2)		Cleavage (Type 3)			Cleavage (Type 4) **			Impact (Type 5)		Max. gap filling (Type 5) [mm]
		Load [kN]	Stress* [N/mm ²]	Load [kN]	Stress [N/mm ²]	Load [kN]	Stress [N/mm ²]		Load [kN]	Residual strength [%]		Energy [J]	Energy/Area* [J/cm ²]	
E5238	1	15	40	32.3	51.7	10	16		6.8	100		43.4	7	
	2	15.5	41.3	32.5	52	9.5	15.2		6.8	100		42	6.7	
	3	15	40	31.5	50	8.9	14.3		6.8	100		40.7	5.5	
ESP110	1	17	45	50	80	10	16		7	100		57	9.1	0.5
	2	16.5	44	51.3	82.1	11.3	18.1		7	100		51.5	8.2	0.3
	3	16.9	45	53	84.8	8.8	14.1		7	100		42	7.8	0.5
ARALDITE 2007	1	18	48	60	96	12	19.2		8.2	100		54	8.6	1.5
	2	17.8	47.5	54	86.4	12.2	19.5		8.2	100		53	8.5	1.5
	3	18.8	50.1	48	76.8	11	17.6		8.2	100		51.5	8.2	1.5
ALDS748	1	6.4	17			3.5	5.6							
	2	6.3	16.8			3.2	5.1							
	3	6.3	26.8			3.6	5.8							
REDUX 338A	1	11.25	30			4.2	6.72							
	2	11.4	30.4			4.1	6.6							
	3	11.5	30.7			3.8	6.1							
EPOXY-WELD 7168	1	11.1	29.6	32	51.7							38	6.1	
	2	11	29.4	34	54.4							38	6.1	
	3	11.1	29.6	30	48							37	5.9	
EVO-STICK (2 PART)	1	7.6	20.3			4.7	7.5							
	2	7	18.7			5.1	8.2							
	3	8.5	22.7			4.8	7.7							

* Average stress or absorbed energy per unit area are obtained from dividing applied load or energy at failure by bond area
** Joints are preloaded by means of bolt and immersed in saltwater for 1000 hrs before testing to destruction

TABLE 3.2 PROPERTIES OF ADHESIVES FOR BONDING STEEL TO STEEL

Type	Supplier	Impact Energy [J]		Cleavage Force [kN]		Shear Force [kN]	
		1st	2nd	1st	2nd	1st	2nd
Araldite 2005	Ciba Geigy	37	38	3.7	3.7	34.0	34.0
Araldite 2004	Ciba Geigy	24	23	2.8	2.7	30.0	29.5
E32	Permabond	31	32	3.8	3.8	36.5	37.0
E34	Permabond	19	19	2.8	2.8	17.0	16.0
9323	3M	27	29	3.5	3.8	35.0	34.0
1838	3M	27	27	3.7	3.8	30.0	29.0

TABLE 3.3 COMPARATIVE PERFORMANCES OF TWO PART EPOXY ADHESIVES

Combination	Specimen No.	Shear Strength		Tensile Strength		Cleavage Strength	
		F[kN]	$\bar{\tau}$ [N/mm ²]	F[kN]	$\bar{\sigma}$ [N/mm ²]	F[kN]	$\bar{\sigma}$ [N/mm ²]
steel/steel	1	13.0	35.0	21.3	34.0	5.2	8.3
	2	12.5	33.0	20.0	32.0	5.1	8.2
	3	12.6	34.0	20.0	32.0	5.2	8.3
steel/GRP	1	4.9	13.0	9.6	15.4	2.9	4.7
	2	4.8	12.8	10.0	16.0	2.5	4.0
	3	5.0	13.3	8.9	14.3	2.4	3.9
GRP/GRP	1	3.5	9.3	4.9	7.8	2.0	3.4
	2	3.6	9.6	5.0	8.0	2.3	3.7
	3	3.5	9.6	5.2	8.3	2.1	3.4

TABLE 3.4 STRENGTH PROPERTIES FOR ARALEDITE -2004 EPOXY ADHESIVE

Thickness [mm]	Specimen No.	Impact energy* [J]	Energy/Area [J/cm2]	Mean energy/Area [J/cm2]
0.05**	1	60	9.6	9.6
	2			
	3			
0.2	1	54	8.65	8.6
	2	53	8.5	
	3	53	8.5	
0.5	1	52	8.3	8.1
	2	50	8	
	3	50	8	
1	1	47	7.5	6.8
	2	40	6.4	
	3	40	6.4	
1.5	1	43	6.9	6.6
	2	40	6.4	
	3	40	6.4	

* Tested at room temperature

** Difficult to achieve

TABLE 3.5 IMPACT RESISTANCE FOR VARIOUS ADHESIVE THICKNESSES
(ARALDITE 2007)

Adhesive	Specimen No	Applied load [kN]	Tensile stress [N/mm2]	Total gauge length* [mm]	Total axial elongation [mm]	Modulus of elasticity [N/mm2]
Araldite 2007	1	25	40	29	0.0102	3750
	2	25	40	29	0.0092	4700
	3	25	40	29	0.0085	6300
Araldite 2004	1	20	32	29	0.008	4700
	2	20	32	29	0.0095	3200

* Total gauge length=29mm (including 0.45mm adhesive thickness)

TABLE 3.6 TEST RESULTS OF TENSILE BUTT SPECIMENS

Temperature [C]	Specimen No.	Applied load [kN]	Shear stress [N/mm ²]	Mean stress [N/mm ²]	% Ultimate stress [%]
18	1	17.6	47	47.2	100
	2	17.6	47		
	3	18	48		
50	1	16.1	43	41.2	87
	2	15.4	41		
	3	14.8	39.5		
80	1	12.9	34.5	34	72
	2	12.2	32.5		
	3	13.1	35		
100	1	10.9	29	25	53
	2	9.4	25		
	3	7.5	20		
120	1	3.2	8.5	15.1	32
	2	7.2	19		
	3	6.7	17.8		
160	1	0.7	1.8	2.4	5
	2	0.9	2.4		
	3	1.1	3		
200	1	0.8	2.2	1.6	3
	2	0.4	1		
	3	0.6	1.5		

**TABLE 3.7 SHORT TERM FAILURE SHEAR STRESS AT ELEVATED TEMPERATURES
(ARALDITE 2007)**

Adhesive	Material combination	Elevated temperature [C]	Sustained applied load [N]	Average shear stress [N/mm ²]	Room temp. shear strength [N/mm ²]	%Shear stress at room temp [%]	Time to joint failure [hrs]
Araldite 2007	steel/steel	80	5000	13.3	47	28.6	>2000(D)
	steel/steel	80	5000	13.3	47	28.6	500
	steel/steel	80	3000	8	47	17	>5000 (D)
	steel/steel	80	2500	6.7	47	14.2	>5000 (D)
	steel/steel	90	3000	8	47	17	>100(D)
	steel/steel	90	3000	8	47	17	>100(D)
	steel/steel	100	2500	6.7	47	17	3
	steel/steel	100	2500	6.7	47	14.2	3
	steel/steel	100	2500	6.7	47	14.2	15
	steel/steel	110	3000	8	47	17	83
	steel/steel	110	1000	2.7	47	5.7	5
	steel/steel	120	1000	2.7	47	5.7	0.7
	steel/steel	120	3500	9.3	47	19.7	0.1
	steel/steel	130	1000	2.7	47	5.7	0.2
	steel/steel	130	2000	5.4	47	11.4	0.2
	steel/steel	165	400	1.1	47	2.3	96
	steel/steel	200	400	1.1	47	2.3	9
Araldite 2004	steel/steel	200	400	1.1	34	3	2640
	steel/steel	200	800	1.3	34	4	16
	steel/steel	250	400	1.1	34	3	0
	steel/GRP	100	300	0.9	17	2	>2000(D)
	steel/GRP	150	200	0.5	17	1	3
	steel/GRP	155	200	0.5	17	1	1.5
	steel/GRP	200	100	0.3	17	0.5	330
	steel/GRP	203	100	0.3	17	0.5	20

TABLE 3.8 CREEP RESISTANCE OF LAP SHEAR JOINTS AT ELEVATED TEMPERATURES

D: Test discontinued

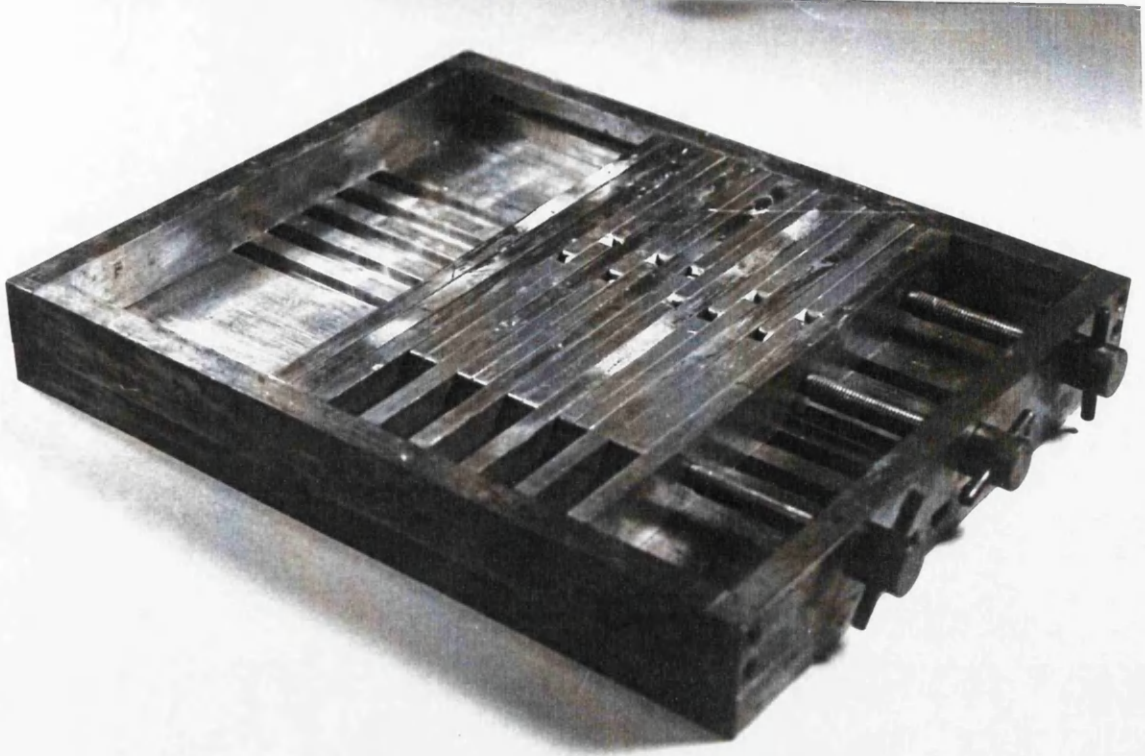


FIGURE 3.1 ASSEMBLY JIG FOR LAP SHEAR SPECIMENS

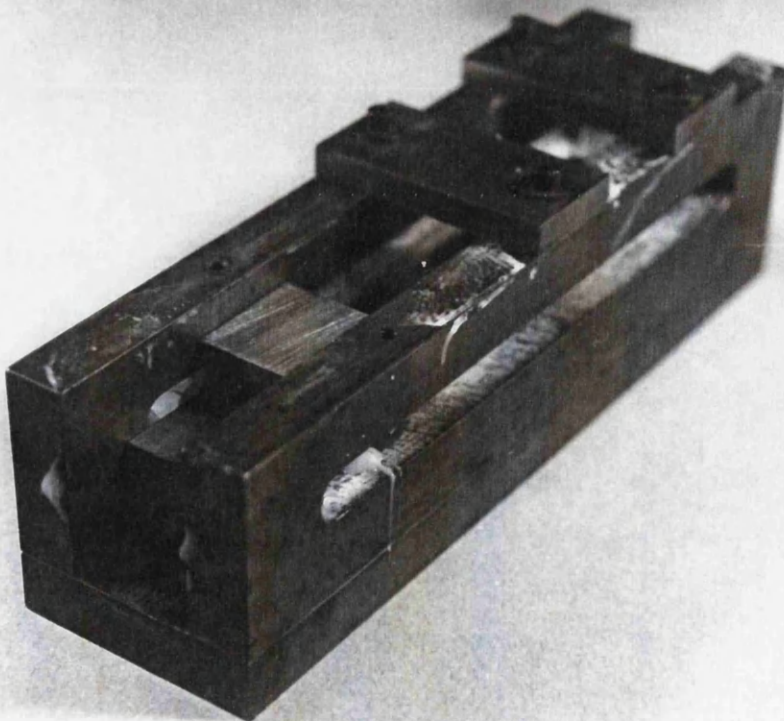


FIGURE 3.2 ASSEMBLY JIG FOR STANDARD IMPACT SPECIMENS



FIGURE 3.3 ASSEMBLY JIG FOR SMALL STEEL/GRP SPECIMENS

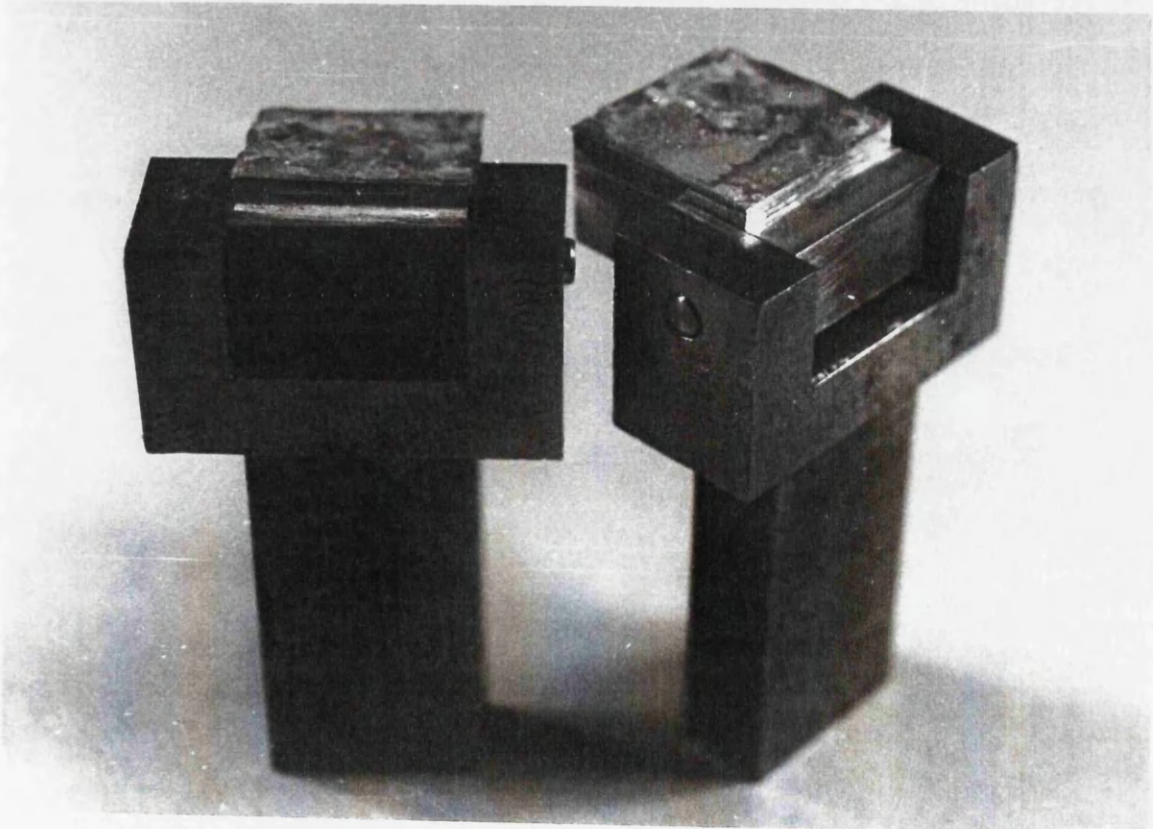


FIGURE 3.4 LOADING YOKES FOR TENSILE CLEAVAGE SPECIMEN

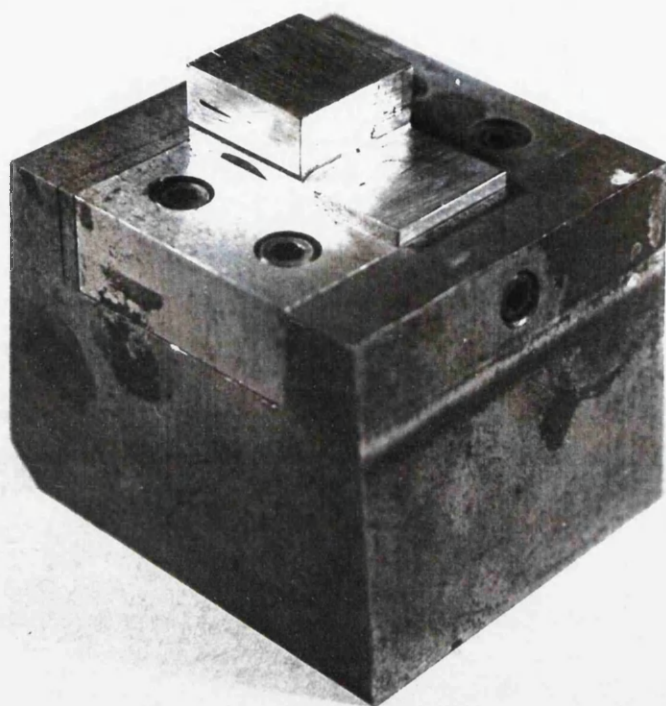


FIGURE 3.5 HOLDER FOR SHEAR IMPACT SPECIMEN

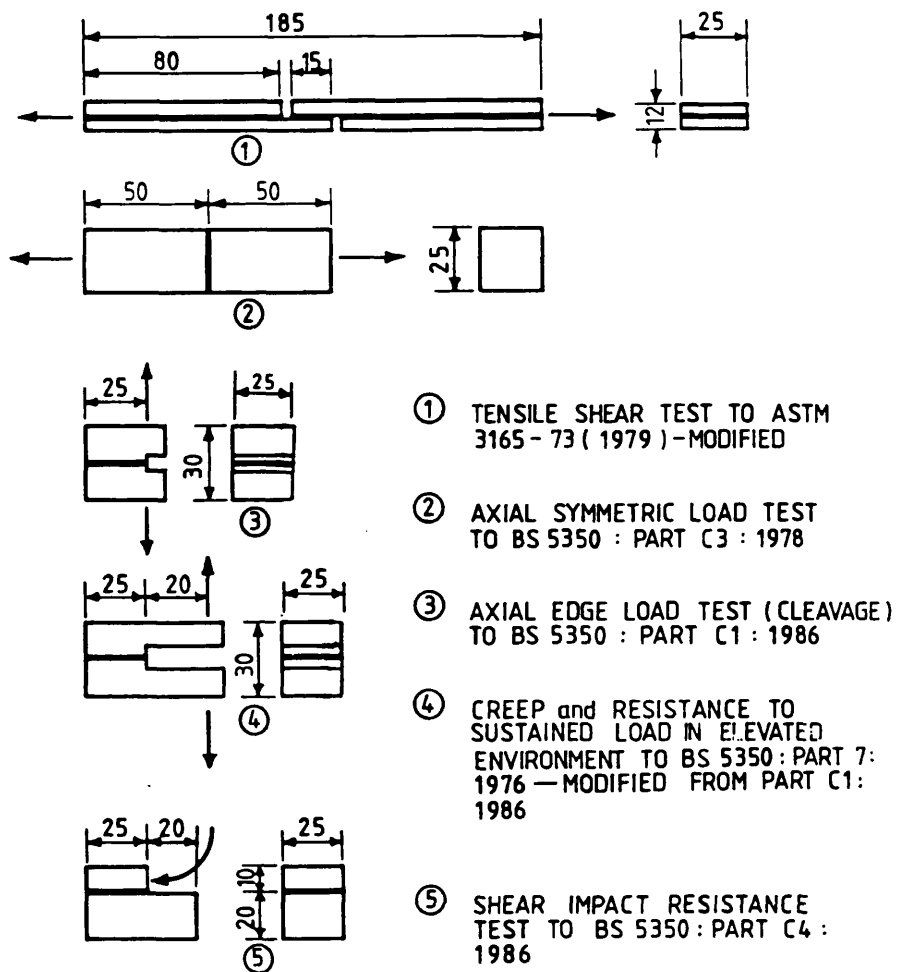
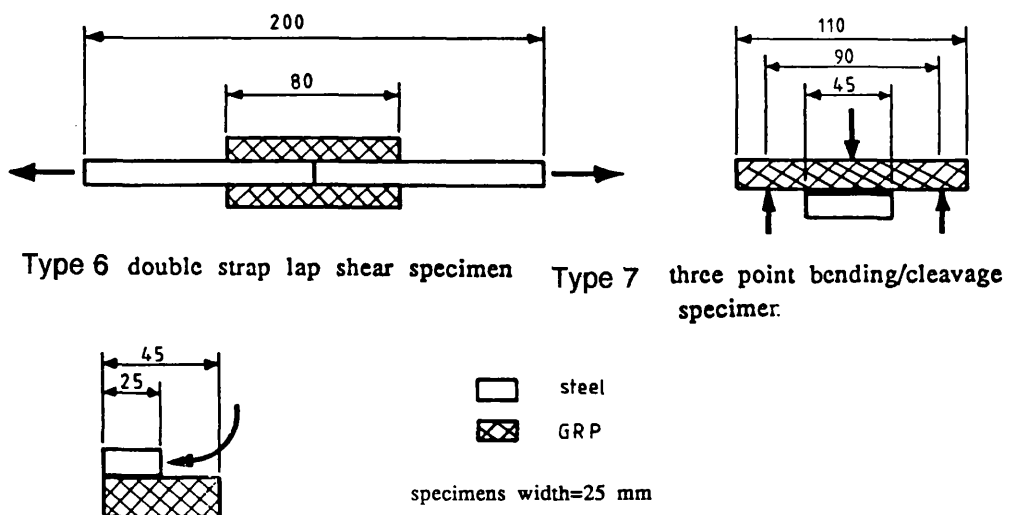


FIGURE 3.6 SMALL STEEL/STEEL TEST SPECIMENS



Type 5 shear impact specimen (modified from BS5350-C4/1986)

FIGURE 3.7 SMALL STEEL/GRP TEST SPECIMENS

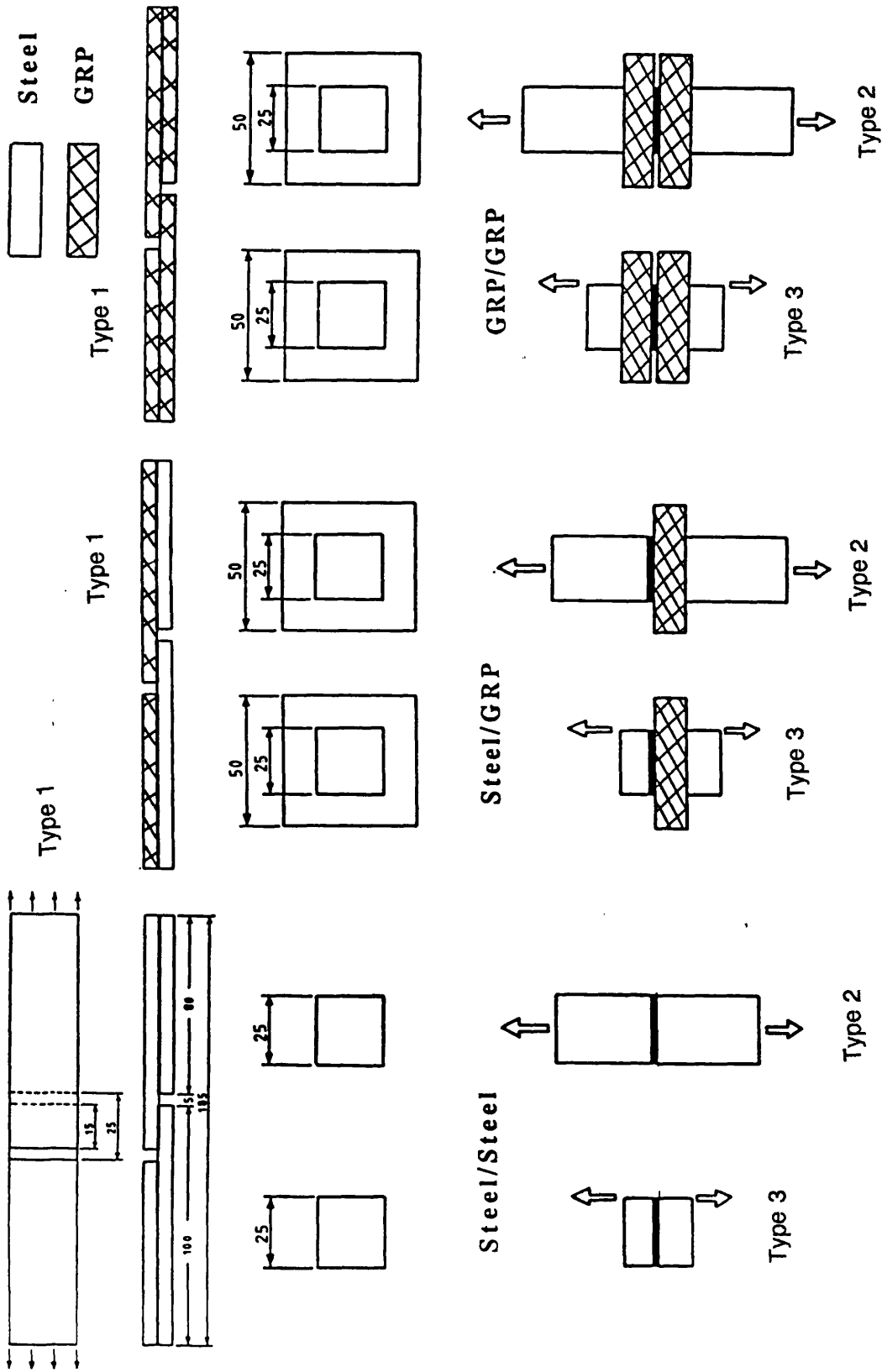


FIGURE 3.8 SMALL TEST SPECIMENS - VARIOUS MATERIALS COMBINATIONS

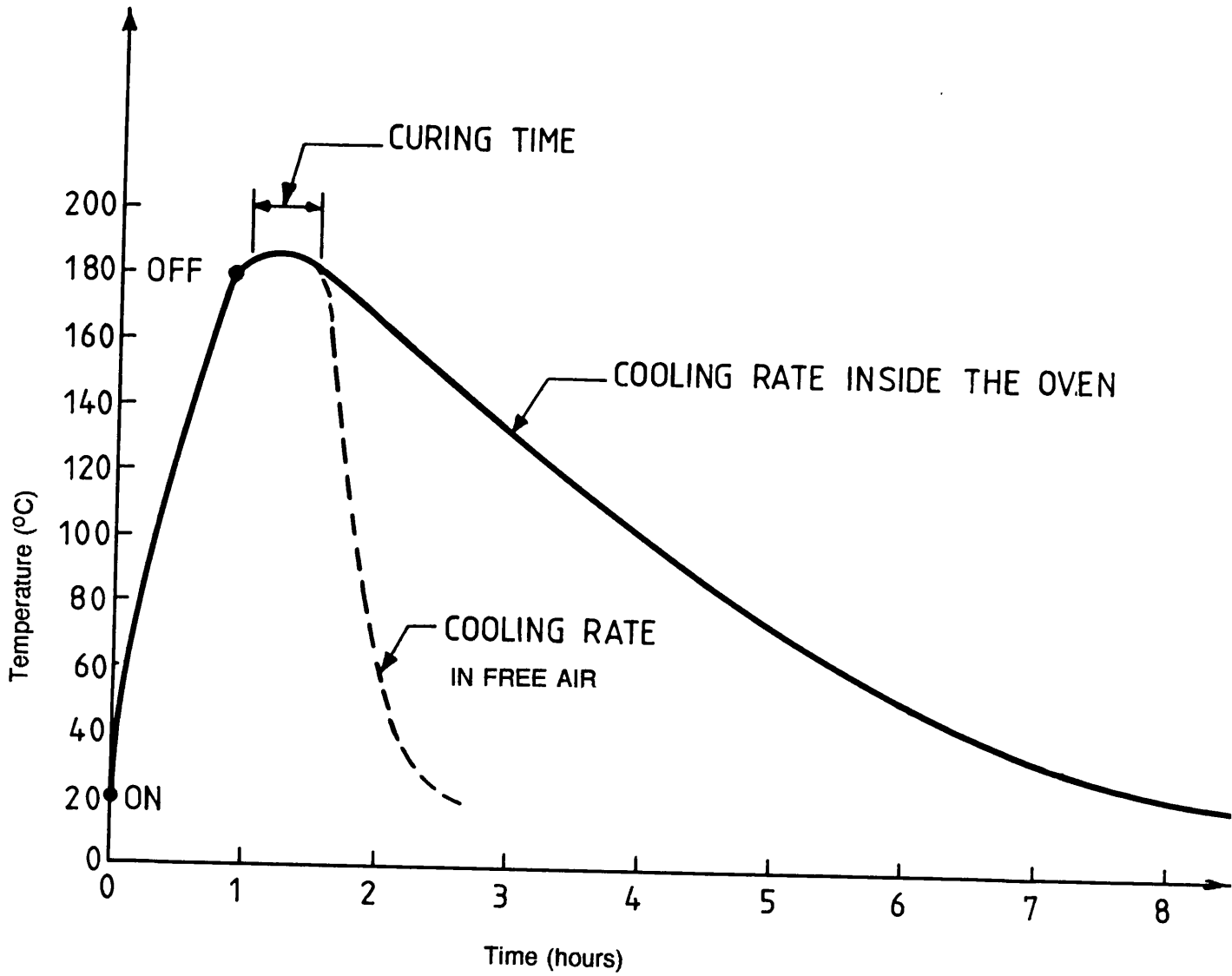


FIGURE 3.9 HEAT CURING CYCLE OF A SMALL ADHESIVE JOINT (ARALDITE 2007)

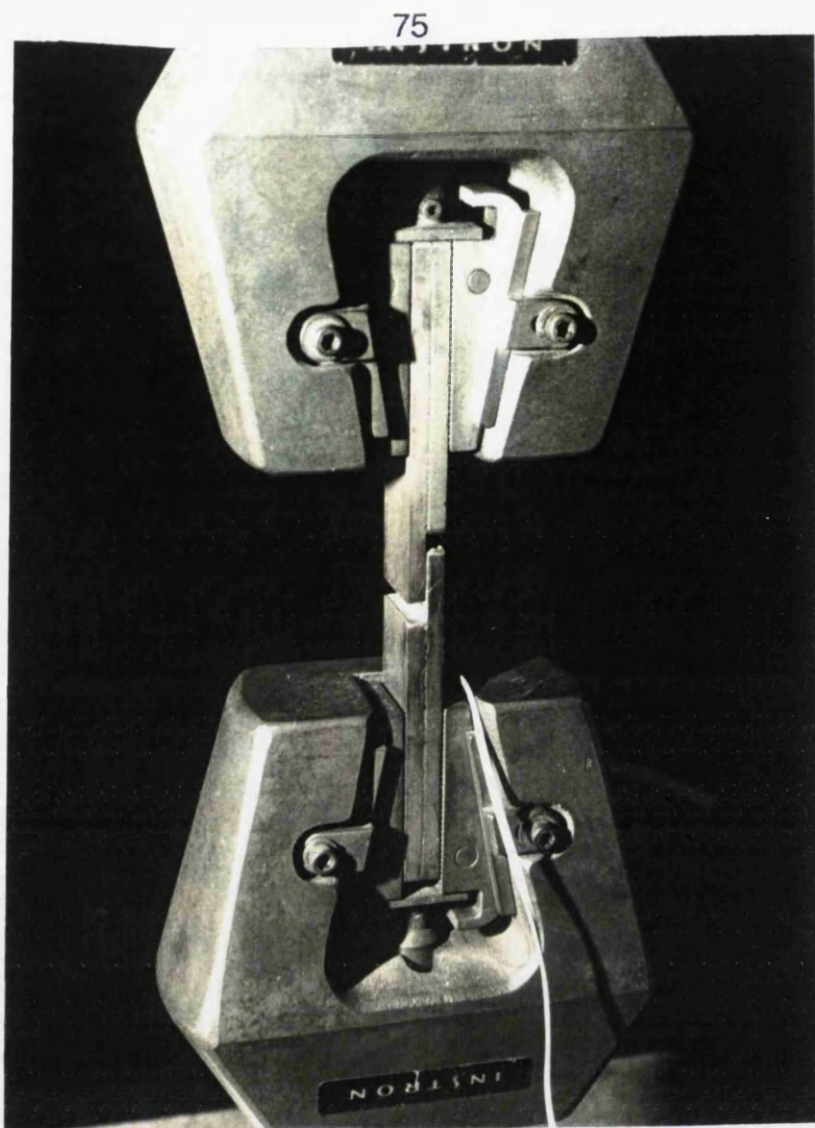


FIGURE 3.10 TESTING OF TENSILE LAP SHEAR SPECIMEN (TYPE 1)

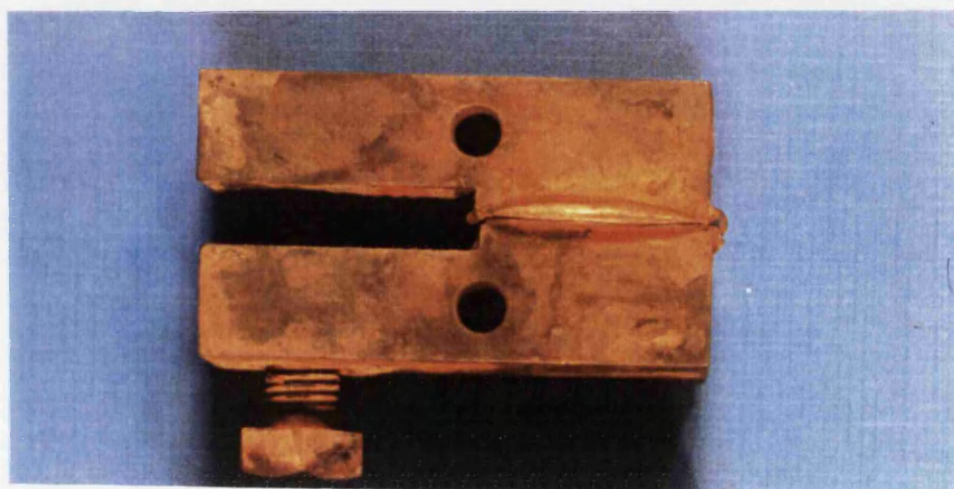


FIGURE 3.11 BOLT LOADED TENSILE CLEAVAGE SPECIMEN (TYPE 4)

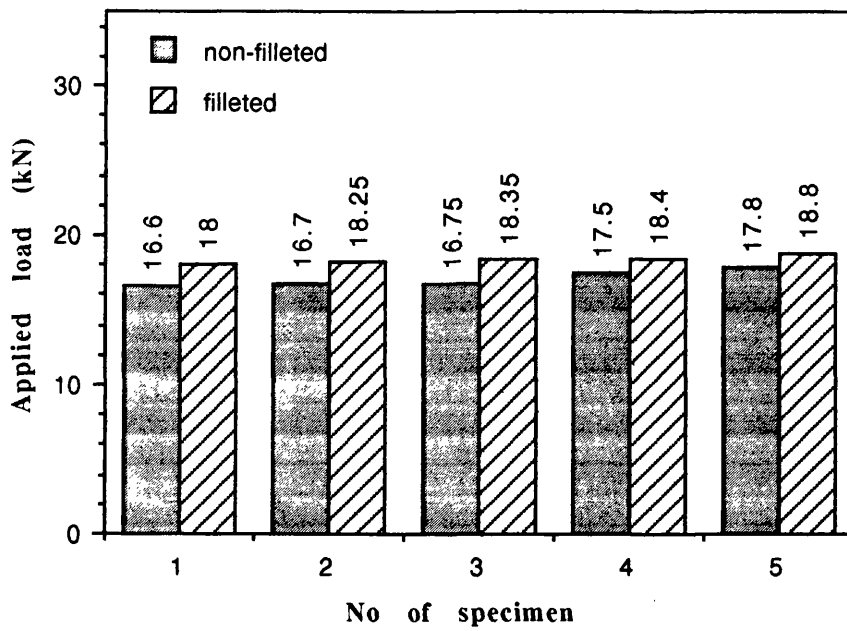


FIGURE 3.12 INFLUENCE OF SPEW FILLET ON JOINT STRENGTH (TYPE 1)

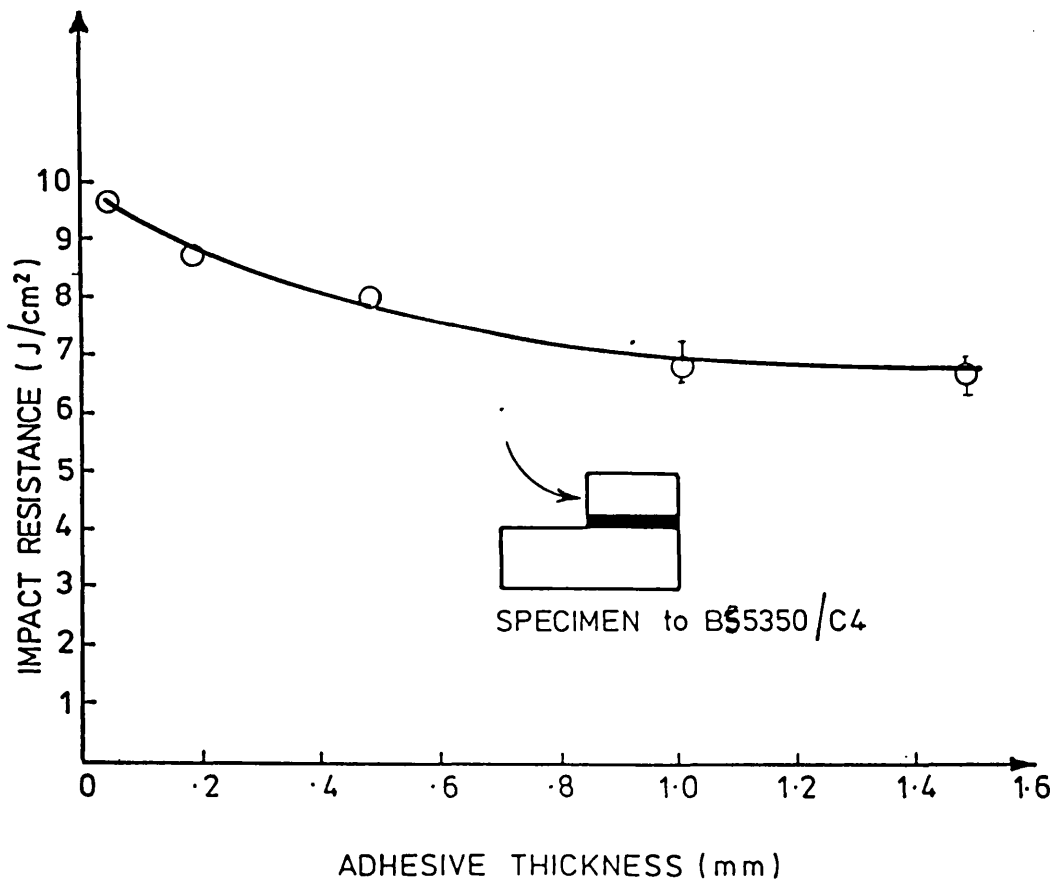


FIGURE 3.13 INFLUENCE OF ADHESIVE THICKNESS ON JOINT STRENGTH (TYPE 5)

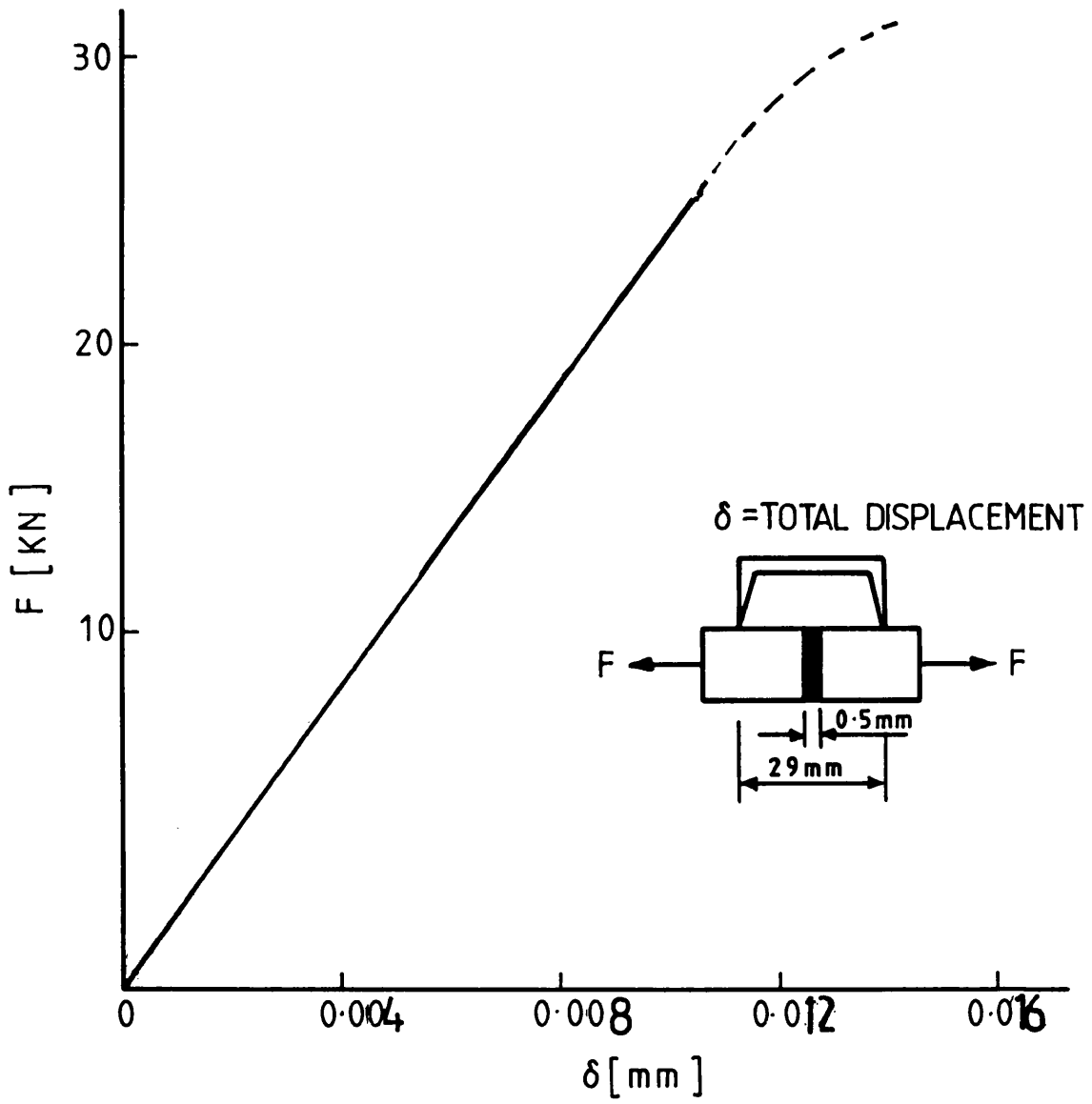


FIGURE 3.14 LOAD- DISPLACEMENT FOR TENSILE BUTT SPECIMEN (TYPE 2)

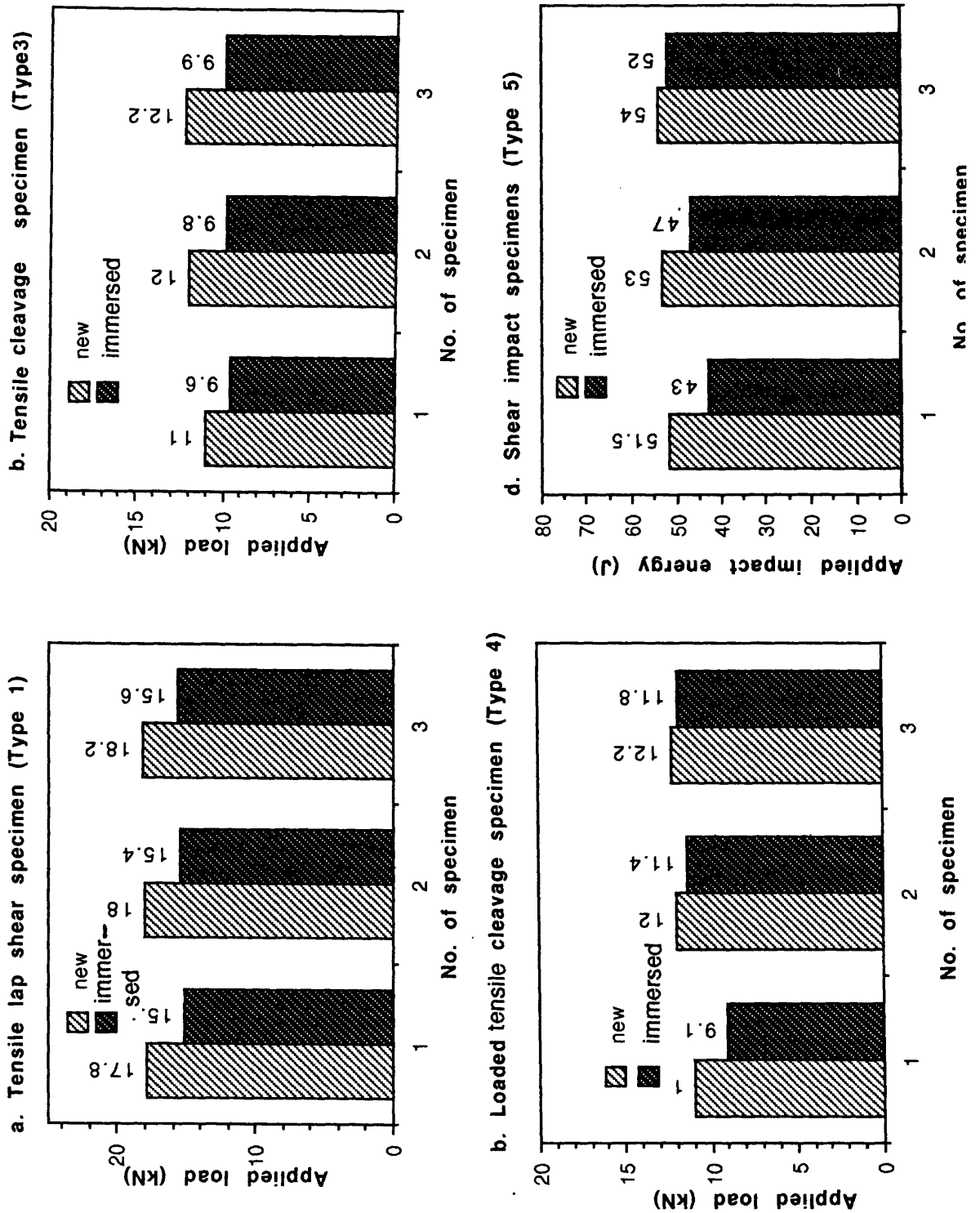


FIGURE 3.15 DURABILITY OF STEEL/STEEL SPECIMENS AFTER 28 MONTHS CONTINUOUS IMMERSION IN SALT WATER (TREATED WITH SILANE)

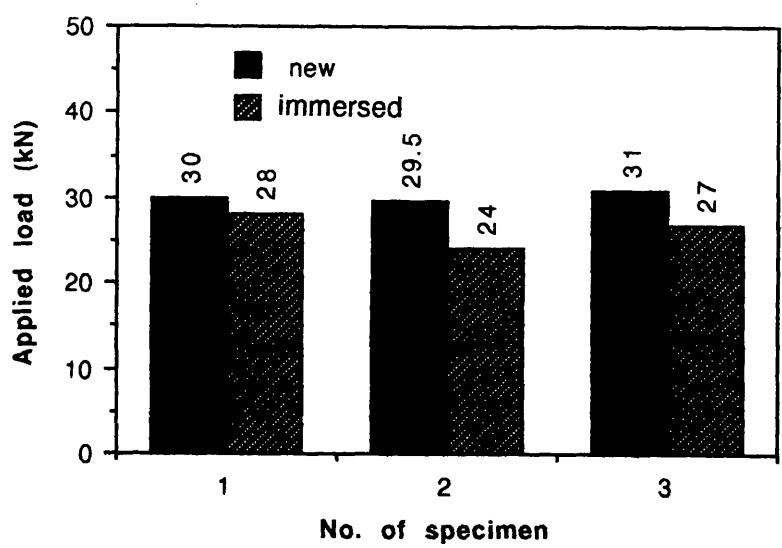


FIGURE 3.16 DURABILITY OF DOUBLE STRAP LAP SHEAR STEEL/GRP SPECIMENS AFTER 18 MONTHS IMMERSION IN SALT WATER (TYPE 6-ARALDITE 2004)

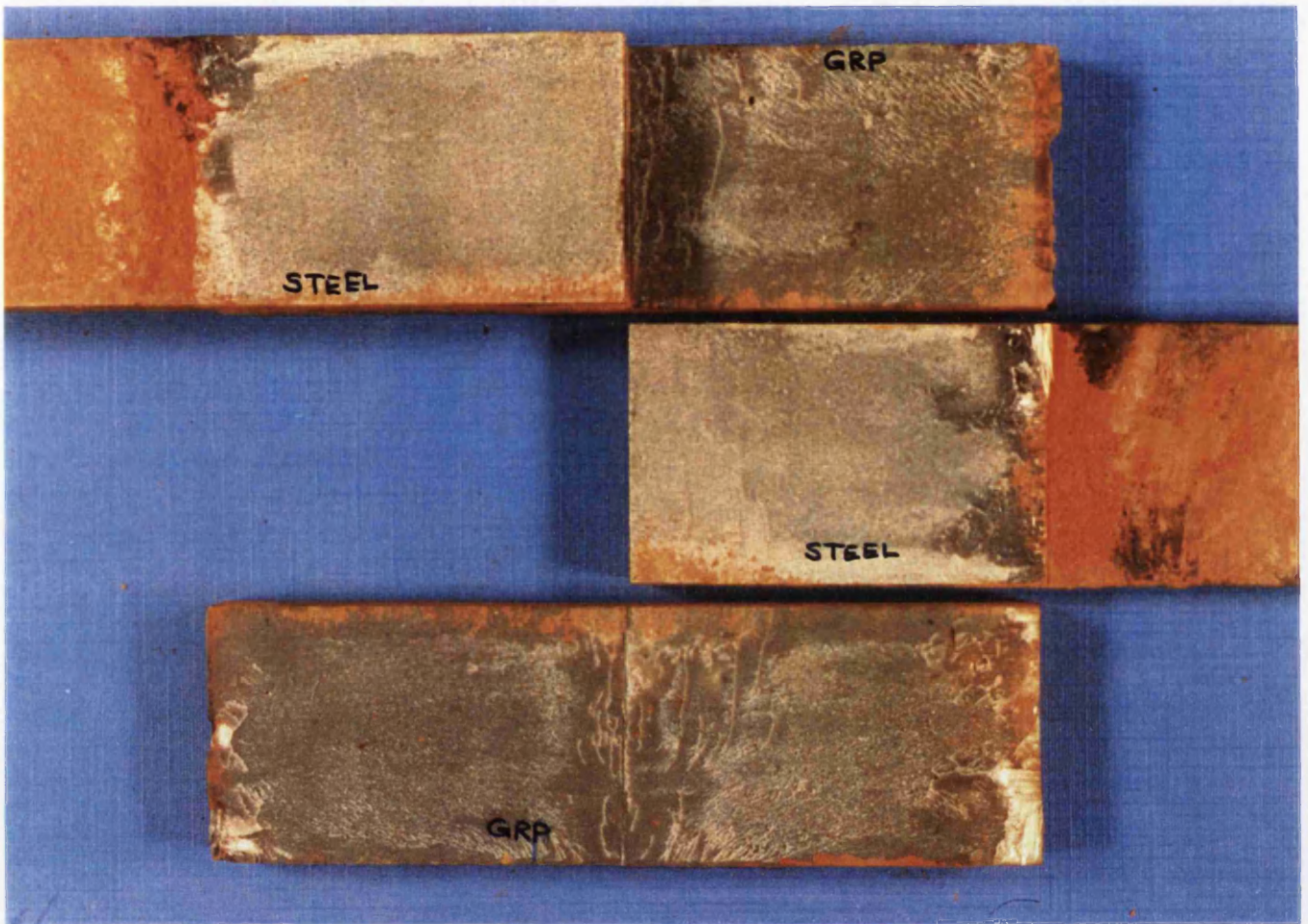
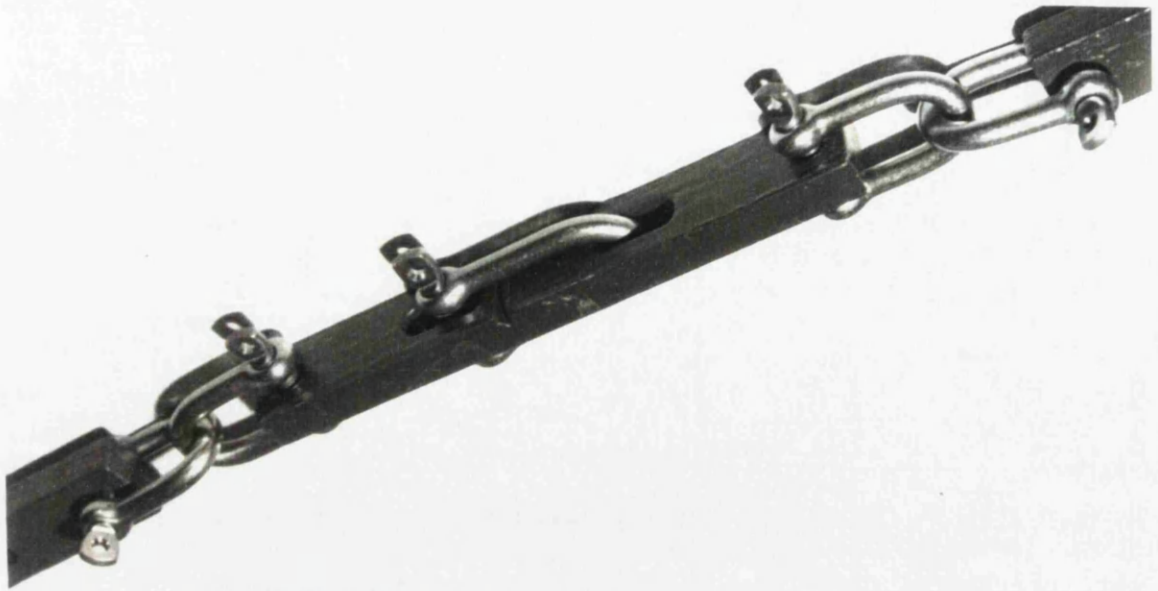


FIGURE 3.17 FAILURE SURFACE OF DOUBLE STRAP LAP SHEAR SPECIMEN AFTER 18 MONTHS CONTINUOUS IMMERSION IN WATER (TYPE 6-ARALDITE 2004)



Lap shear specimen (Type 1)



Deployment of specimens in the Clyde estuary

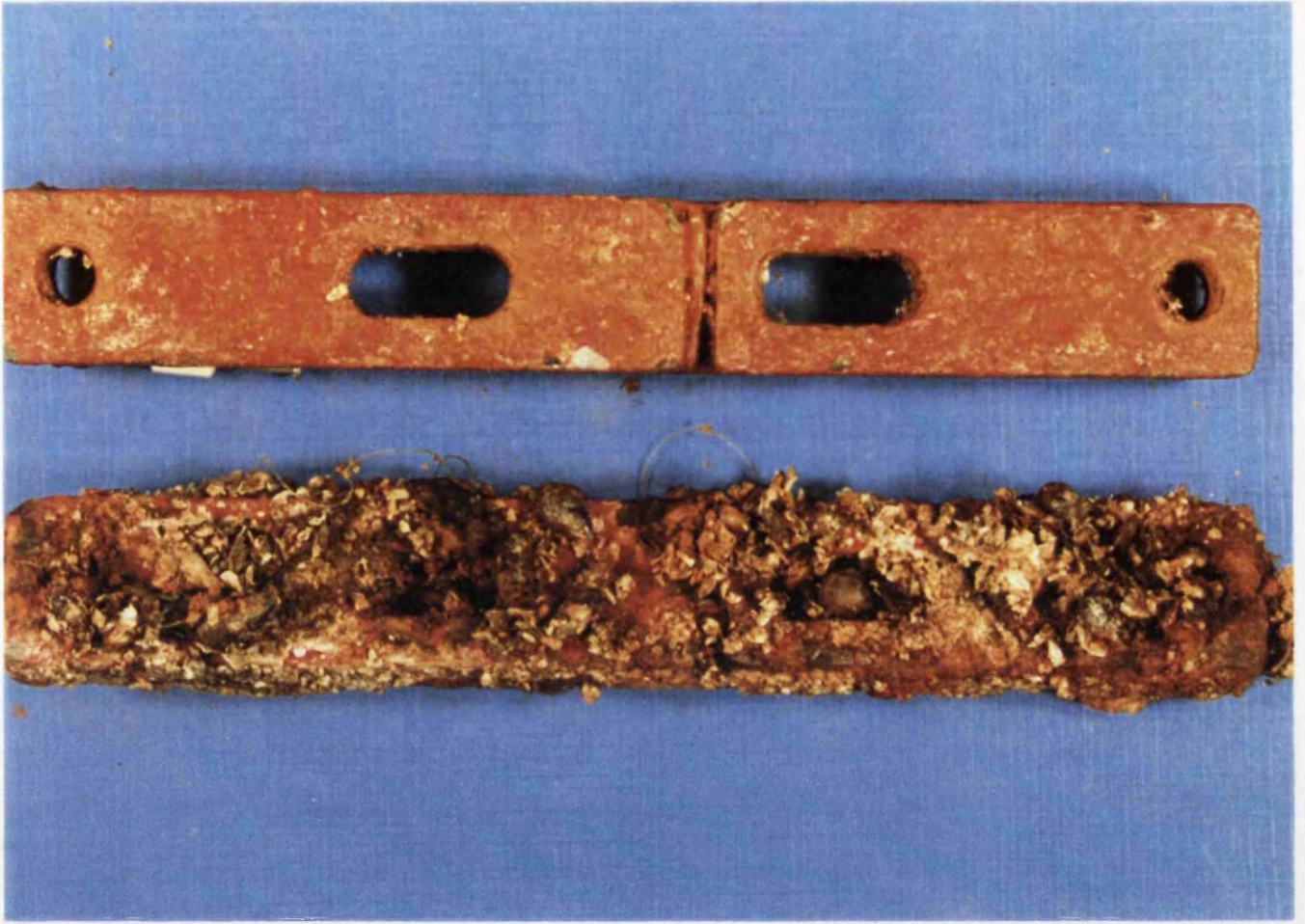


FIGURE 3.19 CONDITION OF A LAP SHEAR SPECIMEN BEFORE AND AFTER CLEANING FOLLOWING TWO YEARS IMMERSION IN SEAWATER (UNDER LOAD)

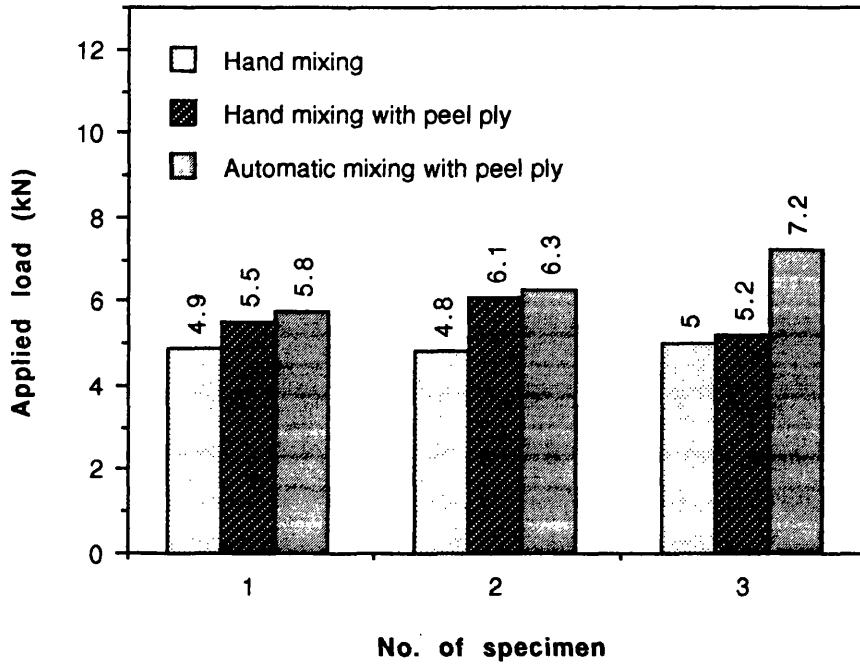


FIGURE 3.20 INFLUENCE OF PEEL PLY AND MACHINE ADHESIVE MIXING ON THE STRENGTH OF LAP STEEL/GRP SPECIMENS (ARALDITE 2004)

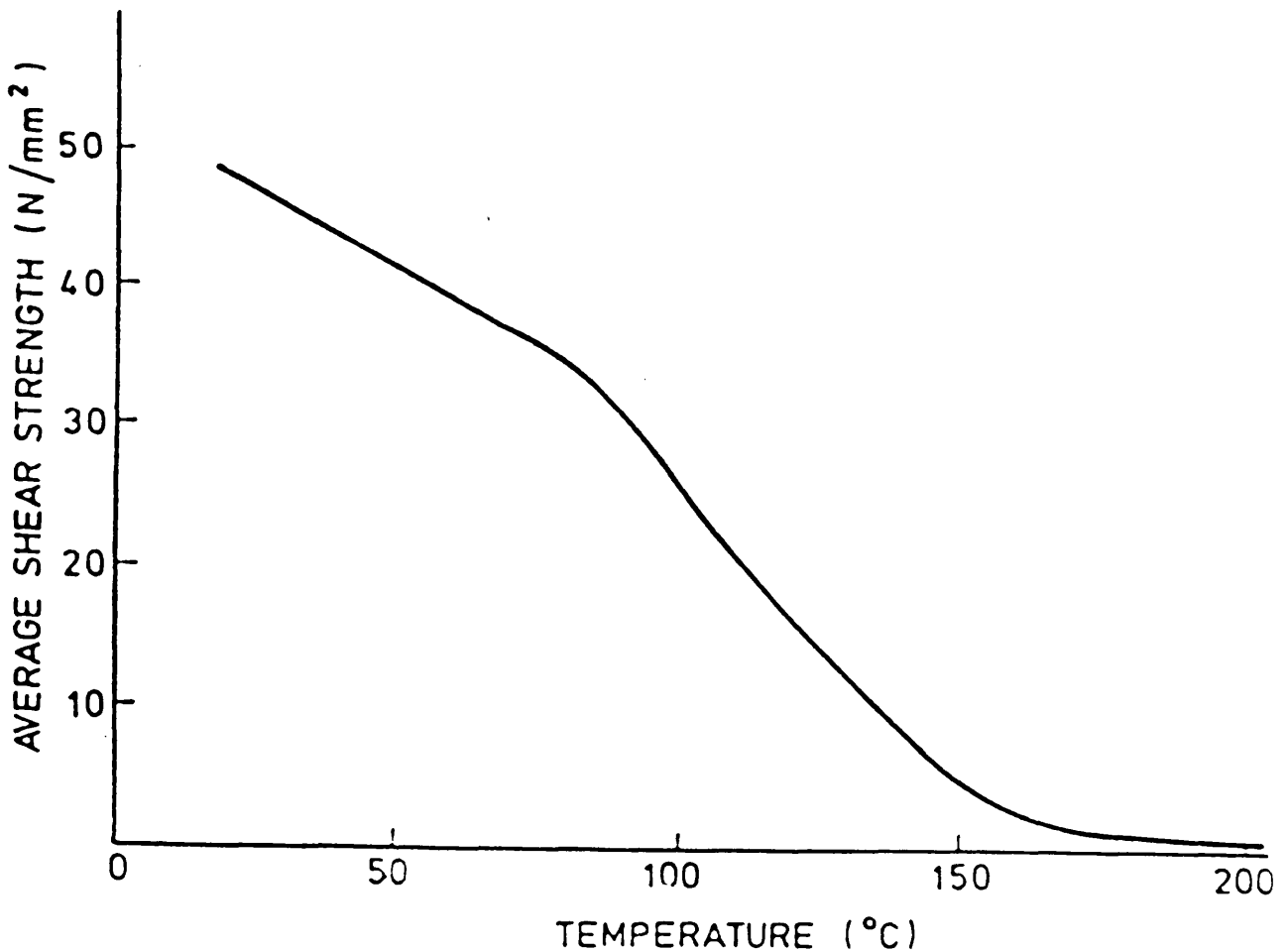


FIGURE 3.21 STRENGTH OF ADHESIVE IN LAP SHEAR JOINT AT ELEVATED TEMPERATURES (ARALDITE 2007)

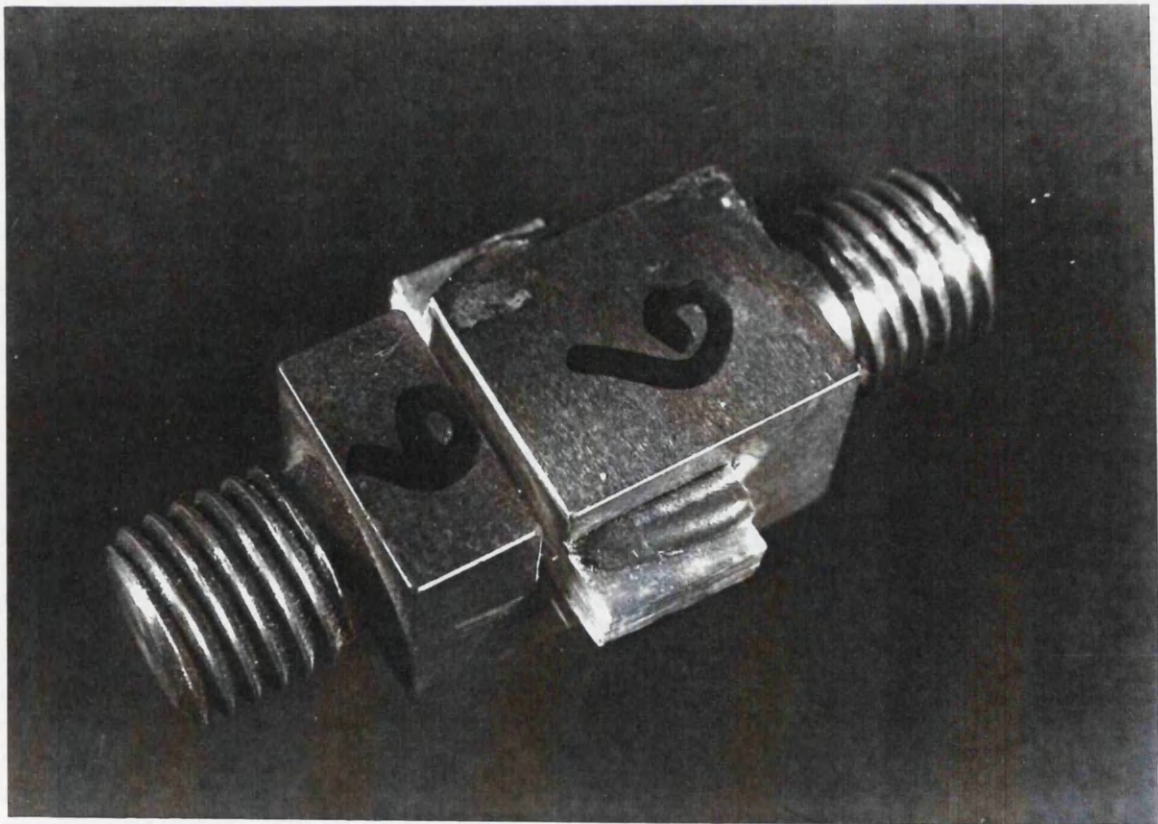
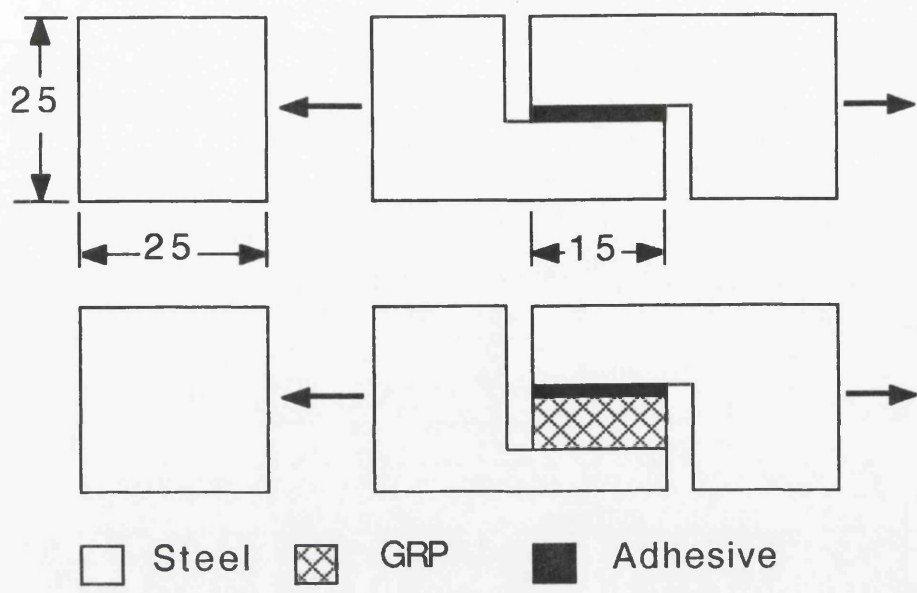


FIGURE 3.22 DETAILS OF LAP SHEAR SPECIMENS USED FOR THERMAL CREEP TESTING

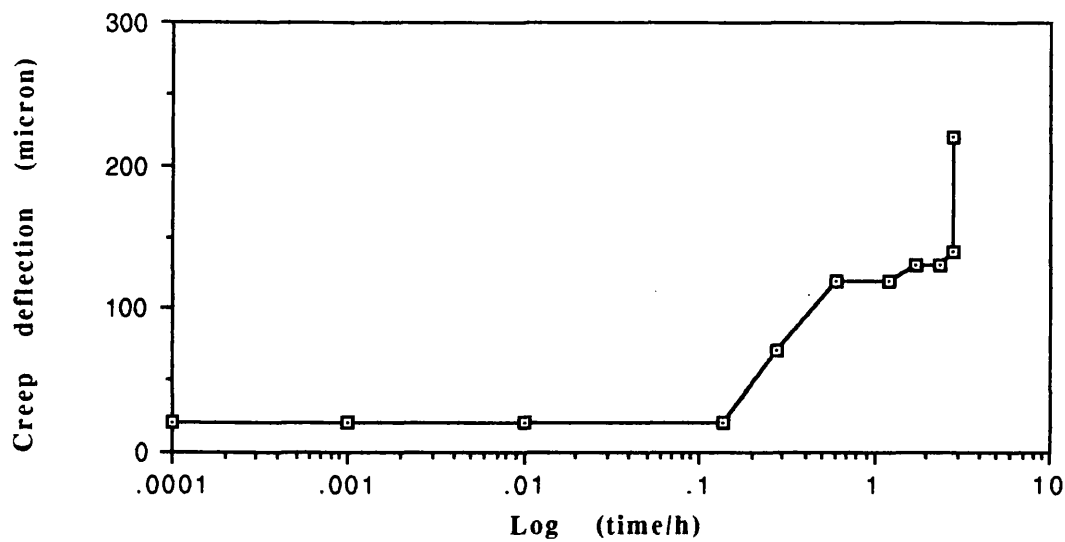


FIGURE 3.23 THERMAL CREEP OF LAP SHEAR SPECIMEN AT A TEMPERATURE OF 130°C/3% OF ROOM TEMPERATURE FAILURE LOAD (ARALDITE 2007)

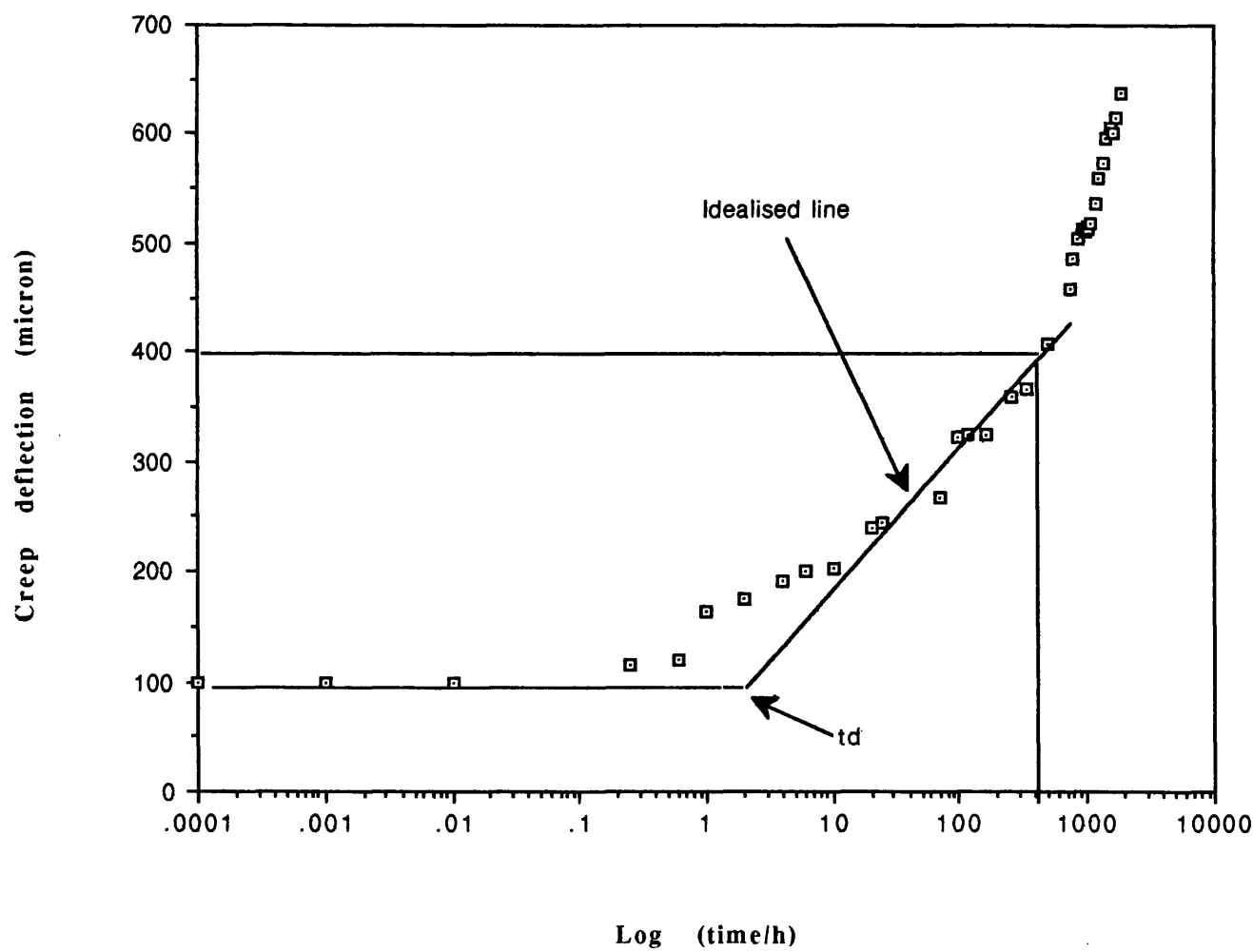


FIGURE 3.24 THERMAL CREEP PROFILE OF LAP SHEAR SPECIMEN AT A TEMPERATURE OF 80°C/25% OF ROOM TEMPERATURE FAILURE LOAD (ARALDITE 2007)

4. ELEMENTARY STRUCTURAL JOINT TESTING

A series of experiments were developed around representative elements of stiffened steel/steel and steel/GRP plated structure. The main objectives in this work were:

- to assess the static strength performance and limitations of thick adherend adhesively bonded structural joints
- to establish a design basis for replacing fillet welding of steel/steel connections between the skin and stiffeners with an adhesively bonded connection
- to establish a design basis for replacing fastener for steel/GRP connections between the skin and stiffeners with adhesively bonded assembly.

Epoxy adhesives Araldite 2007 and Araldite 2004 were used for the bonding of the steel/steel and steel/GRP specimens respectively. Carefully formulated large scale experiments in which the behaviour and design parameters of load bearing joints have been investigated, are presented with their results in this chapter. During this exercise suitable bonding processes for large panel elements were established. Three interrelated design areas and sets of results are presented. These are as follows:

- development of a prototype bonding process for large structural joints,
- assesment of joint design for load bearing joints subject to stiffener transverse and end cleavage forces, and
- testing of large scale (1.5 x 1.2m) stiffened panel elements under lateral loading.

4.1. EXPERIMENTAL JIGS AND FIXTURES

To perform these experiments specialised equipment was selected and a number of jigs were designed and manufactured. These included :-

- High speed (3000 rpm) pneumatic rotary abrasive equipment for abrading steel surfaces which is shown in Figure 4.1.
- Low voltage electrical transformer (60 V/36 kW) power supply for heating which is shown in Figure 4.2.
- 3 kW ceramic insulated low voltage heating elements as shown in Figure 4.3.
- Bench mounted two-part adhesive metering and mixing (static mixture) machine with pneumatic drive pumps as shown in Figure 4.4
- Magnets for clamping mild steel components

- Cantilever loading cleavage test rig for the Instron testing machine (featured in Figure 4.12)
- Cylindrical supports and mandrels for four point bend testing as shown in Figure 4.5

4.2. BONDING PROCESS FOR STRUCTURAL ELEMENTS

Two laboratory techniques were developed for fabricating large specimens as prototypes of practical fabrication techniques for both large load bearing steel structure and steel/GRP fire panels. These specimens included three stiffened panels produced from mild steel plate 1500x1200x8mm bonded to two 102x44mm rolled steel joist (RSJ-7.5kg/m) stiffeners and one GRP 1200x600x15mm plate bonded to a steel square hollow section 50x50mm square hollow section (SHS-7kg/m). The dimensions and configuration details of these stiffeners are shown in Figure 4.6. The bonding processes for the two types (with more emphasis on the steel/steel bonding) are described below.

4.2.1. BONDING OF STEEL/STEEL

The bonding processes for steel/steel specimens are described in the following procedures:

- Cut and machine plates and stiffeners to required dimensions.
- Abrade the bonding surfaces with a flexible grinding wheel to a surface roughness of $5\text{-}10\mu\text{m}$, brush debris out and degrease with an organic solvent such as acetone.
- Dispense as a uniform bead of paste (Araldite 2007) on stiffener bonding surface using an automated or manual dispenser.
- Place components in position and apply clamping pressure sufficient to close the joint by using closely spaced magnetic clamps along the joint. Figure 4.7 shows clamping arrangement for steel/steel panels elements
- Apply the heating elements along the outer skin of the plate and in line with stiffener using magnetic clamps to ensure close contact.
- Operate the automatic heating process using thermocouples to bring the plate temperature to about 180°C and maintain for 20 minutes. Figure 4.8 shows the layout of the heating system and specimen during the bonding process.

- Leave the hot cured steel/steel joint to cool to room temperature or use an air stream to accelerate cooling. Detach clamps and heating elements after which the joint will be capable of being loaded.

4.2.2. BONDING OF STEEL/GRP

The bonding processes for steel/GRP specimens are described in the following procedures:

- Cut and machine GRP plates and steel stiffeners to required dimensions.
- Abrade the bonding surfaces with a flexible grinding wheel to a surface roughness of $5\text{--}10\text{ }\mu\text{m}$, brush debris out and lightly degrease with an organic solvent such as acetone. Although, it is possible to abrade the GRP, the alternative peel ply system was used by simply peeling the knitted nylon ply off the panel.
- Mix the two part (A and B) Araldite 2004 adhesive by using the mixing machine. The mixing ratio and dispensing pressure were specially adjusted for the machine to suit this adhesive. A metallic spatula was used to spread the paste adhesive. It was very important that in this case that adhesive is applied to the GRP surface for maximum wetting at room temperature.
- Place components in position and apply contact pressure sufficient to close the joint by using closely spaced dead weight along the joint (4-off 5 kg along 1.2m stiffener). Figure 4.9 shows the weight application arrangement for the steel/GRP panel element.
- The cold curing adhesive was cured at the room temperature. The cold curing adhesive (Araldite 2004) required 48 hours to fully polymerise at room temperature.
- Remove dead weights after which the joint will be capable of being loaded.

4.2.3. GENERAL CONSIDERATIONS

During these procedures the following should be noted:

- It is important that certain rules concerning safety precautions for working personnel are observed. These relate to skin protection, ventilation, flammability of solvents, and dust from machining cured adhesive and GRP materials.
- Curing temperature across the thickness of the adhesive joint (hot curing)

varies by up to 15°C (higher on the plate compared to the adhesive and stiffener).

- The duration of the hot curing (Araldite 2007) cycle was about 2 hours. This may take the same period for the curing of much larger adhesive joints from room temperature.
- While the time between applying the adhesive and closing and clamping the joint is almost unlimited in the case of the single part adhesive, it is limited to about 10 to 15 minutes (at room temperature) in the case of the mixed cold curing adhesive Araldite 2004
- Changes in the cooling rate (Figure 3.9) of lap shear joints following hot cure (single part adhesive) did not show any difference in the static strength of such joints. This is a useful result in a production environment for full scale fabrication, since it permits optimum utilisation of clamps, heating equipment and time.

4.3. STIFFENED STEEL/STEEL JOINT TESTING

The main aim here is to establish a design basis for replacing fillet welding for grillage steel/ steel connections between plates and stiffeners with an adhesively bonded assembly. Therefore RSJ stiffeners for bonded fillet joints (see Figure 4.6a) were machined to required dimensions of length, width and thickness. Figure 4.10 shows two groups of these machined stiffeners. The stiffeners were bonded to plates of the same grade of mild steel (BS4360-Grade 43A) utilising the bonding process described in Chapter 3 using epoxy adhesive Araldite 2007. Figure 4.11 shows geometric details and primary loading of test specimens used in this investigation. Types of these macro joints (not related to the small standard joints described in Chapter 3) are described below:

- Type 1 refers to the side loaded specimens
- Type 2 refers to the end loaded specimens with square ends
- Type 3 refers to the end loaded specimens with shaped ends

In these tests, the specimens were clamped in the specially designed test rig and loaded at a crosshead speed of 0.5 mm/min. Figure 4.12 shows a test arrangement and Figure 4.13 shows typical load deflection curves for Types 1 and 3 specimens.

4.3.1. EXPERIMENTAL RESULTS

The results from these experiments are presented in Tables 4.1 and 4.2 and also plotted in Figure 4.14. The principal results may be summarised as follows:

- Stiffener end shape - Table 4.1 and Figure 4.14 show that joint Type 3 with a shaped end is up to 50% stronger than Type 2 which had a square cut end.
- Effect of base plate thickness - Table 4.1 and Figure 4.14 show that the joints bonded to 10mm plate could be 100% more structurally efficient than if the same stiffener were bonded to 6mm base plate.
- Resistance to transverse loading - Figure 4.14 shows that tests on joint Type 1 specimens show high strength efficiency of the bonded fillet joint when subject to transverse loading. All specimens with 15-45mm joint width deformed plastically in the stiffener web without noticeable failure of the adhesive.
- Optimum joint width - Figure 4.14 and Table 4.2 indicate that the relationship between joint width and failure load is non-linear. A width of 25mm (for this particular type of joint) may be sufficient to resist, without adhesive failure, both transverse and longitudinal (end cleavage) forces, until the stiffener yields. However a significantly larger joint width may be necessary to resist long term reduction in joint strength associated with service loading and environments. Further discussion on this point raised in Chapter 2 is also contained in Chapter 7.
- Stiffener/plate stiffness imbalance - The results in Tables 4.1 and 4.2 and Figure 4.14 show that the reduction of cleavage stresses depends on reducing the stiffness of the stiffener ends and/or increasing the stiffness of the base plate.
- Thickness of the bonded flange - All tests in Table 4.2 were repeated using a flange thickness of 6mm. There was no significant difference in failure load compared with the original results using a 2mm flange thickness, although direct tensile load carrying capacity was not investigated.
- Cleavage stress - The cleavage stresses at failure shown in Tables 4.1 and 4.2 were obtained from the tensile bending stress equation for a cantilever under pure bending moment detailed in Appendix II. These values are average cleavage stresses. In Chapter 5, the stress analysis will show that actual adhesive cleavage stress is several times higher than this average value. The bending stress in the stiffener web was obtained in the same manner as

shown above.

- Joint strength efficiency - Values shown in the final column of Tables 4.1 and 4.2 are based on calculations of the ratio of the maximum bending stress in the stiffener web to the minimum yield strength for the mild steel used in these tests (230N/mm^2 to BS4 1980-standard steel sections). This method is for comparative purposes only, as it ignores the bending stress developed within the plate as will be shown in Chapter 5. Figure 4.15 clearly indicates the efficiency of Type 1 and some of Type 3 joints in resisting cleavage stresses under an applied bending moment. The joint strength efficiencies in these cases have exceeded the unity value due to plastic deformation. Appendix II illustrates the efficiency calculations.

4.4. LATERAL LOADING OF STIFFENED PANELS

The main aims of these tests were to demonstrate the efficiency of adhesive bonding under lateral bending loads, to determine the level of adhesive shear stress and panel rigidity due to bending and to validate the fabrication techniques developed in this study.

The three 1.5x1.2m stiffened panels described in Section 4.1 were tested to plastic collapse in four point bending under simply supported boundary conditions. Two specimens were tested under a negative bending moment (two inner loading points are in contact with stiffeners and the outer two support points are in contact with plate-designated as AN and BN) and the third under a positive moment (loading and support positions are opposite to the negative moment-designated as AP).

The test arrangement is shown in Figure 4.16 where a negative bending load is applied at two points along the double stiffeners using a 1000 tonne universal testing machine shown in operation in Figure 4.17. Although the load required for the test was small (less than 30 tonne) compared with the capacity of the machine, the choice of facility is dictated by the physical size of the large scale specimens. Strain gauges and a deflection transducer were applied at the centre of each specimen. A typical load deflection curve is shown in Figure 4.18.

4.4.1. TEST RESULTS

Table 4.3 shows the experimental measurements and calculation results at yield and

ultimate bending moment at mid-section of the beam (panel). These results indicate that bending beyond yield has not caused failure at the adhesive except in specimen AN where failure occurred at the stiffener end after plastic deformation of both the stiffeners and the plate. It should be noted that the bonding processes for this particular specimen have not been particularly effective because of poor adhesive gap filling due to inadequate clamping (discussed in Chapter 7). Figure 4.19, shows specimens after testing demonstrating good structural integrity of the adhesive bond under static loading.

Shear stress calculations (bond width=25mm) for this type of test are detailed in Appendix III and results are presented in Table 4.3. This shows that the adhesive shear stress level in these panels is approximately 60% of the nominal shear strength obtained from single lap shear joint (as discussed in Section 3.1). The shear stress can be reduced substantially by increasing the stiffener bonding area. Appendix III also shows the calculations of the flexural rigidity of such composite specimen (steel/adhesive/steel beam) which is theoretically lower than that of a homogeneous one (such as a welded joint). A thorough numerical and experimental analysis was therefore required in order to obtain a more accurate measure of the level of shear stress, its distribution along the adhesive line and the flexural rigidity of bonded beams. This analysis will be developed in Chapter 5.

4.5. STEEL/GRP STIFFENED CONNECTIONS

The main aim of the following experiments to establish a design basis for joining steel stiffeners to GRP skin which can meet the design requirements for offshore fire and blast walls. This series of the stiffened joints is illustrated in Figure 4.20 which includes the following types of macro joints (not related to the small standard specimens described in Chapter 3):

- Type 4 refers to the compression loaded specimens
- Type 5 refers to the tension loaded specimens

Steel/GRP full scale joints were bonded with epoxy adhesive Araldite 2004. The specimens were bonded in the same manner as the small specimens were bonded (see Chapter 3). The features of these joints are shown in Figure 4.21 in which the square hollow section stiffener is replaced in the tension type specimen (Type 5) with flat bar (10mm thick). This facilitated the mounting of the tension specimen on the Instron testing machine to obtain clamped end conditions. These tests attempted to simulate

compressive and tensile explosive overpressure on the bond between GRP skins and the steel supporting frames (stiffeners). The experiments were designed to assess the effect of local cleavage forces which accentuate the joint edge effect at the boundaries between the steel stiffeners and the GRP skin. All specimens were 75mm wide with a span of 500mm between stiffeners and skin thickness varying from 4.5 to 15mm. To simulate an evenly distributed load, the central load was spread to eight points on the surface of an aluminium backing plate separated from the GRP panel by a rubber strip as shown in Figure 4.22. The equivalent static pressure was obtained by dividing the applied load at failure to the area of the GRP skin between the stiffeners (i.e $450 \times 75 \text{ mm}^2$). A typical load deflection curve for the tension specimen is shown in Figure 4.23. This indicates that the bond failure is most likely to take place within the elastic range of the GRP materials.

4.5.1. EXPERIMENTAL RESULTS

The results from these experiments are presented in Table 4.4 and may be summarised as follows:

- The strength of tension type specimens increases with increasing GRP thickness, while in case of the compression type specimens the trend is the opposite. For example, comparison of the average failure pressure of the tension joints for a GRP thickness of 4.5mm with the results for 15mm shows there is increase of approximately 350% in the joint strength of the latter. In the case of the compression mode, comparing the strength of these two thicknesses shows an increase of approximately 100% in the favour of the former. This behaviour may be explained by using the principles of mechanics. In the case of the tension type specimen, the thinner the GRP skin then the higher the cleavage (peeling) forces are at the inner end of the bond. For the compression type specimen, the thinner the GRP skin is, the lower the cleavage forces are, at the outer end of the joint.
- The strength of the compression type specimen is generally higher than that for the tension type. However, there is significant scatter of up to 35% in the strength. This is probably due damage of the bonded surface from the abrasion process and the use of hand mixed rather than machine mixed adhesive, which may cause both voids and wetting deficiency due to the limited pot life of the adhesive after mixing.

- All specimens, except these in compression with 4.5mm thickness, failed at the adhesive as result of local failure of the GRP skin. Unlike the steel/steel joints described in Section 4.3 none of the GRP plates exceeded the elastic limit. It is important to mention here that the load capacities of these joints are well above the minimum design requirements for pressure loading of 0.3 bar estimated as the likely results from an offshore gas explosion.

Many of the above points will be investigated further in Chapters 5 and 7

Joint Type	Joint Width (mm)	Plate Thickness (mm)	Failure for 3 No. 1	Loads Test No. 2	(kN) Pieces No. 3	Average Failure Load (kN)	Adhesive Cleavage Stress (N/mm ²)	Adherend Bending Stress (N/mm ²)	Joint Strength Efficiency
2	15	6	2.95	2.6	3.0	2.85	16.2	56.5	0.25
	15	8	4.6	5.35	6.1	5.35	30.4	106	0.46
	15	10	5.9	6.2	6.0	6.03	34.3	120	0.52
	25	6	5.0	4.0	3.9	4.3	14.7	85.5	0.37
	25	8	8.5	7.75	7.1	7.78	26.6	154.7	0.67
	25	10	8.5	9.1	8.1	8.57	28.9	168.2	0.73
	35	6	4.9	5.5	5.3	5.23	12.8	104.2	0.45
	35	8	8.4	8.3	8.0	8.23	20.1	163.3	0.71
	35	10	9.9	10.0	9.2	9.7	23.7	192.2	0.83
	45	6	6.1	6.2	6.0	6.1	11.7	122.1	0.53
	45	8	9.9	9.8	9.3	9.7	18.4	192.6	0.84
	45	10	11.1	10.3	10.2	10.2	19.3	203.0	0.88

TABLE 4.1 EFFECT OF BASE PLATE THICKNESS AND FLANGE WIDTH ON THE CLEAVAGE STRENGTH

Joint Type	Plate Thickness (mm)	Joint Width (mm)	Failure for 3 No. 1	Loads Test No. 2	(kN) Pieces No. 3	Average Failure Load (kN)	Adhesive Cleavage Stress (N/mm ²)	Adherend Bending Stress (N/mm ²)	Joint Strength Efficiency
2	8	15	4.6	5.35	6.1	5.35	30.4	106.0	0.46
	8	25	8.5	7.75	7.1	7.78	26.6	154.7	0.67
	8	35	8.4	8.3	8.0	8.23	20.1	163.3	0.71
	8	45	9.9	9.8	9.3	9.7	18.4	192.6	0.84
	8	15	8.0	7.5	8.3	7.93	45.1	(157)	(0.68)
3	8	25	11.3	11.4	11.1	11.27	38.6	(224)	(0.97)
	8	35	13.0	12.2	11.8	12.33	30.1	(245)	(1.06)
	8	45	12.6	13.2	13.3	13.0	24.7	(258)	(1.12)

() calculation based on type 2 cross sectional area for comparison

TABLE 4.2 EFFECT OF JOINT'S SHAPE AND WIDTH ON CLEAVAGE STRENGTH

* Specimen No	Yield loading limit							Ultimate loading limit				
	Load (kN)	Central deflection (mm)	Stiffeners bending stresses		Plate bending stresses		Average adhesive shear stress (N/mm ²)	Load (kN)	Central deflection (mm)	Stiffness bending stresses (N/mm ²)	Plate bending stresses (N/mm ²)	Adhesive failure
			(N/mm ²)	(N/mm ²)	(N/mm ²)	(N/mm ²)	(N/mm ²)					
AN	150	3.1	-	-	58	59	22	211	22	498**	550**	Yes
BN	149	3.5	376	421	61	62	22	208	23	498	550	No
AP	140	3.4	345	370	57	58	21	252	24	498	550	No

* N and P denote negative and positive bending moment respectively.

** Ultimate tensile strength of stiffeners and plate material from standard tests.

TABLE 4.3 RESULTS OF FOUR POINT BENDING OF LARGE PANELS (STEEL / STEEL)

GRP thickness [mm]	Specimen No	Load [kN]	Tension mode		Compression mode	
			Average	Pressure	Load	Pressure
			[kN/m ²] *		[kN]	[kN/m ²]
4.5	1	1.4			14	400
4.5	2	1.3	40			
4.5	3	1.35				
8.5	1	2.75			11.0	314
8.5	2	2.00	74			
8.5	3	2.3				
15	1	5.2			7.8	223
15	2	5.6	177			
15	3	7.2				

* 1 Bar = 100 kN/m²

TABLE 4.4 RESULTS OF LOCAL LOADING ON FULL SCALE STEEL / GRP SPECIMENS
(TYPE 4 FOR COMPRESSION AND TYPE 5 FOR TENSION-FIGURE 4.21)

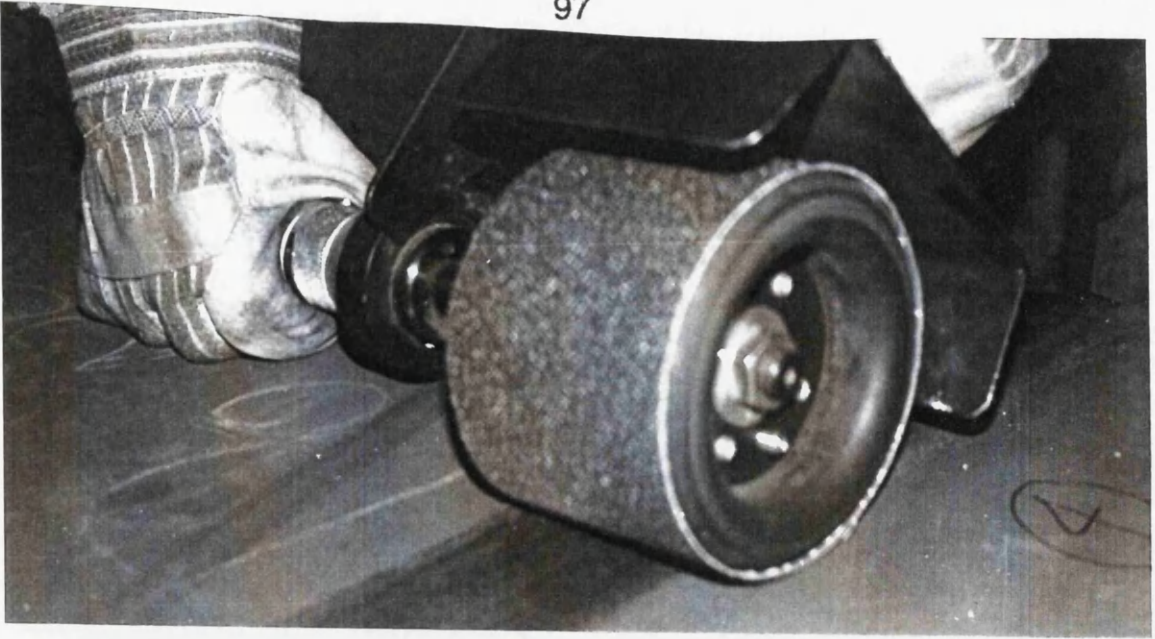


FIGURE 4.1 PNEUMATIC ABRASIVE WHEEL FOR SURFACE ROUGHENING

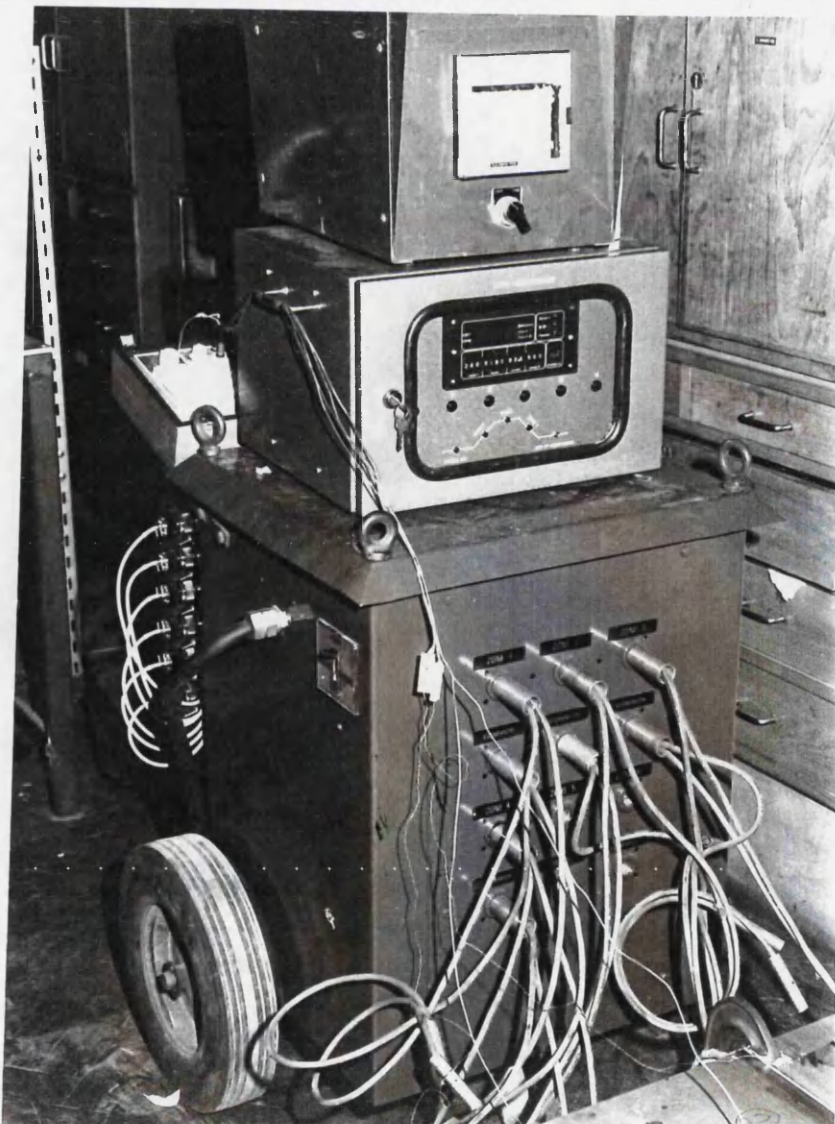


FIGURE 4.2 LOW VOLTAGE HEAT CURING EQUIPMENT (60V)

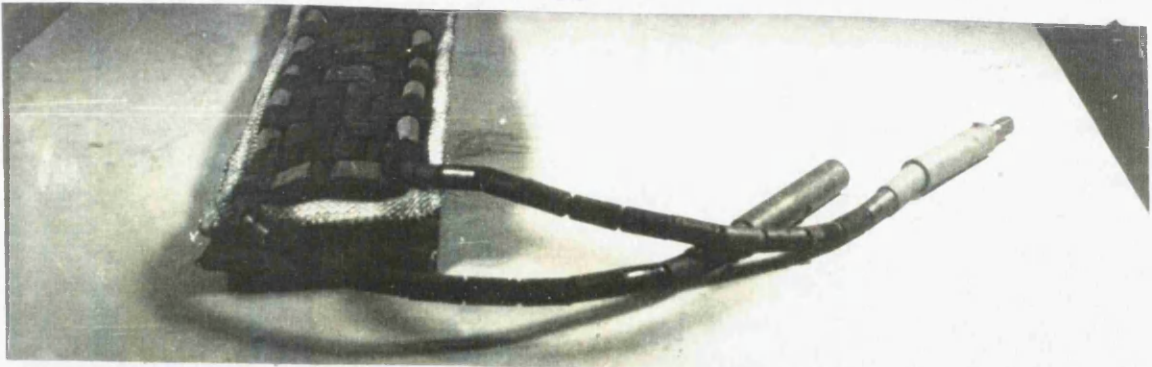


FIGURE 4.3 CERAMIC HEATING ELEMENT (3kW)



FIGURE 4.4 ADHESIVE MIXING MACHINE

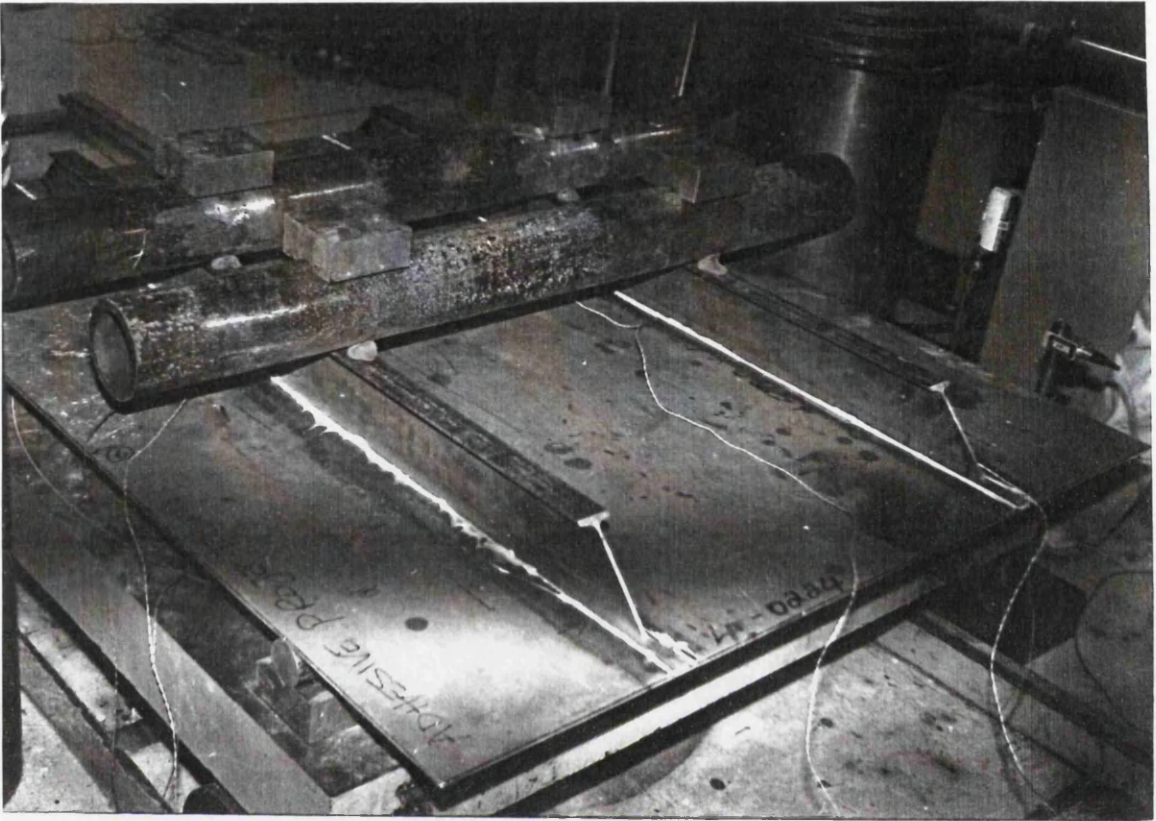
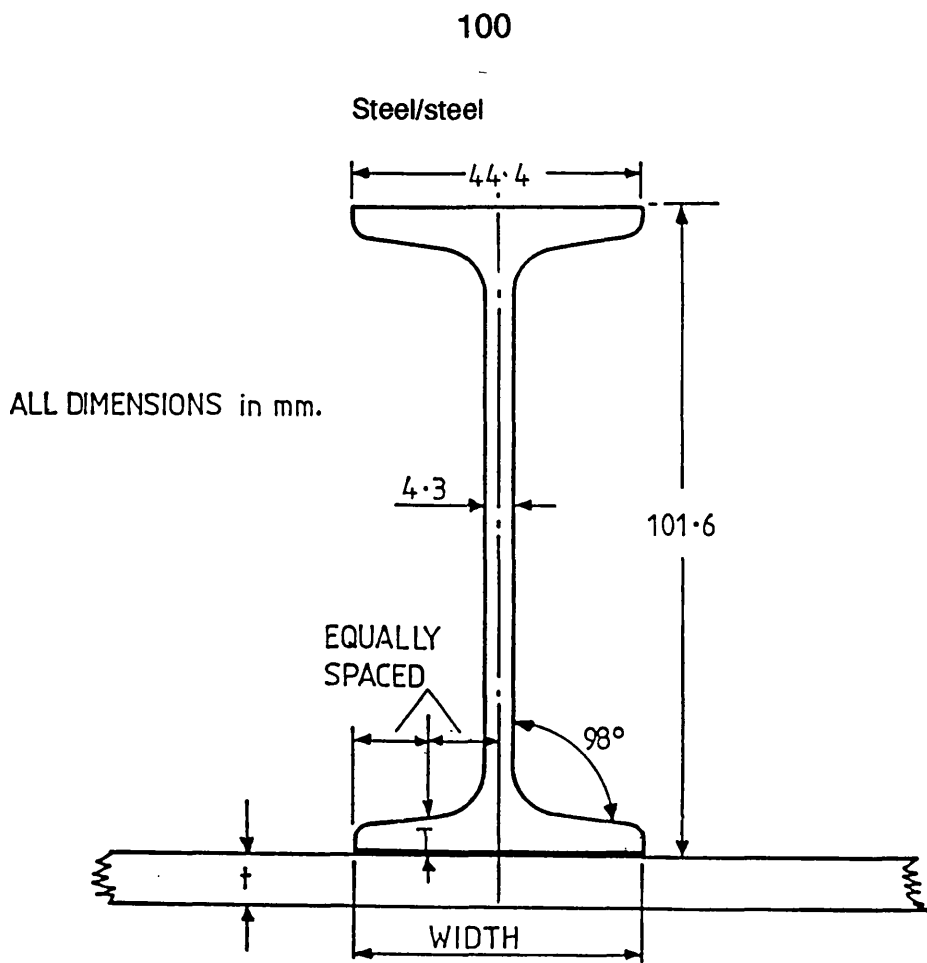


FIGURE 4.5 SUPPORTS AND MANDERLS FOR PANEL TESTING



WIDTH = 15-45 mm
 T = 2 - 6 mm
 t = 6 - 10 mm

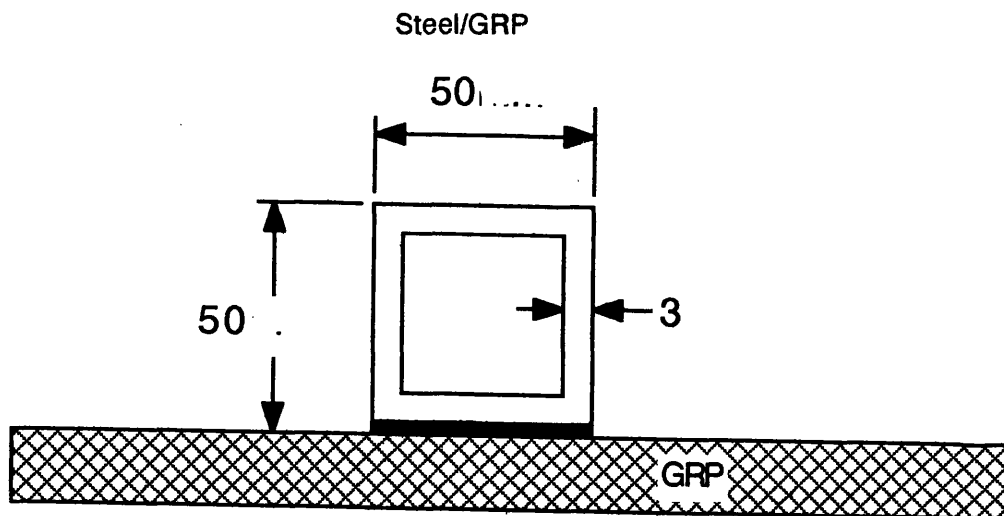


FIGURE 4.6 BONDED STIFFENER/PLATE CONNECTIONS

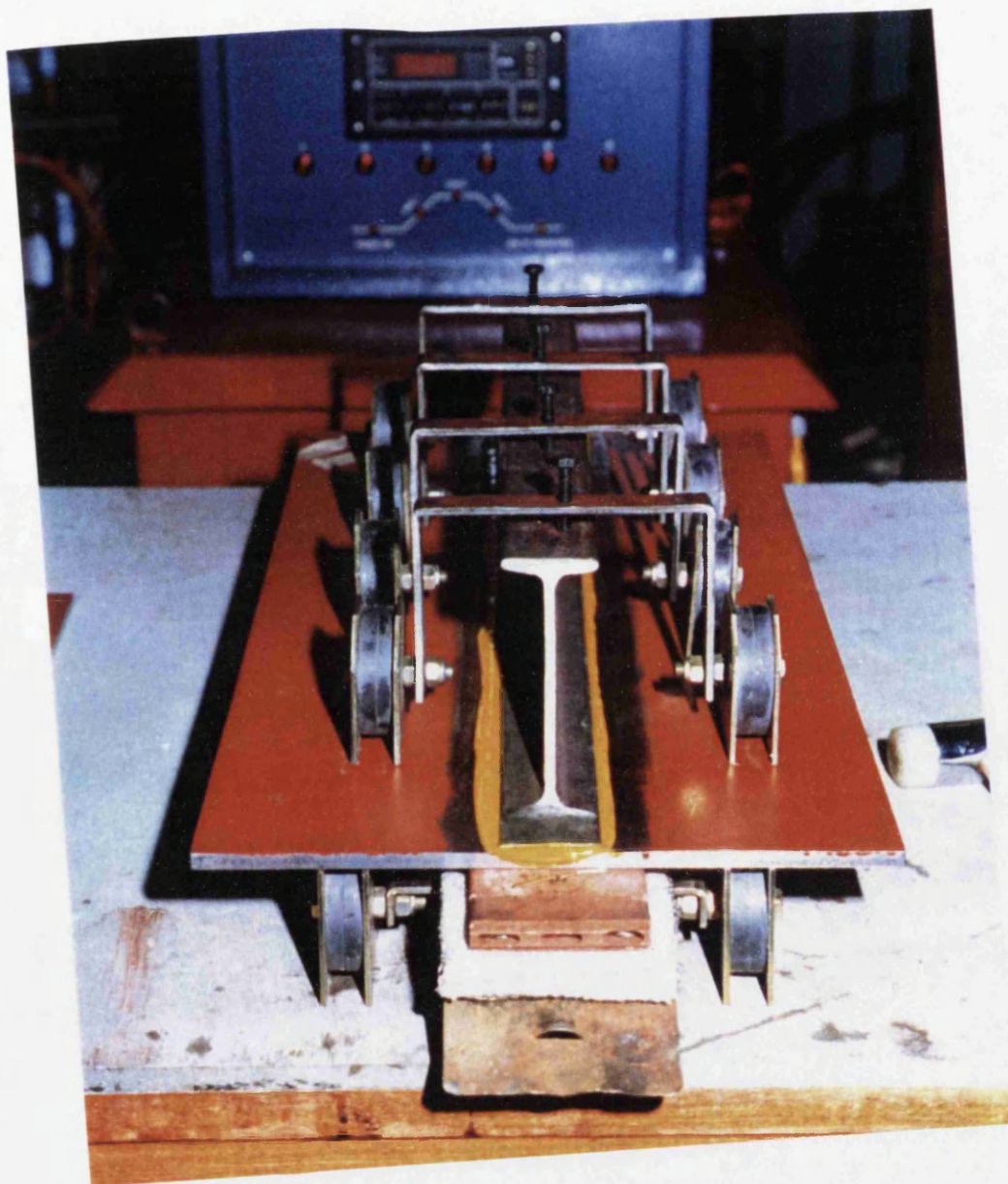


FIGURE 4.7 CLAMPED STEEL/STEEL SPECIMEN (SHOWING HEATING ELEMENT)

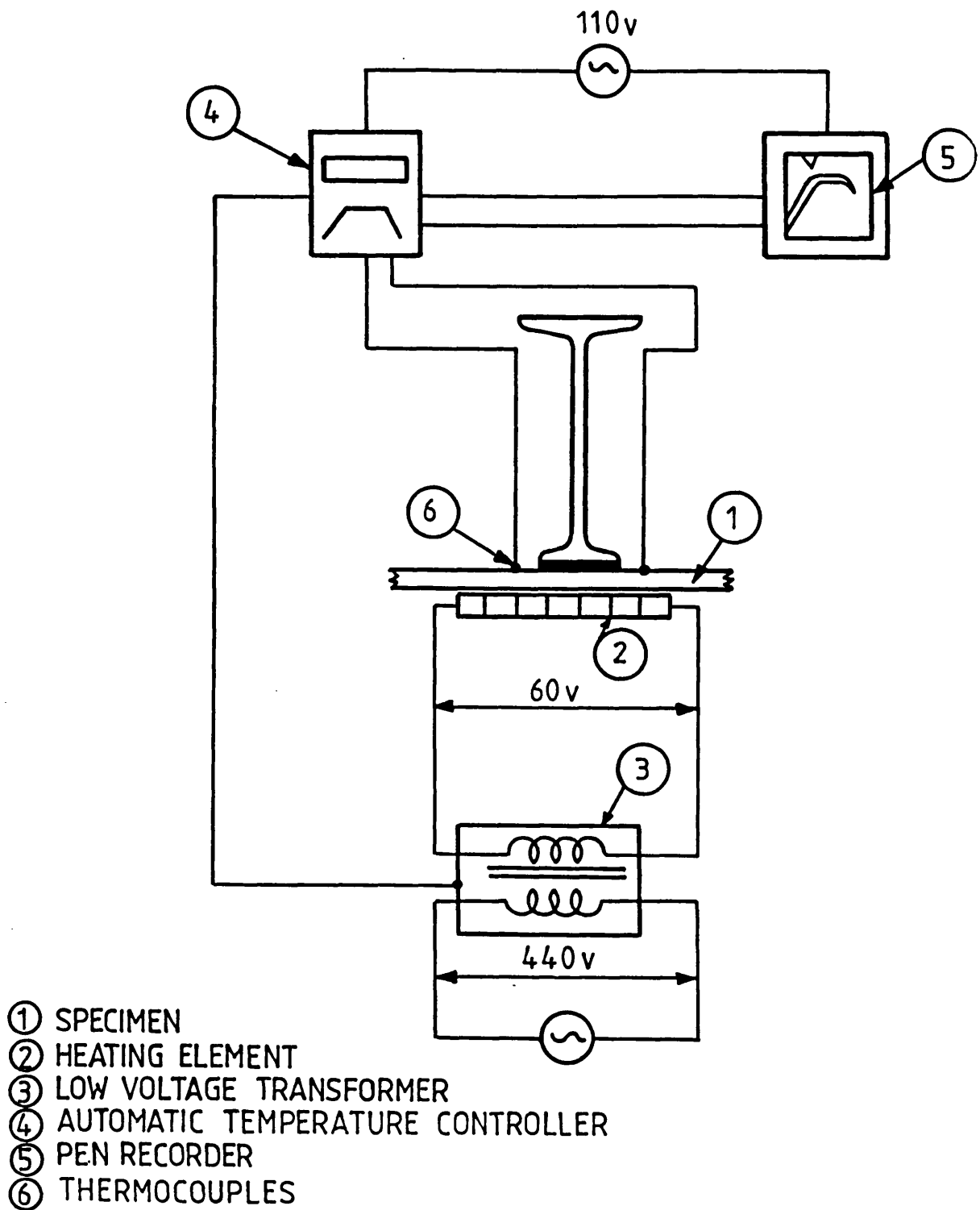


FIGURE 4.8 SCHEMATIC DIAGRAM OF THE HEAT CURING PROCESS

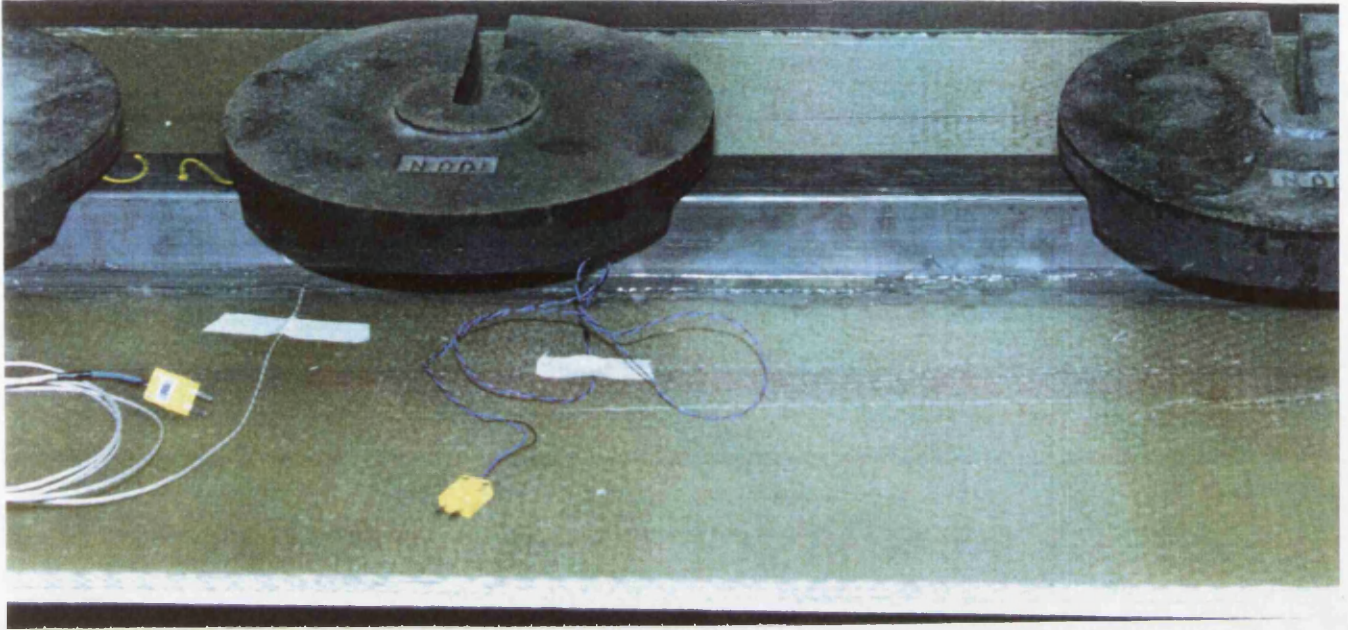


FIGURE 4.9 STEEL/GRP JOINT UNDER DEAD WEIGHT CLAMPING DURING CURING

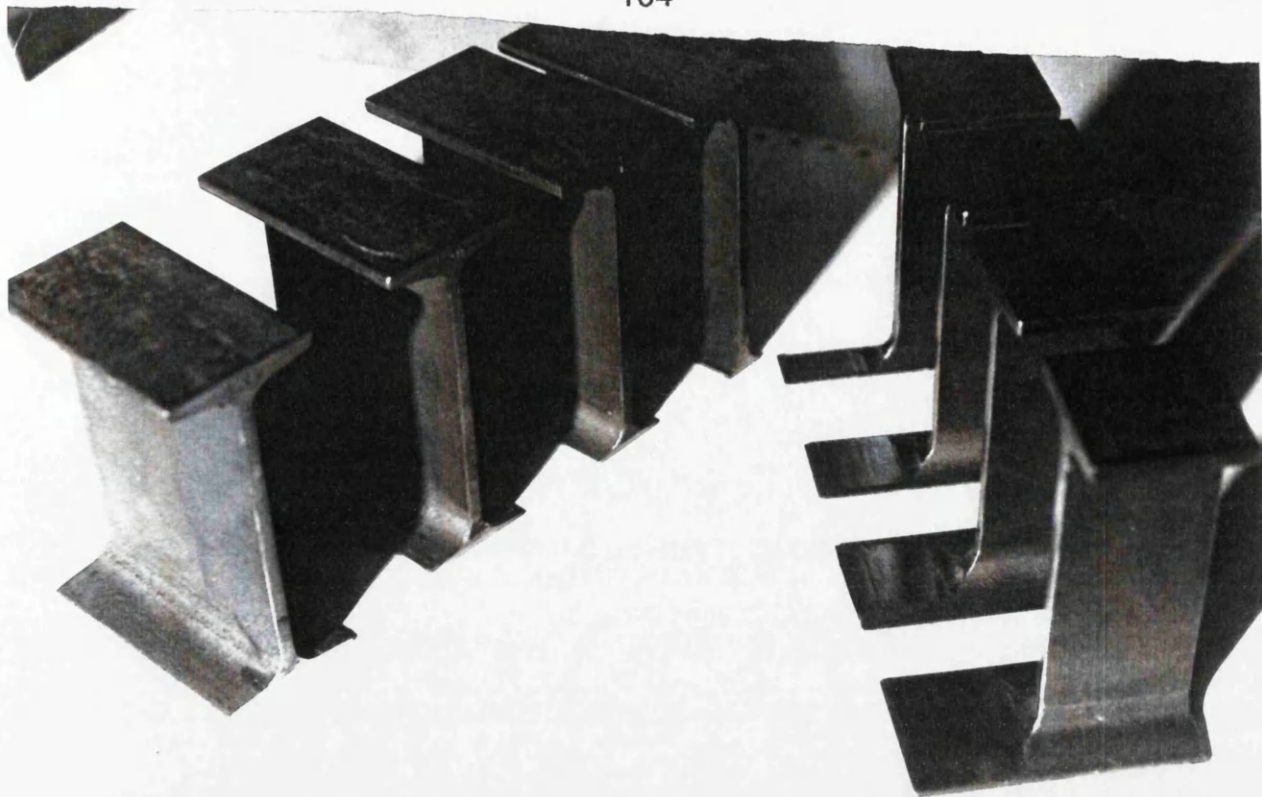


FIGURE 4.10 MACHINED STEEL STIFFENERS (SQUARE AND SHAPED ENDS)

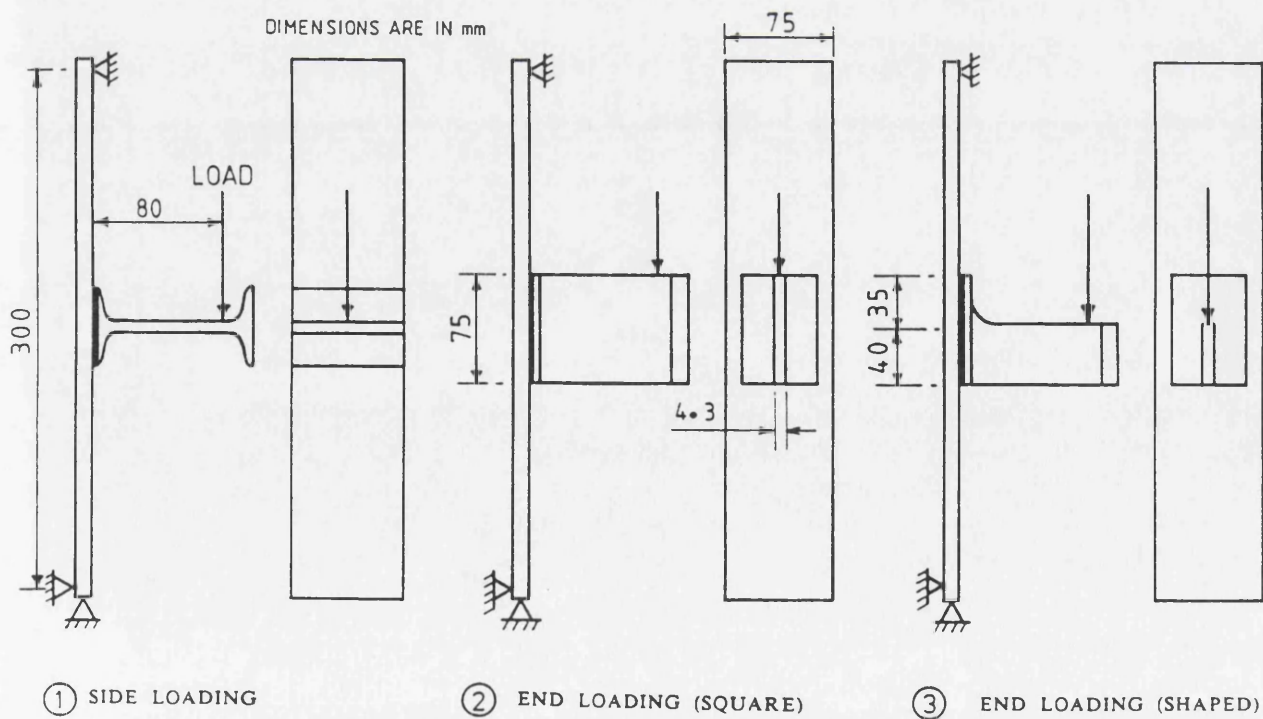
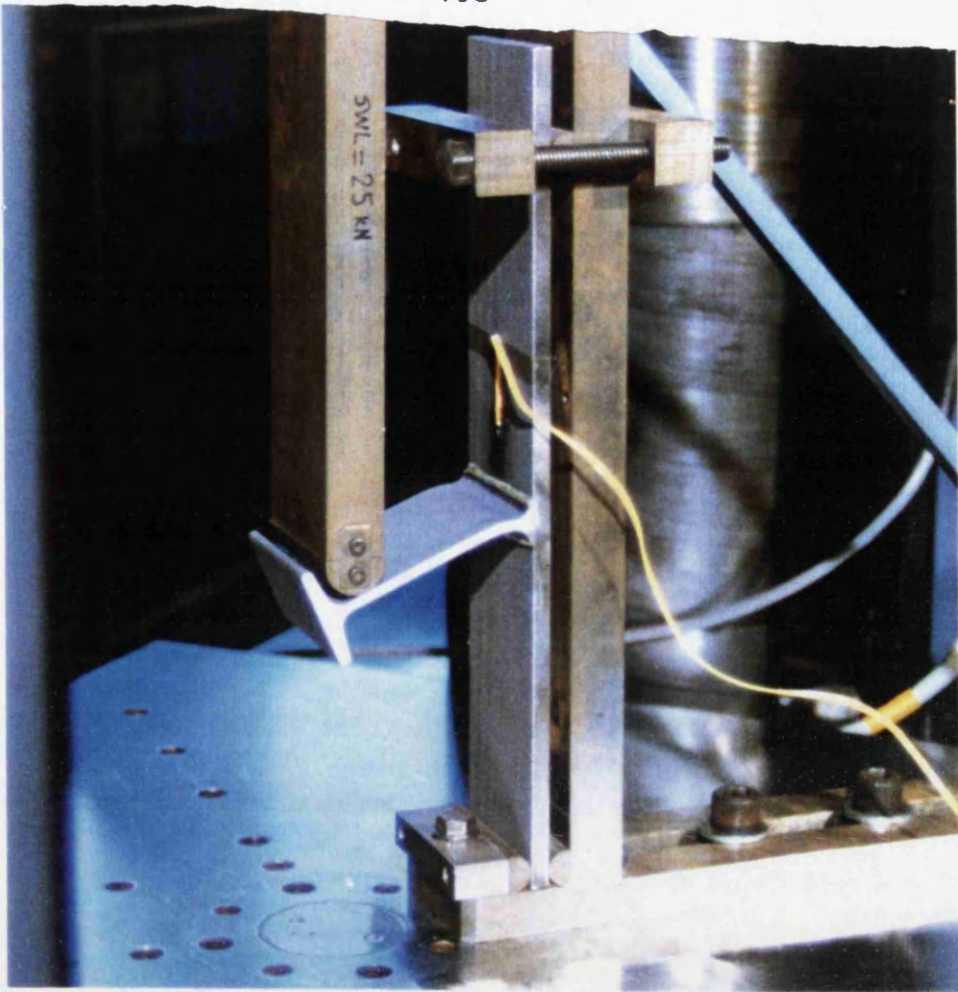
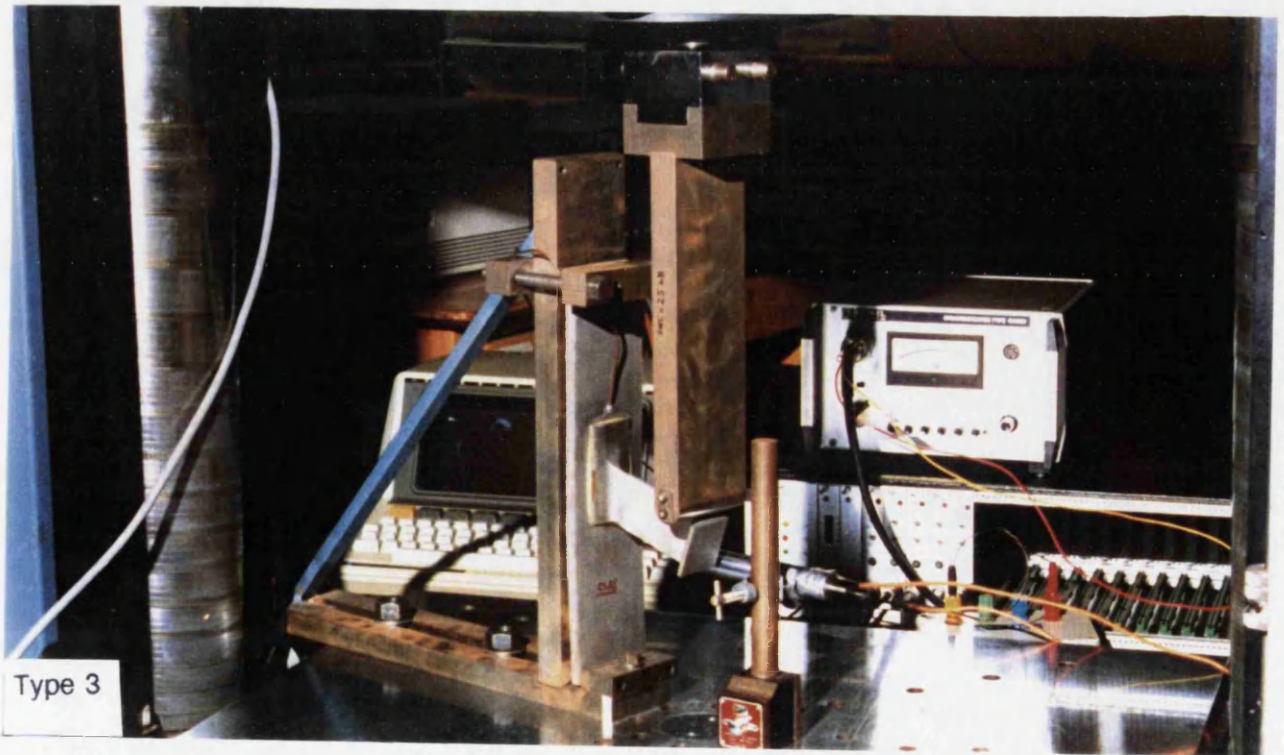


FIGURE 4.11 STEEL/STEEL CLEAVAGE SPECIMENS



Type 1



Type 3

FIGURE 4.12 TESTING OF STEEL/STEEL CLEAVAGE SPECIMENS

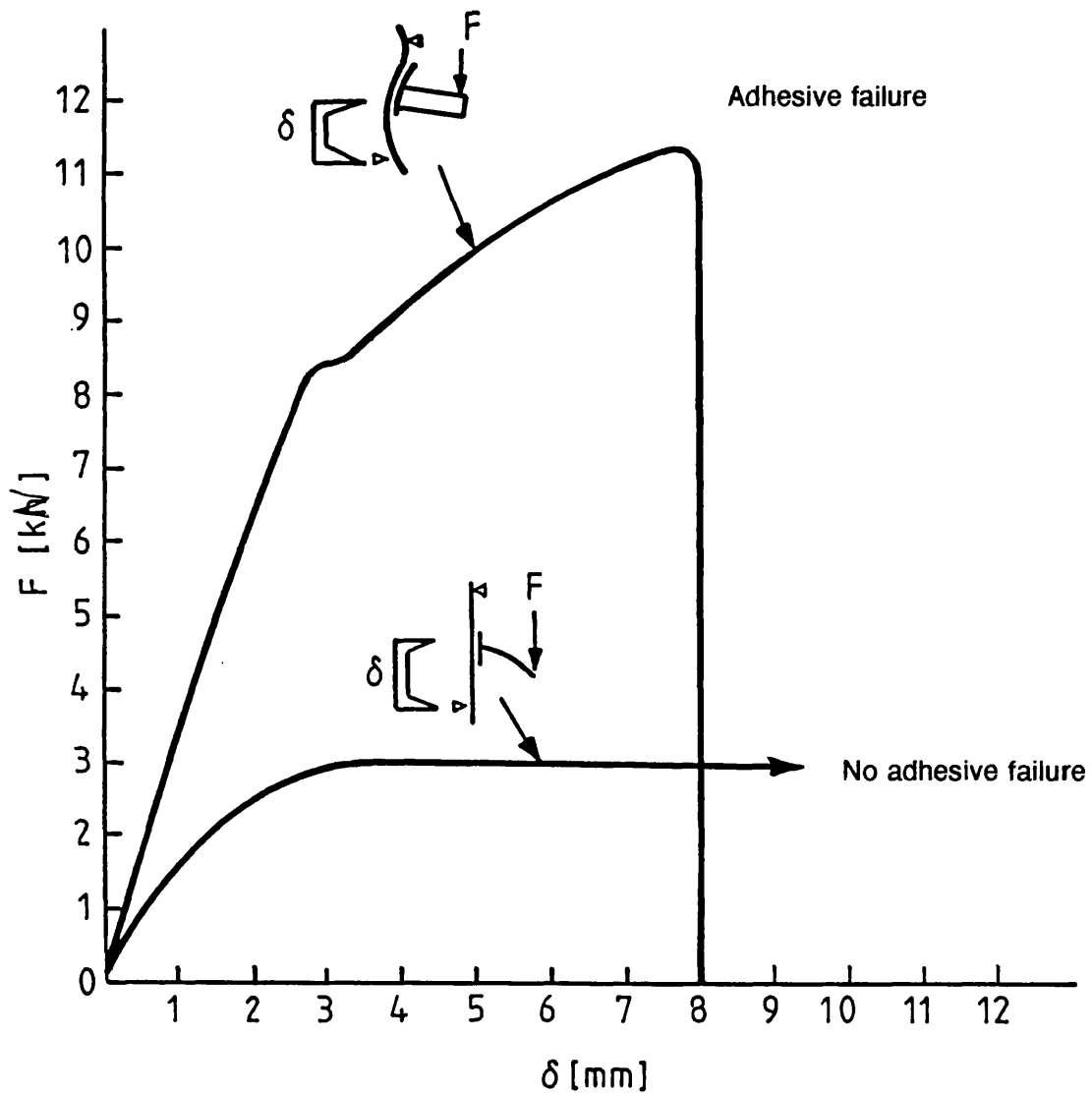


FIGURE 4.13 LOAD-DEFLECTION FOR STEEL/STEEL CLEAVAGE SPECIMENS

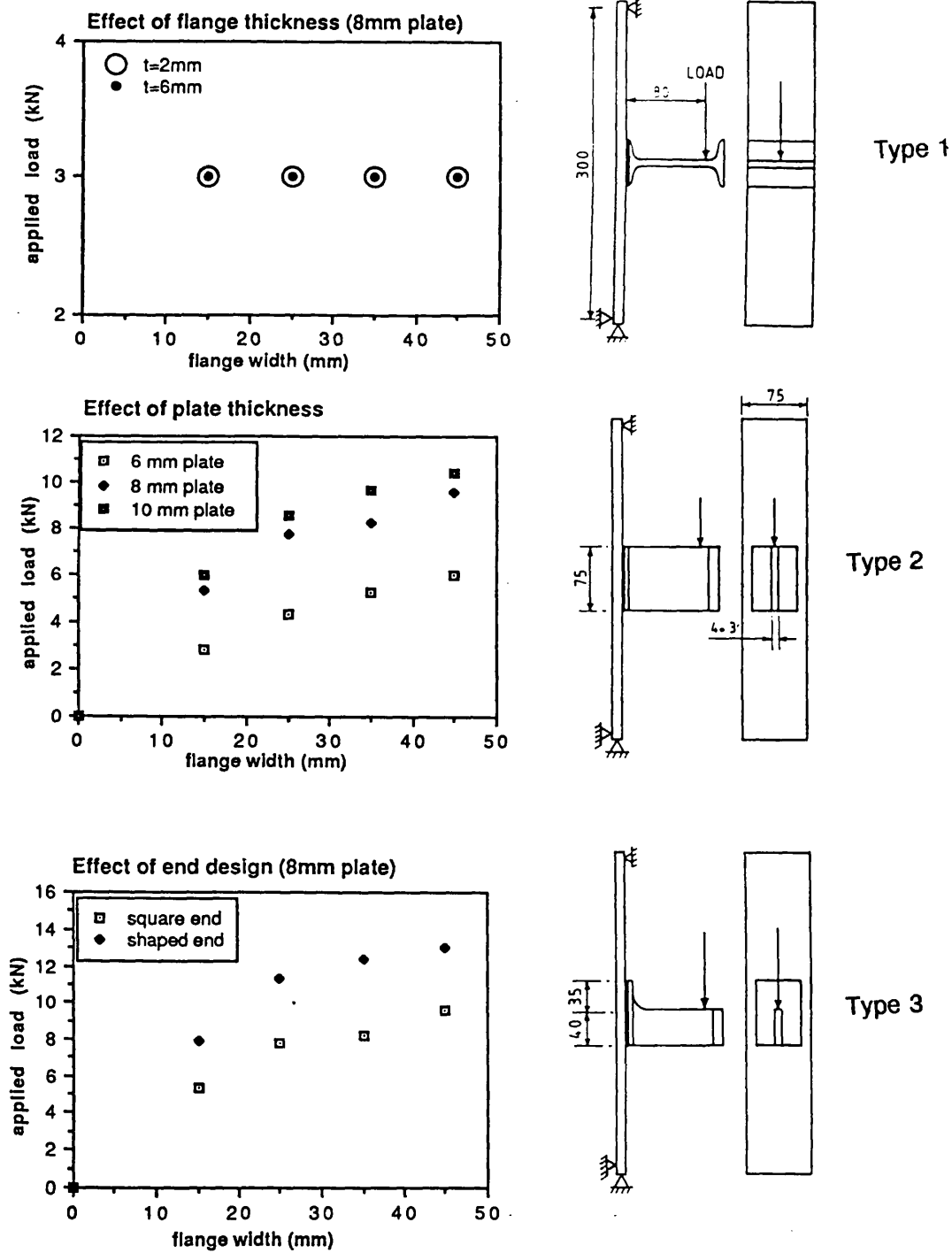
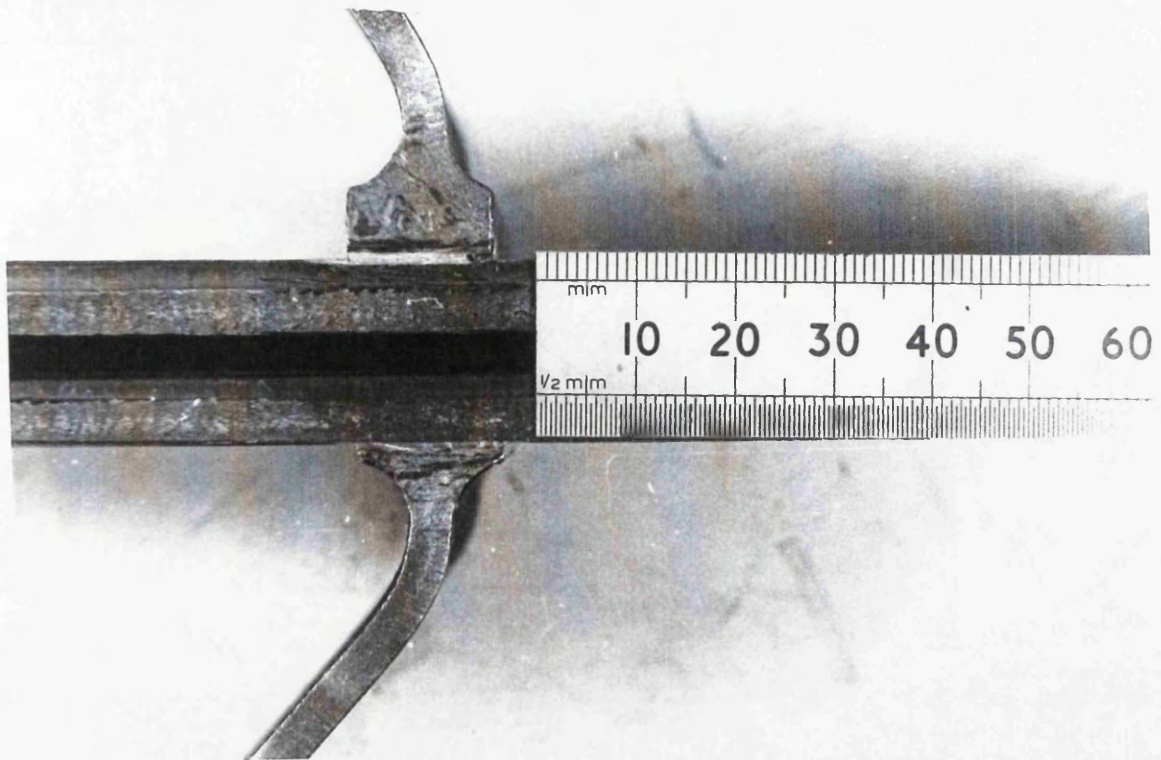
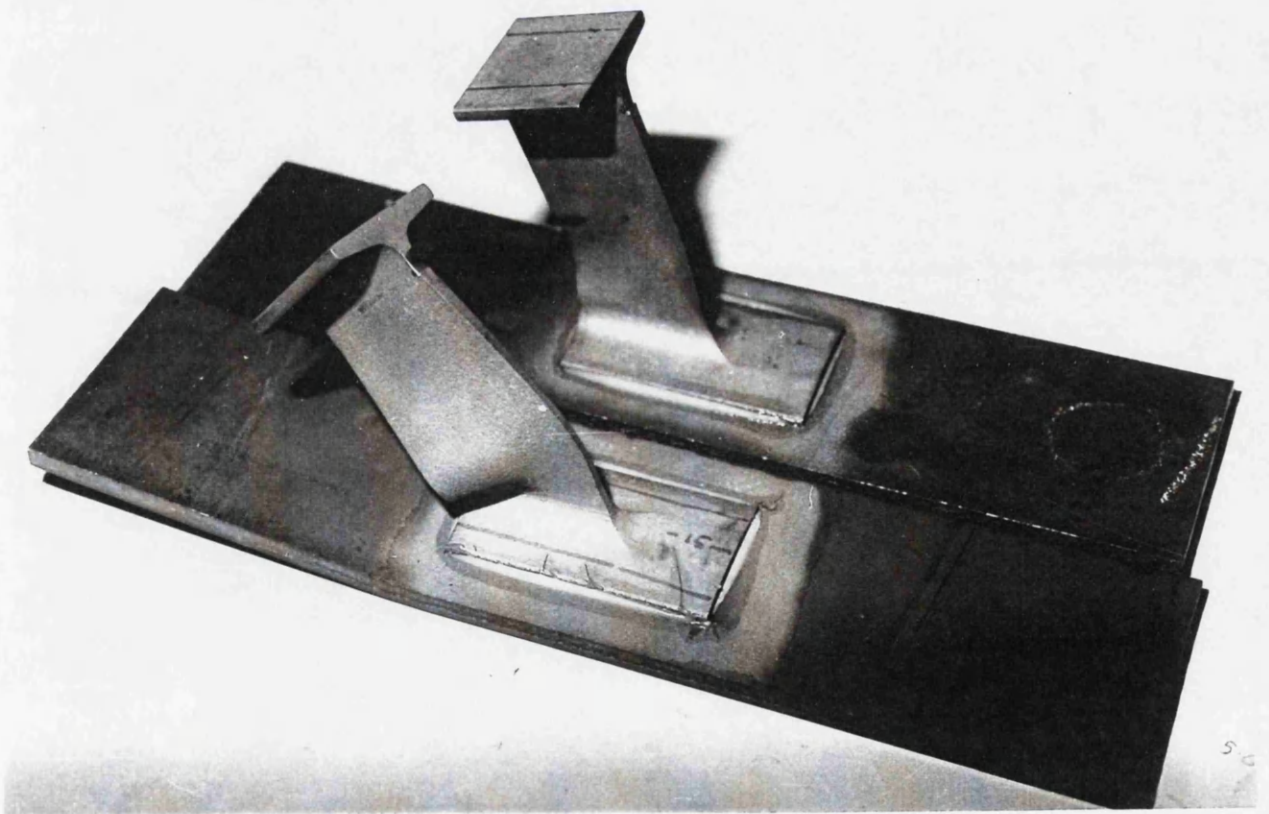


FIGURE 4.14 STRENGTH PERFORMANCE OF STEEL/STEEL CLEAVAGE SPECIMENS



Type 1



Type 3

FIGURE 4.15 DEFORMED STEEL/STEEL CLEAVAGE SPECIMENS (AFTER TESTING)

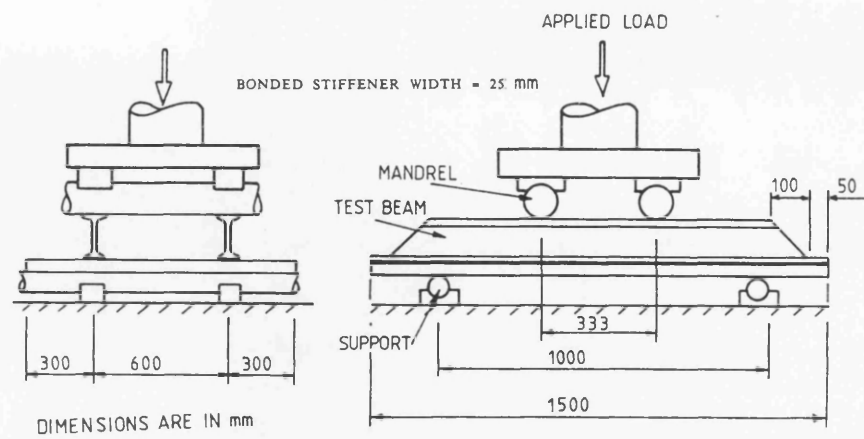


FIGURE 4.16 TEST ARRANGEMENT AND DETAILS OF PANEL TESTING

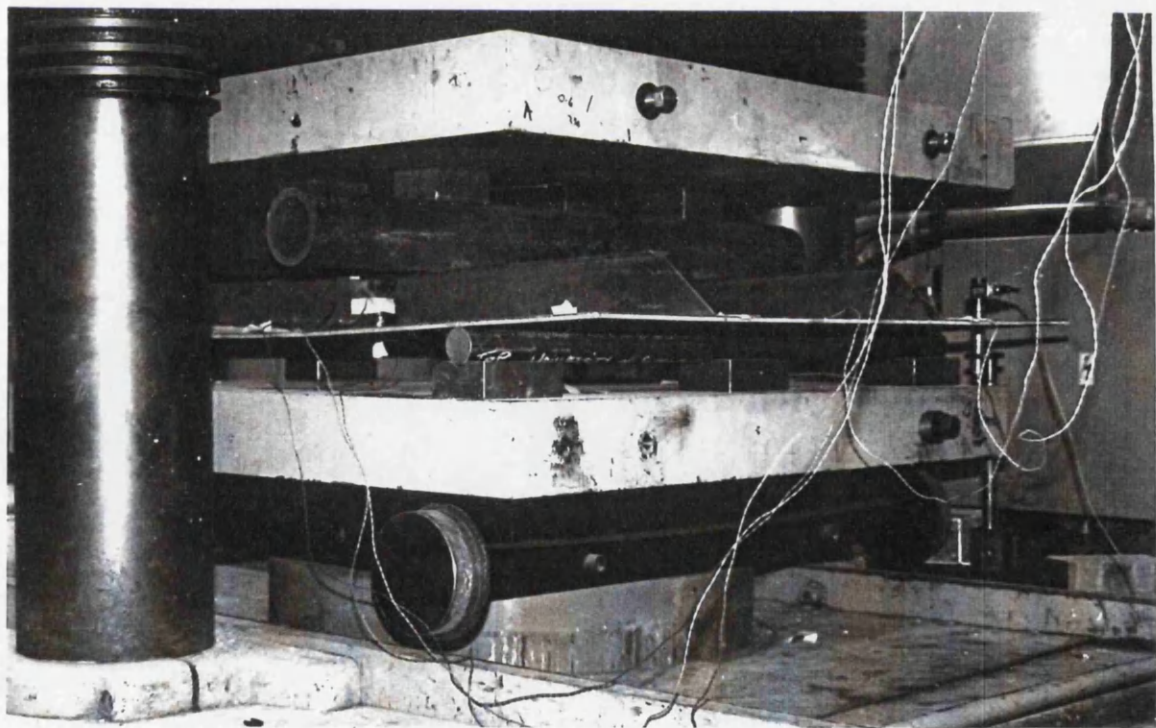


FIGURE 4.17 LARGE STEEL/STEEL PANEL DURING TESTING

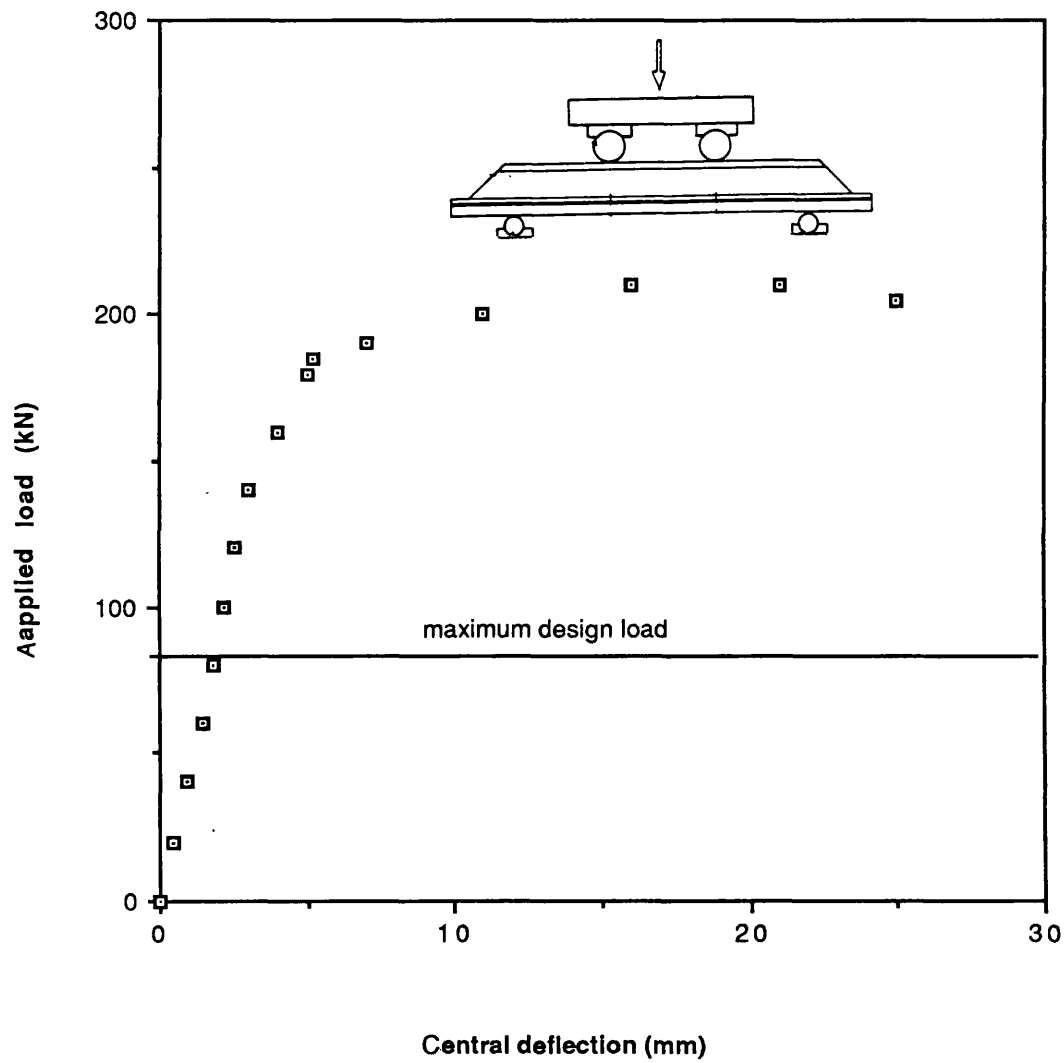
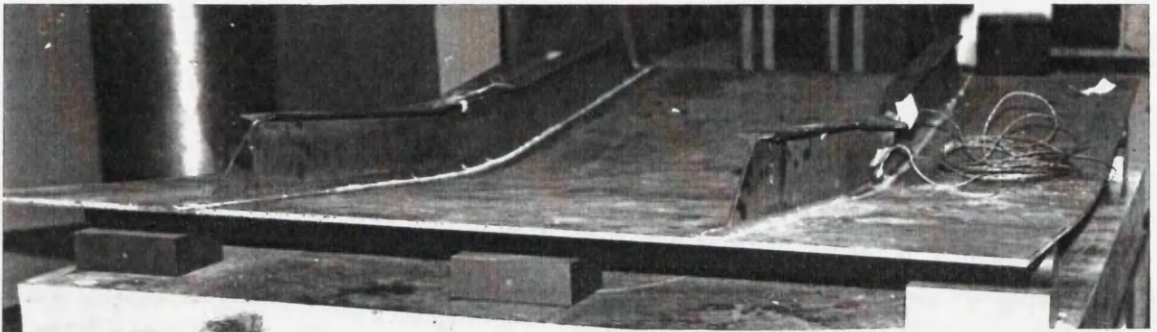


FIGURE 4.18 LOAD-DEFLECTION FOR PANEL TESTING



Specimen AN



Specimen BN



Specimen AP

FIGURE 4.19 DEFORMED PANEL SPECIMENS AFTER TESTING (TABLE 4.4)



FIGURE 4.20 STEEL/GRP CLEAVAGE SPECIMENS

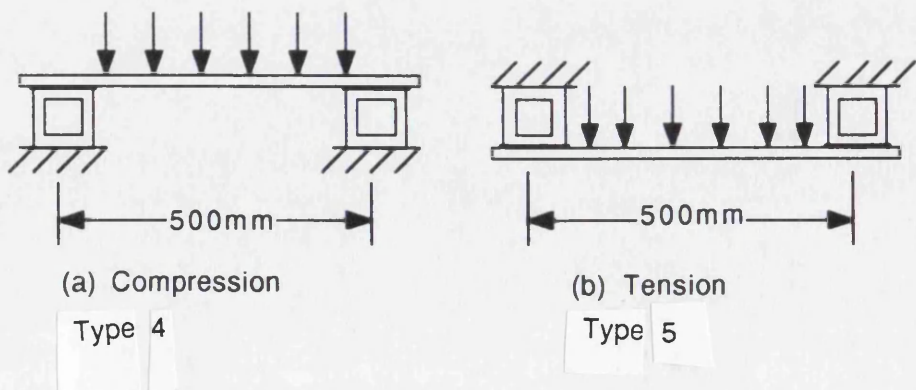


FIGURE 4.21 PRESSURE LOADING ON GRP SKIN BETWEEN STEEL STIFFENERS

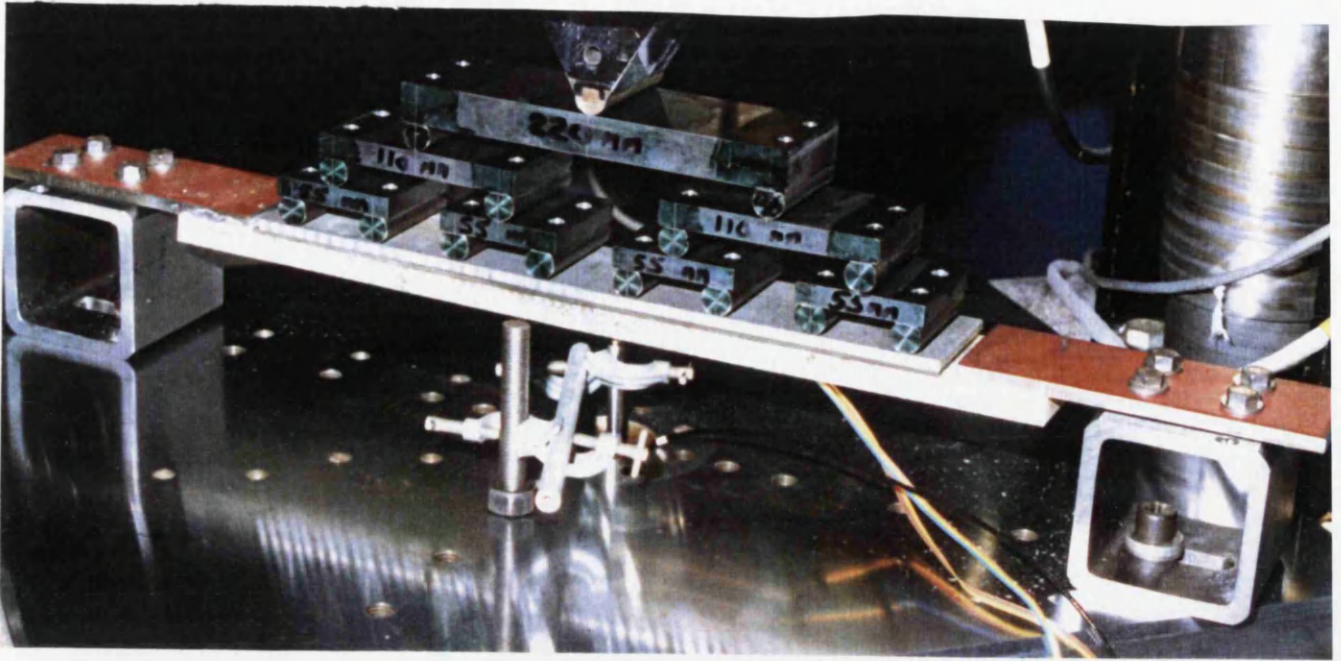


FIGURE 4.22 PRESSURE LOADING TEST ON STEEL/GRP TENSION SPECIMEN (TYPE 5)

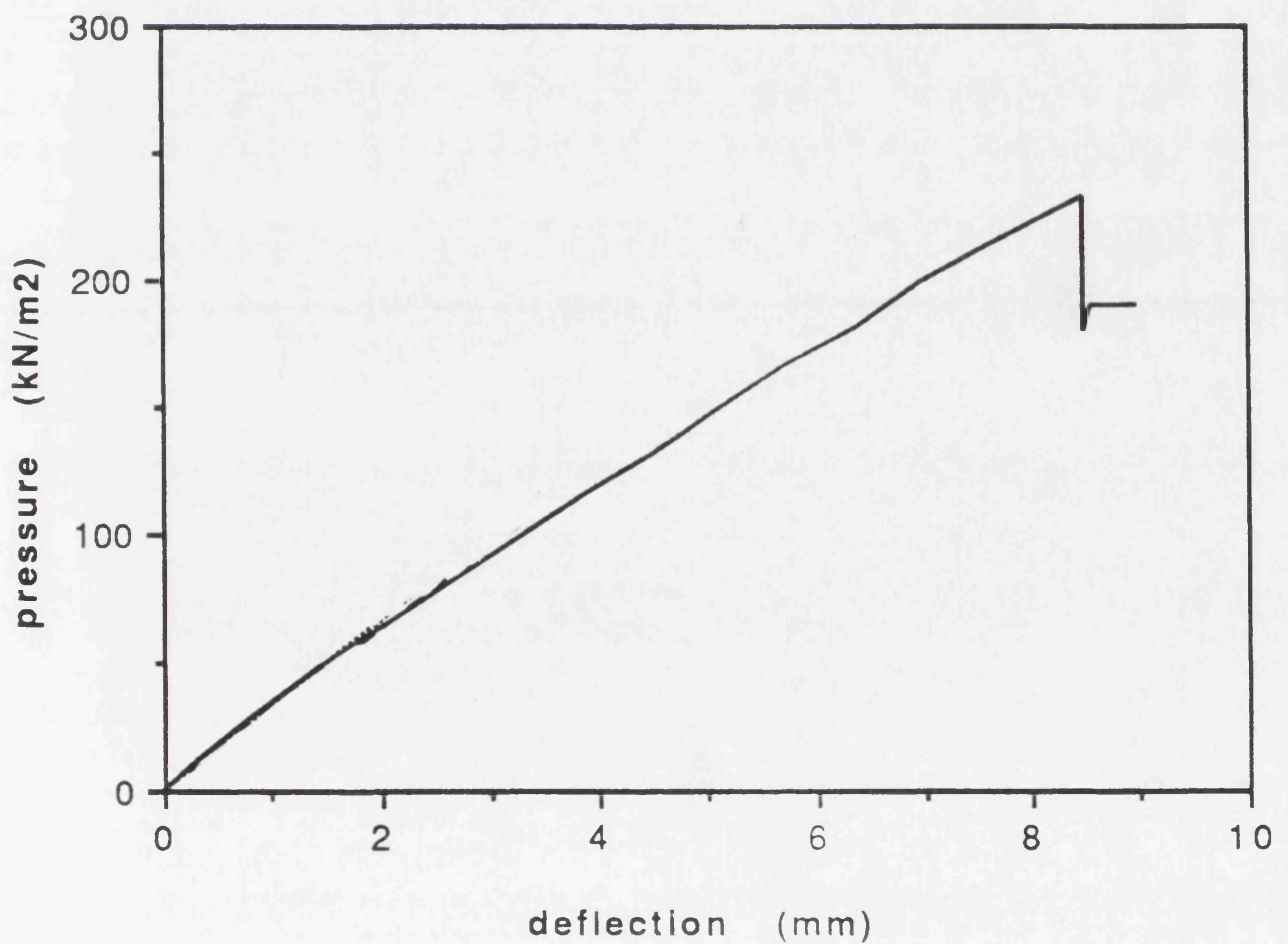


FIGURE 4.23 LOAD (PRESSURE)-DEFLECTION OF STEEL/GRP TENSION SPECIMEN UNTIL FAILURE

5. STRESS ANALYSES

In the previous two chapters, the performances of single part and two part epoxy adhesives have been illustrated through small and large scale mechanical testing. The theoretical models used in this study relate to the types of mechanical testing samples investigated in the previous chapters. This investigation included (i) the determination of stress levels in both small and large scale test pieces (steel/steel and steel/GRP), (ii) the relation between failure stresses in these small and large test specimens and whether or not it is possible to correlate adhesive failure stress of standard small specimens with that of large scale specimens, and (iii) the global behaviour associated with bonded structures, of composite (steel/adhesive/steel) section.

The manufacture and testing of these specimens had to be very carefully controlled in order to obtain accurate measurements of behaviour. During the bonding of specimens, the objective was to obtain a void free bond line with uniform bond line thickness. Accuracy is required in the machining of the dimensions of the adherends to $\pm 0.1\text{mm}$. Special attention to specimens details, bonding and testing jigs was required to avoid possible errors related to variations in adhesive line thickness and incorrect test boundary conditions.

A finite element package, PAFEC 75, was used for all the numerical analyses presented in this chapter. The analyses were based on elastic properties of the materials. Eight noded quadrilateral isoparametric 2-D elements were used. Large numbers of these elements were required (up to 1000 elements) due to the thinness of the adhesive lines (0.2-0.5mm) in relation to thickness of the adherends (5-15mm). Elements were concentrated near the adhesive/adherend zones towards the joint ends where high tensile cleavage stresses were expected. A refined mesh was needed for two reasons. The first was the need for structurally stable elements in severe deformation. Elements with a high length-to-width aspect ratio can collapse when used for meshing a highly stressed area. The second reason was to account for the steep stress gradients towards the ends of bonded joints, which require more detailed stress fields.

The approach to model selection, experimental programme and theoretical analysis are presented in the following sections with results and discussion.

5.1. STEEL/STEEL JOINTS

In this section steel/steel bonded joints modified from the Type1 large cleavage specimen (Figure 4.11) together with the Types 1 and 3 small standard specimens (Figure 3.6) were used for the experimental and theoretical analysis. Epoxy adhesive Araldite 2007 was used throughout in this study.

5.1.1. MODEL IDEALISATION

The physical model was carefully designed to represent the realistic, stiffened skin, load bearing joint in question (grillage connection). Such a model was designed to represent a possible behaviour of the load bearing joint which may be subject to a "tripping" action as a result of a stiffener collapse (Figure 2.9).

Figure 5.1 illustrates diagrammatically the idealisation of such a model. Failure could occur as a result of extreme loading conditions, such as impact loading which causes plastic bending or compressive buckling of the bonded structure. Substructuring involved reducing the problem from one of a complete transverse structure to that individual one is shown in Figure 5.1. This model may also be used to explain local failure mechanisms under ultimate design load or stress levels relating to service conditions, in the transverse direction to an adhesively bonded stiffened structure.

Furthermore, the model represents the influence of joint stiffness on failure load/strength. This is achieved by varying the effective width for the stiffened joint from 200mm to 300mm. These are represented in Figure 5.1 and referred to as follows:

- Type A refers to a model with 300mm span between supports
- Type B refers to a model 200mm span between supports

5.1.2. EXPERIMENTS AND RESULTS

The model test specimens (Figure 5.1) were carefully prepared for bonding in order that the maximum strength was obtained. After correct surface preparation (Chapter 3) had been carried out the adhesive was applied to the surface of the block with only enough smeared on the plate to allow the 0.5mm metal wires, used to control the bond line thickness, to be positioned. Three wires were positioned away from the upper edge of the

joint (where stress levels were expected to be a minimum) and equally spaced across the width of the joint. The two halves of the joint were then joined and checked for alignment before being clamped together. After clamping the joint was again checked for alignment before being put in an oven for curing.

After the specimen had been bonded and cured it was then cleaned up to remove the excess adhesive from around the joint. This has to be carried out carefully to avoid introducing cracks or undercut into the adhesive layer which could cause additional stress concentration in the joint. One strain gauge was then mounted on the plate in a position adjacent to the upper edge of the joint (Figure 5.1).

The experimental set up on the testing machine utilised the same test rig as used for Type 1, 2 and 3 test specimens described in Chapter 4. This rig was designed to hold the specimens in such a manner as to give the required boundary conditions for the structural analysis. The support rollers of the jig were sprayed with dry lubricant (PTFE). The test specimen, in position during this test, is shown in Figure 5.2 which shows the position of applied loading on the block (stiffener). The vertical deflection at the loading point of the specimen was measured with a 25mm gauge-length extensometer attached to the crosshead of the testing machine. Values for load, deflection and strain were recorded. An in-house data logging computer program was modified and used with data acquisition equipment for these tests. The equipment included the following:

- Analogue strain recorder (quarter bridge connection)
- Three channel Micro-Link processing system
- HP 87 micro-computer and display system

The crosshead displacement rate for the experiments was set at 0.2 mm/min and the data logged at intervals of 5 sec until joint failure. The output from these experiments is presented in the form of curves for load-deflection and load-strain as shown for the two test specimens (Type A and B) in Figures 5.3 and 5.4. From these curves and observations during the experiment, it is possible to make the following comments:

- The shapes of load-deflection curves for both models (Type A and B in Figure 5.3a and 5.4a respectively) indicate that the plate in each test was deformed plastically before the failure of the adhesive joints. The value of deflection at failure for Type A specimen is 1.7 times that for Type B specimen. While this is expected behaviour due to increase in span from 200mm to 300mm, the results represent comparative measurements only. This is because the accuracy of measuring the specimen deflection from the crosshead position is relatively low.

- In both cases the maximum strain gauge readings (Figure 5.3b and 5.4b) also indicate that the plate incurred significant bending stresses (assumption of elastic relationship) of 440 and 400 N/mm² for Types A and B respectively. It was also noticed that in both tests the strain gauges debonded due to the excessive deformation.
- The failure load for specimen/model Type A was 12% lower than that for Type B specimen. This is due to the increase in stiffness imbalance for Type A as well as in the bending moment near the adhesive edges. The same trend was noticed when changing the thickness of the plate (Tables 4.1 and 4.2).
- Comparing the failure load for model Type A model(10.37 kN) with that for the cleavage specimen Type 1 (3kN-Figure 4.11), the former is 3.5 times the latter. Both specimens have the same dimensions except that the block in Type A replaced the I section stiffener in Type 1.

5.1.3. NUMERICAL ANALYSIS

The experimental models and results are supported by numerical solutions in order to investigate the range of validity of the various analyses presented in this chapter. Solutions were produced from a general finite element computer package, PAFEC. The input files for these finite element programs are listed in Appendix IV (Sections IV.1 and IV.2) and the mesh details are presented in Figure 5.5. The mesh was constructed using 500, eight-noded, isoparametric plane strain finite elements to represent the adhesive-steel joint with an adhesive thickness of 0.5mm. The figure also shows the details of the smaller elements used towards the tensile region of the bond line and also the five subdivisions through the adhesive thickness. The material elastic properties used in this analyses were:

Adhesive Young's Modulus = 5000 N/mm²

Adhesive Poisson's ratio = 0.35

Steel Young's Modulus = 210000 N/mm²

Steel Poisson's ratio = 0.3

The typical mode of deformation resulting from the finite elements analysis of the Type A model (numerical) is shown in Figure 5.6.

The analysis enabled the variation of dimensions and material properties. The output gave the maximum and minimum principal stresses and the maximum shear stress at the

individual nodes on the element boundaries as well as the centres of these elements. Nodes locations give more accurate results compared with those from the elements. This is because there are significant differences in the sizes of the elements used in such a mesh. The average stresses at each node are generated from the neighbouring elements. This makes the determination of stresses at interface nodes between different materials difficult and these are therefore ignored.

The nodal stress distributions across the 45 mm of the numerical model for Types A and B specimens are plotted in Figure 5.7 and 5.8 respectively. The stresses in these two figures vary through the adhesive thickness (0.5mm) and are given for positions 0.1 and 0.4 mm above the plate surface. In these distributions both the maximum and minimum principal and maximum shear stresses are plotted. From these results the following observations are possible:

- The distribution of stresses across the joint is highly nonlinear and peak stresses are restricted to a very small region of the joint. The level of the stress towards the tension end is high for polymeric type materials. This may suggest that plastic deformation of the adhesive has occurred, but it is difficult to assess this without knowing the inelastic properties for the adhesive.
- The maximum principal stresses in the adhesive near the plate surface shown in Figures 5.7a and 5.8a, at 0.1mm above the plate surface (tensile failure stress), are about 30% higher than those shown in Figures 5.7b and 5.8b, at 0.4mm above the plate surface (ie. 0.1mm below the stiffener/block surface). The stresses at the edge nodes were ignored in all cases due to the singularity problems.
- The maximum tensile principal stress is 170 N/mm^2 and the maximum shear stress is 80 N/mm^2 , which are about 90% higher than values for average tensile and shear stresses, obtained from standard butt (90 N/mm^2) and lap shear specimen (45 N/mm^2) type tests (Table 3.2-Araldite 2007).
- There is a very good agreement between the maximum principal failure stresses of adhesive for models Types A and B (principal stresses at distance=0 -Figures 5.7a and 5.8a). In fact there is a stress difference of 2% higher in the favour of Type B. This despite a failure load difference of 12% in favour of physical model Type B (Figures 5.3 and 5.4).

Two types of standard specimens models were also analysed numerically with the aim

of relating adhesive failure stresses in small specimens with those occurring in a stiffener/plate joint under failure loading conditions. These geometries were the tensile lap shear (shear) and the tensile edge loaded butt (cleavage) joint (Types 1 and 3 - Figure 3.6). The mesh details and boundary conditions are shown in Figures 5.9 and 5.10 for shear and cleavage respectively. The input files for the finite element programs are listed in Appendix IV (Sections IV.3 and IV.4), with the same mesh concepts and the same materials properties and adhesive thickness (0.5mm) considered in the previous finite element analysis.

The experimental failure load was based on a one-off carefully prepared specimen for each model. The failure load values, with were 17 kN and 12 kN respectively for the shear and cleavage joints (typical values of Types 1 and 3). It should be mentioned here that the Type 2 (butt joint) was excluded in this investigation due to the very significant scatter observed in failure load, as will be discussed further in Chapter 7.

The numerical results from analysing these two type of joints are plotted in Figure 5.11 for the shear joint and in Figure 5.12 for the cleavage joint. From these results the following observations may be made:

- The stress distribution, for the lap shear model, as expected, is a non-linear along the specimen overlap (15mm). As in the previous case, because of the mathematical singularity problems at the end of the joint, the stresses have been ignored at the ends of the joint.
- Figure 5.11a shows that at a distance 0.1mm above the lower adherend surface, the shear and tensile stress levels are significantly higher at the left hand side of the joint (Figure 5.9). This trend is the opposite at 0.4mm (0.1mm below the upper adherend surface) as shown in Figure 5.11b. This would suggest that it is possible to predict the location of failure initiation in the joint .
- The stress distribution in the cleavage joint represents the stress level at any point through the thickness as shown in Figure 5.12. This is because the level of stress and distribution is found to be the same at 0.1, 0.2, 0.3 and 0.4mm above the surface of the lower adherend. Again, there are uncertainties in the stress levels at joint edges and these are ignored.
- Comparing the maximum tensile stress from the tensile cleavage model (Type 3 standard specimen) analysis, which is 112 N/mm^2 , with that obtained from the tensile lap shear model (Type1 standard specimen) of 169 N/mm^2 , shows the latter is 50% higher than the former. This suggests that, either the failure

stress of the adhesive is difficult to establish with the use of tensile cleavage specimen due to high stress concentration (singularity problems) or as in the case of the standard tensile butt specimen (Type 2), the cleavage geometry is very sensitive to loading misalignment which can cause failure loads to be lower than expected (Chapter 2).

- There is again very good agreement between the maximum principal stresses (failure tensile stresses) between Types A and B (Figures 5.7a and 5.8a) and the lap shear joint model (Figure 5.11a), with less than a 3% difference between them.

5.1.4. ANALYTICAL SOLUTION

The classical stress analysis theory used in this research is one developed recently¹⁰⁰ from principal analyses in lap shear joints. This analysis however has been made more suitable for a variety of sandwich configurations such as L, T and T-peel joints. The basic analysis models the adherends as cylindrically bent plates of different flexural stiffness and the adhesive as an elastic interlayer transmitting only direct or cleavage stresses. As the upper and the lower adherends are completely independent, joints with adherends of different thicknesses and materials can be analysed. In order to utilise the analyses, boundary conditions for sandwich configurations should be defined in the manner illustrated in a diagram in Appendix V (Figure V.1). This diagram shows the positive direction of these boundary forces and moments. The derived expression from this theory is as follows:

$$\frac{\sigma_y}{k_a} = A \cos \alpha x \cosh \alpha x$$

The main equations and constant definitions are detailed in Appendix V.

It should be noticed here that the upper part of this sandwich configuration represents the block part of the experimental model. Appendix V also details the calculations to determine the above constants. The calculations of forces and moments generated at the boundary of the model specimen have also been detailed in Appendix V .

Cleavage stresses on the tension side of the joints for model A and B were calculated (Appendix V) using the above formula and are presented in Table 5.1. This table also includes (i) the tensile average stress values at the joint edges, from the finite

element analyses (Figures 5.7a and 5.8a) and (ii) bending stress results from analytical methods, which treat the block attachment as a cantilever (in a similar manner to that shown in the previous chapter (Section 4.3.1). The values calculated from the sandwich analytical and finite element analysis suggest that there is some agreement (see Table 5.1). The difference in the stress values at the end of the joint is approximately 18% higher in the finite element analysis. This agreement which initially appears to be good, on closer investigation may be questionable as will be discussed in Chapter 7. The cantilever bending moment calculation (Section 4.3.1) on the other hand produces stress level at the adhesive four times lower than that obtained from the other two methods. This is because this approach does not include the bending moments at the plate.

5.2. STEEL/GRP TENSION JOINT

In a similar manner to the previous section, the level of tensile (cleavage) stress in the adhesive (Araldite 2004) was investigated with reference to the steel/GRP tension specimen (Type 5-Figure 4.22). The failure stress was then compared with that of the standard steel/GRP tensile lap shear specimen (Type 1-Figure 3.8).

5.2.1. MODEL IDEALISATION

In this model the failure mechanism was assumed to be restricted to the pull-out mode of the GRP skin away from the the square section frame due to pressure loading. It consisted of a stiff GRP plate which represented the stiffener/frame with clamped boundary conditions. The physical model used here had the same configuration as steel/GRP tension specimen (Type 5-Figure 4.21) as shown in Figure 5.13

5.2.2. EXPERIMENT AND RESULTS

The bonding process of this specimen (14.5 mm GRP thickness) was carried out in the same way as for Type 4 specimen except that the peel ply and adhesive mixing system were used in this case (Chapters 3 and 4). The thickness of adhesive was controlled to 0.5mm. A spew fillet of 1.5mm leg length was machined after the curing of the joint. The same testing machine, logging system and static loading conditions as in the previous

experiment (Section 5.1.2) were used. Figure 5.14 shows the experimental results of load, central stress and deflection for the pull out test. From this figure the following observations can be made:

- The pressure of 2.3 bar (230 kN/m^2) at joint failure is approximately 30% higher than the average failure pressure of 1.8 bar for the earlier experiments (Table 4.4). This is due mainly to the use of peel ply and automatic mixing equipment used for these experiments. A similar effect was observed on small lap shear joints, as discussed in Chapter 3.
- The experimental tensile bending stress at mid-span of the GRP skin at adhesive joint failure load was approximately 50 N/mm^2 (Figure 5.14b) represents approximately 25% of the ultimate tensile strength of the GRP material (Table 1.1).

5.2.3. NUMERICAL ANALYSIS

In an attempt to predict failure in the pull-out joint described above a finite element method was used in the similar manner described in section 5.1.3. The woven roving GRP and Araldite 2004 epoxy adhesive material (in addition to steel) elastic properties used in this analysis were:

Adhesive Young's Modulus	=	4000 N/mm^2
Adhesive Poisson's ratio	=	0.35
GRP Young's Modulus	=	14000 N/mm^2
GRP Poisson's ratio	=	0.13

The input file for this analysis is detailed in Appendix IV (Section IV.5). Typical boundary conditions, detailed mesh at the fillet and adhesive stress distribution at 0.1mm above the GRP surface are shown in Figure 5.15. From this figure it can be observed that the tensile cleavage stress is well above the average values obtained from standard steel/steel tensile butt specimen (Type 2-Table 3.4-Araldite 2004). This may suggest that the stress has exceeded the elastic limit of the adhesive.

As for the steel/steel joints (Section 5.1.3), a standard steel/GRP tensile lap shear specimen (Type 1) was also analysed for correlation with the larger joint described above (Figure 5.15). The input file for this analysis is detailed in Appendix IV (Section IV.6) and the stress distribution for this model is shown in Figure 5.16. From this figure there is a good correlation (as in the steel/steel case). The failure stress of the

lap shear joint (failure load=6.35 kN with maximum principal stress=152 N/mm²) is within approximately 10% of that predicted for the large steel/GRP tension model (failure load=230 kN/m² with maximum principal stress=165 N/mm²). This comparison assumes that the simulated loading and boundary conditions for the tension model gives a good representation to the actual joints. The reliability of this failure prediction is discussed further in Chapter 7.

5.3. FLEXURAL BEAM LOADING

A bonded structural beam under lateral loading, such as the stiffened beam described in Section 4.4, may be expected to behave differently from a beam with continuous/homogeneous material throughout its section. This section addresses this problem, in particular the stresses and deflections in a small model beam representing such an adhesively bonded (composite) structure. In addition, the adhesive shear stress resulting from an applied bending moment in a bonded beam will be assessed and compared with that obtained from the lap shear joint analysis. In this study steel/steel joints bonded with Araldite 2007 epoxy adhesive are considered.

5.3.1. MODEL IDEALISATION

The beam model is illustrated in Figure 5.17. This model simulates the loading imposed on an adhesive layer within an element of load bearing related structure subjected to lateral loading in the longitudinal direction of the stiffener (Figure 5.17a). A symmetric section was then assumed with simply supported boundary conditions as shown in Figure 5.17b. This assumption was made to obtain a simplified model as well as to have the neutral axis of the beam at the centre of its section.

The dimensions of this model were arbitrarily chosen and restricted to a support span of 30mm and a width of 25mm. This was considered adequate to enable direct comparison with the shear stress distribution obtained from lap shear joint (15mm overlap and 25mm wide). A concentrated load was assumed as shown in Figure 5.17 and thus, the assessment of the bending shear (interlaminar) stress in the adhesive line is possible. Figure 5.17d shows another beam model of the same dimensions to that shown in Figure 5.17c, but of homogeneous steel material (continuous transverse section) which was intended to represent an equivalent welded structure (without residual

stresses or defects).

The two beam models will be referred to as follows:

- Type C is a bonded beam
- Type D is a solid beam

These models enable assessment and comparison of flexural stiffness for such bonded structures and, in conjunction with composite beam theory, permitted analysis of the interface between bonded adherends (and not between adhesive and adherend).

5.3.2. EXPERIMENTS AND RESULTS

The required steel strips were manufactured to the exact dimensions (Figure 5.17) from mild steel, by milling and grinding. The surface preparation prior to bonding and curing of the adhesive was carried out in the same manner as for the small scale specimens described in the previous Chapters 3 and 4. However, more care was taken in applying the adhesive and closing the joint to avoid air entrapment within the adhesive line. In order to control adhesive line thickness, a specially designed bonding jig was manufactured with a very high accuracy to give a uniform 0.5mm adhesive thickness along the joint. Figure 5.18 shows this jig and the technique used to control the bondline thickness. After curing, the adhesive line thickness was checked using a microscope. One strain gauge was mounted on the centre of each specimen (one specimen was bonded and the other was solid) to measure tensile bending stress along the outer surface of the steel.

An extensometer system was developed to measure the displacement of the centre of the beam specimens during testing. This used two guide pins which were incorporated within a specially designed test rig on the Instron testing machine. The general arrangement is shown in Figure 5.19. The extensometer was calibrated for a maximum displacement of 0.5mm. This figure also shows the three point bending supports and loading mandrel which were carefully designed and machined to ensure full contact with the specimen and to provide simply supported boundary conditions.

Prior to loading of specimens dry lubricant (PTFE) liquid was sprayed on the supports and mandrel to reduce friction at the contact points with the specimen. The specimen was then loaded under a cross head speed of 0.2mm/min. The values of strain and deflection at the centre of the specimen were logged as a function of central loading. The results for the bonded (laminated) and homogeneous (solid) flexural short beams

are plotted in Figures 5.20 and 5.21 respectively. From these results and observations during the tests the following comments are possible:

- The bonded beam has a distinctly linear force-deflection response before gross plastic deformation (Figure 5.20a). The same response is observed in the force-strain curve (Figure 5.20b.). This figure also shows that the plastic deformation eventually caused debonding of the surface strain gauge. No joint delamination (adhesive debonding) occurred, but crazing (stress whitening) was observed on the sides of the plastically deformed specimen as shown in Figure 5.22.
- The solid beam, which had the same dimensions as the bonded one, exhibited a higher level of stiffness within the elastic range. The elastic stiffness of the solid beam was found to be approximately 60% higher than the bonded equivalent (5.20a & 5.21a). In addition, the yield and plastic strength are significantly higher for the solid beam.
- At a force of a 15 kN (In the linear range for both specimens), the surface strain level was approximately 20% higher for the bonded beam (compare Figures 5.20b and 5.21b). This comparison may be more reliable than that for global stiffness due to the likely contribution from the adhesive material deformation as well as steel indentation at the contact points.

5.3.3. ANALYTICAL THEORY

For laminated materials such as the bonded (laminated) model in this study, classical beam theory was modified to apply to the stacking sequences and bonding of individual plies in case of the polymeric composite materials. It has been shown by Hoff¹⁰⁷ and Pagano¹⁰⁷ that layered beams in which the plies are oriented symmetrically about the midplane possessing orthotropic axes of material symmetry in the plies which are parallel to the beam edges can be analysed by the use of laminated beam and plate theory. A beam such as that shown in Figure 5.23 can be analysed by classical beam theory if the bending stiffness EI is replaced by equivalent stiffness $E_x^b I$ defined in the following manner:

$$E_x^b I = \sum_{k=1}^n E^k I^k \quad (1)$$

Where E_x^b is the effective bending modulus of the beam, E^k is the modulus of the kth layer relative to the beam axis, I^k is the moment of inertia of the kth layer relative to midplane, and k is the number of layers in the laminate. For bending of symmetric laminates, the relation between stress and moment resultants and their definitions⁽¹⁰⁷⁾ are detailed in Appendix VI and for a two ply beam (k=2) yield the following equations:

$$\sigma_x^{(2)} = \frac{h}{2} \cdot f_1^{(2)} \cdot \frac{M}{I} \quad (2)$$

$$\tau_{xz}^{(2)} = f_1^{(2)} \frac{h^2 Q}{8I} \quad (3)$$

Where $\sigma_x^{(2)}$ is the bending stress at the skin of the beam, $\tau_{xz}^{(2)}$ is the interlaminar shear stress at the centre of the beam and $f_1^{(2)}$ represents an interface coefficient which is a function of beam curvature in the longitudinal direction. This curvature depends on the continuity condition between bonded adherends. The value for this coefficient is unity for a beam section with homogeneous material ($f_1^{(2)} = 1$). This means that there is continuity between two plies (ie solid beam). The interlaminar shear stress is often of interest in laminated beams which include adhesively bonded metallic joints carrying lateral loading, but the calculation of stresses often assume a homogeneous section ignoring the discontinuity between layers produced by adhesive lines.

Bending and shear stresses can, therefore be determined with some degree of certainty by utilising the experimental values (from Figures 5.20b and 5.21b). First the interface coefficient $f_1^{(2)}$ for the bonded beam may be determined by substituting the following values in equation(2), as follows:

$\sigma_x^{(2)} = 357 \text{ N/mm}^2$ (bending stress from experiment), $I = 2083 \text{ mm}^4$, $h = 10 \text{ mm}$,
 $M = 112500 \text{ Nm}$ and therefore:

$$f_1^{(2)} = \underline{1.32}$$

Thus the interlaminar shear stress can be calculated by substituting the following values in equation (3), as follows:

$$f_1^{(2)} = 1.32, Q = 7500 \text{ N and therefore:}$$

$$\tau_{xz}^{(2)} = \underline{52.8 \text{ N/mm}^2}$$

Therefore without considering the interface (bonding) factor, adhesive and adherend stresses in such structural configurations would be underestimated by 32%.

5.3.4. NUMERICAL ANALYSIS

In order to validate the above analysis a finite element model of the bonded beam specimen, the mesh of which is shown in Figure 5.24, was used in conjunction with an input file detailed in Appendix IV (Section IV.6). The model has a concentrated central load with simply supported boundary conditions. The size of elements is reduced significantly at both ends of the beam. The element sizes and type and analysis conditions are similar to those used in the previous numerical studies (Section 5.1.3). The resulting maximum shear stress distribution along the 15mm from either edge of this model, at the centre of the adhesive line (no variation in the adhesive stresses through its 0.5mm thickness) is plotted in Figure 5.25. The same diagram also shows two values of the interlaminar shear stresses. One is derived above from equation (3) and the other based on a homogeneous section ($f_1^{(2)} = 1$). From this figure the following observations are possible:

- There is a difference in the maximum shear stresses between the value obtained from equation (3) (52.8 N/mm²) and that obtained from the finite element analysis (58 N/mm²). The latter method produced approximately 9% higher stress than the former. This comparison is based on the stresses deduced at 0.5 mm from either end of the bonded beam model.
- The shear stress value is influenced by the compressive normal stress arising from the loading contact points. This is noticeable at the centre of this short beam, but can also be seen at the support positions (one end of the beam is shown in Figure 5.25). This may explain the reduction in the shear stress towards the centre. The variation between the ends and centre of the specimen is more than 100%. The stress values near the ends are more representative of the actual level of the interlaminar shear stress in the model. For a longer beam this variation may be less pronounced.
- The stress distribution (from Figure 5.25) is compared the shear stress distribution obtained from the finite element analysis of the 15 mm lap shear joint (Type 1-Figure 5.1), in Figure 5.26. The values for shear stresses for

both the standard overlap and beam joints have been based on an applied load of 15 kN. The figure indicates the possibility of a more uniform shear stress distribution in a beam-like joint (assuming a limited effect from the compression stress at the points of loading) compared with that expected in a lap shear joint. The ratio of the stress variation between the positions of 0 and 7.5mm along the two joints is approximately 75% higher in the case of the lap shear joint .

Further discussion of the above points will be presented in Chapter 7.

MODEL TYPE	FAILURE LOAD [kN]	ANALYTICAL(1) (PEEL ANALYSIS) CLEAVAGE STRESS [N/mm2]	F.E (2) MAXIMUM PRINCIPAL STRESS [N/mm2]	SIMPLE (3) CANTILEVER BENDING STRESS [N/mm2]
A	10.374	149	169	33
B	11.643	148	170	37

- (1) From Appendix V
- (2) From Figures 5.7 and 5.8 (0.1mm from plate surface)
- (3) Obtained in the same manner shown in Appendix II

TABLE 5.1 COMPARISONS OF ADHESIVE STRESS ANALYSES IN LARGE STEEL/STEEL
CLEAVAGE JOINTS (FIGURE 5.1)

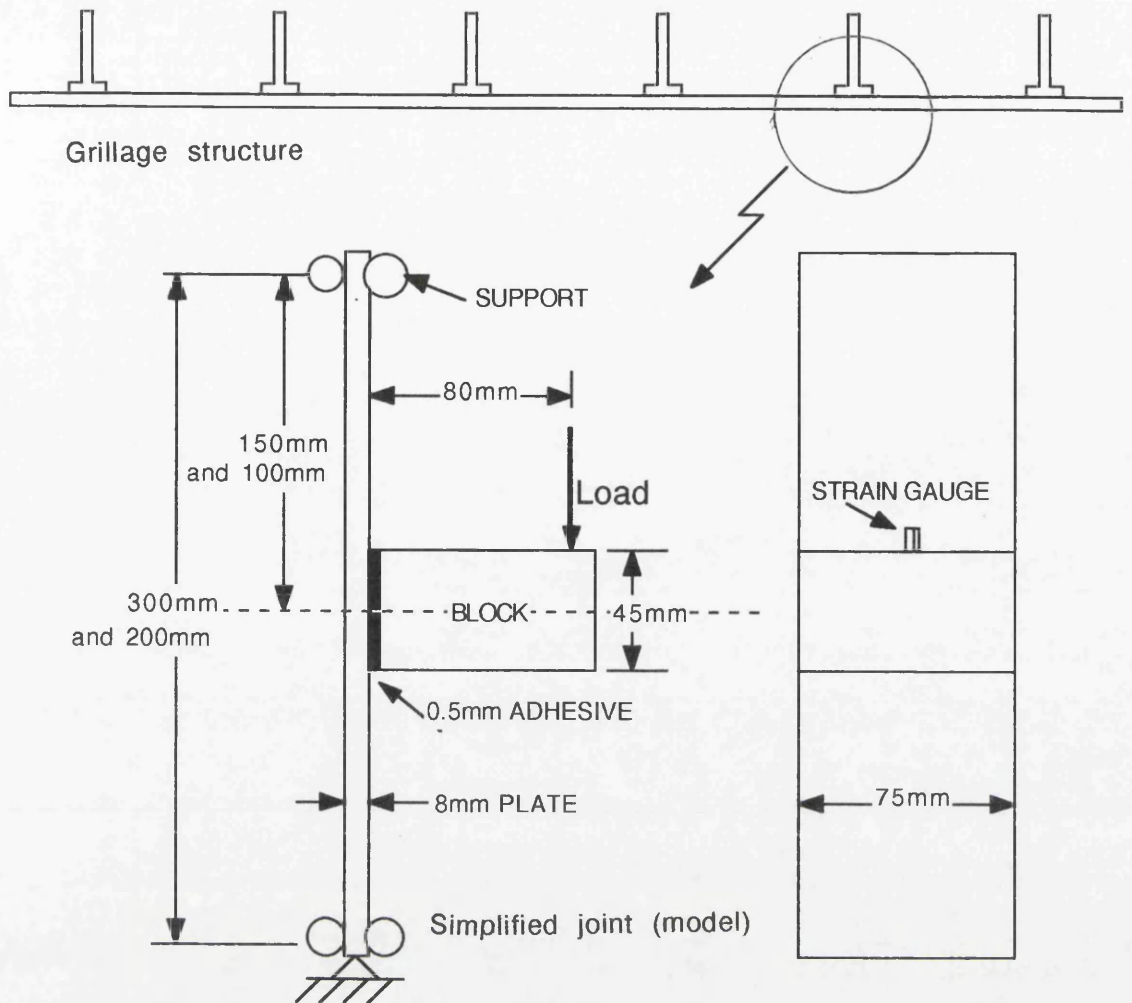


FIGURE 5.1 IDEALISED MODEL FOR STRESS ANALYSIS (SIMILAR TO TYPE 1-CHAPTER 4)

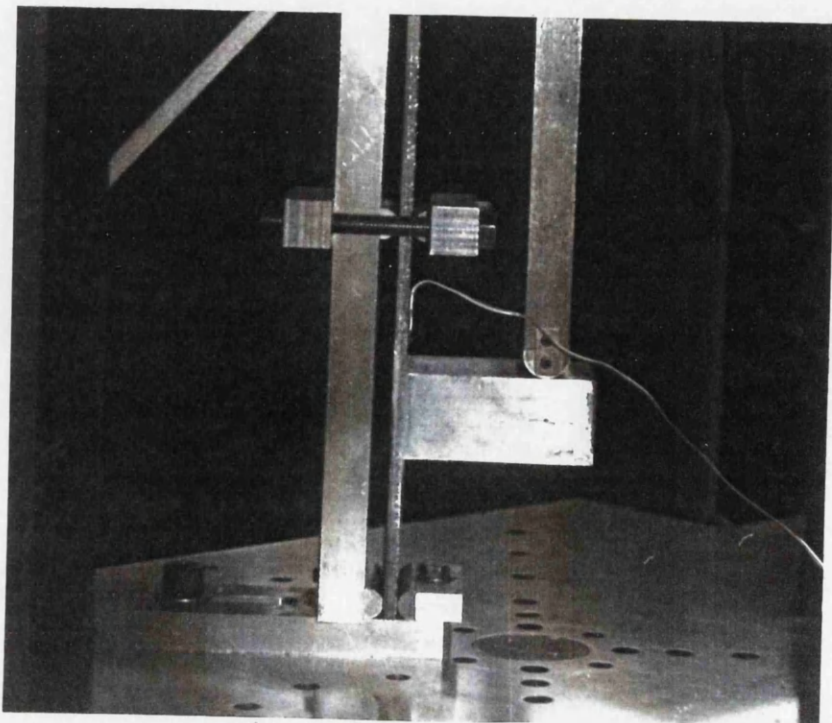
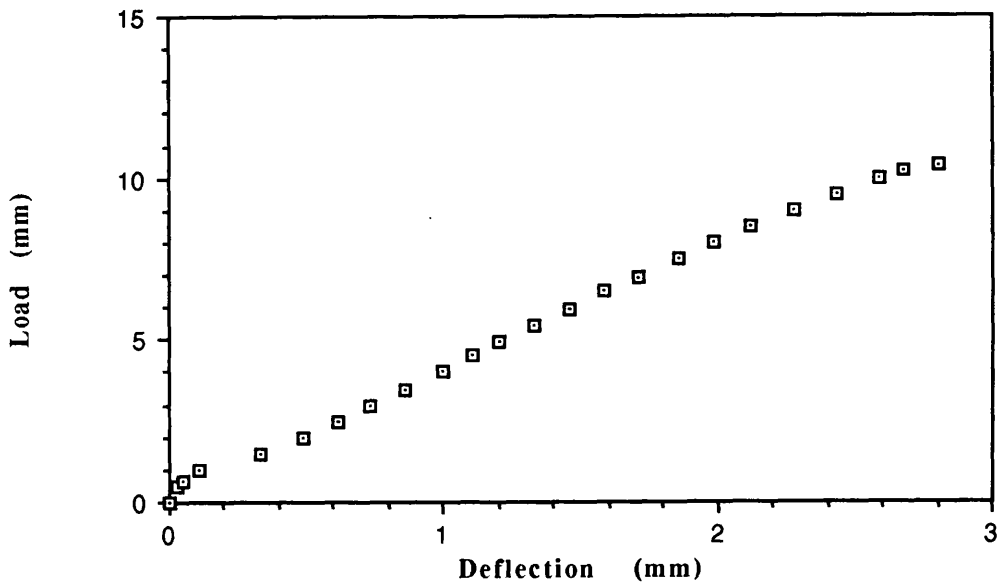
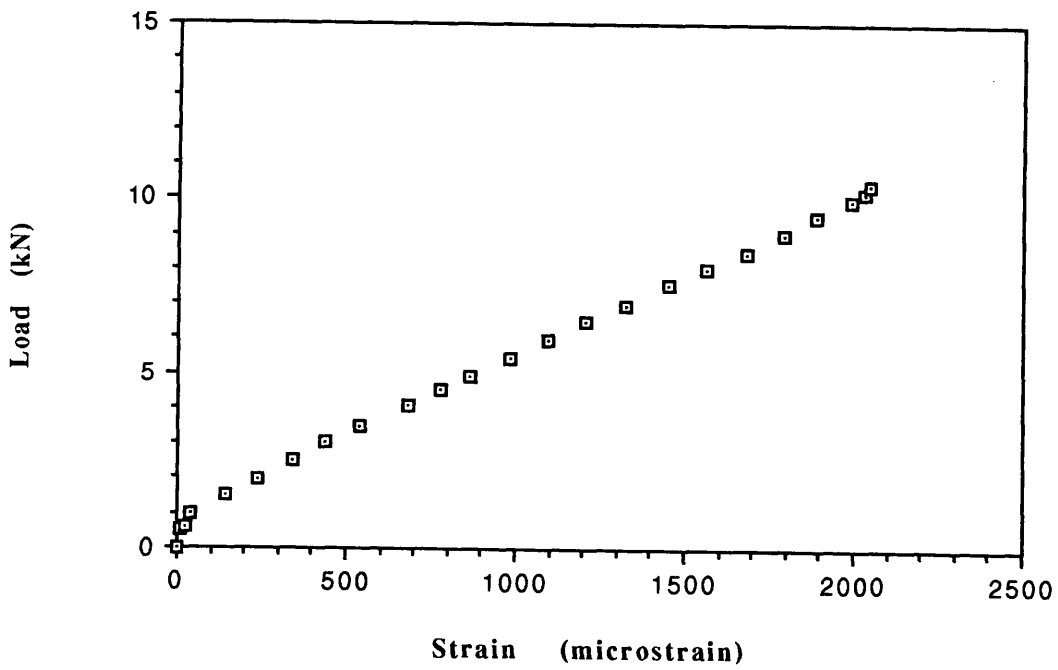


FIGURE 5.2 STEEL/STEEL STIFFENER SPECIMEN (PHYSICAL MODEL) DURING TESTING

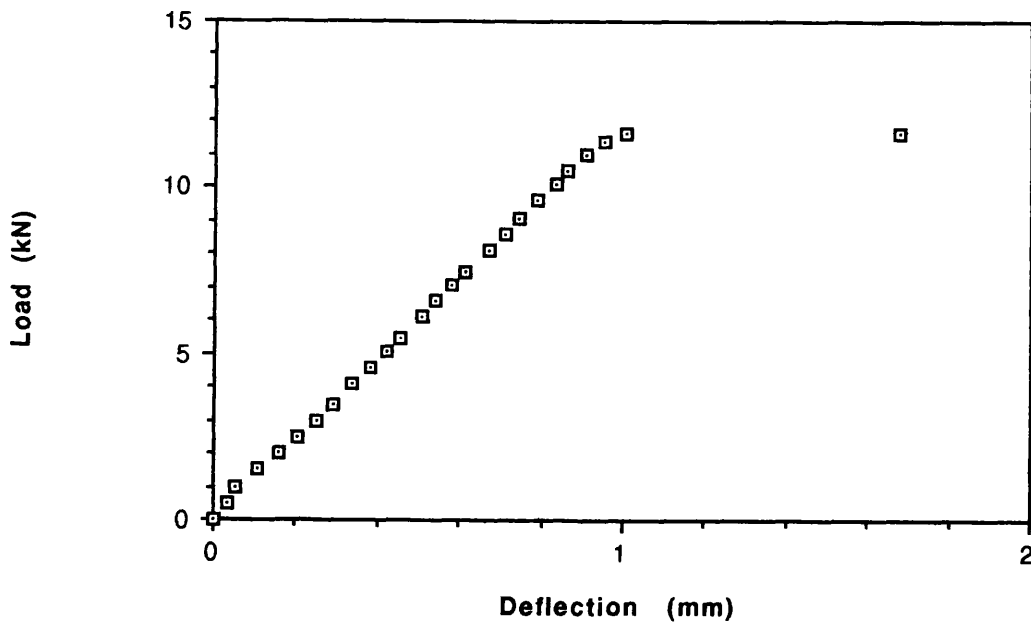


a. Load- central deflection

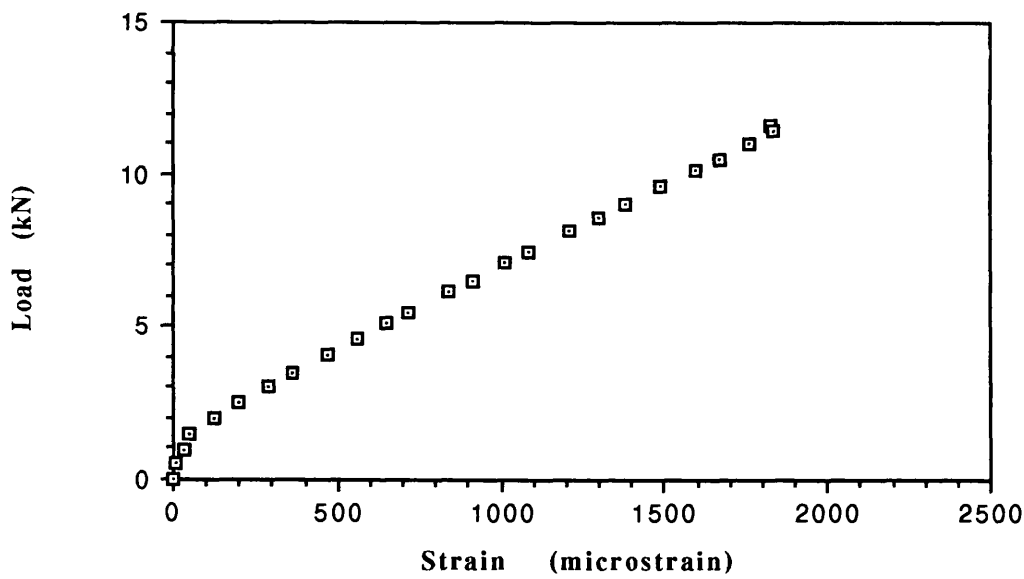


b. Load-strain

FIGURE 5.3 TEST MEASUREMENTS OF MODEL TYPE A UNTIL ADHESIVE FAILURE



a. Load- central deflection



b. Load-strain

FIGURE 5.4 TEST MEASUREMENTS OF MODEL TYPE B UNTIL ADHESIVE FAILURE

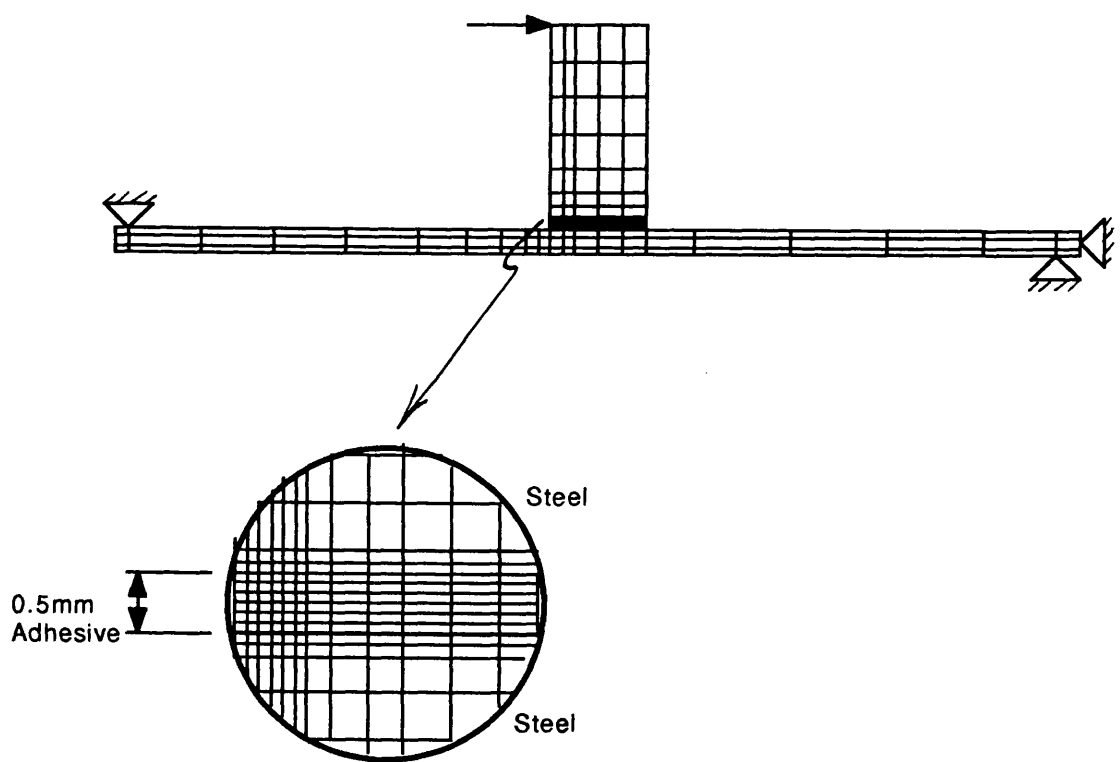


FIGURE 5.5 FINITE ELEMENT MESH FOR NUMERICAL MODEL (TYPE A OR B)

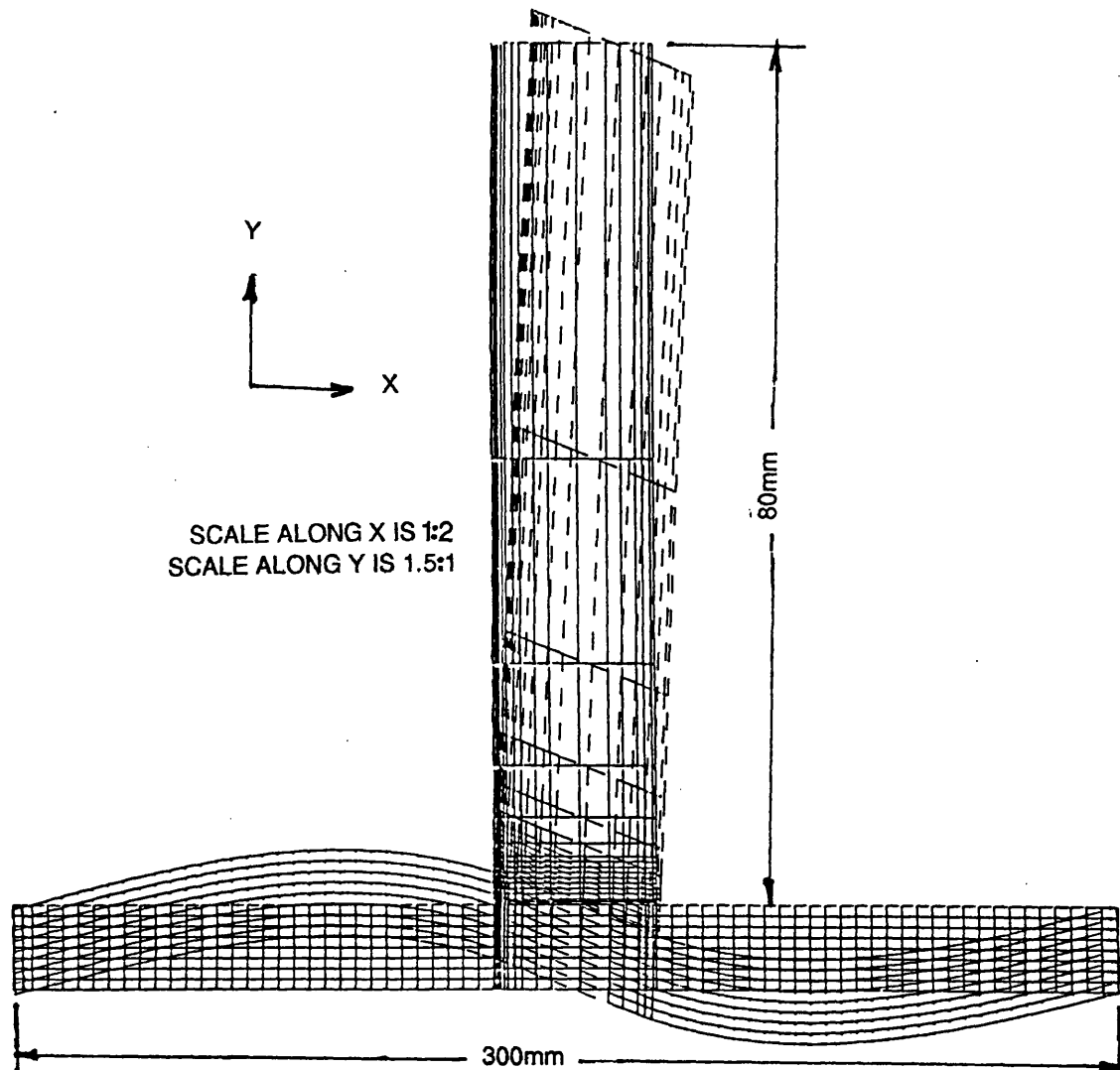
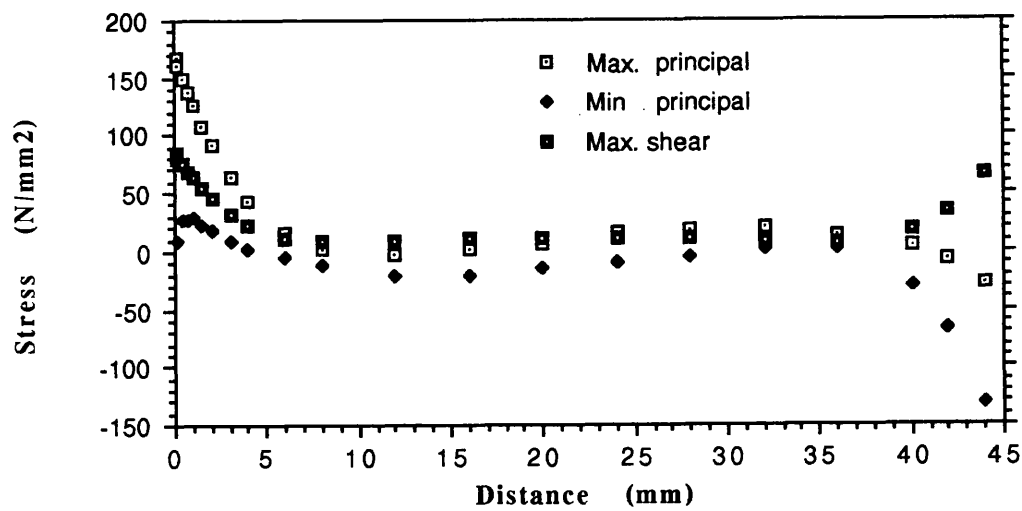
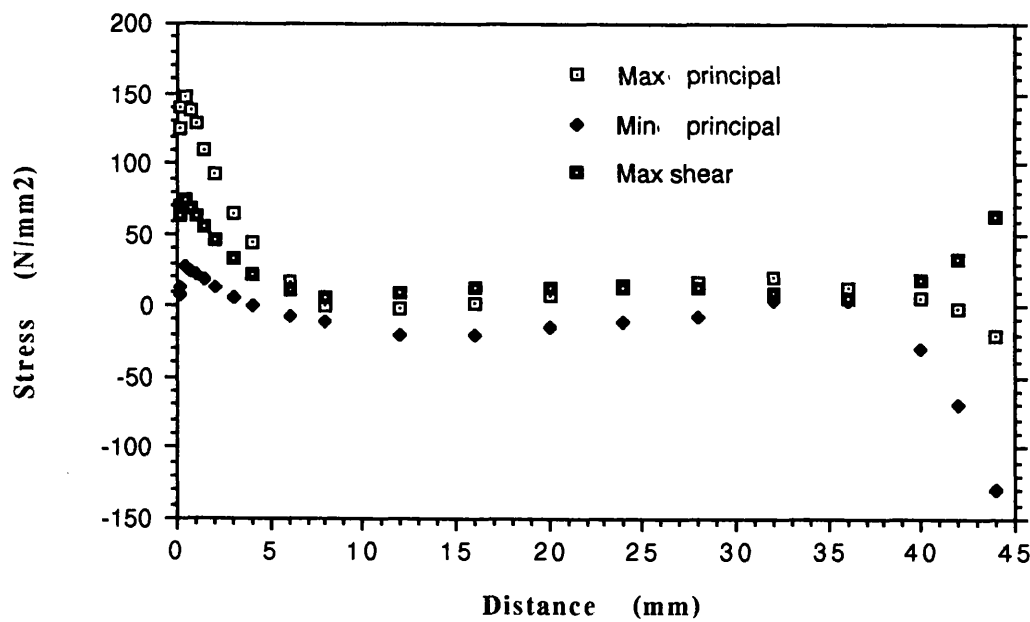


FIGURE 5.6 ELASTICALLY DISPLACED NUMERICAL MODEL (TYPE A OR B) UNDER LOADING

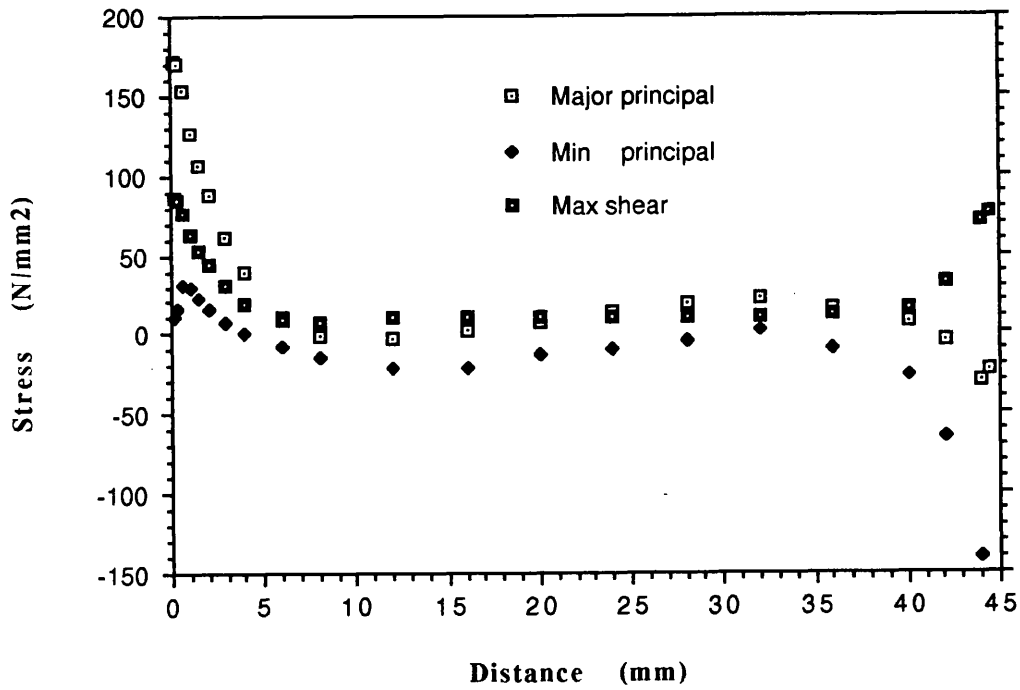


a. At 0.1mm from lower adherend surface

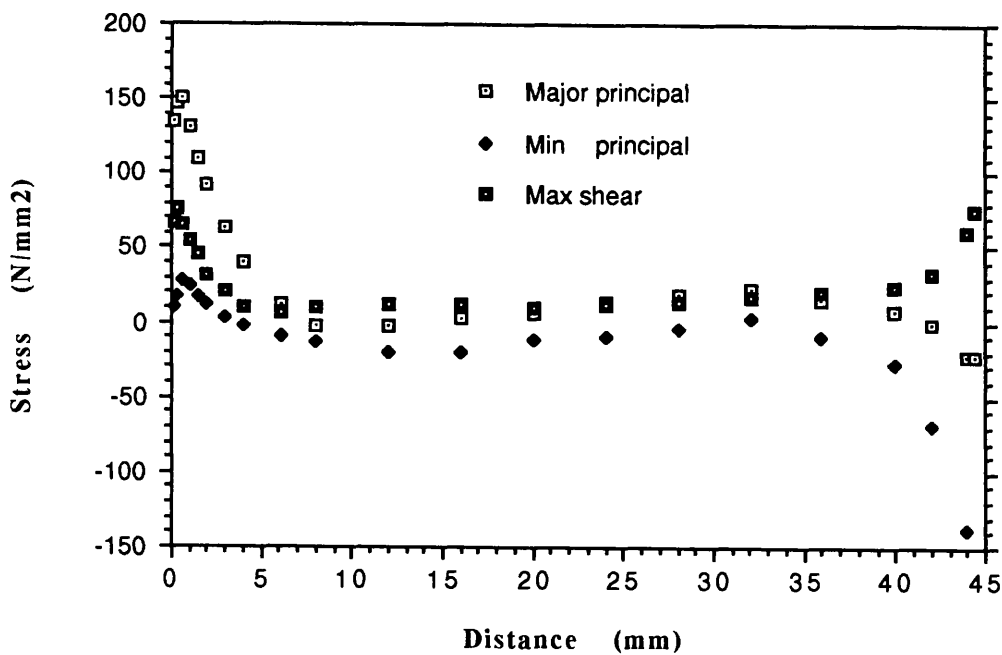


b. At 0.4mm from lower adherend surface

FIGURE 5.7 STRESS DISTRIBUTION ALONG ADHESIVE LINE FOR NUMERICAL MODEL (TYPE A) AT ADHESIVE FAILURE



a. At 0.1mm from lower adherend surface



b. At 0.4mm from lower adherend surface

FIGURE 5.8 STRESS DISTRIBUTION ALONG ADHESIVE LINE FOR NUMERICAL MODEL (TYPE B) AT ADHESIVE FAILURE

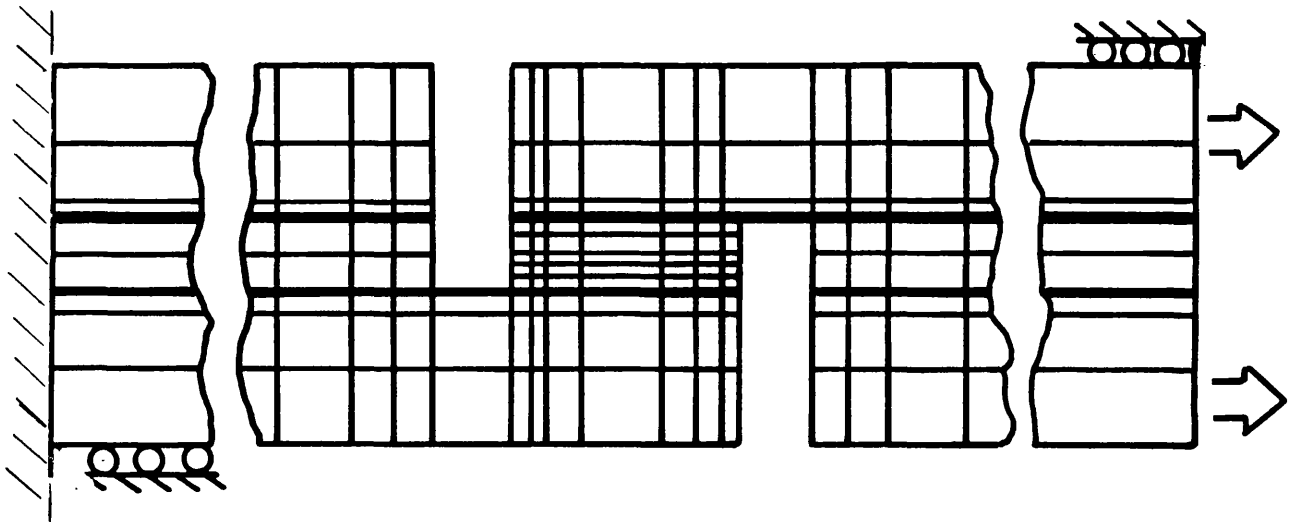


FIGURE 5.9 NUMERICAL MODEL FOR STANDARD STEEL/STEEL LAP SHEAR SPECIMEN
(TYPE 1-CHAPTER 3)

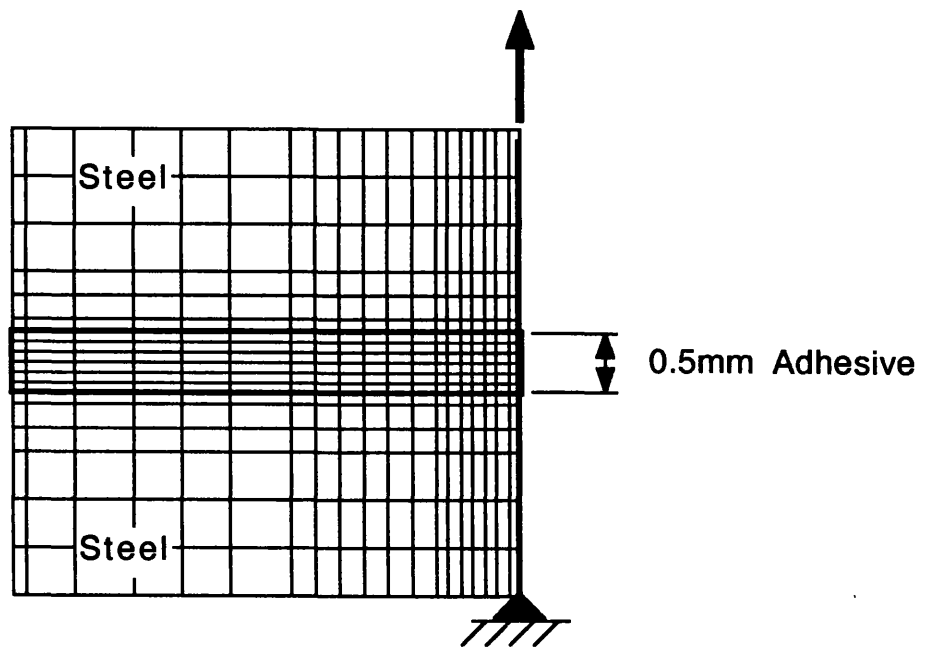
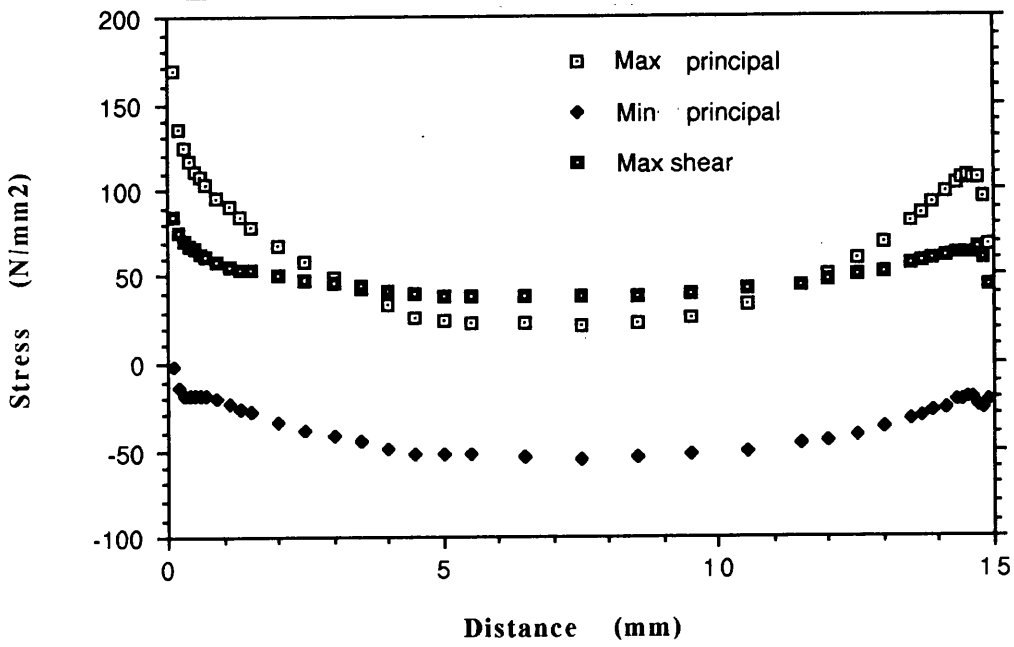
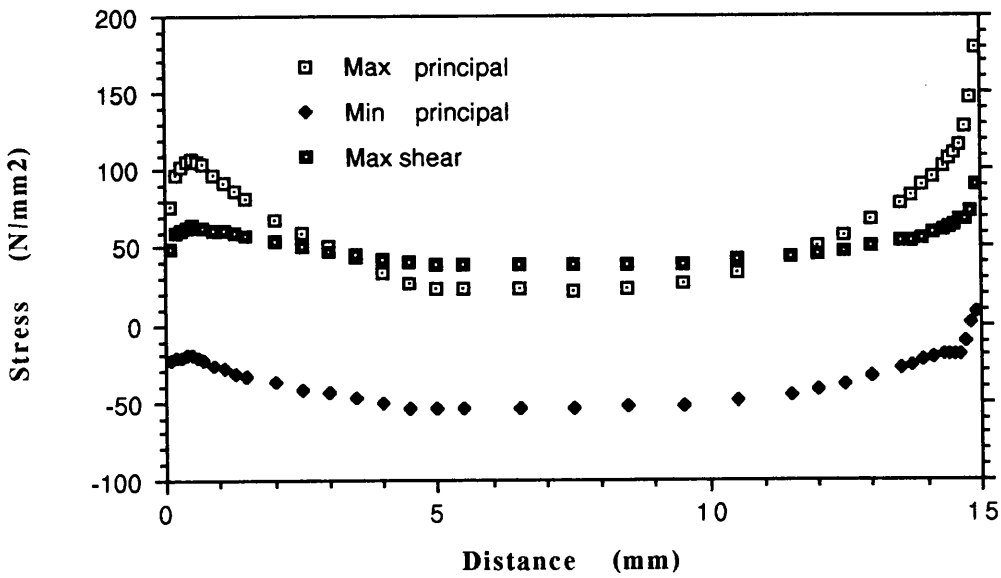


FIGURE 5.10 NUMERICAL MODEL FOR STANDARD STEEL/STEEL TENSILE CLEAVAGE SPECIMEN
(TYPE 3- CHAPTER 3)



a. At 0.1mm from lower adherend surface



b. At 0.4mm from lower adherend surface

FIGURE 5.11 STRESS DISTRIBUTION ALONG ADHESIVE LINE FOR NUMERICAL MODEL OF STANDARD STEEL/STEEL LAP SHEAR SPECIMEN (FIGURE 5.9) AT ADHESIVE FAILURE

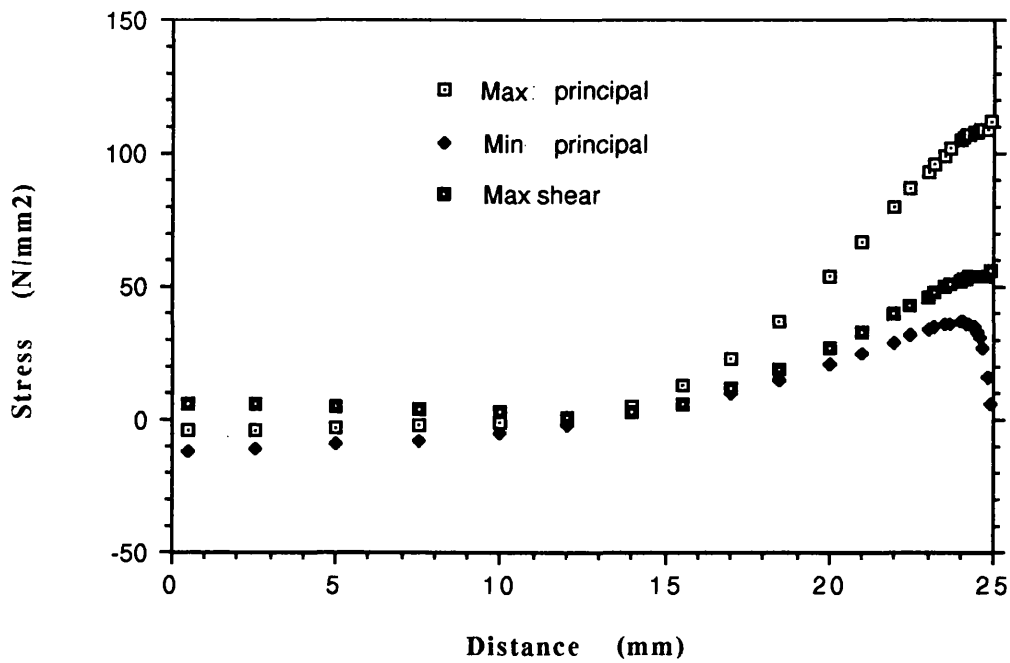
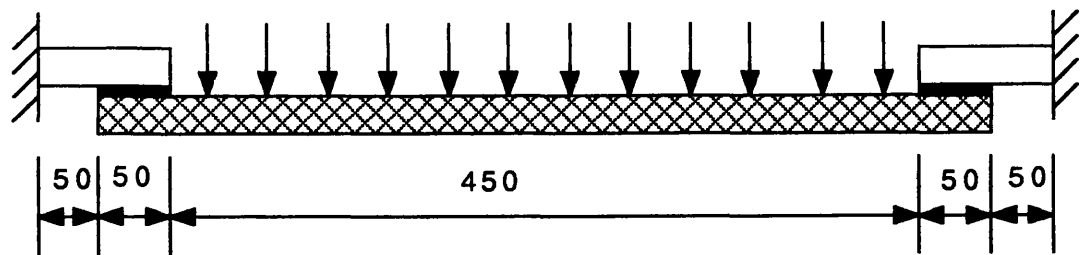


FIGURE 5.12 STRESS DISTRIBUTION (UNIFORM THROUGH THICKNESS) ALONG ADHESIVE LINE LINE FOR NUMERICAL MODEL OF STANDARD STEEL/STEEL TENSILE CLEAVAGE SPECIMEN (FIGURE 5.10) AT ADHESIVE FAILURE



Dimensions are in mm (not to scale)




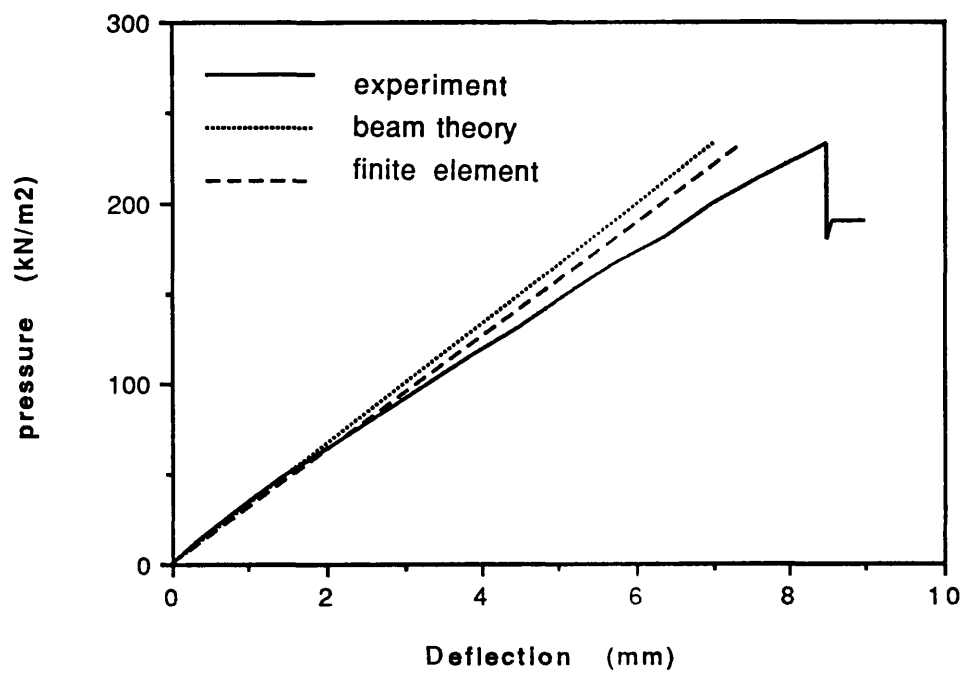
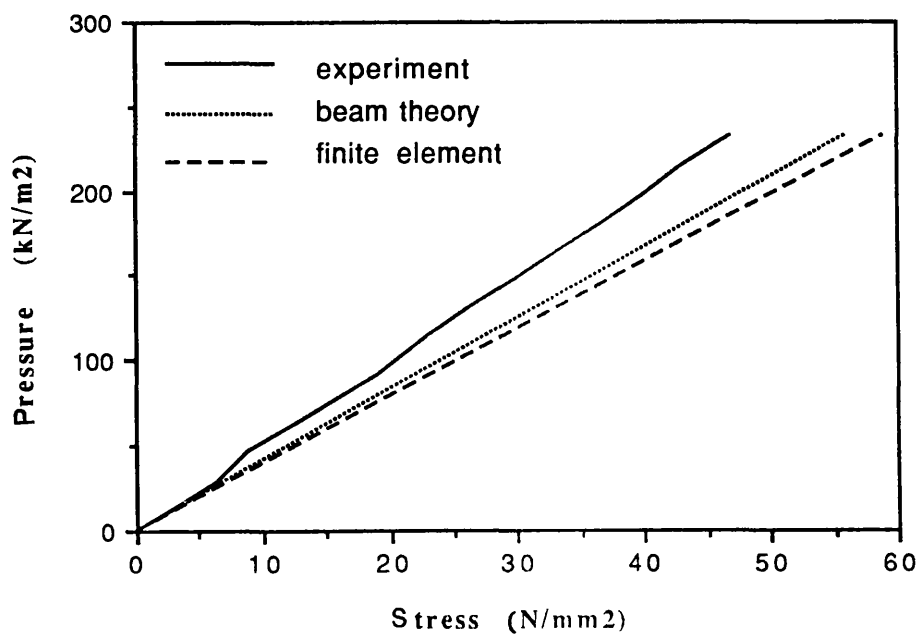
-  Steel 10mm thick and 75 mm wide
-  Adhesive (Araldite 2004) 0.5mm thick and 75mm wide
-  GRP 14.5mm thick and 75mm wide

FIGURE 5.13 IDEALISED MODEL FOR STRESS ANALYSIS (SIMILAR TO TYPE 5-CHAPTER 4)



a. pressure - central deflection curves



b. Pressure - central skin stress curves

FIGURE 5.14 TEST MEASUREMENTS FOR STEEL/GRP STIFFENER SPECIMEN UNTIL JOINT FAILURE

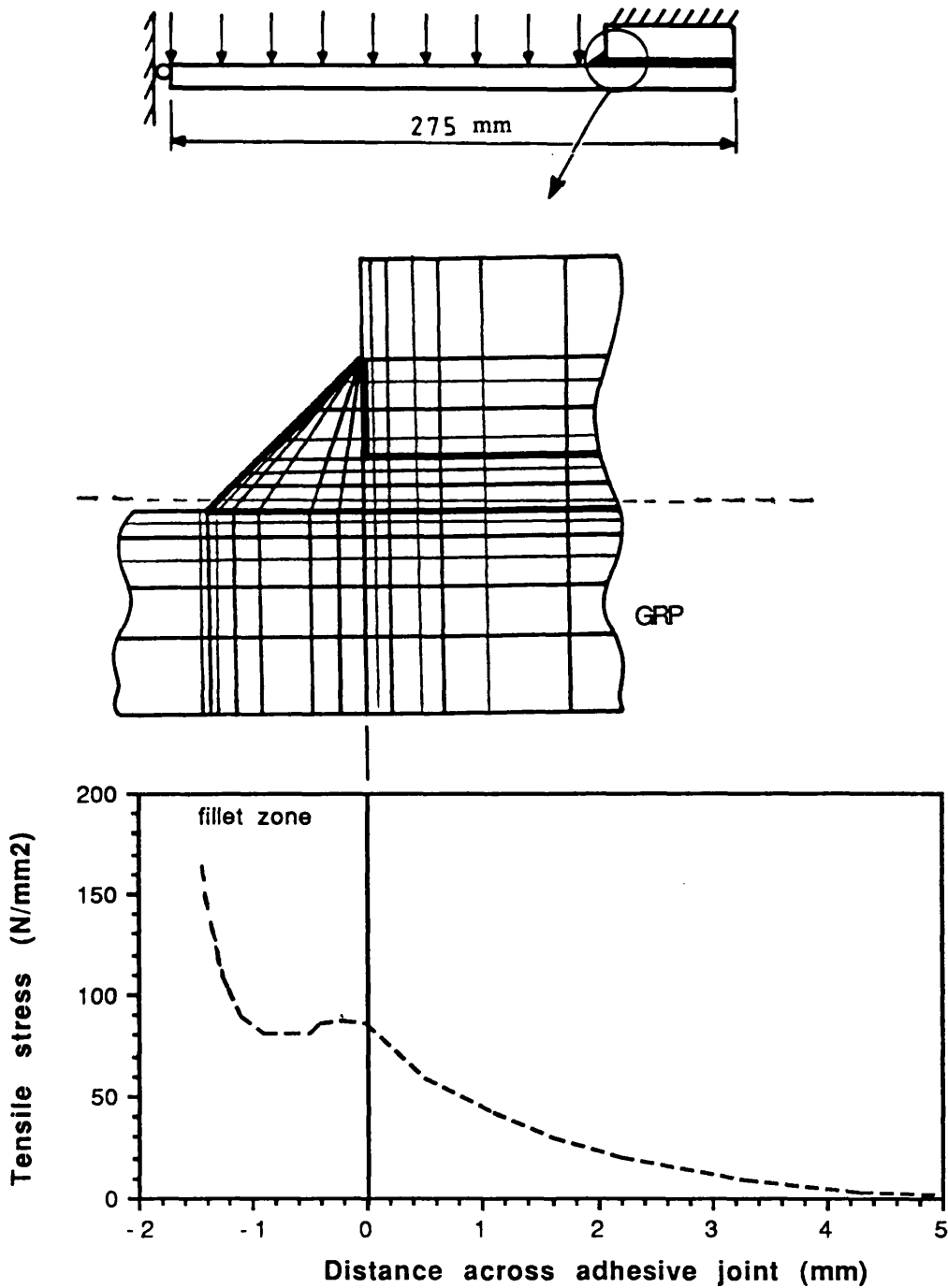


FIGURE 5.15 MESH AND STRESS DISTRIBUTION (0.1mm FROM GRP SURFACE) FOR STEEL/GRP NUMERICAL MODEL AT FAILURE UNDER 2.3BAR PRESSURE LOADING

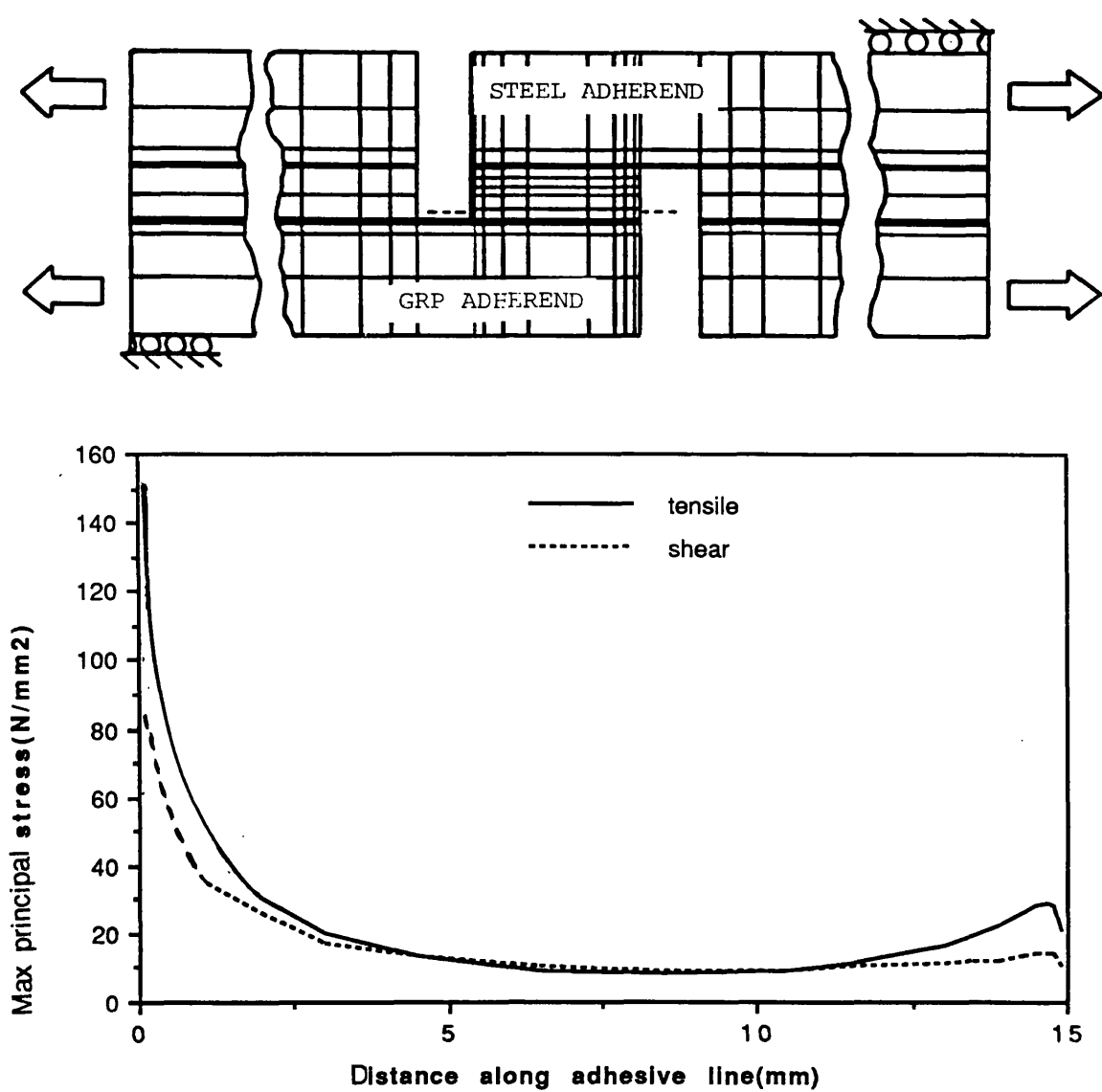
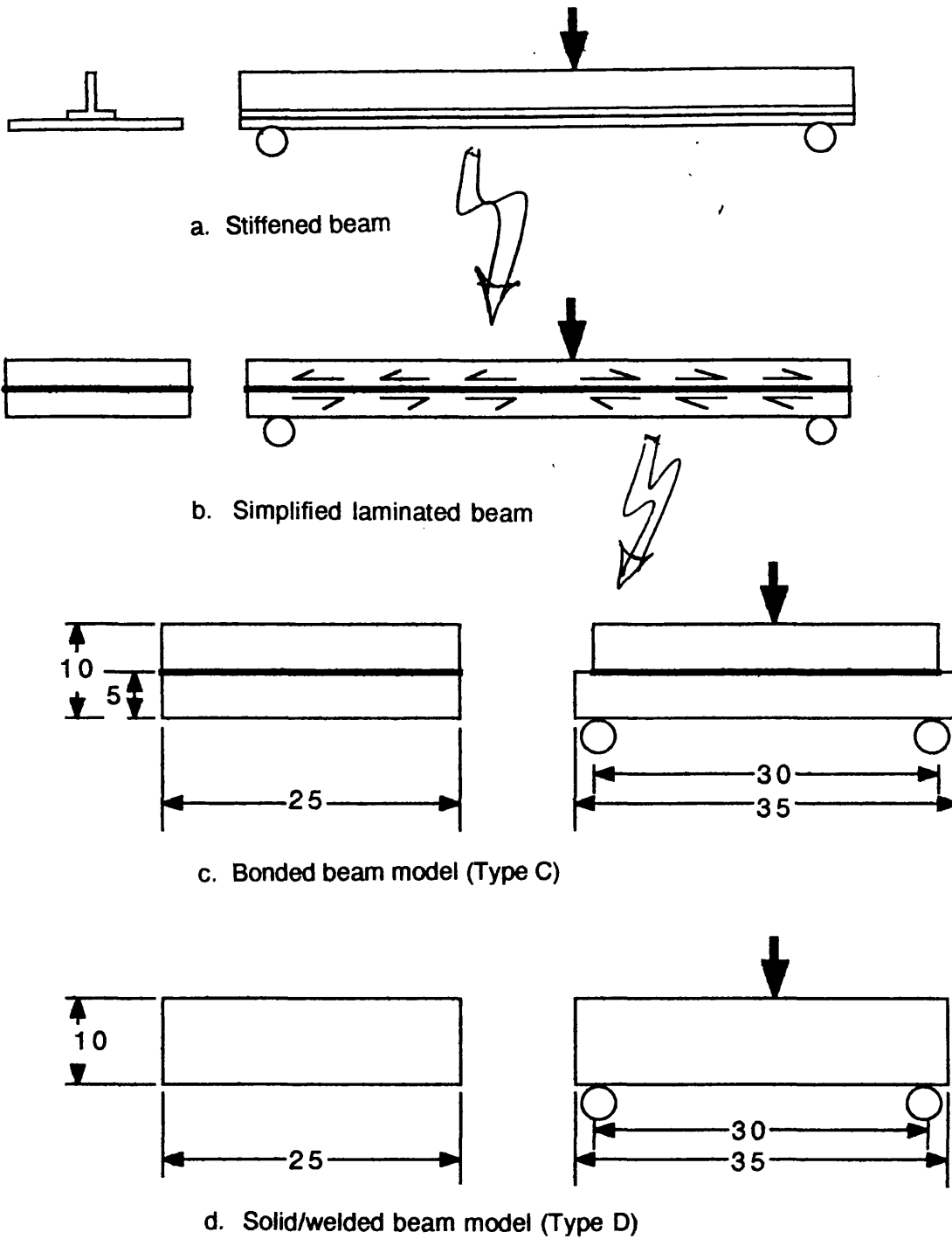
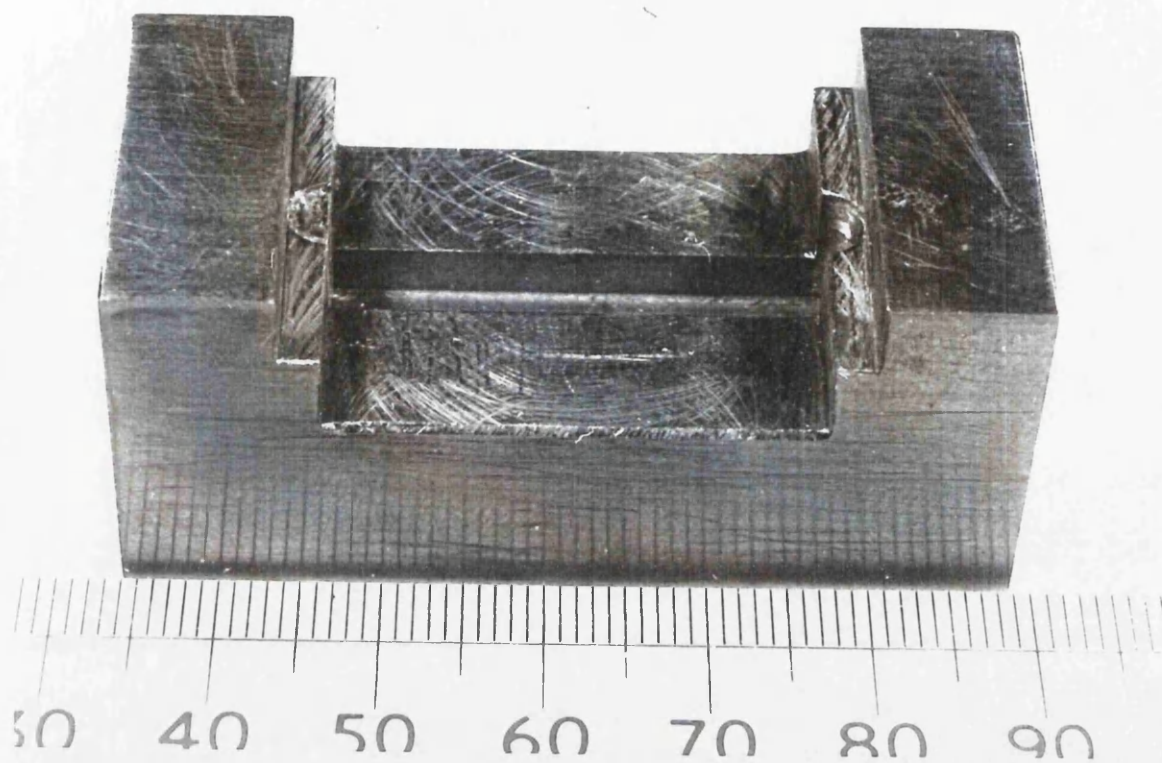


FIGURE 5.16 NUMERICAL MODEL AND STRESS DISTRIBUTION IN LAP SHEAR JOINT (TYPE 1) AT FAILURE (0.1mm FROM GRP SURFACE)

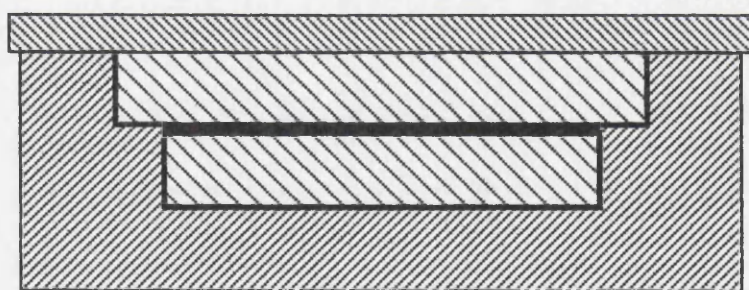


Dimensions are in mm

FIGURE 5.17 IDEALISATION OF STEEL/STEEL BEAM MODEL (TYPES C AND D)



a. Bonding jig



- 0.5mm thick adhesive
- ▨ 5mm thick steel adherends
- ▨ Steel bonding jig
- ▨ Clamping plate

b. Schematic details for clamping of specimen

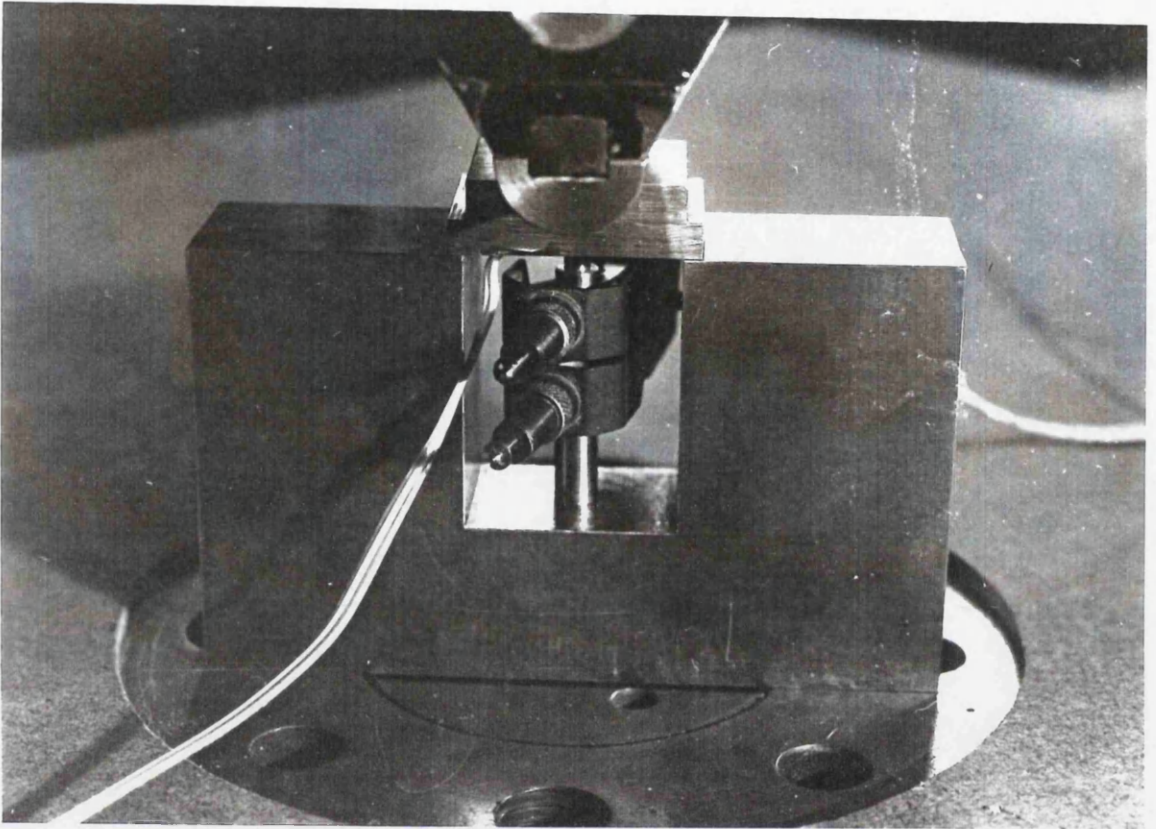
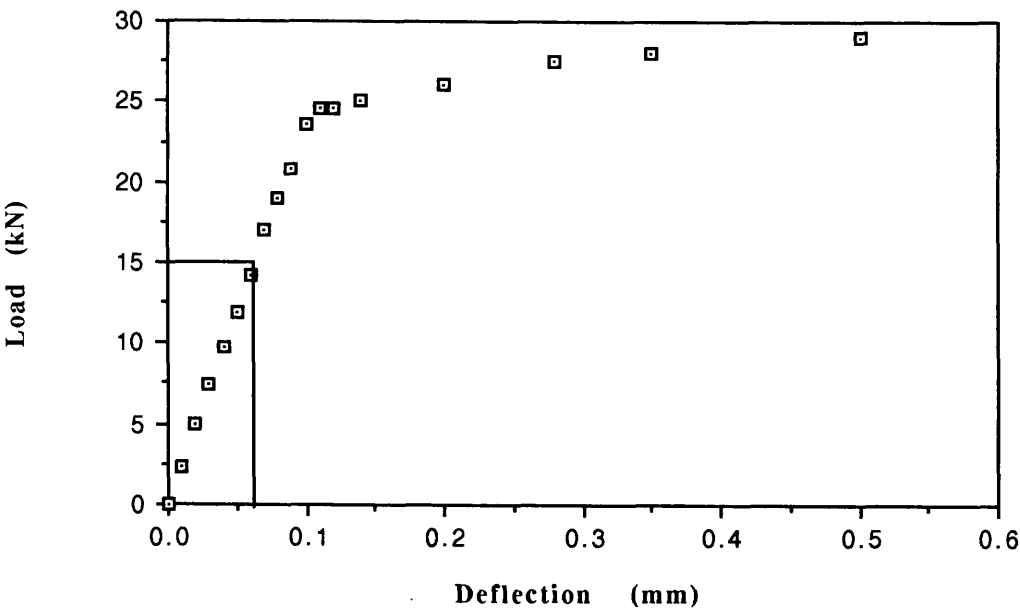
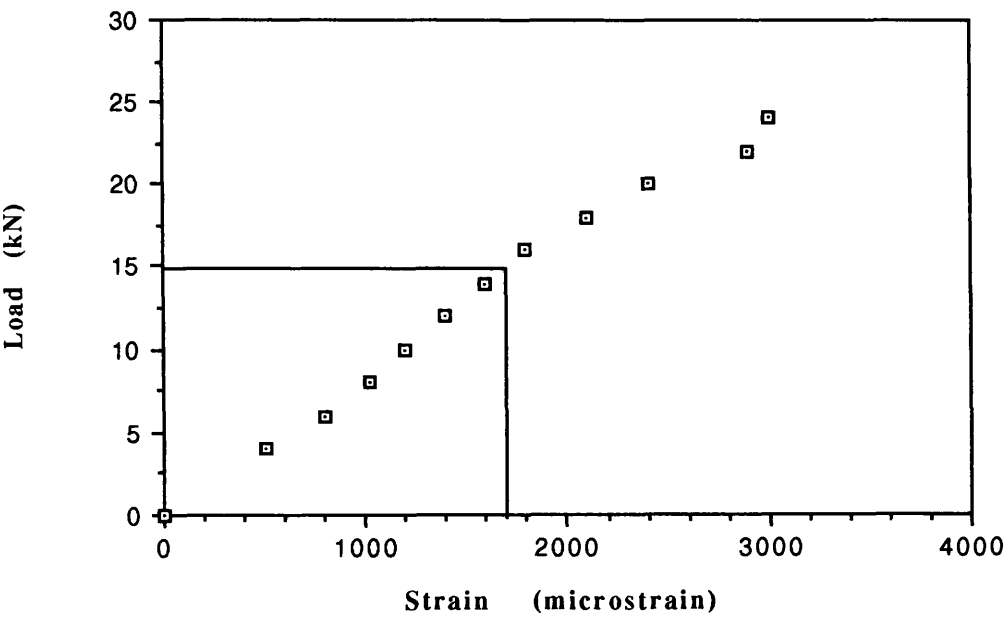


FIGURE 5.19 BONDED BEAM MODEL DURING TESTING

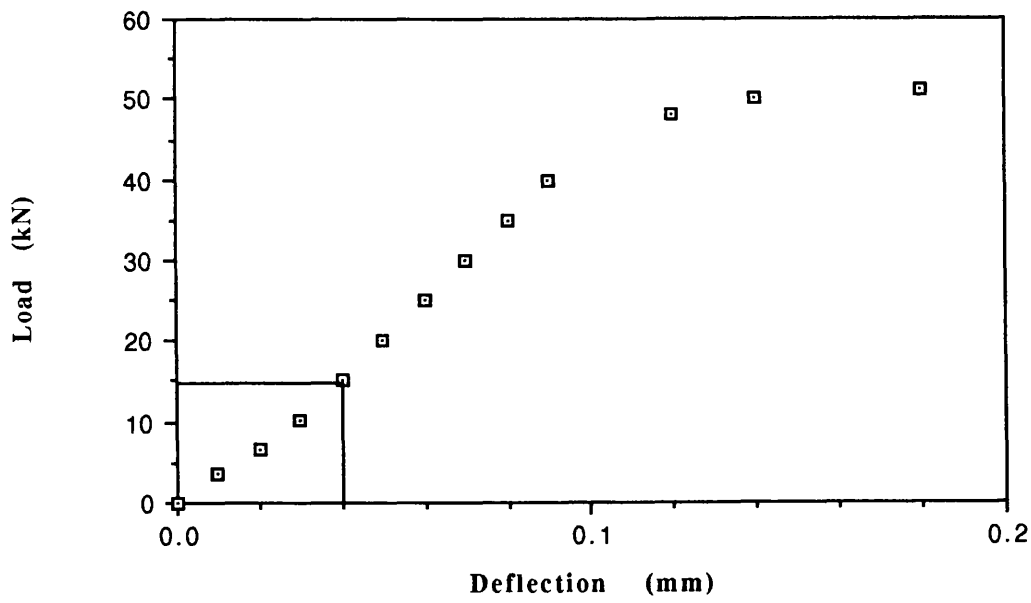


a. Load-central deflection

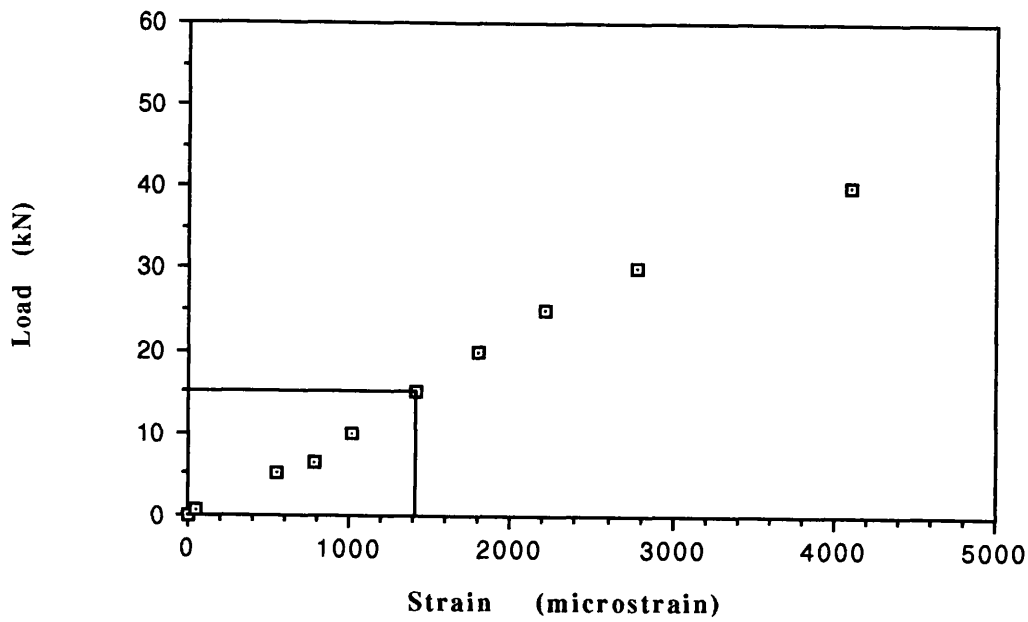


b. Load-strain

FIGURE 5.20 TEST MEASUREMENTS FOR THE BONDED BEAM (MODEL TYPE C)



a. Load- central deflection



b. Load-strain

FIGURE 5.21 TEST MEASUREMENTS OF THE SOLID BEAM (MODEL TYPE D)

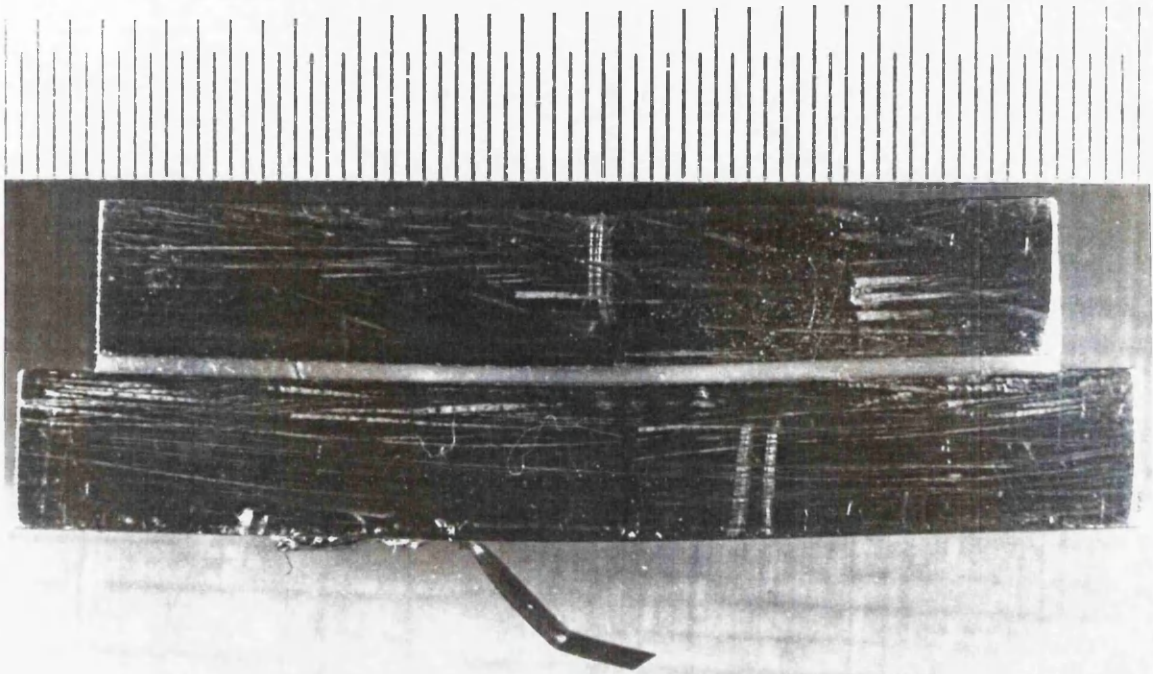


FIGURE 5.22 DEFORMED BONDED BEAM SPECIMEN

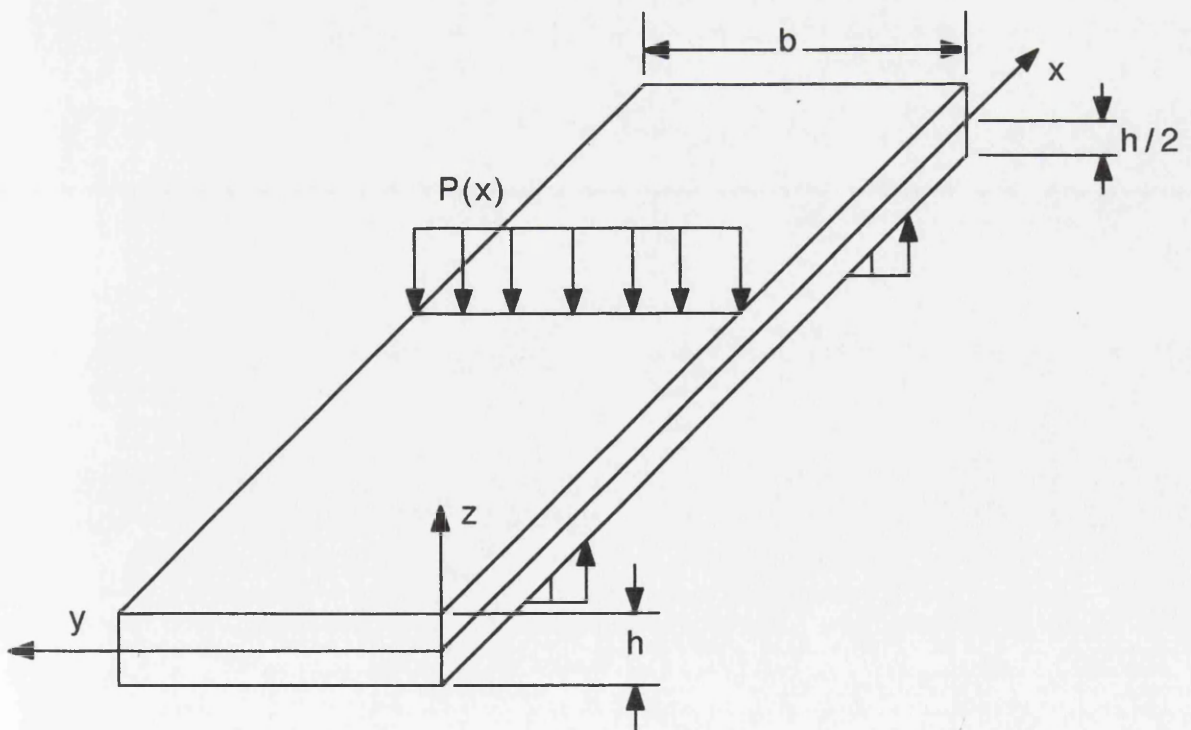


FIGURE 5.23 ANALYTICAL BEAM MODEL

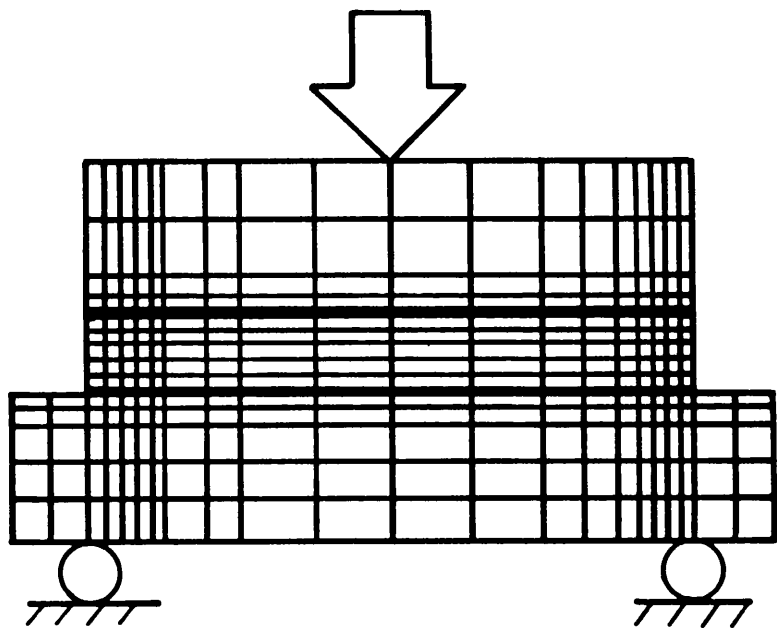


FIGURE 5.24 NUMERICAL MODEL (TYPE C)

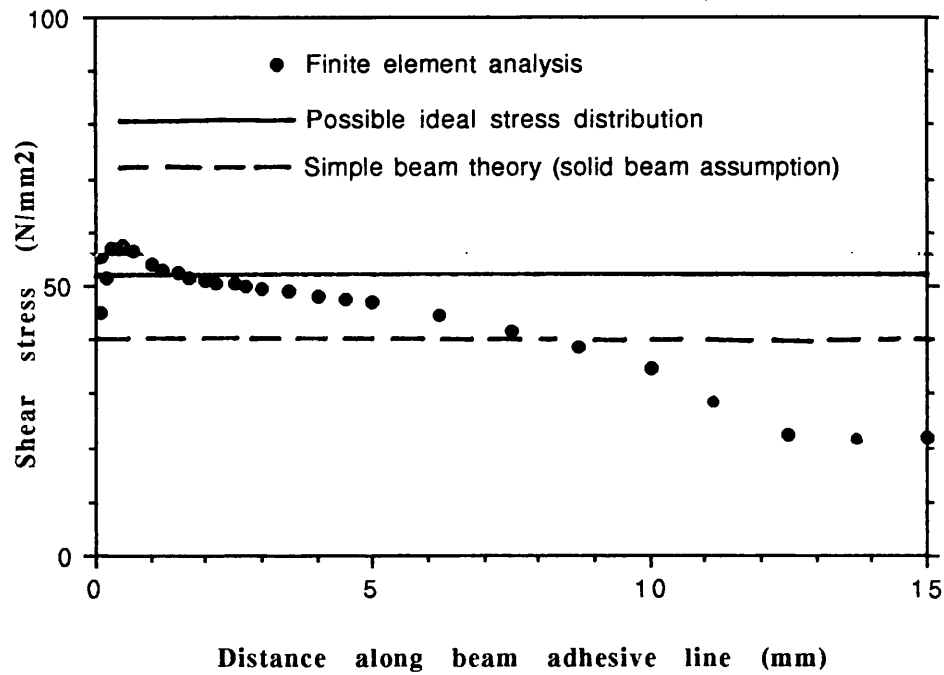


FIGURE 5.25 SHEAR STRESS DISTRIBUTION ALONG ADHESIVE LINE OF THE BONDED MODEL

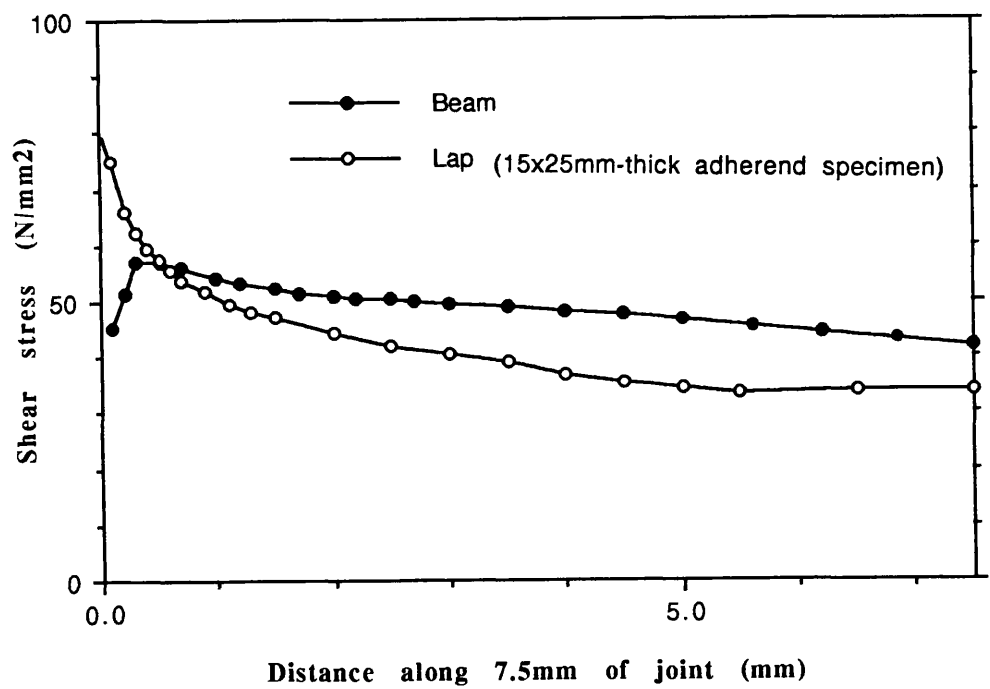


FIGURE 5.26 COMPARISON OF SHEAR STRESS DISTRIBUTION ALONG ADHESIVE LINE FOR BEAM MODEL TYPE C AND STANDARD LAP SHEAR SPECIMEN MODEL

6. DESIGN LIMITATIONS

The most short term limitations associated with the use of adhesive bonding are the problems of impact loading and fire conditions as reviewed in Chapter 2. This thesis attempts to assess these two unrelated problems through two examples in order to provide general guidelines for designing with structural adhesives. The first limitation is the need of the steel/steel bonded structures to resist impact loading, since it is otherwise difficult to accept the replacement of welding. The second limitation is that, while it is attractive to use the polymeric composite materials to improve the thermal insulation of lightly loaded walls, during fire the bonded joints within such a system must not fail before the failure of the remainder of the structure (assuming adhesive bonding is the preferred joining method).

Epoxy adhesive Araldite 2007 was used for most of these larger experiments for the first case study but a limited number of specimens were bonded with epoxy adhesive ESP110 for comparison. The latter adhesive possesses a modulus of elasticity significantly higher than the former. In the second case study the epoxy adhesive Araldite 2004 was used. While each of these studies relates to specific application requirements, the objective is to highlight the limitations and potential of structural adhesives in general.

6.1. LATERAL IMPACT RESISTANCE

In order to gain some insight into the parameters affecting impact resistance, three different stiffener end conditions were examined as shown in Figure 6.1. Types A and B had their ends machined to reduce the cleavage forces and Type C is with square ends. The adhesive thicknesses considered here are in the range 0.2-0.5mm and 1.5-2.0mm to examine the effects of adhesive thickness. Some specimens were mounted with two strain gauges at the centre, one on the web side and the other on the outer surface of the stiffener flange or plate depending on whether the impact direction was from stiffener or plate side. The strain gauges enabled assessment of the adherend stresses in highly loaded areas. Centre and support positions were marked on the beams and their straightness was checked to ensure proper contact with the free falling striker(hemispherical nosed) and supports.

Twelve specimens, each comprising 600x300x8mm plate and single stiffener were

fabricated (adhesively bonded) in the manner described for the large panel elements in Chapter 4.

The experimental programme for this investigation may best be described under the following subheadings.

6.1.1. DEVELOPMENT OF TEST RIG

The free fall impact testing rig was modified from an existing facility to allow a wide range of impact energies to be applied to bonded beam specimens. The salient features of this rig are shown in Figure 6.2 in which a range of predetermined masses up to 6.4kg, guided in a vertical tube, can be raised to specific heights, up to 12.5m, and released. The striking masses have a spherical hardened indenter of 90mm diameter. The specimen is mounted in a bending rig in such a manner that the beam and striker axis are centered between the two supports. The supports comprise sets of rollers to allow mounting of the beam facing the striker either from the plate or stiffener sides. These supports prevent the beam from bouncing when struck and also provide simply supported boundary conditions.

Instrumentation was designed and selected for recording strain, strain rate and energy absorption during impact. Figure 6.3 shows some of this apparatus located in the confined space of the stair well in which comprised the dropweight tower. Figure 6.4 shows the schematic layout, dimensions and instrumentation details of the test rig. The apparatus consisted of a two channel transient recorder, quarter bridge amplifiers, oscilloscope and X-Y plotter for strain measurements. Two infra-red switches were placed 500mm apart near the bottom end of the fallway tube to measure impact speed through a digital timer. The time recording starts when light reflected from sensitive tape mounted on the striker is detected by the upper infra-red switch and stops when detected by the lower one.

6.1.2. TEST PROCEDURES

Prior to each test the strain measurement equipment was calibrated. Suitable ranges for the plotter and the oscilloscope were chosen and the infra-red light switches and timer operations were checked.

The specimens were tested with simply supported boundary conditions. Six of them

were instrumented with strain gauges. Predetermined masses were raised to a specific height and freely dropped onto the centre of the specimen. By monitoring the striking and return velocities of the striking masses the energy absorbed by the specimen was determined. The striking impact velocity is measured as the ratio of the distance between the two infra-red switches to the time recorded. The average rebound height was monitored visually in the range of 1-1.5m. The energy calculations are presented in Appendix VII.

After each impact strike the two strain values were recorded, and plotted through the two channel recorder and oscilloscope. Typical expanded strain against time records are shown in Figure 6.5. A 50kHz square wave cycle was also plotted as a reference to scale the strain rate as a ratio of peak strain to time. From this it can be seen that the strain rate for these specimens is about 10^3 s^{-1} . This is regarded as a very high strain rate for normal impact conditions. However it should be borne in mind that both striker and specimens are very rigid with respect to the position of the impact strike (short stiffener web under compression loading).

After each impact the specimen was visually examined to determine whether or not it had debonded. To assess the residual strength up to two further impact tests were carried out from a height of up to 12.5m, or until significant adherend deformation and/or bond line failure occurred. The failure of each specimen after repeated impact was measured as both a function of local denting damage and the proportion of adhesive debonding along the adhesive line.

6.1.3. TEST RESULTS

Table 6.1 summarises the test results to which the following notes refer:

- In the case of plate side impact, measured stresses on stiffener flange (centre of beam) opposite to the struck side indicate very high strain levels without failure of the adhesive. The stiffener stresses exceeded the material yield stress.
- Dynamic impact forces and adhesive shear stress were calculated from an equation based on composite beam theory detailed in Appendix VII. The calculation assumed static loading conditions. The estimated forces are based on the strain values measured at specimen surface (adherend). It can be seen that these forces are relatively high and this may explain the high level of strain rate recorded. The forces and shear stresses produced by striking the specimen

from the plate side were difficult to calculate due to the onset of yield in the stiffeners.

- Many of the impacted specimens exhibited considerable residual strength. Figure 6.6 shows such a specimen with noticeable plastic deformation after testing.
- Lower impact resistance is recorded when the impact loading is from the plating side in comparison with resistance to impact from stiffener side. It is possible that cleavage forces due to rotation of the struck plate (plate side impact) about the adhesive joint contributed to this weakness. In addition to that the stiffener side impact can produce local deformation of stiffener which can absorb considerable energy.
- The impact resistance is greatly improved by shaping/tapering the stiffener end thereby reducing the induced end cleavage stresses. This observation is similar to that noticed in the case of the statically loaded specimens (see Section 4.3). These improvements are reflected by the increased number of strikes required to cause debonding.
- Adhesive failure after repeated tests suggests that Araldite 2007 adhesive is more tolerant to impact loading compared to the ESP110 epoxy adhesive. This is probably because the latter possesses a higher modulus of elasticity which generates higher cleavage stresses.
- In general, the thinner the adhesive line (bond line) the better the impact resistance. This confirms at a larger scale the observations on small scale shear impact specimens shown in Figure 3.13 (Chapter 3).

6.2. FIRE RESISTANCE

For fire resistant bonding there are at least three requirements. These are:

- The adhesive should not revert to its monomer molecular (liquid) form when subject to elevated temperature. Instead it should, at worst, decompose and char.
- The adhesive must generate minimal smoke density and toxic fumes.
- Good engineering design is essential for the use of adhesive bonding in fire applications. The joint must be kept at relatively low temperature near the cold face of the structure. The latest hydrocarbon fire test requirement is for the cold face temperature rise to be not more than 139°C above the ambient

temperature.

Two series of fire tests were undertaken which were largely concerned with the adherend rather than the adhesive on the assumption that adhesive failure would initiate at the interface due to elevated temperature. The series of tests included small and large experiments which are described below together with the results.

6.2.1.SMALL SCALE EXPERIMENTS

An initial batch of nine, baseline, fire test specimens (100mm x 100mm) of GRP panel material in thicknesses ranging from 4.5 to 15mm were sent to Fire and Materials Ltd. for cone calorimeter tests, together with measurement of rear face temperature so as to assess the effect of fire on the adhesive joints. The first three specimens were tested without insulation and gave poorer results than expected. It was therefore decided to evaluate the effect of 6mm knitted silica fabric insulation bonded (clad with epoxy adhesive) to the exposed surface (hot face) and coated with intumescent paint on further specimens. Figure 6.7 shows some of these specimens. Figure 6.8 illustrates the temperature/time profiles associated with the rear surface (cold face) of the first four baseline specimens tested in horizontal orientation. The effect of the additional layer of insulation on the overall performance of the panel is marked despite the higher incident energy and difficulty in preventing ignition of the specimen at the edges. The presence of the knitted silica barrier significantly reduced the burn off of resin at the front face and the measured levels of resultant ignition products. The presence of the intumescent paint was however of uncertain value in the single test as there was insufficient incident flame to initiate intumescence as expected.

Tests on eleven additional small samples were carried out using the cone calorimeter unit to measure the rate of heat release and the concentration of smoke and gas emissions as well as the thermal gradient through the thickness of these samples. A summary of these results is presented in Table 6.2 for an incident heat flux density of 60kW/m².

A sample of full test analysis details including thermal, chemical and physical test results are presented in Appendix VIII. From Table 6.2 the following observations are possible:

- The heat release rate was reduced by the use of intumescent paint. This improvement however applied only for the first 5 minutes. After the intumescent paint chars and disintegrates it loses its effectiveness.

- The effectiveness of the knitted silica insulation is shown through a significant reduction of both heat release rate and rear face temperature. Corresponding reductions also occurred in both rate of mass loss and smoke yield.
- Comparing these results with those predicted from the initial batch of test pieces the increase from 30 to 50 kW/m² heat flux did not produce a proportional increase in rear face temperatures. This may be due to the contribution of combustion products to the heat release rate.

6.2.2. LARGE SCALE TEST

Using the fabrication techniques described in Chapter 4, a 1.2 x 1.2m panel, 100mm thick, was fabricated incorporating layers of structural and thermal insulating materials such as GRP, wood and silica face with a stainless steel vapour barrier (see Figure 7.9). One half of the panel was based on a bonded structural member of 15mm GRP with a bonded (Araldite 2007) steel stiffener while the other half used a similar skin element of 15mm phenolic coated birch plywood with a nailed top hat stiffener. A limited number of lap shear test specimens were used to indicate the strength of adhesively bonded joints between pultruded materials, plywood and GRP adherends in order to qualify the bonding of the pultruded frame which supports the fire insulation materials. Panel fabrication included, where appropriate, the use of peel ply, automated adhesive dispensing and simple clamps. Outer skin stainless steel was held in place by stainless steel fasteners connected into the GRP pultruded frame. The frame was adhesively bonded to GRP and wood skins with Araldite 2004.

This 1.2 x 1.2m panel was tested at Warrington Fire and Materials Centre (WFMC) using an indicative hydrocarbon fire test which employed a furnace providing a temperature time curve to the Norwegian Petroleum Directorate (NPD) code. Twenty one thermocouples were placed across the surface or embedded through the thickness of the multilayered panel and these provided very useful measurements. The set up of the panel against the furnace is shown ready for testing in Figure 6.10 in which the two halves of different structural materials can also be seen. The schematic layout of a set of thermocouples is illustrated in Figure 6.11 and the corresponding temperature/time curves are given as Figures 6.12 to 6.16. From these curves and observations during the experiments the following points should be noticed:

- The performance of the furnace in terms of time/temperature profile provided a

slightly lower heating rate than the NPD standard in the first few minutes but a slightly higher rate after that (Figure 6.12). The maximum temperature inside the furnace was above 1150°C after one hour.

- From Figure 6.13 it can be seen that the temperature of the stainless steel outer surface reached a temperature of 1000°C after 15 minutes and closely followed that of the furnace thereafter.
- As in the case the thermal creep tests in Chapter 3 (Table 3.8), temperature at the adhesive bond between steel/GRP (Figure 6.14) exceeded 120 °C (well above the glass transition temperature of the Araldite 2004) without joint failure. During the test there was no visible sign of distortion in the adhesive or slipping of the steel stiffener (5kg).
- The rise in rear face temperature for the GRP upper and lower quadrants(Figure 6.15) passed class H60 rating for fire walls to the NPD code. The code requires that the increase in rear face temperature not to exceed 139°C above the initial temperature (20-22°C on this occasion).
- Figure 6.16 shows that rear surface temperatures at the plywood upper and lower quadrants achieved only an H55 rating. This may be improved by increasing the plywood thickness.
- The fire test was terminated after 75 minutes of continuous testing. This was due to an edge effect on the panel which led to external ignition of the plywood side edge at pultruded frame edge members.
- At the end of the test the panel was removed from the furnace and dropped unintentionally onto the floor. Despite the impact it was returned to Glasgow as a single unit. The weight loss after the test was 7kg from an original panel weight of 65kg. This relatively small loss is the result of the stainless steel vapour barrier at the hot face of the panel preventing any surface ignition during the test.
- The panel was then dismantled by removing the stainless steel face first. The silica fabric suffered considerable shrinkage which may have led to local loss of insulation.
- The effectiveness of the insulation layers is well demonstrated in Figure 6.16 as both a function of temperature and time within the upper quadrant of the GRP side of the panel.
- With the removal of the fabric, it can be seen from Figure 6.17 that the internal

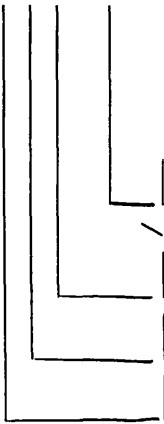
frames of the panel (pultrusions) were charred, having lost most of their resin, but surprisingly still in good shape. The bonded pultrusions were still attached to the rear panels through the charred epoxy adhesive (Araldite 2004).

- The 15mm GRP skin suffered delamination to a depth of about 5mm from the inner surface. This was mainly due to resin boil off as the temperature reached about 500°C. The outer skin of the GRP however showed no signs of damage and Figure 6.18 shows the delaminated layers and steel to outer skin adhesive bonds with no sign of fracture. The plywood outer skin charred to about 70% of its thickness except in the area enclosed at the steel top hat section where it failed completely at the end of the test.

Further discussion to the above results is will in Chapter 7.

TEST[1] SPECIMEN	HEIGHT [m]	MASS [kg]	VELOCITY [m/s]	ABSORBED ENERGY [J]	ADHEREND BENDING [N/mm ²]	IMPACT FORCE (KN)	ADHESIVE SHEAR STRESS [N/mm ²]	NO. OF REPEATED DROPS FROM 12.5m	DEPTH OF DENTING DAMAGE [mm]	% DEBOND IN ADHESIVE LINE
AA1/S	12.5	6.4	14.2	565	307	215	33,	2	7.0	60
AB2/S	12.5	6.4	14.2	565	300	210	32	1	5.0	100
AC1/P	10.0	6.4	12.5	420	405	-	-	1	1.5	60
AD2/P	10.0	6.4	12.5	420	420	-	-	0	1.0	05 AT MID-SPAN
BA1/S	12.5	6.4	14.2	565	305	215	32	2	7.0	00
BB1/P	12.5	4.5	14.2	400	[3]	-	-	1	0.5	100
CA1/S	12.5	2.2	14.2	195	-	-	-	0	2.0	100
CB1/S	12.5	2.2	14.2	195	-	-	-	2	4.0	100
AD1/P[2]	10.0	6.4	12.5	420	-	-	-	0	1.0	100
AE1/P[2]	10.0	6.4	12.5	420	-	-	-	0	1.0	100

NOTES:
[1] Test specimen designations denote the following:
Test specimen type (see Figure 6.1)
Sequence Letter
Type of adhesive: 1 - Araldite 2007
2 - ESP 110
Position of central impact loading:
S - from stiffener side
P - from plate side

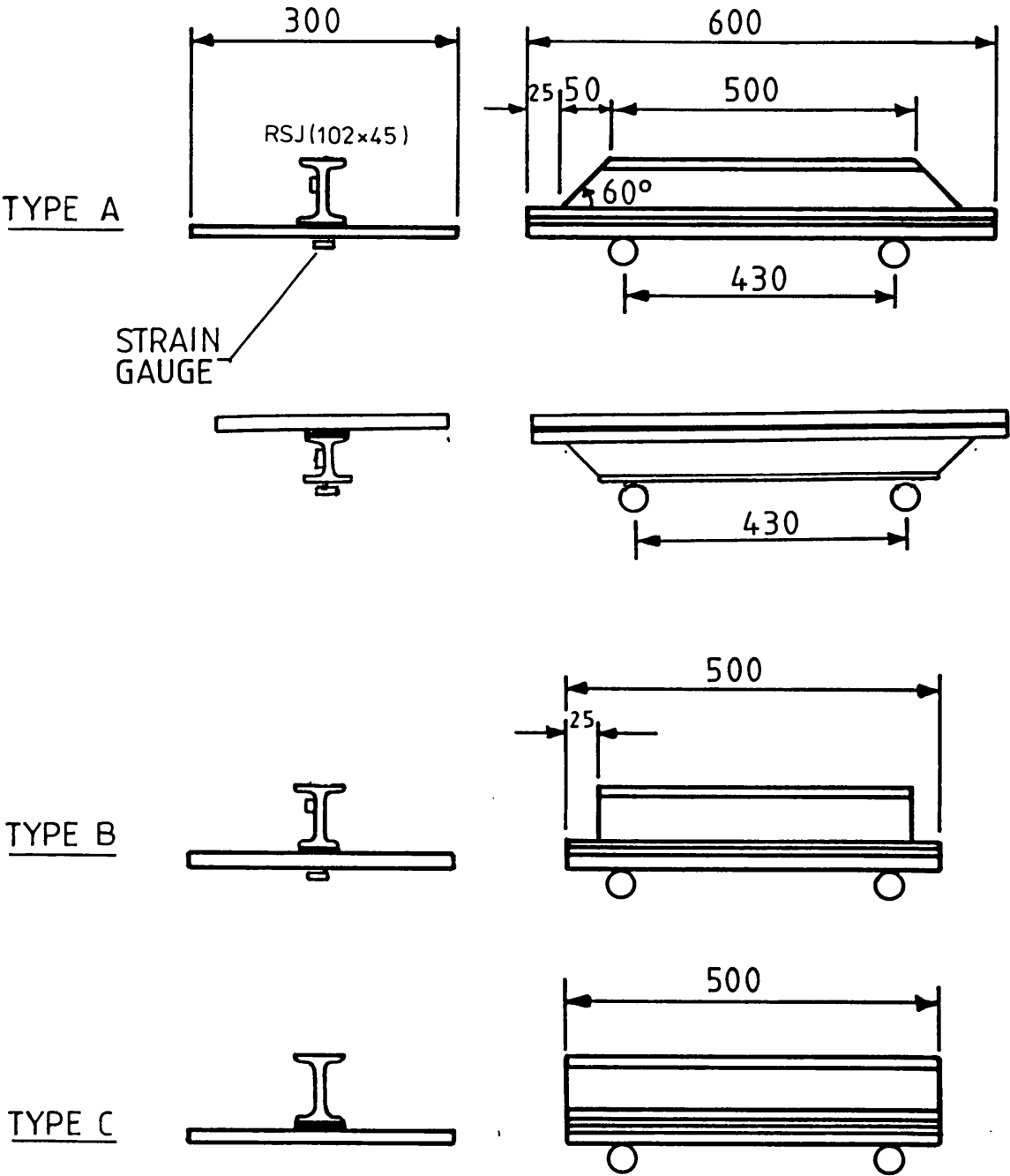


[2] Adhesive thickness 1.5mm - 2mm.
[3] No stress measurement was undertaken.
[4] Test temperature 120-150C

TABLE 6.1 IMPACT TEST RESULTS

SAMPLE IDENTIFICATION	MATERIAL/THICKNESS [mm]	HEAT RELEASE RATE AFTER 5 MINUTES [kW/m ²]	TIME TO REACH 200°C AT REAR FACE [min]
AB	5mm GRP + 6mm silica + intumescent paint	7.8	7.5
BA	8mm GRP + 6mm silica + intumescent paint	11.0	10.5
BC	8mm GRP + 6mm silica	87.0	10.0
DA(1)	14mm GRP + 12mm silica	<9.0	STOPPED AFTER 10 MINS
DB	14mm GRP + 12mm silica + intumescent paint	0.6	33.0
EA	8mm GRP + 6mm silica + 4mm GRP + 6mm silica + intumescent paint	1.0	33.0
EB	8mm GRP + 6mm silica + 4mm GRP + 6mm silica	2.5	32.0
2	14mm GRP	156.0	9.5

TABLE 6.2 SUMMARY FROM CONE CALORIMETER TEST RESULTS AT 60kW/m²
HEAT FLUX (SEE APPENDIX VIII)



DIMENSIONS ARE IN mm

FIGURE 6.1 IMPACT TEST SPECIMENS

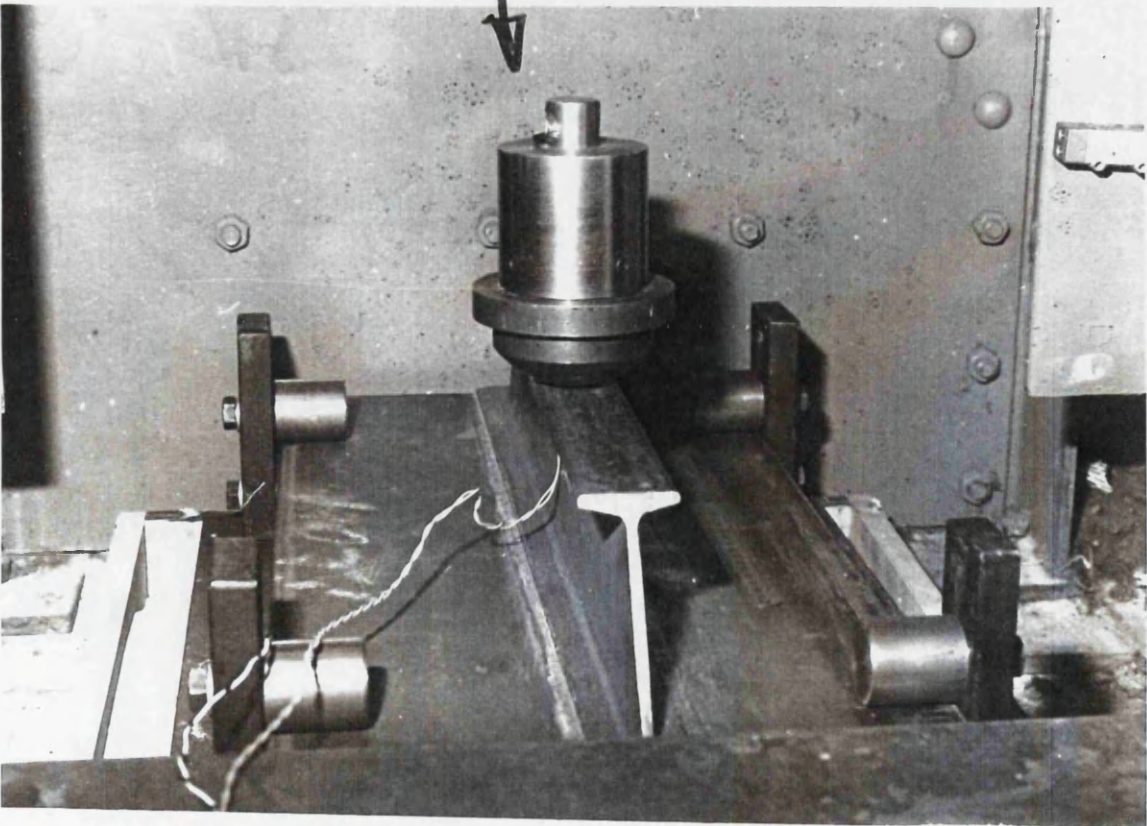
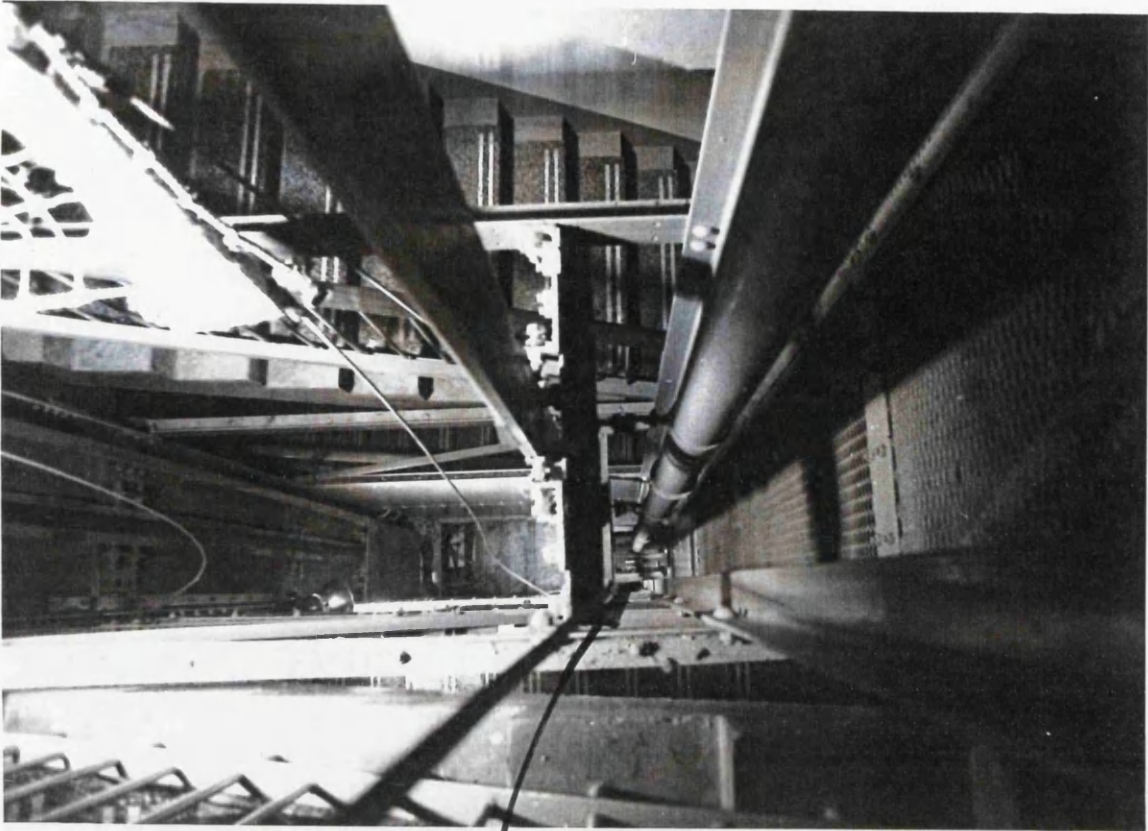


FIGURE 6.2 IMPACT TEST RIG (AT STAIRWELL)

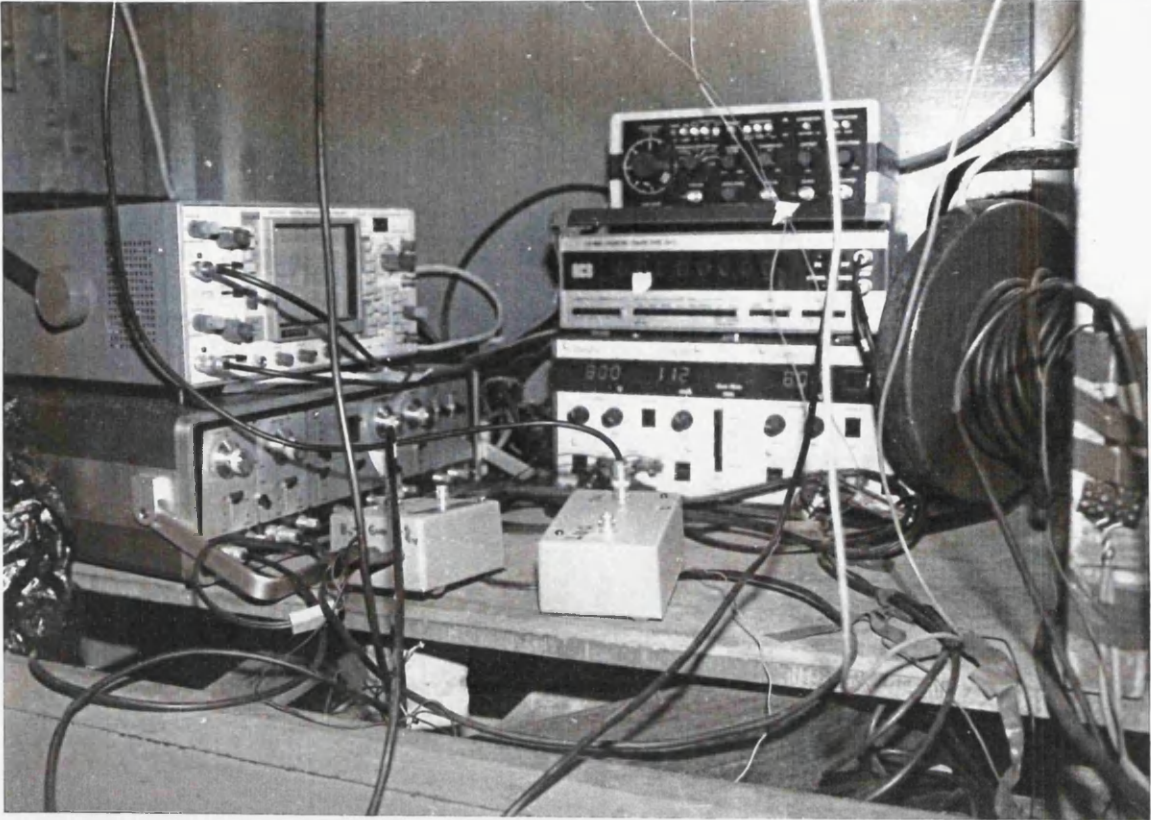


FIGURE 6.3 INSTRUMENTATION FOR IMPACT TESTING (AT STAIRWELL)

ALL DIMENSIONS IN mm.

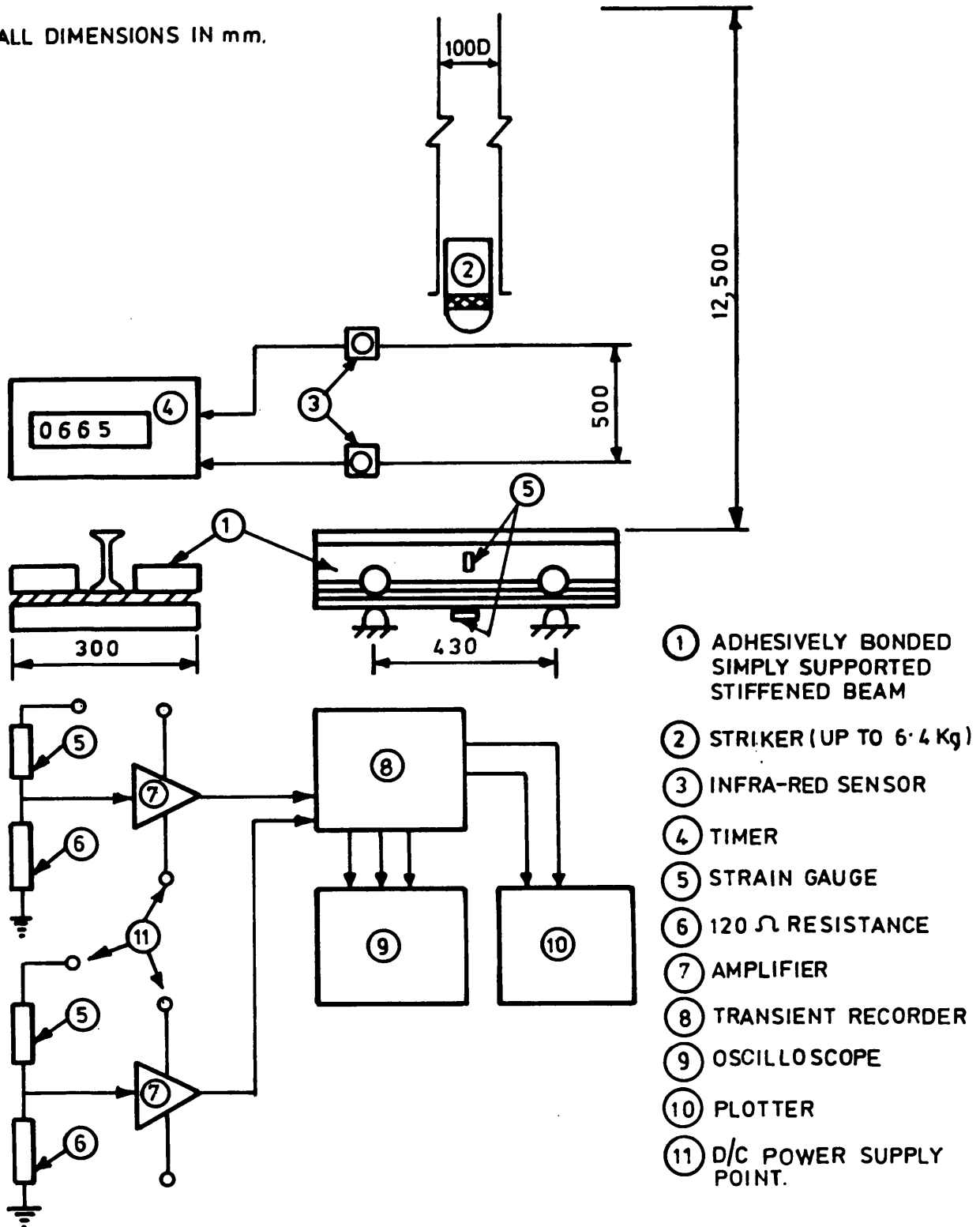
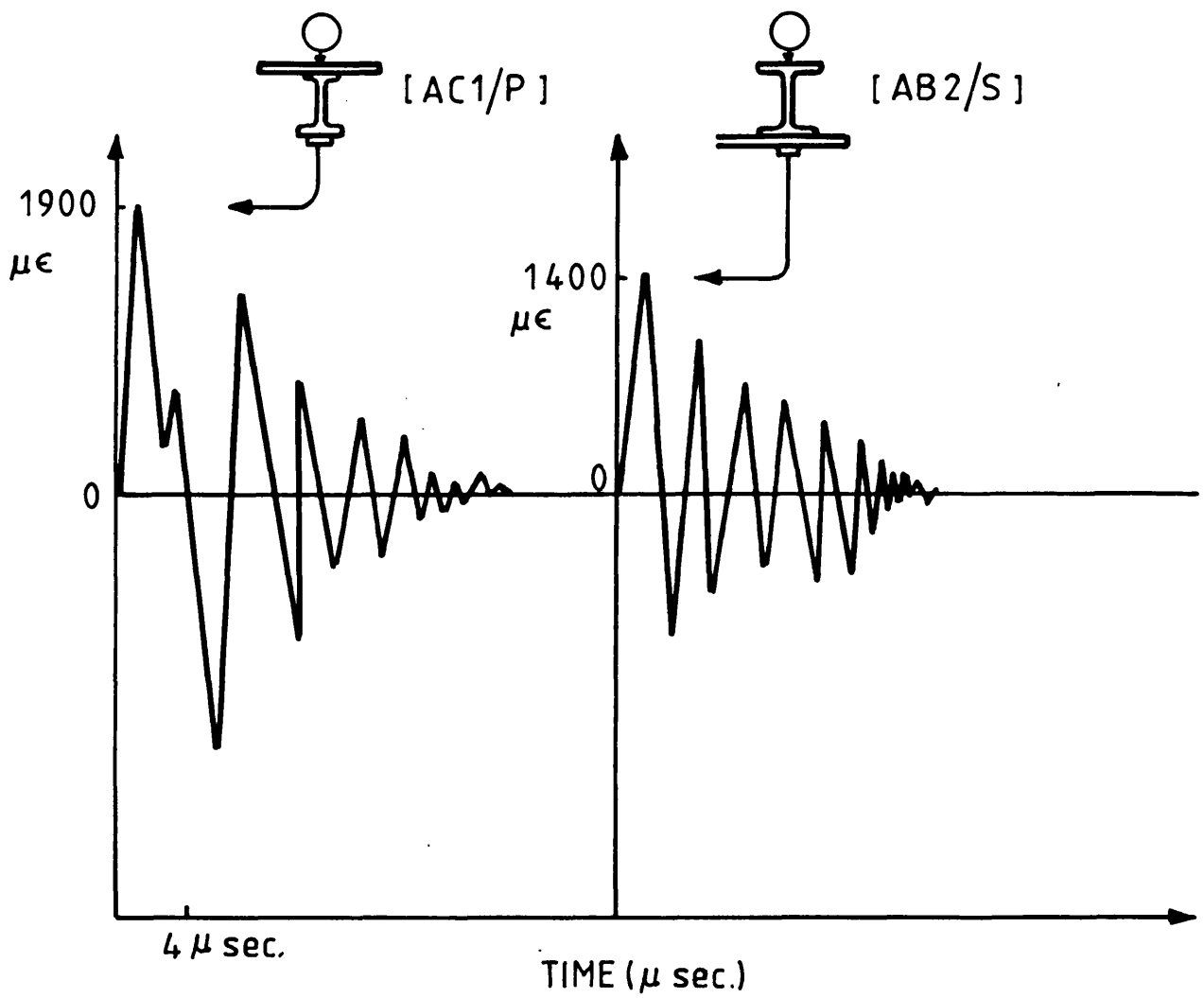


FIGURE 6.4 SCHEMATIC DETAILS OF TEST RIG AND INSTRUMENTATION



50 kHz
REFERENCE
SQUARE
CYCLES



FIGURE 6.5 TYPICAL STRAIN-TIME CYCLES OF IMPACT TESTS



FIGURE 6.6 DEFORMED SPECIMEN AFTER REPEATED IMPACT LOADING (SHOWING STRIKER)

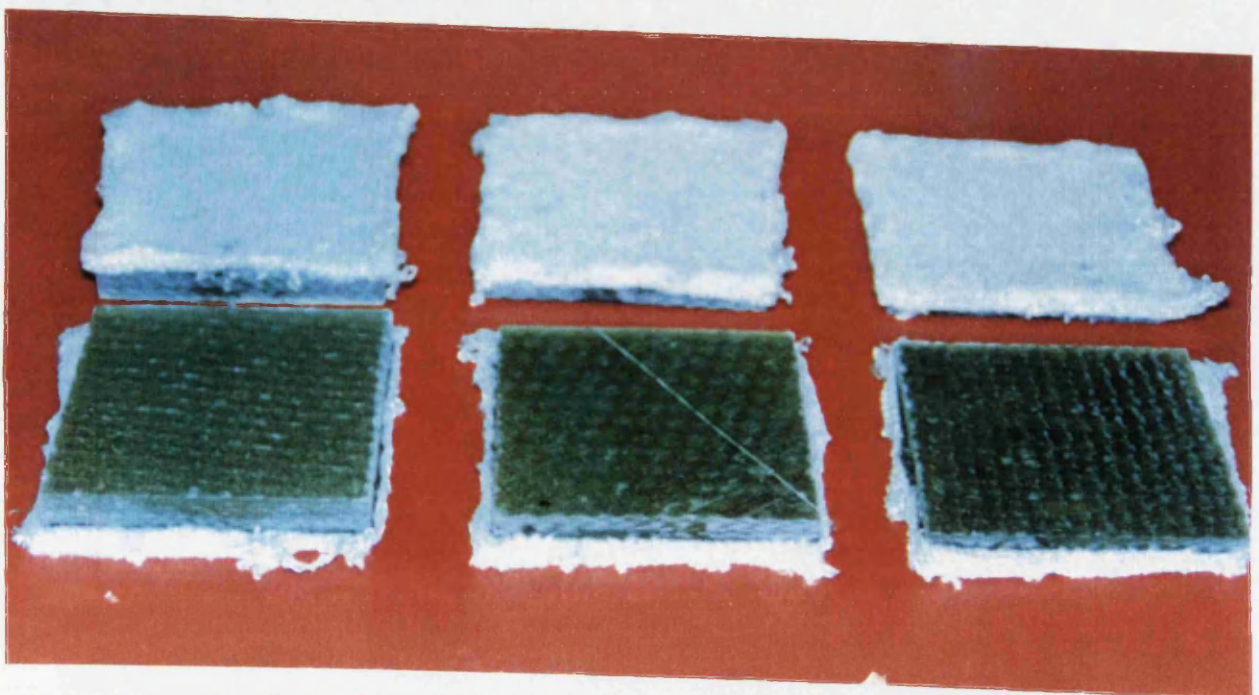


FIGURE 6.7 100x100mm GRP (INSULATED) SPECIMENS FOR CONE CALORIMETER FIRE TESTING

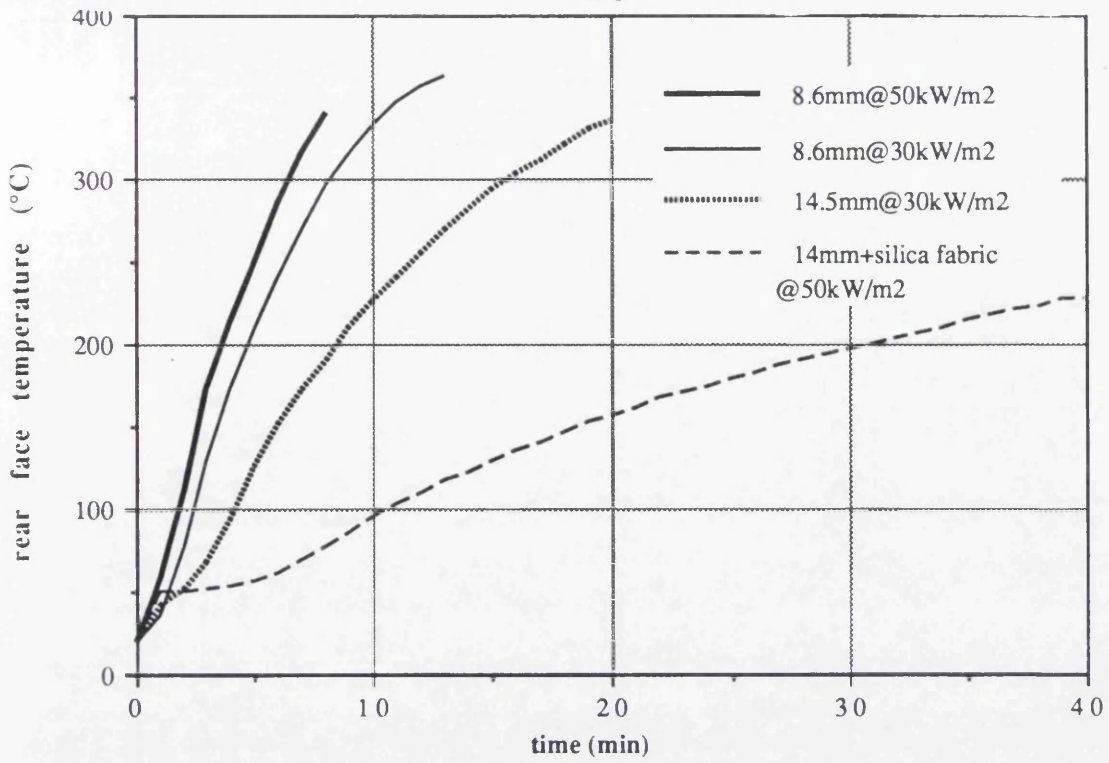


FIGURE 6.8 RESULTS OF REAR FACE TEMPERATURE FROM CONE CALORIMETER TESTS



FIGURE 6.9 INSULATION LAYERS OF PANEL

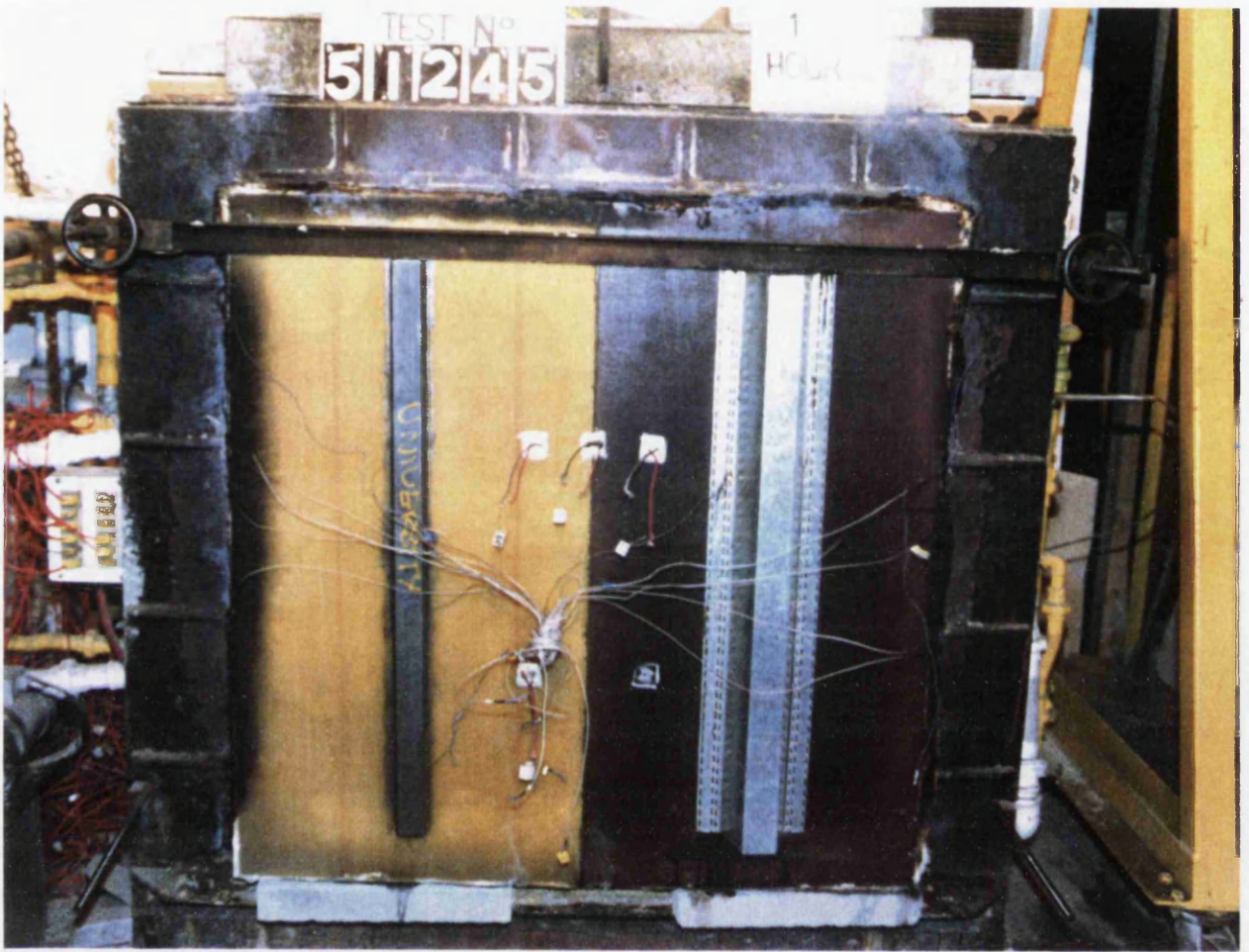


FIGURE 6.10 1.2x1.2m COMPOSITE PANEL (BONDED) UNDERGOING HYDROCARBON FIRE TEST

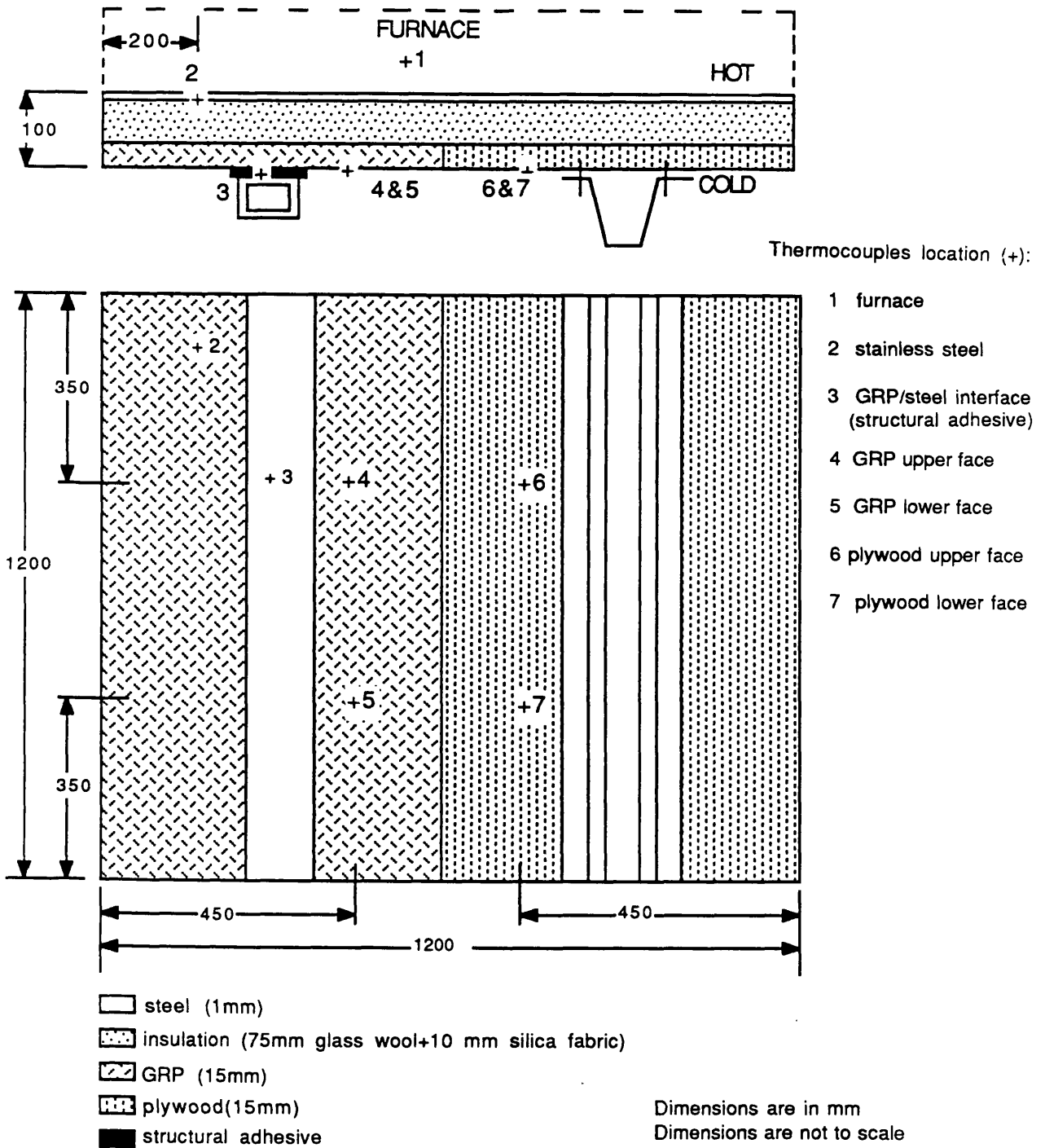


FIGURE 6.11 DETAILS OF FIRE TEST PANEL SHOWING THERMOCOUPLE LOCATIONS

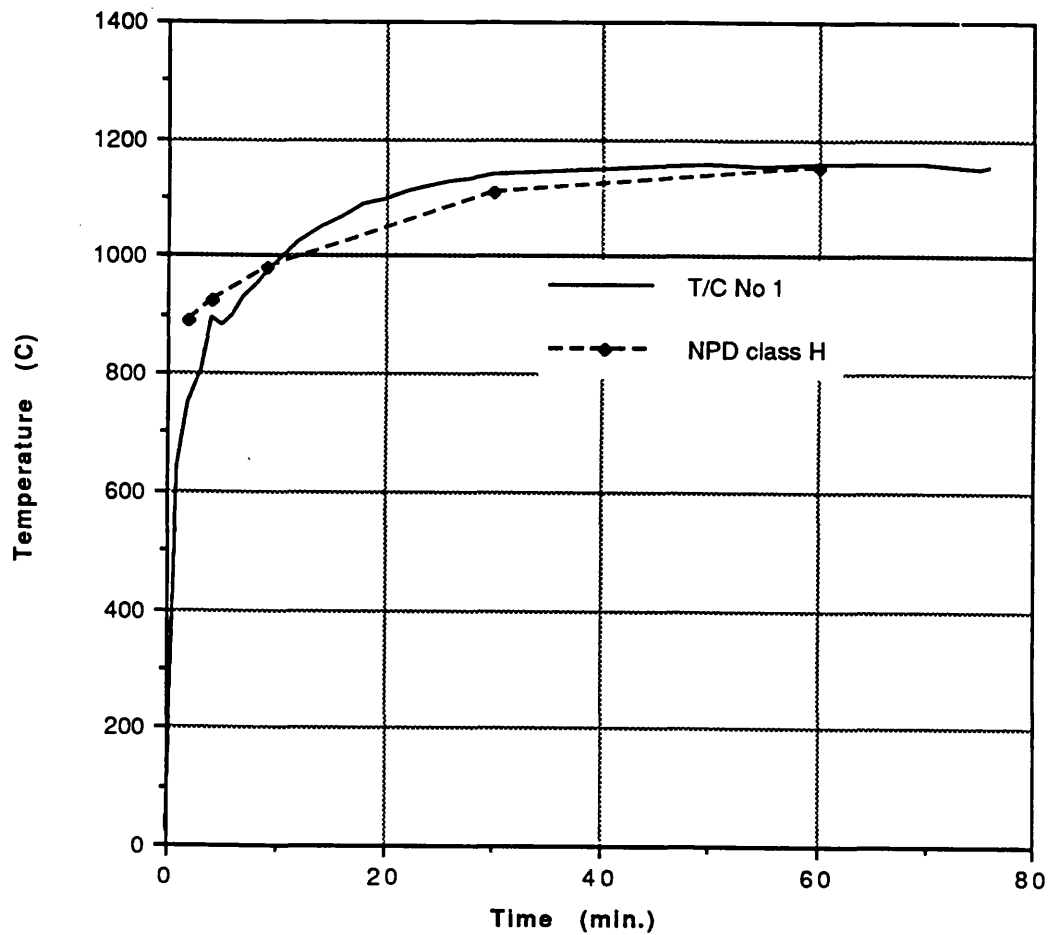


FIGURE 6.12 TEMPERATURE PROFILES FOR TEST FURNACE AND HYDROCARBON FIRE

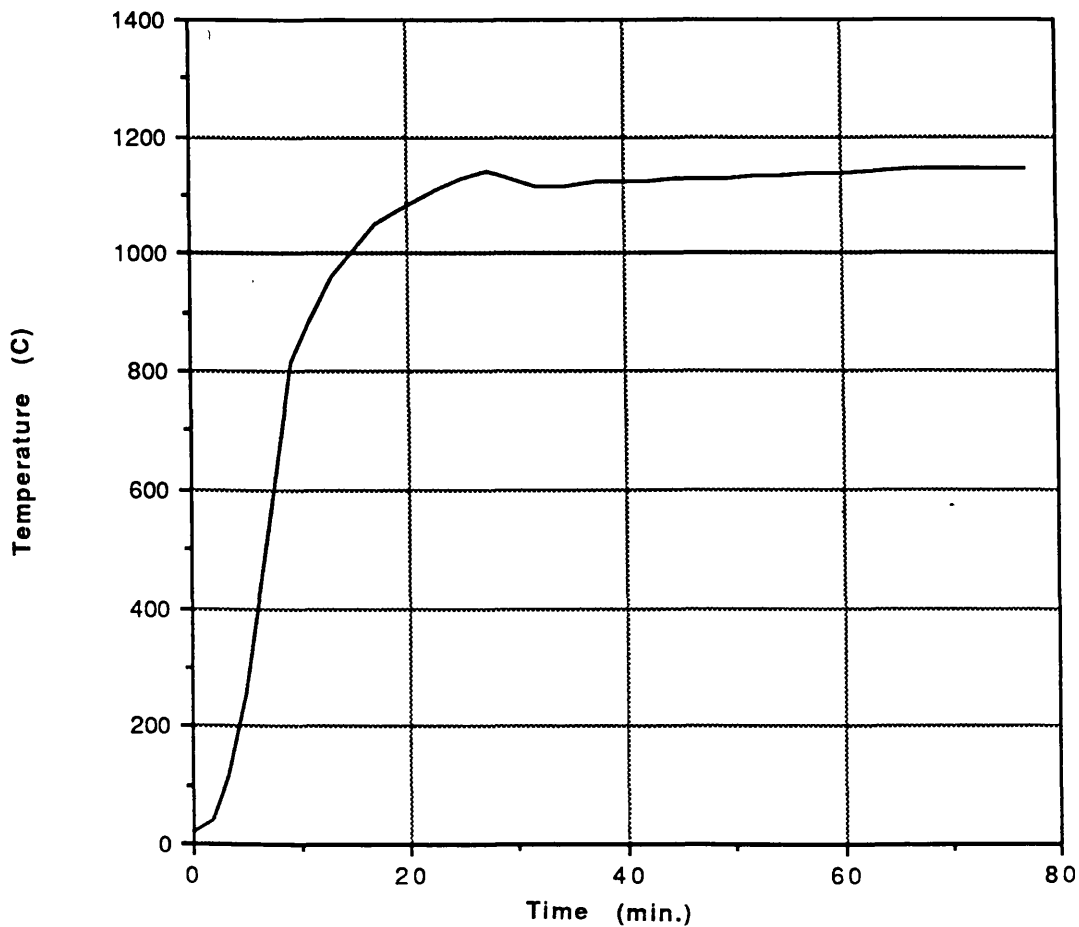


FIGURE 6.13 TEMPERATURE PROFILE OF STAINLESS STEEL SURFACE (T/C 2)

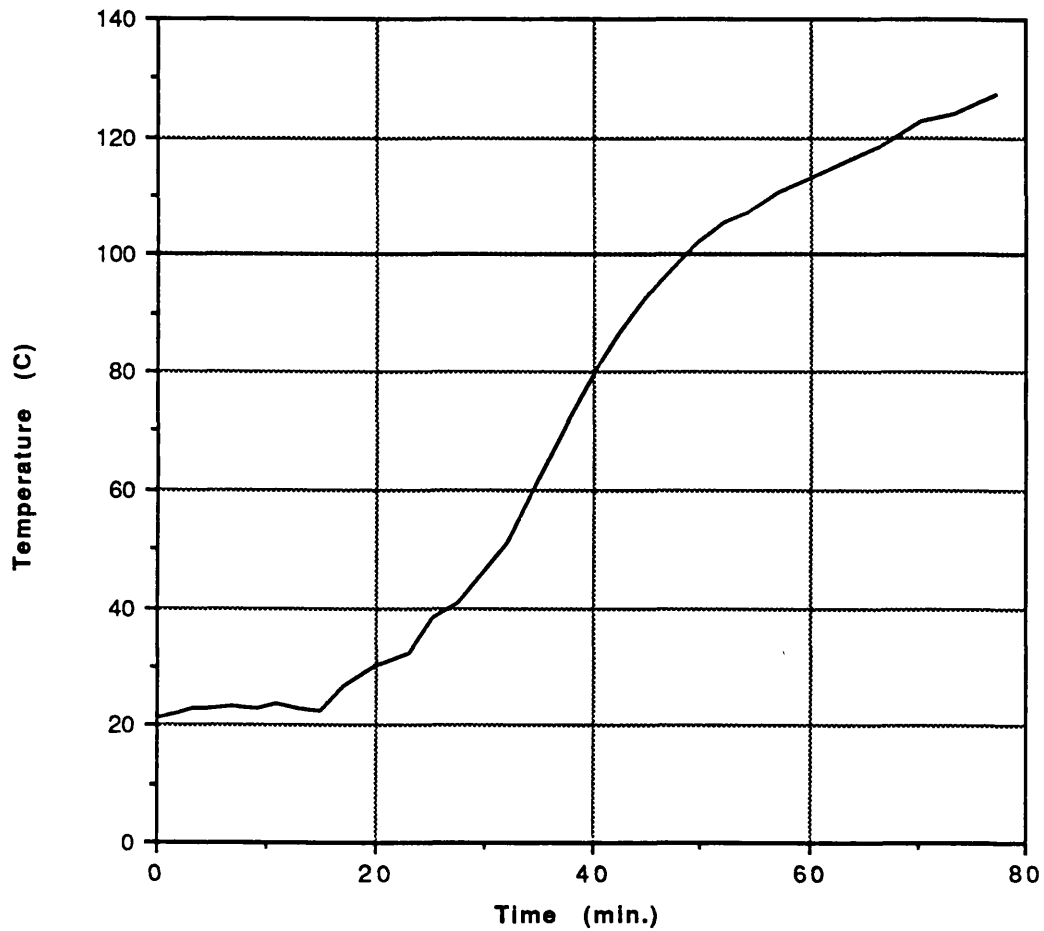


FIGURE 6.14 TEMPERATURE PROFILE OF ADHESIVE LINE AT STEEL/GRP JOINT (T/C 3)

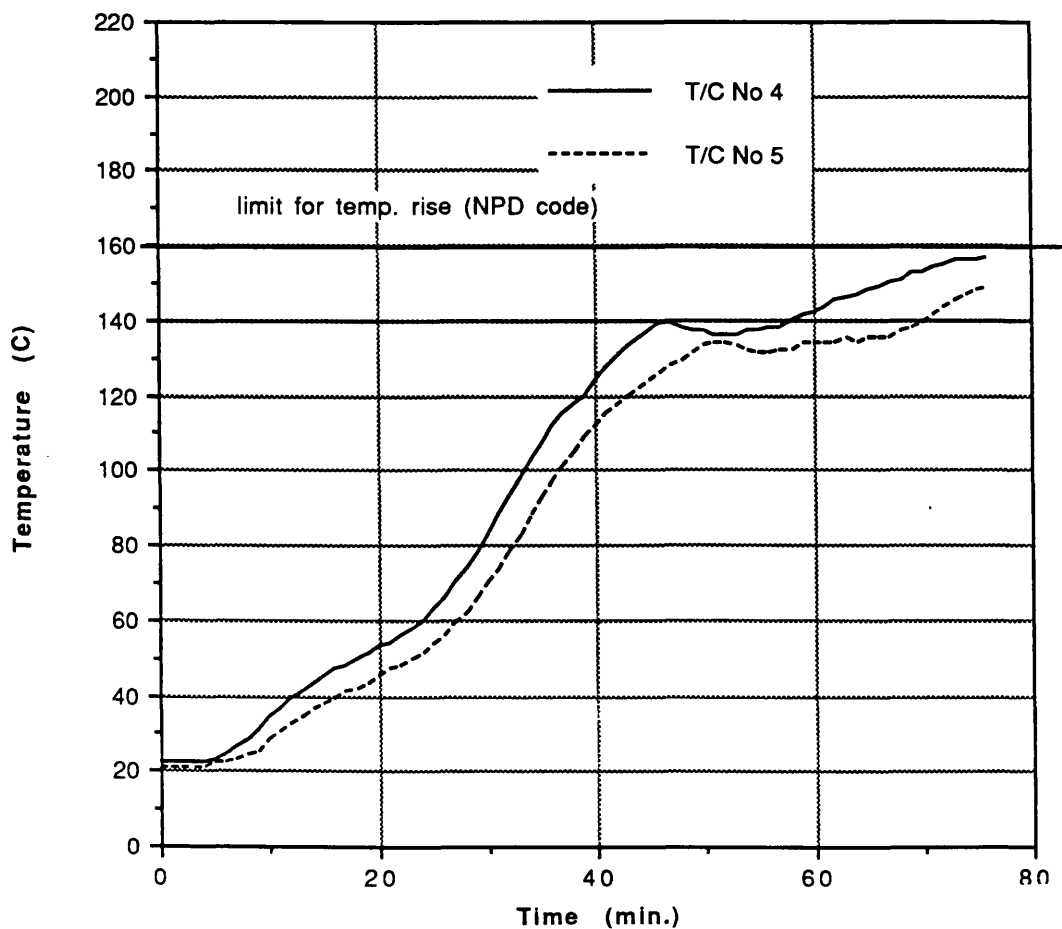


FIGURE 6.15 TEMPERATURE PROFILES FOR GRP REAR SURFACE

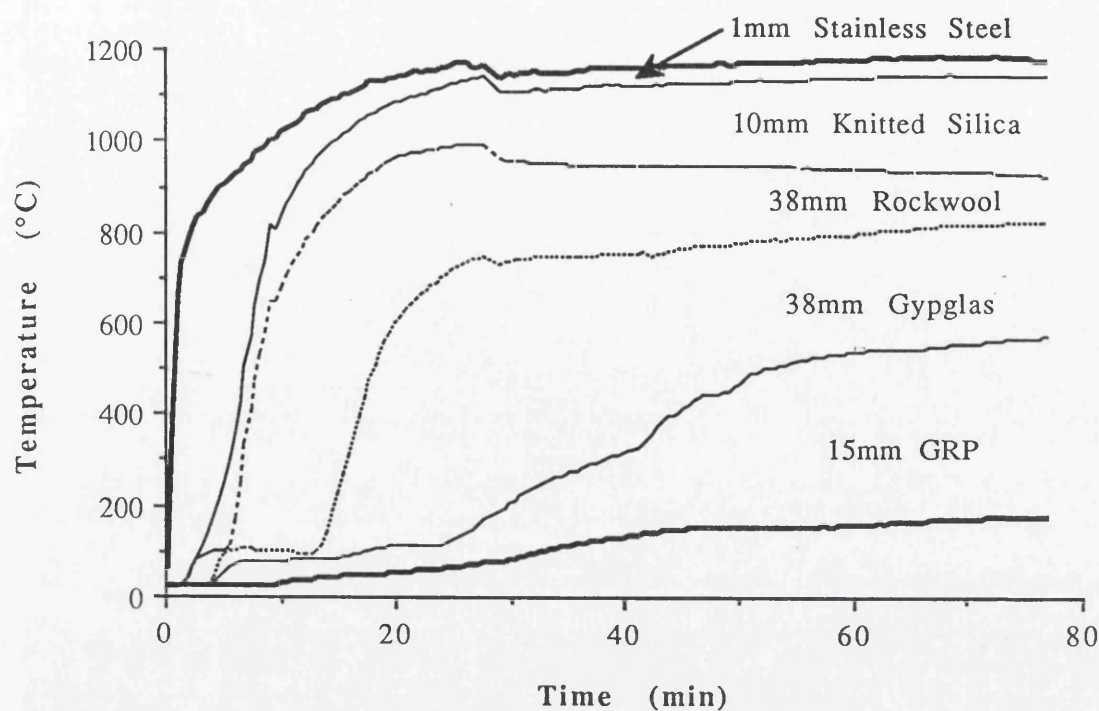


FIGURE 6.16 THERMAL GRADIENT THROUGH MULTI-LAYERED INSULATION OF GRP PANEL

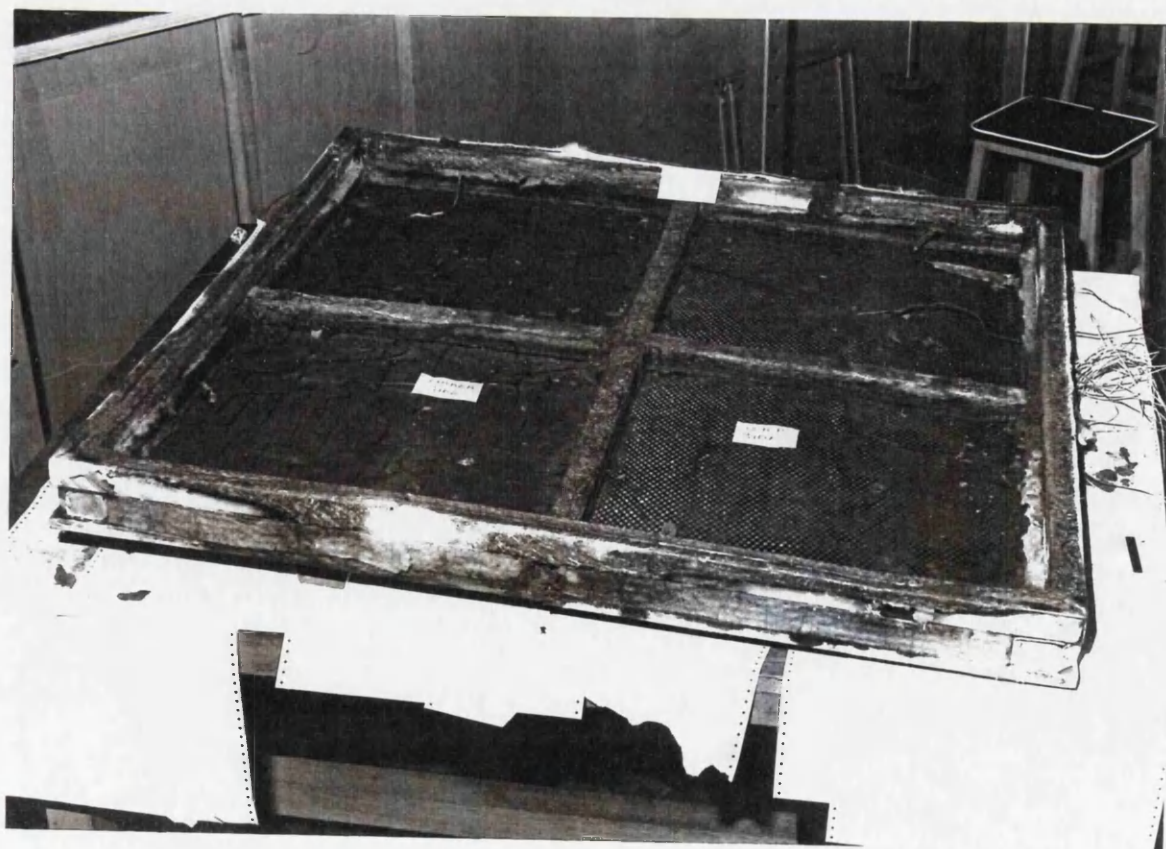


FIGURE 6.17 PANEL AFTER TESTING (STAINLESS STEEL AND INSULATION LAYERS ARE REMOVED)

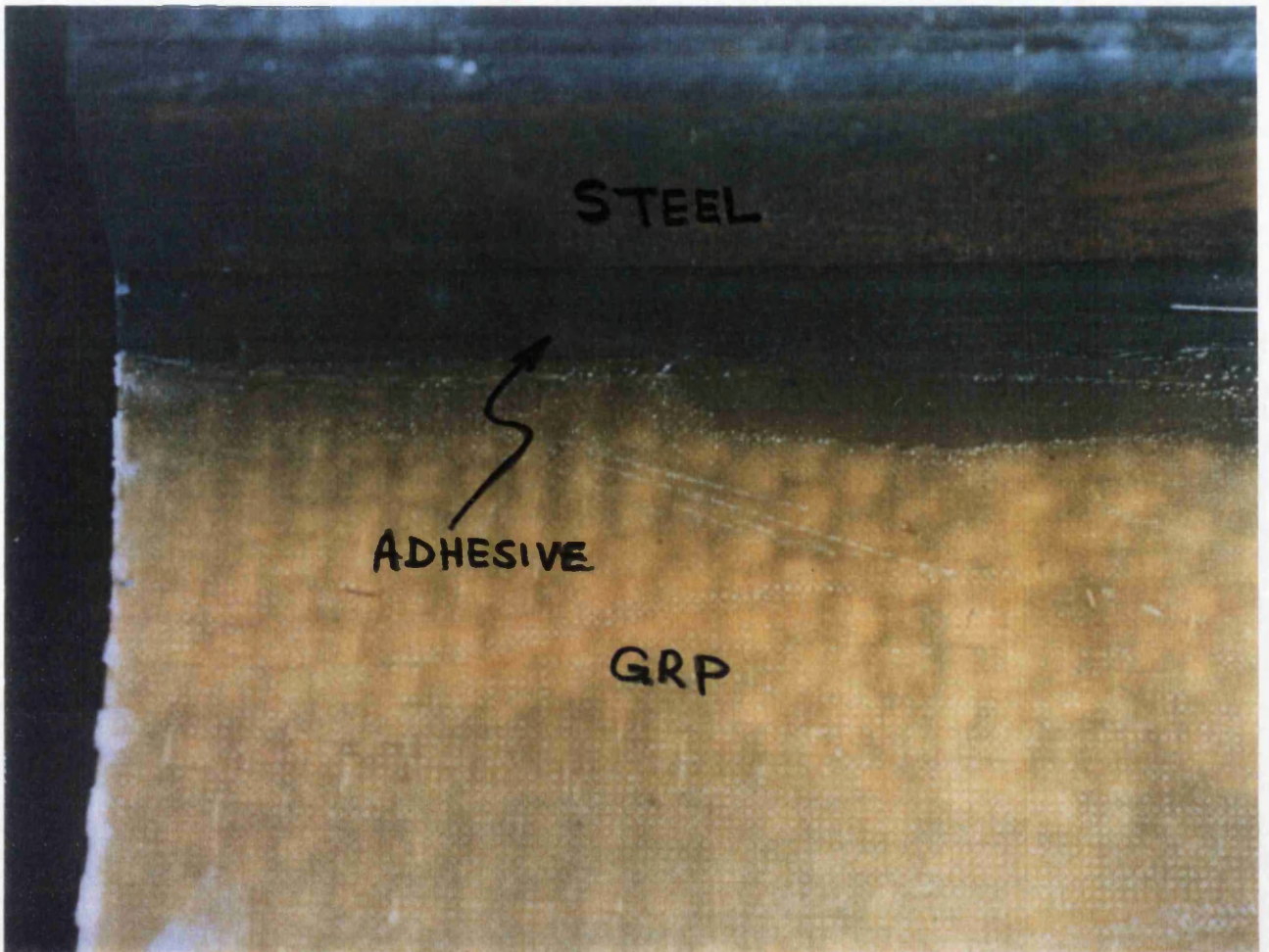


FIGURE 6.18 ADHESIVE JOINT OF PANEL AFTER TESTING

7. GENERAL DISCUSSION

The previous chapters presented an evaluation of adhesive bonding technology with reference to two applications. These are steel/steel bonds for stiffened plate structure for light, ship-type construction and steel/GRP bonds for fire/blast barriers of offshore platforms. The following subsections relate not only to these specific applications, but to wider applications of structural adhesives in novel designs. Some points have been already discussed in the previous chapters.

7.1. ADHESIVE SELECTION

The choice of Araldite adhesive 2007 for the bonding of steel to steel was dominated by the strength requirements. Initial strength is important for durable long term adhesion in order to counteract losses in the interface strength with time. In chapter 3 it was shown that after two years in a wet environment losses in strength of approximately 10% could be expected. A selection criterion including a combination of cleavage strength and shear impact resistance may be adequate to satisfy the overall strength. This is because the cleavage test reflects the tensile strength criterion and the shear impact reflects the shear strength as well as impact resistance. These comparative strength values are similar for both Araldite 2007 and ESP110 (Table 3.2) despite the fact that the toughening mechanism in the latter includes rigid metallic particles. In addition to the limited gap filling capabilities (0.5mm) of epoxy adhesive ESP110, feedback from users (communication with Alcan International Laboratory) suggested that it may have relatively poor resistance to longer term durability in a wet environment due to the use of metallic toughening particles. These could lead to corrosion within the bulk adhesive in an exposed joint.

In general a high performance adhesive should provide both rigidity for high tensile strength and low creep rates combined with flexibility to resist high peeling and impact forces. These are obvious conflicting requirements. Gap filling is also an important selection criterion and it is relatively difficult to achieve despite the claims of some adhesive manufacturers. There will be considerable problems relating to materials production and strength properties in order to achieve the necessary thixotropic material characteristics. These include the increased content of toughening particles (rigid or rubber based materials) and hence the related change in strength properties of

the adhesive as well as mixing, packaging and dispensing processes required during the manufacture and application of the adhesives.

At first sight the selection of Araldite 2004 from the candidates for steel/GRP bonding might not appear to be obvious. Its strength and impact resistance are not the best in the group (Table 3.3). The others (except E34) achieve their strength through greater ductility. However, the penalty associated with higher mechanical properties is a low glass transition temperature, which greatly reduces performance in creep and at elevated temperatures. Araldite 2004 has "a track record" of good durability in high humidity environments with minimal aging (private communication with Ciba-Geigy Plastics). In addition, the strength and Young's modulus of this adhesive are relatively well balanced with those of the polyester resin to which it is bonded in the GRP applications¹²⁹. Other considerations for a two part adhesive must include "pot life" after mixing which, although short at 30 minutes, is likely to be adequate for fabrication when automated mixing and dispensing systems are employed.

While the efforts of adhesive manufacturers are geared towards development of suitable adhesives for structural applications, equal attention should be paid to surface preparation. Therefore the choice of an adhesive should also incorporate the use of appropriate primers and likely surface topography among other factors. These considerations were not extensively studied in this current investigation.

Present trends (with few exceptions) in the development of a wider use of adhesive bonding rely normally on "existing structural adhesives to stimulate new applications" (as has been the case for this study) rather than to start with a structural requirement and manipulate the joints and adhesive characteristics to satisfy a defined need. Some adhesive users (such as Ford, Alcan and Rover) have recently developed their own adhesive formulations, in most cases to meet requirements other than strength of the adhesives. These other factors include ease of bonding processes in automated production environments and long term durability.

7.2. BONDING PROCESSES/FABRICATION

The success of an adhesively bonded structure depends to a very large extent on the quality of the surface preparation of the adherends employed. This aspect was therefore incorporated from the beginning. Conclusions regarding bonding process variables (some based on only one or two test specimens in order to obtain general views) include

the following:

- There is no appreciable difference in the joint strength between joints whose adherend surfaces are abraded or grit blasted. This applies to both steel and GRP surfaces and was demonstrated on Types 3 and 5 specimens (macro joints- Figures 4.10 and 4.15). The implication of this is the possibility of utilising semi-automatic abrasive systems for preparing the surfaces of large/long plates. Such equipment (developed for abrasive belts-3M Ltd) is already in use for abrading large horizontal surfaces for platforms in the civil engineering industry.
- The "as received" GRP surface produced a joint strength of only 20-50% of the equivalent well prepared steel/GRP specimen. This scatter appears to depend both on adhesive type (brittle or flexible) and joint configuration. This was demonstrated by Types 6 and 7 small specimens (Figure 3.7).
- The "as received" surface of hot rolled mild steel produces about 50% of the strength of typical (well prepared steel/steel specimen -hot curing adhesives) joint strength¹²³, investigated with reference to Type 1 small specimens (Figure 3.6).

It is clear that bonding surfaces without mechanical preparation (or peel plies) will always produce joints which are weaker than can be achieved with structural adhesives. This may be due to the absence of mechanical interlocking mechanism "hooking" between adhesive and adherend as it was demonstrated on peel test specimens elsewhere²⁴. In the case of the GRP there is the additional problem of residual mould release agents such as silicone materials which can be effectively eliminated by the material removal of the surfaces and/or chemical degreasing. Much research work in these areas¹³⁰ justifies the use of "as received" zinc coated and uncoated oily rolled steel surfaces by the cost saving advantages without a clear view on the cost effectiveness of this approach, in relation to possible degradation in the adhesive strength (at the interface) and associated consequences of failure.

It has become clear, in the case of the GRP adherends that the use of a peel ply can give good strength (Figure 3.20) as well as a cost advantage due to the absence of an abrasive process. The cost of incorporating the peel ply during the production of the panels (adherend material) is insignificant in comparison with normal resin rich finish to panels (private communication with Vosper Thornycroft Ltd). However, long term integrity of adhesive joints, at the interface with the peel ply surface may depend on the

type of the mould release agent used for panel moulding. In many cases these are silicone based materials which must be removed by wiping with solvents. In addition, it is important to know the effect of anti-aging additives used within the resin matrix of these panels. This is particularly important when the GRP is subject to elevated temperatures during a warm curing process¹²².

Mixing equipment is essential in the case of the two part adhesives (for any materials combination) not only in producing a repeatable and air free adhesive (stronger joint) but also to control the limited "pot life" of the adhesive by mixing the required amount at a given time. Such equipment is expensive and may need to be justified against the cost of single part adhesives (mainly applicable to metallic joints) which otherwise require heat curing equipment. The cost of producing a thermally insulated steel/GRP panel for hydrocarbon fire resistance will be considerably higher than that in the case of general steel/steel panel (without thermal insulation). Therefore the investment in semi-automated plant including mixing and dispensing systems may be justified.

Adhesive Araldite 2007 has shown good gap filling capabilities in both small and large test pieces. Proper clamping is however essential to ensure adequate contact pressure along the adhesive joint and therefore smaller gaps to be filled with the adhesive. Figure 7.1a shows a visible bond defect resulting from incomplete gap filling resulting from inadequate clamping of a large panel specimen. Although after opening such a joint for inspection (following a successful mechanical testing) a significant area was bonded as shown in Figure 7.1b. The author however would like to investigate in future research the hot cure of a large joint/panel element with thick (up to 2mm) adhesive line in a vertical position in order to monitor the possibility of adhesive flow at elevated temperatures during such fabrications. Techniques for using sealing tape system have apparently been used successfully (communication with Permabond Adhesives Ltd).

In the case of steel/GRP bonding it is important to maintain the minimum clamping force (deadweight) so that stress built up in the joint after curing and releasing the clamping force, is very low. Excessive clamping force may cause debonding after the release of the clamping force, especially when a lightly toughened adhesive such as Araldite 2004 is being used for bonding.

Surface preparation of corrosion-resistant steels has not progressed to a level equivalent to that of aluminum because of the latter's association with aircraft

applications. However recent attempts to produce durable steel joints has led to new developments in the field of silane primers¹²⁴ (for details see Section 7.4). In the case of large structural applications such as marine structures there may be scope for integrating the the use of existing epoxy shop primers, as a part of the surface preparation, or to incorporate corrosion inhibiting materials within the adhesive formulation. An alternative strategy is the possibility of designing the joint against wet environments by active methods such as incorporating sealant or by use of the sandwich design concept.

The author believes that even a confident first time user of the adhesive for a major structural application would wish to complement the adhesive joints with other joining methods or to consider fail-safe design. In addition to the psychological barriers, the problems of impact and fire risks may dictate such a decision. A feasibility study based on this research carried out by a steel fabricator/manufacturing company¹²⁸ examined the possibility of using the manual arc welding process in conjunction with the bonded joint (both ends of a 1m long beam were fillet welded at an L stiffener to an 8mm plate attachment) without significant damage to the bonded joint. The heat affected adhesive areas were only charred locally due to the intensity of the heat from welding and did not spread further because of the poor thermal conductivity of the adhesive and large heat capacity of the bonded steel beam. This fabrication method may be more suitable for steel rather than aluminium adherends due to high thermal conductivity of the latter. More work is required in this area to understand the impact of a damaged zone caused by adjacent welding.

In principle, production of adhesively bonded structures in the marine industries seems to be straightforward provided it is carried out by adequately trained personnel (little skill is required relative to welding) using simple modifications of existing equipment. Changes in design may require new optimised standard steel sections compatible with proposed joint configurations, but this need not to be a practical or economic barrier to large scale production. Qualifying destructive testing and visual inspection of the squeeze-out of the adhesive are likely to remain the main quality control technique at this stage. Much work remains to be done in developing cost effective and reliable NDT methods, especially the ultrasonic techniques, for adhesively bonded joints. Small debonded areas or voids included in an adhesive joint between thin adherends can be detected relatively easily¹²⁵. In adhesive joints with thicker adherends only large size defects may be detected by using low frequency ultrasonic

methods¹²⁵. Other suitable methods for thick adherend applications include the low-frequency vibration of coin-tap test from which a vibration signature may be produced to assess whether large debonding or large voids exist in a joint. No technique is yet available to successfully detect poor adhesion in range of adhesive joints. There may be scope for monitoring the strain behaviour in an adhesive joint by embedding strain gauges or optic fibre elements within a critical zone. This however, requires sophisticated instrumentation, and in order to justify the use of such techniques they must be used in a very important application. Much research is still required to establish this technology which may prove to be the only reliable method for long term quality assurance of adhesive joints.

In full scale production environments automated jigs and adhesive dispensing equipment may be used together with additional advantages obtained from using peel plies to provide ideal bondable surfaces on GRP panels. Applications of well designed jigs which control positioning and avoid disturbance during cure are especially important when using relatively short "pot life" adhesives. The production (bonding processes) of steel panels (for example) would require at least seven operations including surface roughening, degreasing, marking of components, application of adhesive, positioning of clamps or pressure devices, curing and removal of the clamping or pressure devices. In the bonding of a large aircraft wing using a hot curing technique the full bonding cycle of the above operations takes about 24 hours¹²⁶. There is a scope for reducing this time substantially in the case of steel panels due to relatively easier processes of clamping (using magnets which cannot be used in the case of the aluminium) and heat curing (using low a voltage heating system rather than an oven). The other advantage with steel is that curing temperature for epoxy adhesives can be brought up to 200°C to initiate cure cycles of approximately 10 minutes without the risk of causing metallurgical damage in the microstructure of the steel. It was noticed when bonding the panel elements described in Chapter 4 (Section 4.2) that a variation of up to 20°C existed across the thickness of the adhesive line (adhesive cure at 180°C). This, however is regarded as an acceptable allowance for curing single part epoxy adhesives by the adhesive manufacturers. Temperature differences of up to 60°C were measured between the plate and stiffener in some positions. Such temperature variations may lead to a build up of residual stresses within the adhesive if one of the bonded components is clamped.

7.3. EXPERIMENTAL EVALUATION METHODS

In the development of adhesive applications, experiments are the most important and reliable technique available for evaluating adhesives, adhesive joints and the performance of bonded structures. There are however two requirements. The first is that the experiments should reflect the strength level relating to their engineering application. The second consideration is that the experimental hardware is suitable, reliable and compatible with the nature of the bonded joints.

Small scale specimens are usually used to determine comparative properties of adhesives. In addition, in this research, the choice of these specimens was dominated by the need to produce a cleavage mode of failure in stiff joints for both steel/steel and steel/GRP specimens. This reflected the importance of the cleavage (tensile) stresses in the relatively heavy structural applications considered here for adhesive bonding. Small specimens of Types 2 and 3 (Figure 3.6) represent "very rigid" joints while Type 1 can be regarded as a "semi-rigid" joint due to its relative flexibility as a result of the deflection generated from the bending moment. This feature (in the author's opinion) makes the lap shear joint more relevant to the behaviour of stiffened plated structures in comparison with other small test specimens (steel/steel). Stiffened plated structures may experience a combination of shear stresses (bending shear) and cleavage stresses due to the transverse moments on the joint between the plate and stiffener. The same can be said for the small steel/GRP lap shear specimens of Type 1 (Figure 3.8). However, steel/GRP specimens Types 2 and 3 (butt and cleavage respectively-Figure 3.8) may not be regarded as rigid joints. This is because the low modulus, as well as lamination organisation in composite materials, makes such joints rigid adjacent to the steel adherend but flexible on the GRP side. Thus Types 2 and 3 steel/GRP joints may be regarded as useful specimens in evaluating the local behaviour of the composite plated stiffened structures where failure of the joint occurs as a result of GRP delamination, as discussed in Section 7.5.

The large scale specimens for steel/steel and steel/GRP joints were formulated and designed to represent actual structural joints and to study their behaviour under the ultimate loading conditions. In reality, possible loading equivalent to the magnitude of failure loads in these specimens can only arise as a result of extreme environmental loading, impact or explosion blast conditions. The other possibility of failure is long

term fatigue loading under service conditions. The preliminary indications show that adhesives can provide good fatigue performance in stiffened joints subject to light loading in a low humidity laboratory environment¹²³. Even with convincing results that adhesives can provide joint strengths well above normal design limits, it is likely that a first time user of adhesive bonding will demand a maximum load limit (e.g plastic deformation) from the bonded structure even if he considers lightly loaded design.

All the experiments were carried out using testing machines and hardware which are typically used to test metallic specimens. This has produced problems in measuring the properties and behaviour of the thin adhesive line such as the small strain to determine modulus of elasticity and creep deflection. In particular the use of standard machine grips for testing butt specimens has shown a significant scatter in joint strength (Table 3.2) up to 30%. The results from the larger cleavage steel/steel specimens (Tables 4.1 and 4.2) have also shown strength scatter up to 30% due to difficulties of accurately controlling the loading alignments for the large number of specimens which were produced and tested. It was difficult to apply, for large number of specimens very accurate machining, bonding and testing, due to time limitation. However specimens (Types A and B-Chapter 5) used for the theoretical analyses were very carefully manufactured, bonded and aligned during testing.

The test models and rigs used in the large scale impact experiments (Section 6.1) are intended to represent a structural element of a practical stiffened/panel. It is felt, however, that this produced conservative results because the use of relatively short specimens led to high frequency response and development of high cleavage stresses at the ends of the adhesive joint. The impact resistance in this investigation was measured at a temperature of approximately 15°C. Other temperature ranges could affect the impact resistance due to the temperature sensitivity of Young's modulus in the adhesive tested. The instrumentation used in the impact study produced some difficulties in measurement of strain rates in the adherends. This was because of the high stiffness of the short specimens, the relatively high impact velocities, the contribution from the inertia forces and the limited reliability of amplifiers used (normally used for measuring low frequency response).

Despite the reservations discussed above, it is felt that the principal joints, their behaviour and adhesive requirements have been evaluated satisfactorily. The final stage of such development requires the testing of a full scale sample of load bearing structure. This will require extensive collaboration with industry. Such a demonstration might

include the fabrication and testing of a large steel panel for a marine application.

As a result of the experimental evaluation in this study many problems have been identified and refinements have been made to the experimental hardware and software. These included the use of thermal creep and impact testing in addition to static loading criteria to measure the properties of a bond line.

7.4. THEORETICAL EVALUATION METHODS

Proper representation of the test specimens boundary conditions is an important factor in obtaining the correct stress distributions, particularly in the case of the lap shear specimen test in which the position of the loading points can influence the results. Restraint and loading conditions are meant to simulate the real boundary of the specimens tested for example, in the Instron testing machine.

Good agreement between theoretical results and experiment measurements, at the adherend surfaces is, very important in validating stress analysis, as in any bonded joint analysis, because it is very difficult to obtain experimental strain measurement in the adhesive line due to difficult accessibility. Table 7.1 compares theoretical adherend stress values for models Types A and B (steel/steel-Chapter 5) which result from finite element analysis with stress values measured from experiments (Figure 5.3). This comparison is based on an applied load of 8kN for the two models (due to debonding of the strain gauges at loads above this level). These results indicate that theoretical stresses are between 5% and 15% higher than those obtained by experiment. The accuracy of such measurements is influenced by the exact positioning of the strain gauge 5 mm from the edge of the joint (Figure 5.1). In these circumstances this correlation is regarded by the author as a good.

The correlation between failure stress for the lap shear joint and that for model A and B exhibits scatter of about 10%. This percentage is based on a product of 3% experimental and 6% theoretical scatter as discussed in Chapters 3 and 5. This correlation is based on the assumption that adhesive stress value 0.1mm from the adherend/adhesive interface are compatible between the small and the large specimens. Lap shear joints with fillets were also analysed. The stress level, again, was high 0.1mm from the lower adherend/adhesive interface (Figure 7.3a) but slightly higher (by approximately 5%) near the sharp corner of the upper adherend/adhesive. This effect was however ignored due to geometrical complexity in this area as mentioned in

Chapter 2 (Figure 2.21). Further discussion of this point is presented in Section 7.5.

In the case of the simulated pressure testing (steel/GRP) there were difficulties in exactly modelling the experiment numerically. These were largely due to ignoring the contributions, from both the rubber and aluminium strips, to the GRP beam stiffness. The assumption of a clamped boundary condition of the test model may also give rise to errors. The correlation between the stress in this model and the standard steel/GRP test specimens/model (Section 5.2.3), might therefore be unreliable. The influence of these strips would be even more pronounced in testing a model with a thinner GRP skin because their contribution to the measured beam stiffness would be relatively higher.

The results from elastic finite element analysis are encouraging and the author is not aware of similar attempts to evaluate failure of a bonded joint in this manner. Whatever the numerical approach used, the present technique can only be regarded as qualitative, because of the exact interface topography is not modelled and because of the uncertainty associated with the final element in a joint at which a singularity in the stress distribution occurs causing widely varying values of adhesive stresses^{98,113}. This is even more complex in the case of composite materials where it is difficult to numerically identify the exact location of the interface region between the resin matrix and the adhesive.

The analytical method based on the peel analysis showed reasonable agreement with the finite element analysis (Table 5.1). However, on closer investigation it is clear that the stress equation (Appendix V) is very sensitive to the adhesive thickness. For example, assuming an adhesive thickness of 0.1mm produces stresses five times that obtained with a 0.5 mm adhesive thickness. The results are also very sensitive to a change in plate thickness. Such design formulae are therefore more useful for thin adherends applications.

The following modifications, assumptions and observations are associated with the laminated beam theory analysis used in Chapter 5

- The beam model did not have a large length to width ratio. This makes it more suitable for cylindrical bending rather than beam bending but this theory states that the two modes of bending are applicable.
- The analysis equations apply to beams with a large radius of curvature (due to bending) and hence to small loading conditions
- The theory applies to a symmetrical beam section and therefore needs

modification to suit stiffened sections and panel elements

- From the interface coefficient equation $f_1^{(2)} = (Q_{11}^{(2)} \cdot D_{11}^{*(2)}) \cdot \frac{h^3}{12}$ (Appendix VI) the following design parameters can influence the behaviour of beam joints:
 1. the modulus of elasticity and Poisson's ratio of the adhesive and adherend,
 2. the thickness of the beam section,
 3. the equivalent modulus of elasticity of the section,
 4. the curvature of a beam with different adhesive thicknesses. It may be assumed that a bonded beam with a "near zero" adhesive line thickness should behave as a solid beam and hence; $f_1^{(2)} = 1$

7.5. DESIGN LIMITATIONS

The four possible limitations to the use of adhesive bonding require that some guidance be given to assist designers who are considering adhesives as a primary joining method. These areas of limitation are fire, thermal creep, impact and durability in wet environments, which are discussed below.

The main requirements of polymeric adhesives used for bonding structures in which fire is a design criterion are the ability to retain adequate strength to support the structure and to produce minimum harmful fumes as a result of its combustion. These requirements are clearly difficult to meet unless adhesive is incorporated in a suitable design. The same applies to a composite which is self (resin) bonded to meet the above requirements unless it is sufficiently insulated and protected. This is the approach used in this study where the insulation design used with the steel/GRP construction played the prime role in providing a fire resistant construction as demonstrated in Chapter 6. Fire resistance remains the most serious drawback in using adhesives for joining structures in which fire is a possibility rather than a probability and where insulation is prohibited by cost or other factors. The concept of fail-safe design in such cases must be considered. A possible example is the design of decks where plating is supported on a horizontal frame and where in case of fire, the joints are under compression (self weight of the deck plating) and therefore the plating retains its location on the frame but with reduced resistance to in-plane and normal loading.

The strength of the heat cured toughened adhesive used in this study has been taken well above that expected of an adhesive to resist impact loading. A significant resistance to impact loading was demonstrated by a number of repeated impacts and only partial

debonding of the joints. However, although adequate for most design purposes it is unlikely to compete with very high shock resistance inherent in welded joints in such applications as warships where high energy ballistic impact must be accommodated.

The impact resistance of a bonded steel framed GRP structure has been reported to be good with reference to air blast associated with weapons explosion adjacent to ship superstructure⁴⁷. The adhesive used in that study was ductile and a limited number of bolts supplemented the adhesive joint. It is unlikely that the brittle adhesive used in the current steel/GRP study (Araldite 2004) would be capable of resisting such high strain rate explosive loading. However, the author feels that the failure mechanism at the GRP/adhesive interface may help in absorbing impact energy through the micro-failure of the fibres near the interface. The possible generation of high speed fragmentation, however, needs to be assessed. Such localised high energy is unlikely to be absorbed by the fire insulating materials which constitute about 50mm of the total thickness of the fire/blast panel developed in this study, but can be dissipated within the structural GRP layers.

In real load bearing bonded structures joints are much more continuous and unlikely to have the same simply supported end conditions used in laboratory studies. This is, especially true where plating is supported by a framework of continuous stiffeners. To verify this contention a large scale test structure is required for further experimentation which has been beyond the scope of this research programme.

The question of the durability in a wet environment is a point of natural concern. Unlike the two previous probabilistic limitations, a wet environment is a continuous design condition for marine structures where highly corrosive metals such as steel are used. The durability data obtained in this study is limited to three years and, although it has shown very encouraging results, the expectation of a structural life of 25 years demands more data in this area. However it is also important to simulate the service environment and the joint conditions for the bonded structure rather than trying to obtain accelerated test data. Recent published research¹²⁴ into the durability of steel joints which were treated with silane primer, has shown that when immersed in 50° C water for 400 hours they retained their full strength while a batch of similar, untreated, joints lost 50% of their strength under the same conditions. Only one silane treated lap shear specimen (site tested-with the adhesive joint sealed and painted) tested in this programme has not shown a noticeable difference in comparison with its equivalent untreated specimen (Section 3.4.2) in the sea environment after 17,000

hours of continuous exposure while under load.

The retained strength in the silane treated specimens was about 85% when tested saturated after 25000 hours (lab conditions) in comparison with dry unaged specimens. This loss in strength is believed to be mainly due to corrosion processes at the interface, which was noticed from close examination of the failure surface of lap shear and cleavage joints as shown in Figures 7.2a and 7.2b respectively where it can be seen that there are traces (brown spots) of oxide. These test conditions are extreme since the joints in a bonded structure are continuous rather than in this case where the joint was small (15x25mm) with four surrounding edges. The author feels that the durability of bonded structures in the marine environment is acceptable on two grounds. The first is that the initial strength of the adhesive in lightly loaded stiffened joints is well above the static strength requirements for these structures (fire walls, minor bulkheads and secondary decks for examples). Many of these structures are stiffened internally within the enclosed spaces where exposure to wet environments is limited to condensation. The alternative to single skin is the double skin sandwich design especially in the case of steel constructions. Polymer composite materials tend to absorb moisture and that may lead to moisture attack at the adhesive/adherend interface.

Another limitation is thermal creep of a structure/joint subject to sustained loading. The results of this study (Chapter 3) suggests that adhesives of relatively high glass transition temperatures (90-120°C) may be limited to 15-20% of their maximum failure load when subject to a continuous temperature of say 80°C. Such a temperature is likely to be experienced by a steel structure in a desert environment during the day time of the peak summer seasons¹²⁰. At temperatures in excess of 200°C where the adhesive is being charred there may be resistance to sustained load of only 2% of the ultimate failure load (Table 3.8). The strength requirement in the case of the fire wall design is very low since the shear stress for the bonded structure subject to the maximum service wind loading¹²⁷ is approximately 0.5 N/mm². This is below the 2% of the maximum strength value.

Considering the limitations imposed by thermal creep (for example) as the main design criterion for an elevated temperature application (up to 80°C) there should be a minimum factor of safety of 6 against the ultimate strength of the adhesive. This is the product of 5 for the loading factor and 1.2 as an uncertainty factor (based on the reliability of bonding processes-Section 3.3.4). This however does not include

consideration of the possible degradation in joint strength due to wet environments (assuming these two extremes are unlikely to be present simultaneously)

7.6. LOCI OF SURFACE FAILURE

The author has examined the following failure surfaces in an attempt to understand the mechanism of failure initiation in both the adhesive and at the interface of joints which are subject to short term quasi-static loading. This is in order to recommend bonding processes and practical design concepts.

7.6.1. STEEL/STEEL LAP SHEAR JOINT

For a given strain rate, adherend type and thickness and adhesive type and thickness, the failure mechanism in a lap shear joint is governed by two factors: stress concentration and the porosity and defects of the glue line. Araldite 2007 adhesive contains micro voids on curing as part of the toughening mechanism for the adhesive. Most of the joints examined did not include significant voids at the critical regions which could have influenced the strength and therefore the failure mechanism of the steel/steel the lap shear joints appears to be dominated by the stress concentration at the ends of adhesive/adherend interface. To explain the failure mechanism in the lap shear joint, it has been divided into zones as shown in Figure 7.3 for ease of explanation. Numerical analysis of the lap shear joint (Figure 5.11) has shown that stresses are maximum at points 2 and 3 (Figure 7.3a) and the stress concentration pattern (from both the F.E analysis and observation-Figure 7.3b) suggests that it is a maximum towards the interface. Therefore initiation of adhesive failure at one of these points would be expected and thus should not be interpreted as an adhesion weakness due to the condition of the surface preparation of the adherend. At areas in the middle of joint the failure surface suggests a clear shear failure as shown in Figure 7.4. This is "a secondary failure" (a term used to denote a failure which follows failure initiation in the joint) due to separation mechanisms between the adherends as illustrated in Figure 7.4b. Examination of zone c1 using a scanning electron microscope (SEM) micrograph suggested that there was no significant residual adhesive on the fracture surface when compared with fresh grit blasted steel surface (see Figure 7.5).

This proposed failure mechanism assumes no spew fillet left on adherend A above

point 1 (Figure 7.3) because this will influence the stress distribution pattern such that failure initiation should start at point 1 or 4 instead of point 2 (see Section 7.2). A typical failure of a filleted joint is shown in Figure 7.6 which seems to initiate near point 1 instead of point 2 (compare with Figure 7.3).

In the cases of the butt and cleavage joints, finite element analysis (Section 5.1.3) suggests that there is no stress concentration towards the interface and thus the failure is normally cohesive (as shown in Figures 7.7) unless the surface conditions are not ideal (e.g. improper surface preparation or interface corrosion). This makes the cleavage type specimen more suitable for investigation of interface problems particularly since butt joints are sensitive to load alignment and produce significant scatter in their failure strength.

7.6.2. STEEL/GRP LAP SHEAR JOINT

In the case the lap shear joints bonded with the relatively brittle adhesive, Araldite 2004, failure initiation always appears to be at point 1 (assuming adherend A is steel one in Figures 7.3 and 7.8). This is despite the suggestion from the finite element results that the stress is higher at point 2 (assuming adherend C is the GRP). Stresses are always higher at the left hand side of the joint due to high deflection of the GRP in comparison with the steel at the right hand side of the joint (Figure 7.3). That this may be due to one or more of the following reasons;

- It is difficult to produce a square cut adhesive joint at the GRP ends in comparison with the steel due to the possibility of causing damage to the GRP. This means adhesive is left at the corner in point 1 (i.e the joint may be regarded as having a spew fillet) and it is therefore possible that the adhesive failure would initiate from there.
- Following the small failure initiation at point 2 the joint, under considerable deformation, will be subject to shock loading (impact) which causes the brittle adhesive to depart from zone a1 completely (see Figures 7.3 and 7.8).
- That this is a characteristic of the brittle adhesive which may possess insignificant toughening mechanisms and thereby behaves differently from a ductile toughened adhesive in such a joint. As such it is vulnerable to crack initiation at point 1 between the brittle adhesive and the rigid steel adherend.

The failure of a cleavage specimen can be seen in Figure 7.9 in which failure

initiation is from the GRP which is under tension. This makes this type of specimen very unsuitable for correlation of failure stresses with tension type specimens (for example) as it fails at a significantly lower load than predicted from the stresses in the adhesive joint.

7.6.3. STEEL/STEEL STIFFENED JOINTS

The location of the adhesive joint failure is in agreement with the observations made from the examination of the failure surface described in Section 5.2. This includes the following:

- failure initiated from the tension edge,
- failure is confined to a smaller area of the joint and
- failure started from a position nearer to the plate surface rather than the stiffener/block surface.

Examination of the failure surface shown in Figure 7.10 indicates two well defined areas. The failure mechanism in this joint may be explained as in the case of the lap shear joint. The failure may have initiated at an area near to point 2 where the bending stiffness of adherend C is much lower than that for adherend A. Zone c1 shows adhesive failure due to the stress concentration towards the interface (in agreement with the finite element analysis-Figure 5.7 and 5.8). The close up examination of zone c1 with the SEM micrograph of fracture surface shown in Figure 7.11a, suggests residual of traces of adhesive material but the same type of fringes can be observed on the grit blasted steel surface shown in Figure 7.11b. The opposite zone (interface of a1/b1-Figure 7.10) contains the adhesive which shows whitening features. This suggests either a crazing effect due to micro cracks and/or plastic deformation of the adhesive which is at a high stress level. Examination in the SEM for this zone is shown in Figure 7.12 which shows microcracks running in all directions. It can be also concluded from the smooth topography of this failure surface (no stretched adhesive materials) that adhesive failure has occurred, as was suggested earlier.

In the case of end cleavage loading for Type 2 and 3 large scale cleavage specimens (Figure 4.13) it is interesting to notice that the failure surface for the Type 3 cleavage specimen (shaped end) is different from that of the Type 2 cleavage specimen (square end) as shown in Figure 7.13. Three observations may be made from these specimens :-

- Type 3 has larger whitened adhesive zone than Type 2 which suggests that a

larger area of the Type 3 joint has experienced cleavage stresses. This was also reflected in the magnitude of the failure load (Table 4.1).

- Adhesive failure has occurred from the plate side of the Type 2 specimen because it is more flexible relative to the stiffener (square end). The Type 3 specimen indicates a different failure mode (i.e adhesive failure has occurred from the plate side) because the shaped end of the stiffener (1.5-2mm thick) is more flexible than the plate. The implication of this is that within a bonded joint/structure it may be possible to produce a strength advantage by controlling the surface preparation of the critically stressed areas.
- The "secondary failure" which followed the failure initiation in Type 2 and 3 specimens has shown that the middle part of these joints displays a thumb nail pattern of the fractured surface as shown in Figure 7.14. This circular adhesive patterns radiates from the most highly stressed from center under the stiffener flange. The hill and valley pattern indicates that there are signs of deformation in the adhesive in the surrounding flange area. This suggests that a wide stiffener with a thin flange could give improved resistance against impact loading by absorbing energy through adhesive deformation as a result to the flange deformation.

7.6.4. STEEL/GRP TENSILE CLEAVAGE JOINT

Analysis of the tensile cleavage joint (large scale specimen Type 5) has suggested that the failure would initiate in the adhesive near the fillet edge, towards the GRP surface. Figure 7.15 shows the position of failure initiation in the adhesive associated with delamination in the GRP. It is believed that the failure initiation in the adhesive is a result of the delamination within the GRP thus decreasing the resistance to the bending moment. This increases the deflection nearer the edge of the joint and hence increases the cleavage stresses which initiate the failure. The thicker the GRP skin the higher the delamination strength and hence the stronger the steel/GRP joint. On examination of the failure surface (Figure 7.16), the fracture shows debonding at the polyester resin/adhesive interface as well as a plucking failure within the fibres. This is believed to be largely influenced by the stiff nature of both the adhesive and the resin matrix. If a tougher adhesive was used it would produce a different failure pattern by improving the stress distribution. Furthermore the use of a toughened resin matrix for the GRP would

add an extra strength advantage to the joint.

7.7. DESIGN IMPLICATIONS

The analysis of Types C and D models (beam specimens-Section 5.3) clearly indicates that there is a distinction between welded (continuously) and bonded steel stiffened structures in the term of stress level and structural stiffness. Both tensile bending stress within the adherends and interlaminar shear stresses within the bond line have been shown to be higher than those obtained by applying normal beam stress calculations. The differences in stress and behaviour of the two test models imply that the effect of the interface condition between bonded adherends should be considered in designing with adhesive. This would be influenced by bond line thickness and type of adhesive and therefore needs further investigation. The results of the experiments in this study suggests that an adhesively bonded single skin stiffened steel plate structure may present about 15% weight penalty (i.e 15% increase in the material thickness to give the same bending stress of equivalent solid beam) and also produce a lower plastic strength capacity in a bonded steel/steel structure. However, the relevance of this depends on whether a weight design criterion in stiffened structures fabricated by welding processes is dictated mainly by ultimate strength or also by production and corrosion considerations. In lightly loaded structures, it is more likely that the first criterion would have the minimum consideration and therefore the others will dominate the resultant weight. The production of a stiffened panel, in the author's opinion, may be influenced by production trends which attempt to produce a uniform structure of the same plates and scantling dimensions and to save cost by implementing heavier panels which are easier and cheaper to fabricate (see Figure 2.4). There are minimum thickness requirements for the mild steel plate in the marine structures (5.5mm for Lloyd's Register of Shipping) to combat the problem of corrosion. In the case of adhesive bonding this problem may be reduced by the absence of metallurgical damages and corrosion crevices, which are generated by the welding process.

While it is difficult to generalise the results from the beam analysis, in allowing a margin of say 30-40% for adhesive and adherends stress calculations in a stiffened steel bonded structure, this can be at least an initial guide in designing steel structures which are subject to lateral loading. Perhaps there is potential for producing guidelines for different section configurations including bonded sandwich structures,

which are beyond the scope of this thesis.

In an attempt to investigate the effect of different beam sections as well as the influence of the bond area between the adherends, solid and bonded models were developed as shown in Figure 7.17. In these models the position of the neutral axis was maintained at the bond line centre. When these short beam models were tested, they behaved in a similar manner of that to model Types C and D (bonded and solid rectangular section beams respectively). These two models were not considered for analysis due to significant indentation at the contact points.

In highly loaded structural applications it is structurally more efficient to consider the design of sandwich construction against single skin design¹²⁹. Such a configuration is difficult to implement in the case of welded structure unless the sandwich skins are wide apart to give accessibility for the welding processes. Sandwich configuration, however, is a logical design development in the case of adhesive bonding. A closed sandwich may also provide a solution to limiting the environmental attack of the adhesive joint. The implementation of this would require to answer many questions which include quality control (visual inspection), joint design and fabrication methods.

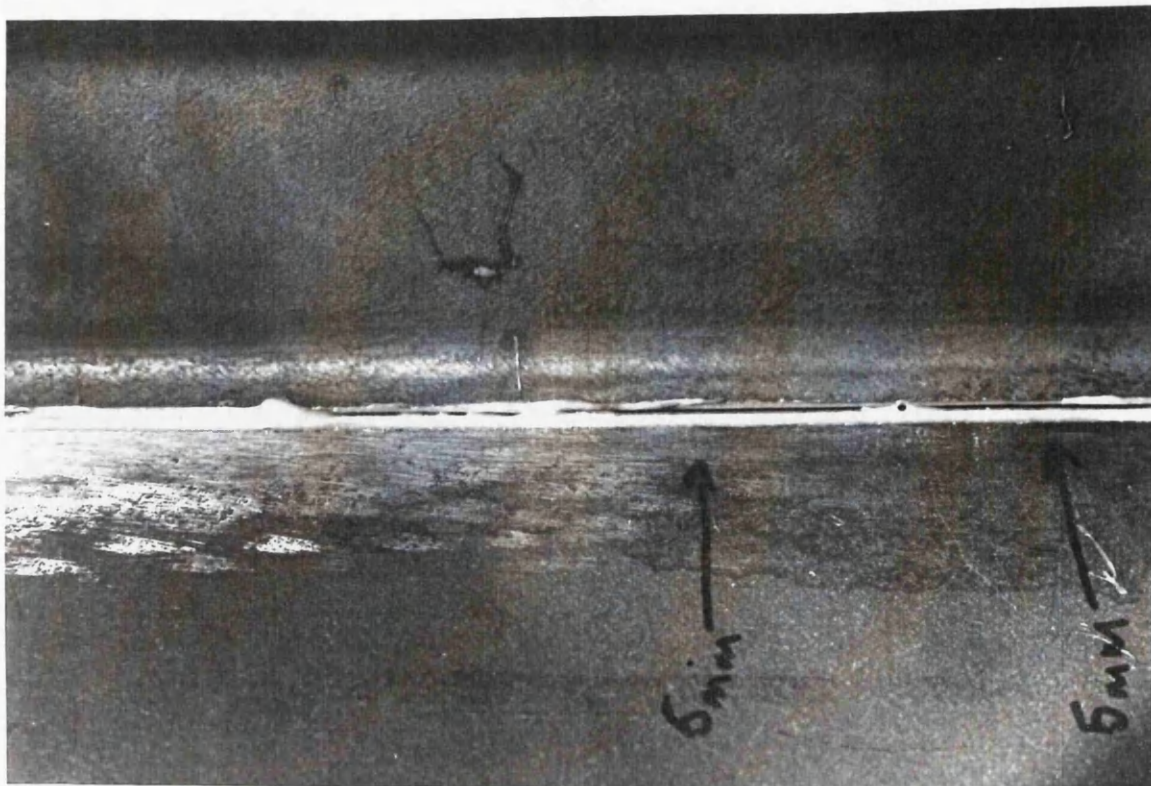
In the case of GRP construction, a single skin design is more acceptable, for two reasons, if the stiffener is of composite material too. The first reason is that adhesive bonding will produce a structure/panel which is structurally compatible with the bolted one. Secondly the influence of the degradation/oxidation at the joint interface is expected to be lower in the case of polymeric materials than for the steel adherends. The problem of water absorption in such materials are potentially largely reversible when composite joints are subject to dry weather conditions.

In the case of incorporating fire/heat insulation materials with steel/GRP for fire/blast walls, the strength properties of these materials should be incorporated within the structural joint as they may have an important role in improving the structural stiffness and resisting the overall and local impact loading. The fire insulation materials used in this study (Chapter 6) were supported by pultruded frame bonded to the GRP and hence this would reinforced the structure.

Other design problems which need careful considerations are the repairability and fabrication in an open site such as an offshore platform. Consideration of these factors will influence the choice of the adhesive, its dispensing and curing methods and the configuration, as well as surface preparation of the adherends. This in turn would lead to compromises in the mechanical properties of the adhesives.

MODEL TYPE	F.E STRESS ANALYSIS [N/mm2]	EXPERIMENT STRESS ANALYSIS [N/mm2]
A	266	262
B	290	336

TABLE 7.1 ADHEREND (STEEL) STRESS FROM EXPERIMENT AND FINITE ELEMENT ANALYSIS AT ADHESIVE FAILURE (FIGURE 5.1)

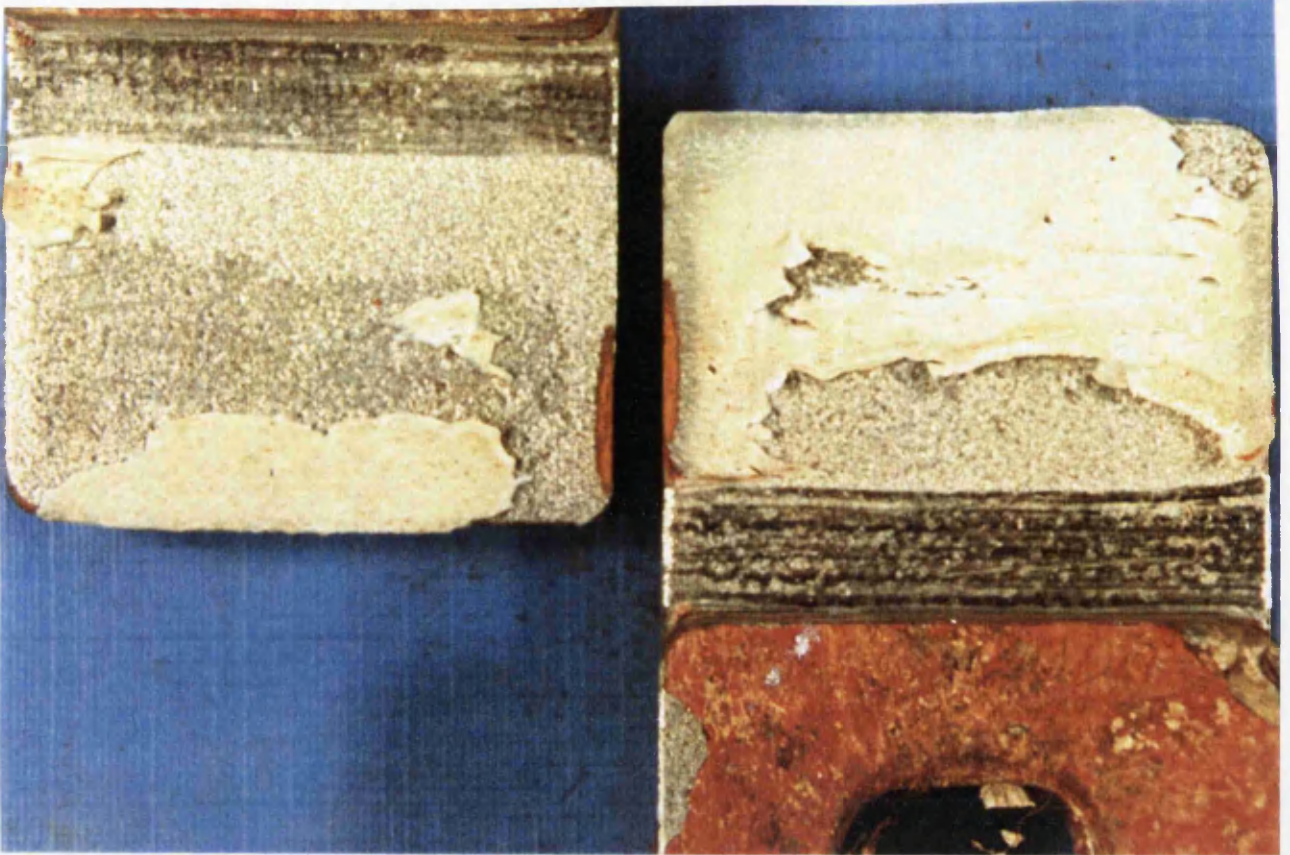


a. Before testing

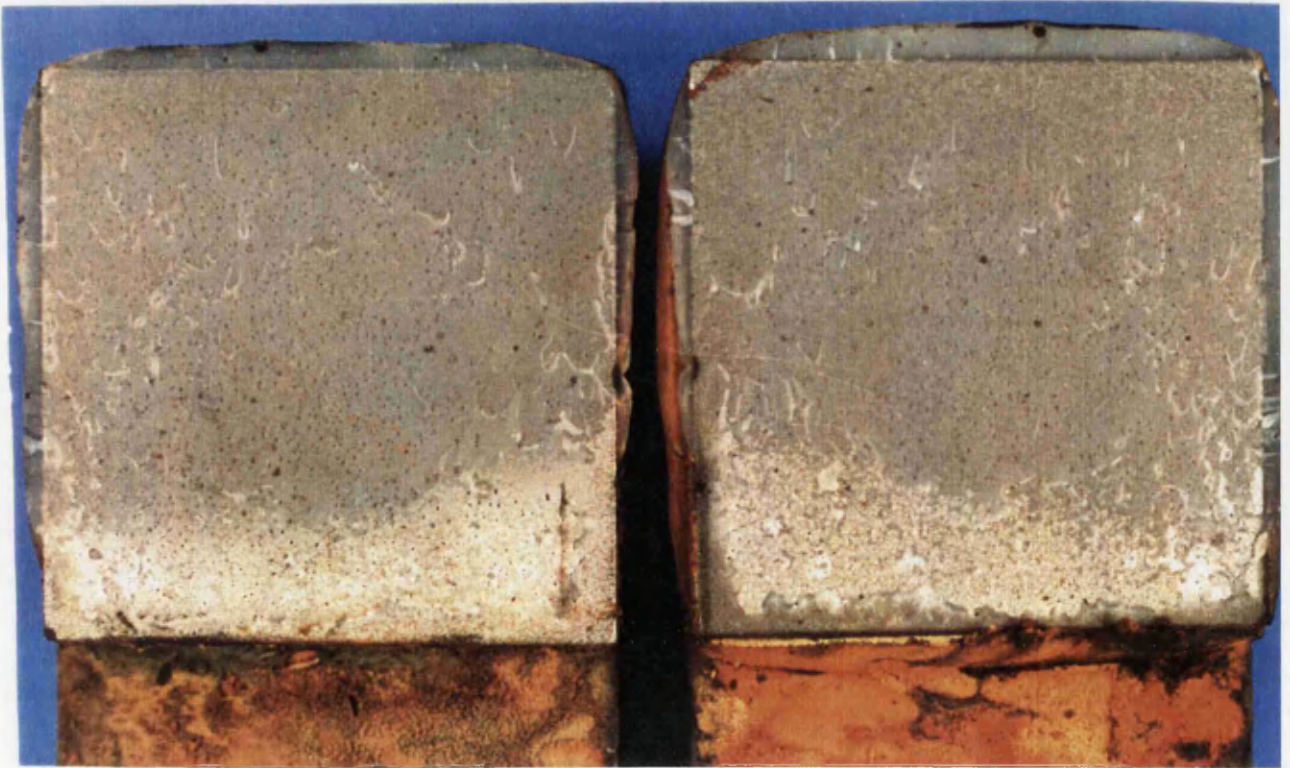


b. After testing and opening

FIGURE 7.1 GAP FILLING DEFICIENCY OF ADHESIVE IN LARGE PANEL JOINT

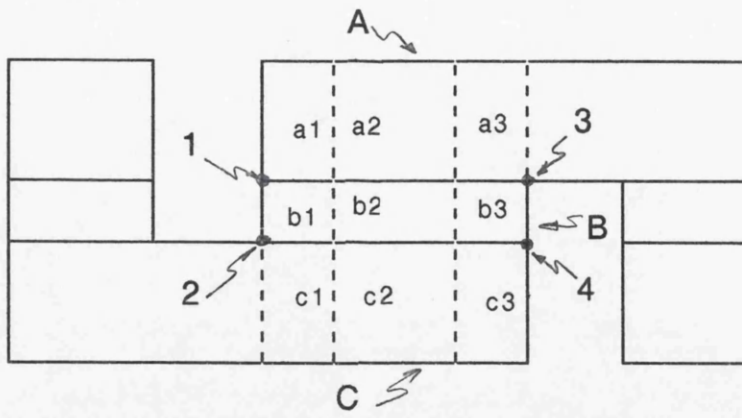


a. Lap shear

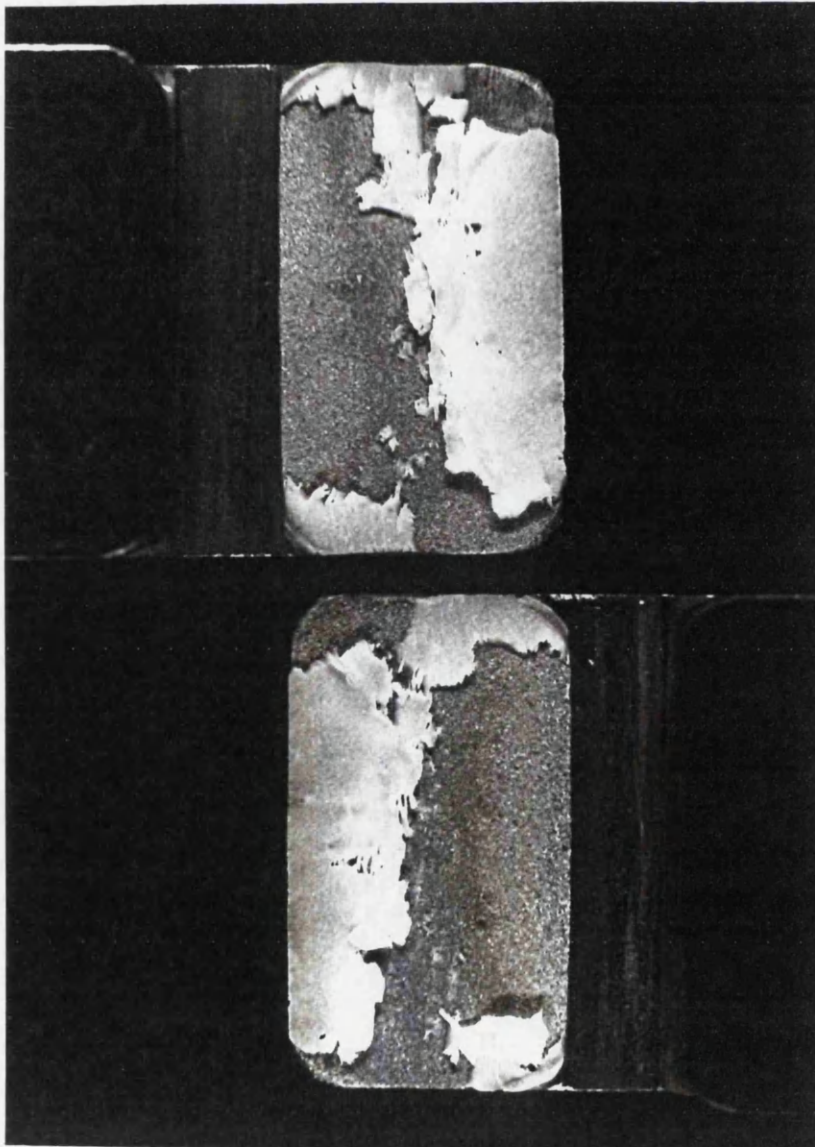


b. Cleavage

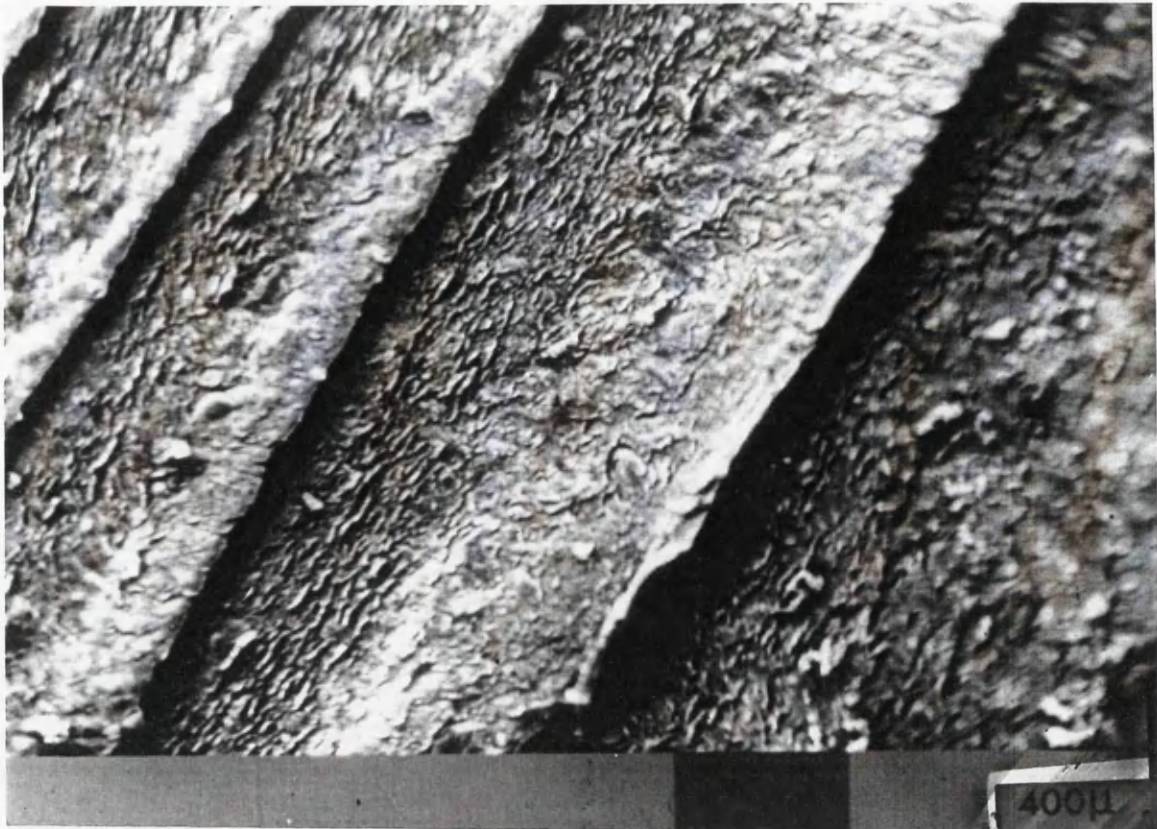
FIGURE 7.2 FRACTURED SURFACES OF STANDARD STEEL/STEEL SPECIMENS AFTER 28 MONTHS CONTINUOUS IMMERSION IN SALTWATER



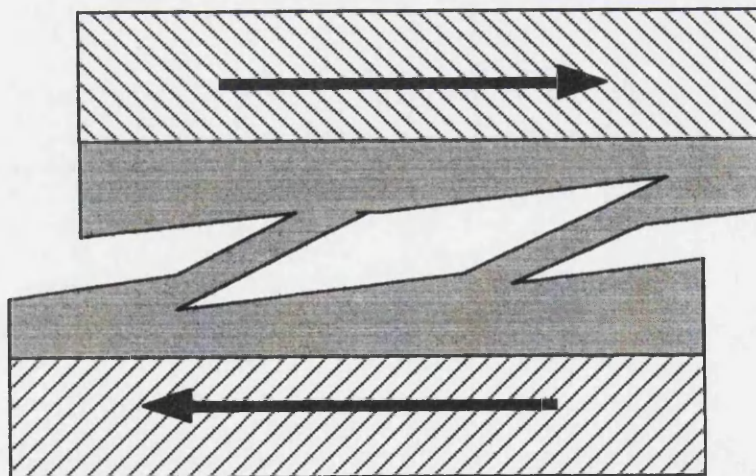
a. Schematic representation



b. Fracture surfaces (no spew fillet)

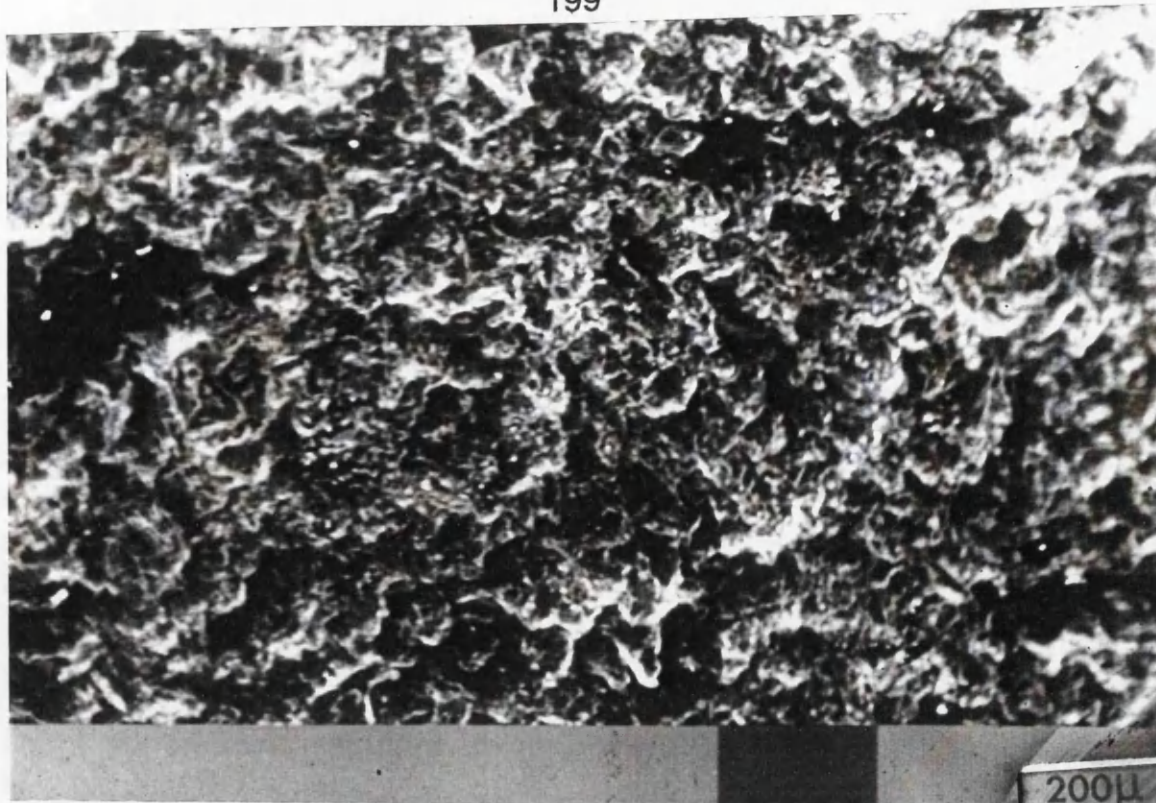


a. SEM micrograph

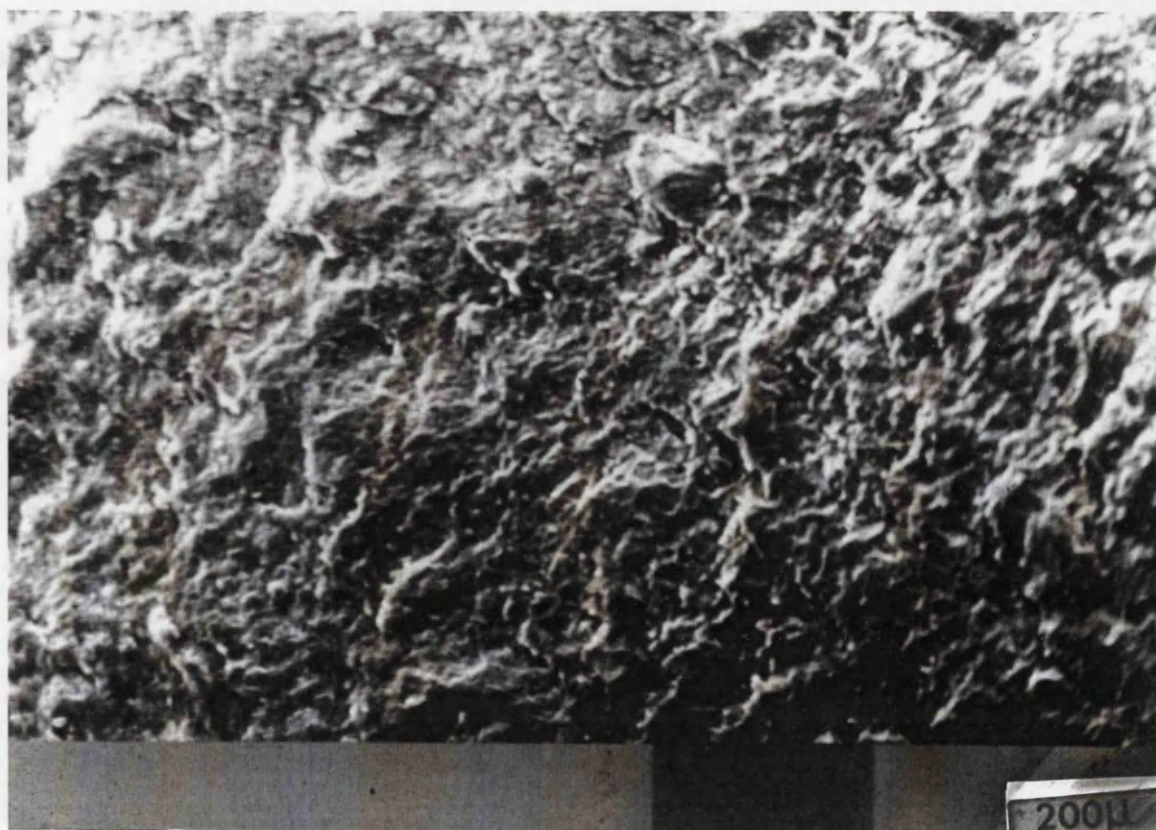


b. Schematic representation showing force directions

FIGURE 7.4 POSSIBLE MECHANISM OF STEPS FORMATION IN STEEL/STEEL STANDARD TENSILE LAP SHEAR SPECIMEN AS A RESULT OF JOINT INITIAL FAILURE



Fractured adhesive joint (adhesively!)



Grit blasted

FIGURE 7.5 SEM MICROGRAPHS COMPARING TWO STEEL SURFACES

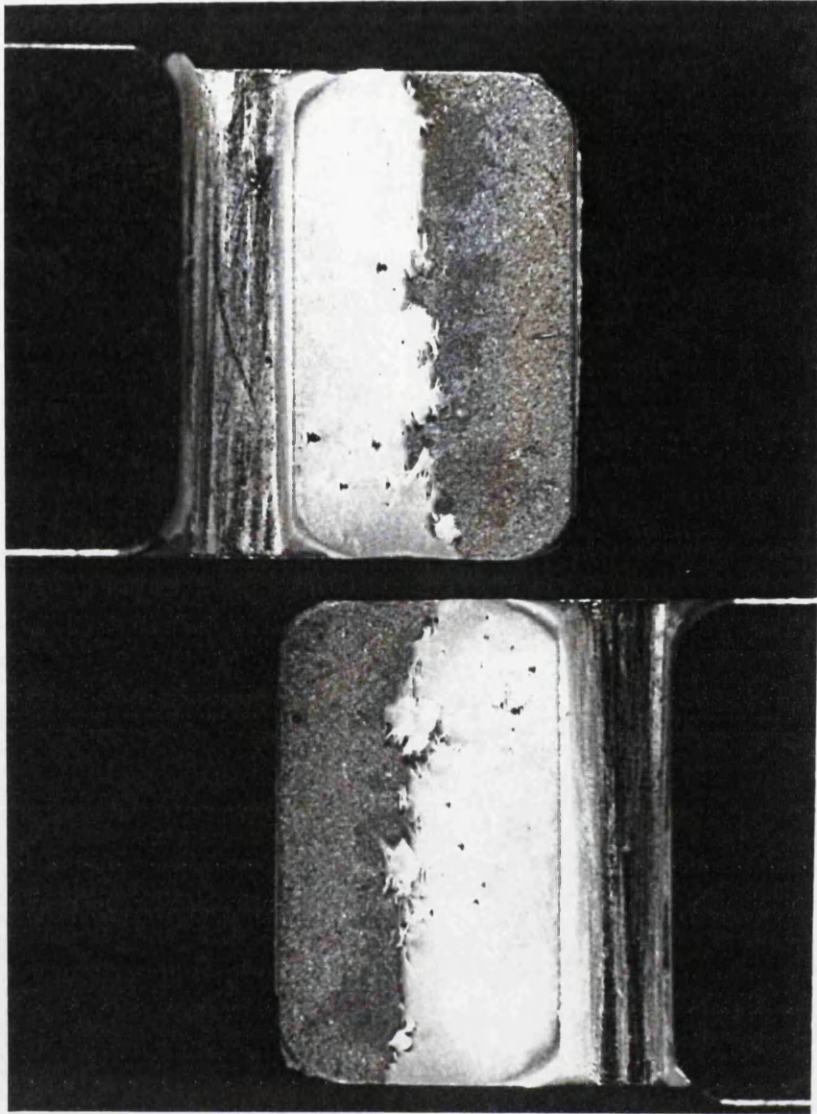


FIGURE 7.6 FRACTURED SURFACES OF LAP SHEAR SPECIMEN (WITH SPEW FILLET)

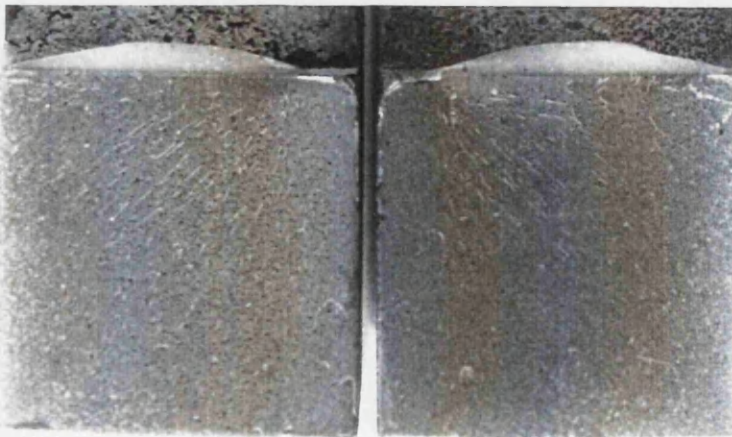


FIGURE 7.7 FRACTURED SURFACES OF TENSILE CLEAVAGE SPECIMEN (STEEL/STEEL)

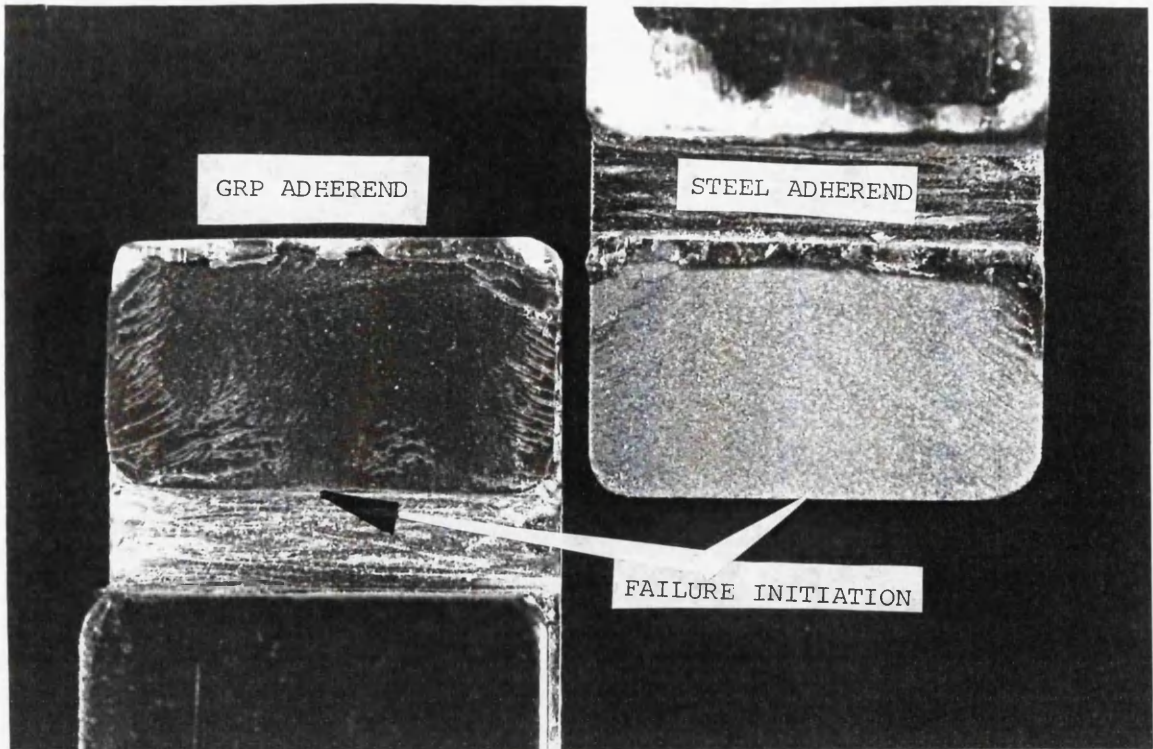


FIGURE 7.8 FRACTURED SURFACES OF LAP SHEAR SPECIMEN (STEEL/GRP)

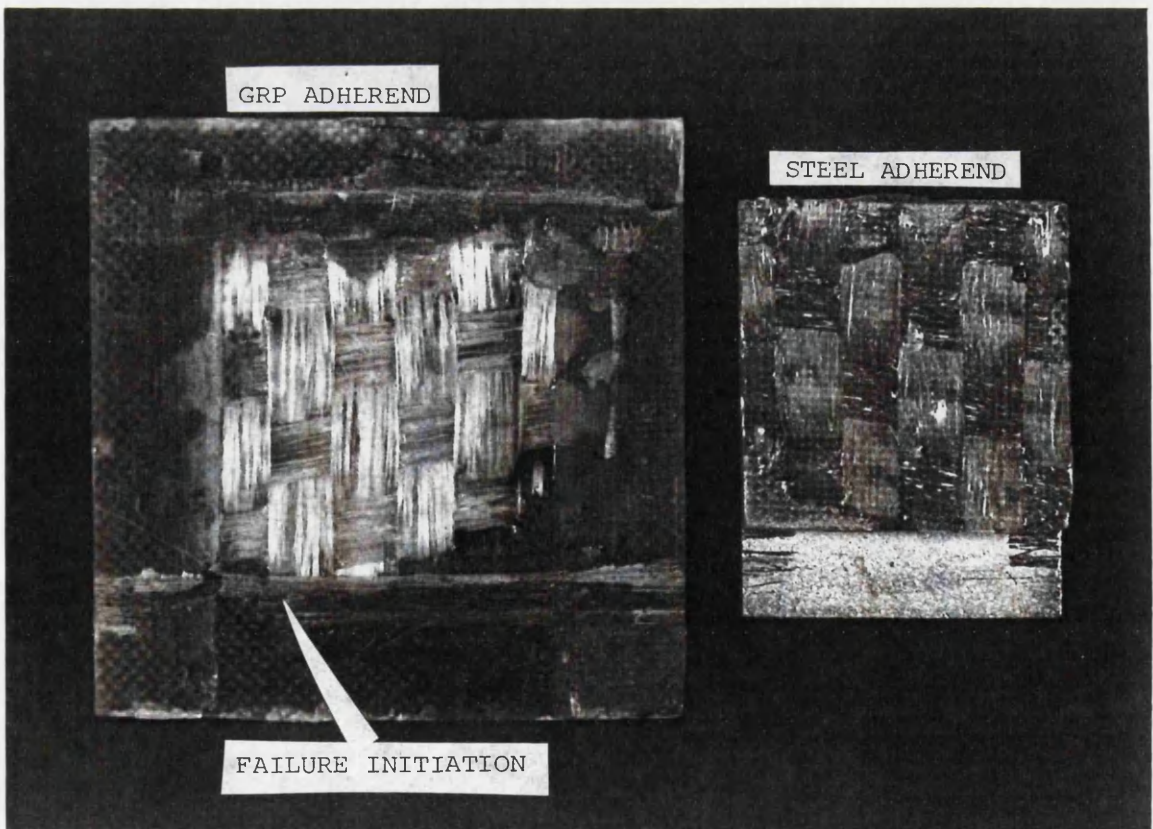
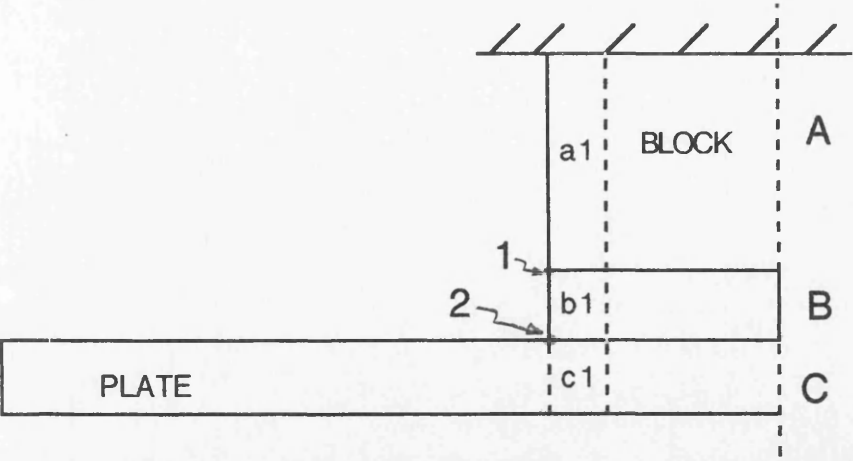
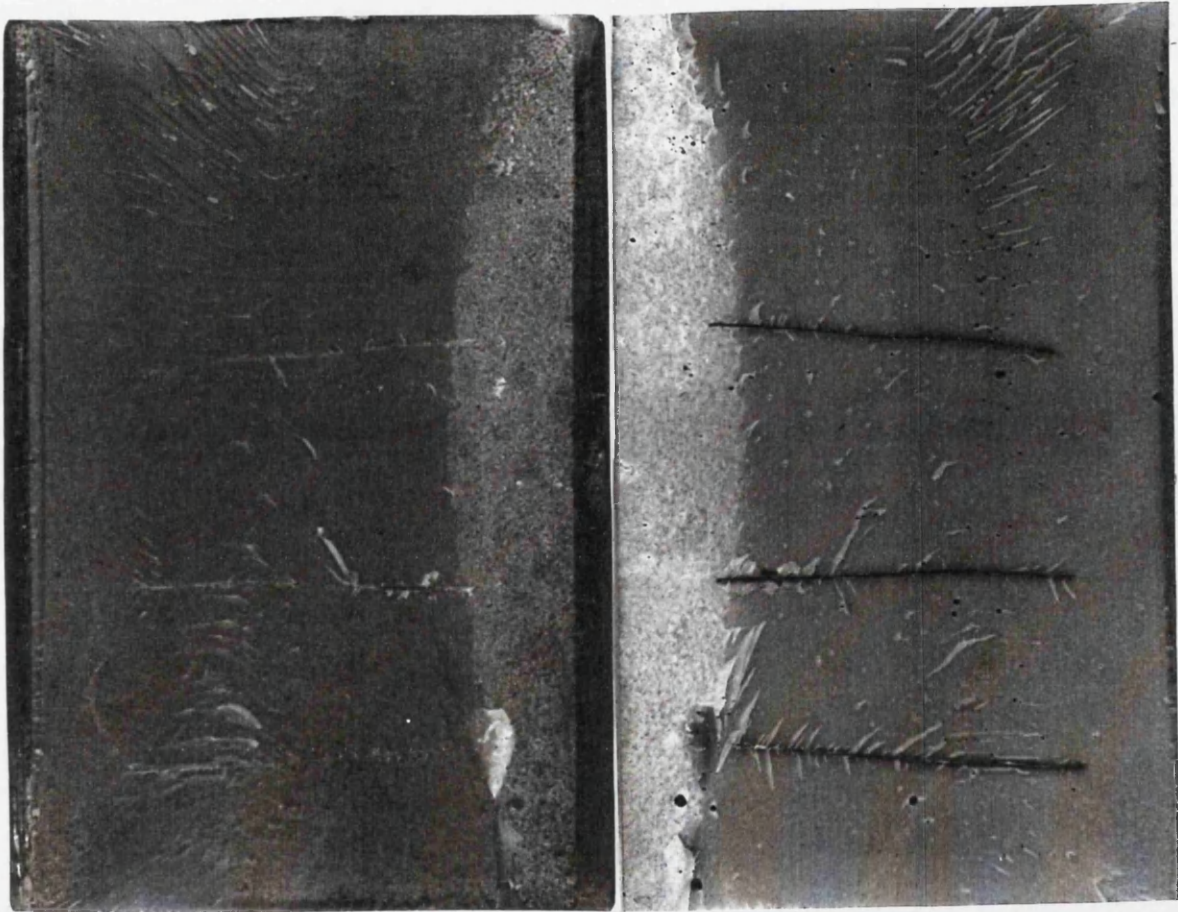


FIGURE 7.9 FRACTURED SURFACES OF TENSILE CLEAVAGE SPECIMEN (STEEL/GRP)

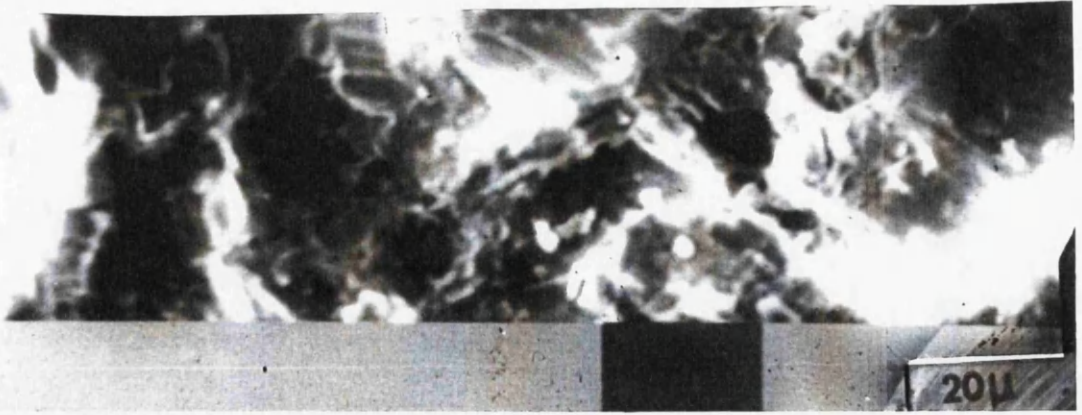


a. Schematic representation

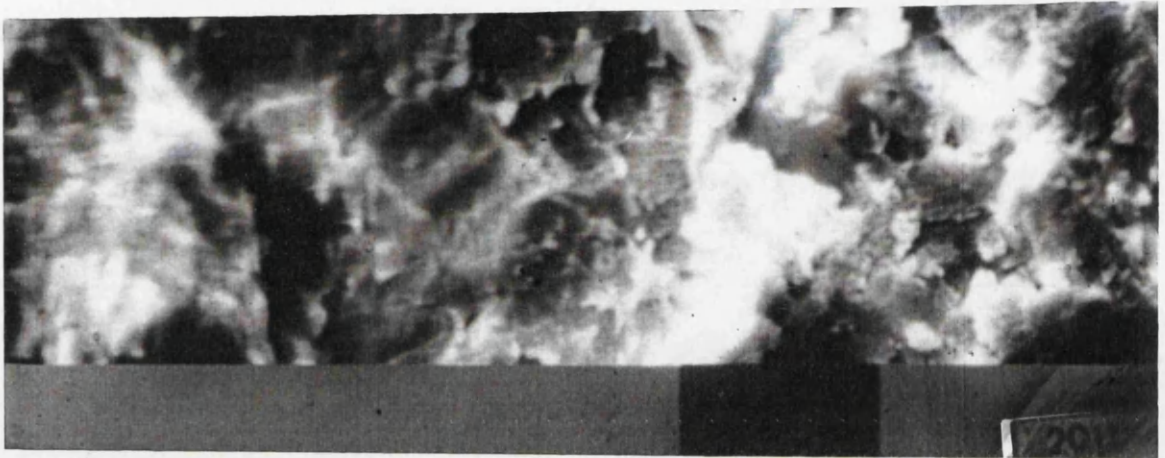


b. Fracture surfaces

FIGURE 7.10 LOCUS OF FAILURE OF STEEL/STEEL JOINT (MODEL TYPE A-FIGURE 5.1)



a. Fractured adhesive joint (at c1/b1 location-Figure 7.10)



b. Grit blasted

FIGURE 7.11 SEM MICROGRAPHS COMPARING TWO STEEL SURFACES

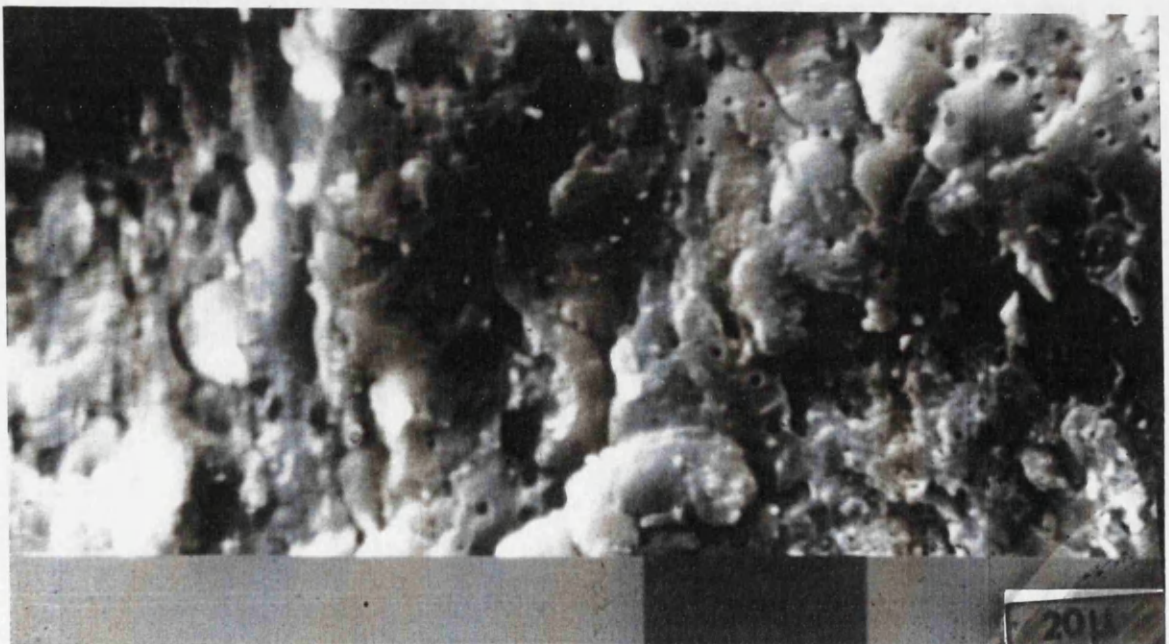
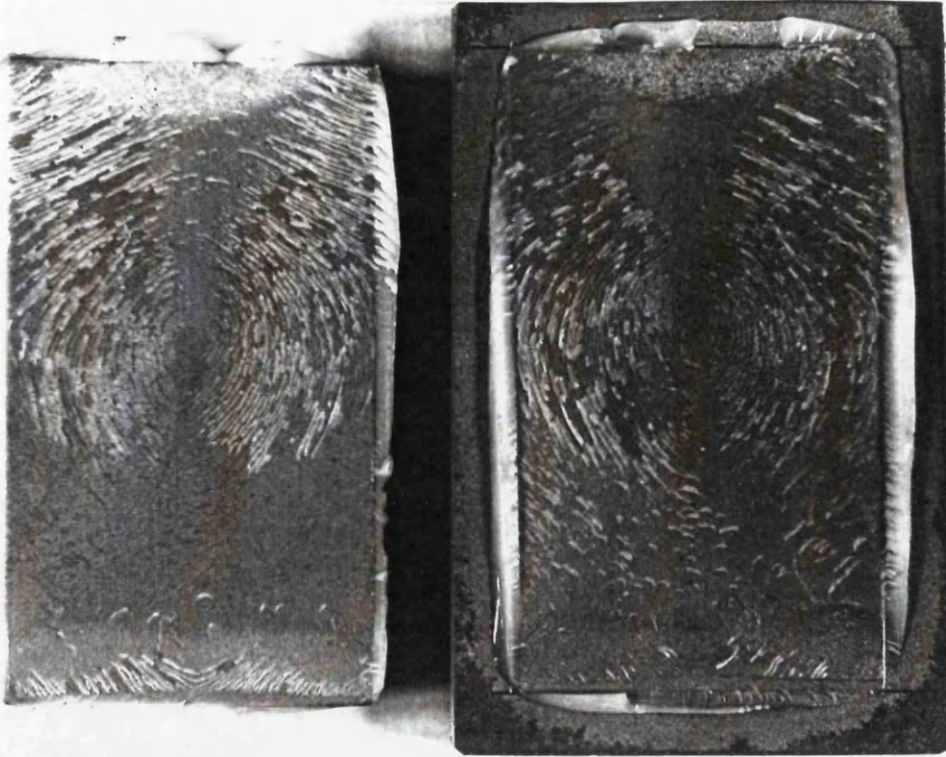
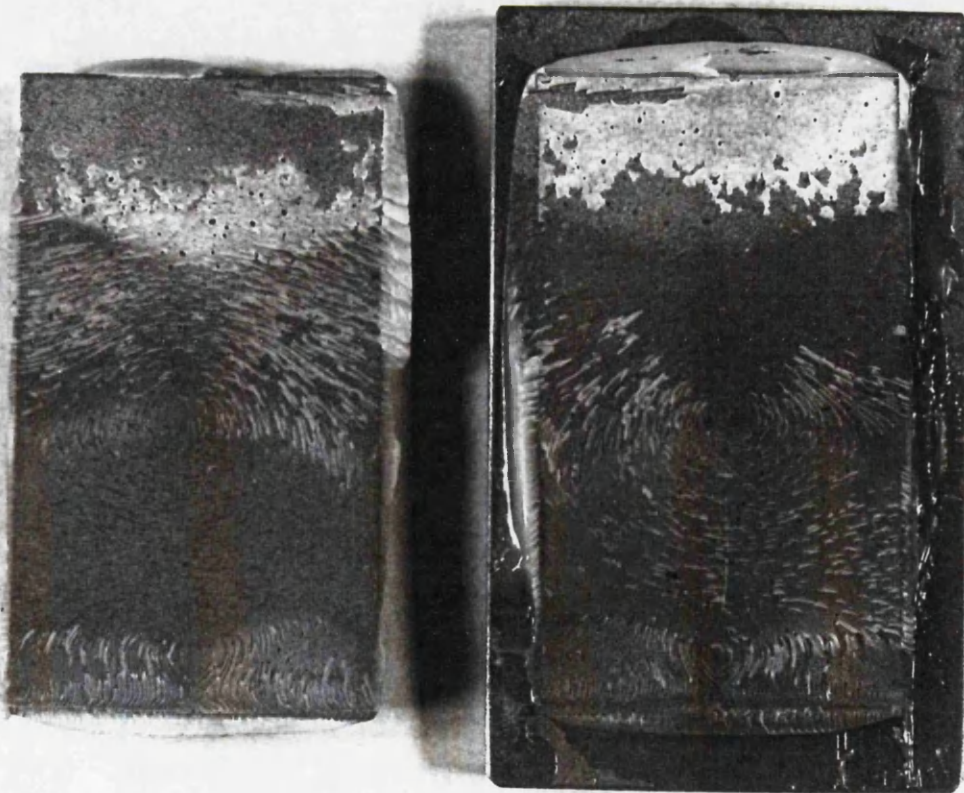


FIGURE 7.12 SEM MICROGRAPH OF ADHESIVE SURFACE INDICATING ADHESIVE FAILURE (LOCATION AT a1/b1-FIGURE 7.10)



a. Type 2 (square end)



b. Type 3 (shaped end)

FIGURE 7.13 FRACTURED SURFACES COMPARING TWO CLEAVAGE SPECIMENS (Figure 4.11)

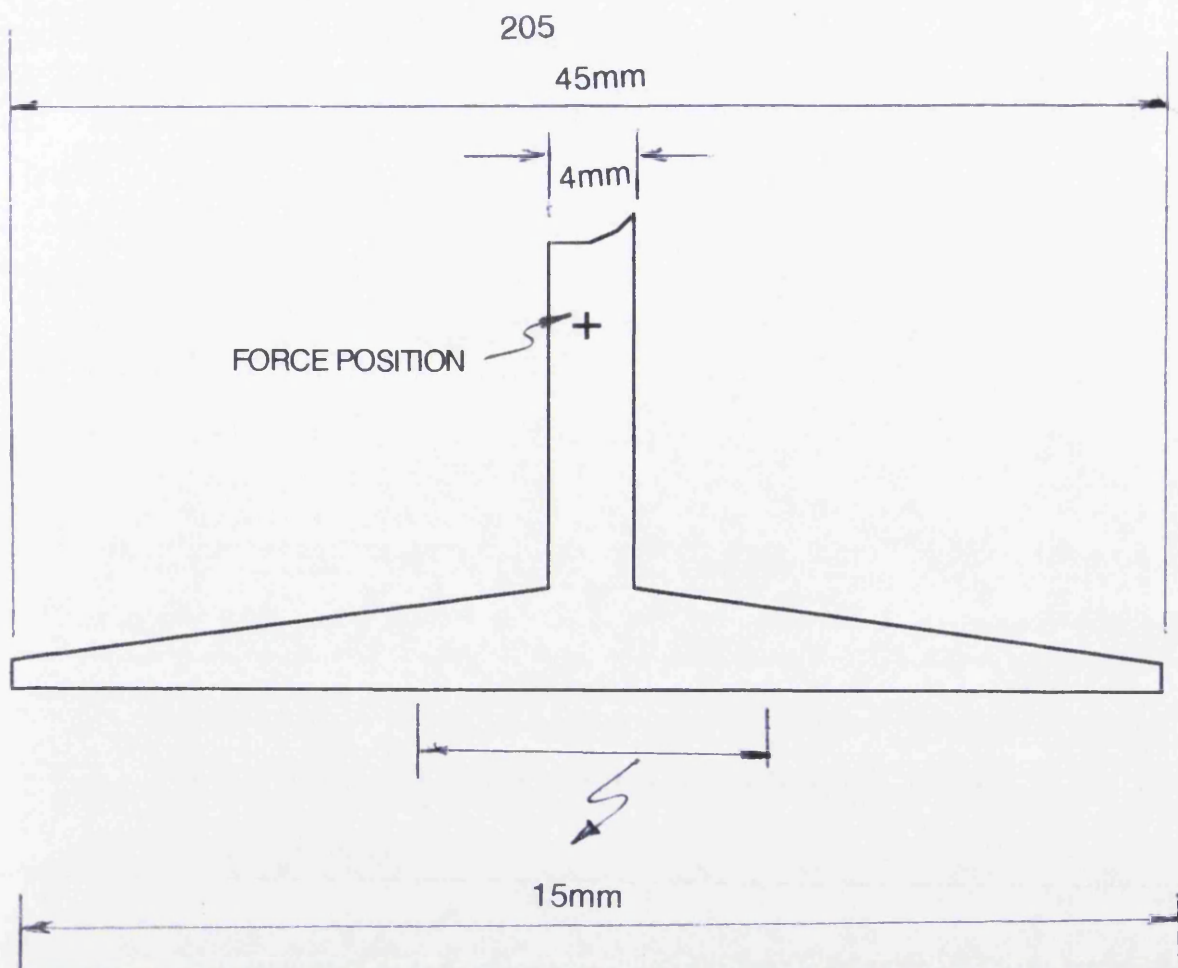


FIGURE 7.14 FRACTURE STIFFENER SURFACE OF CLEAVAGE SPECIMEN (TYPE 2)

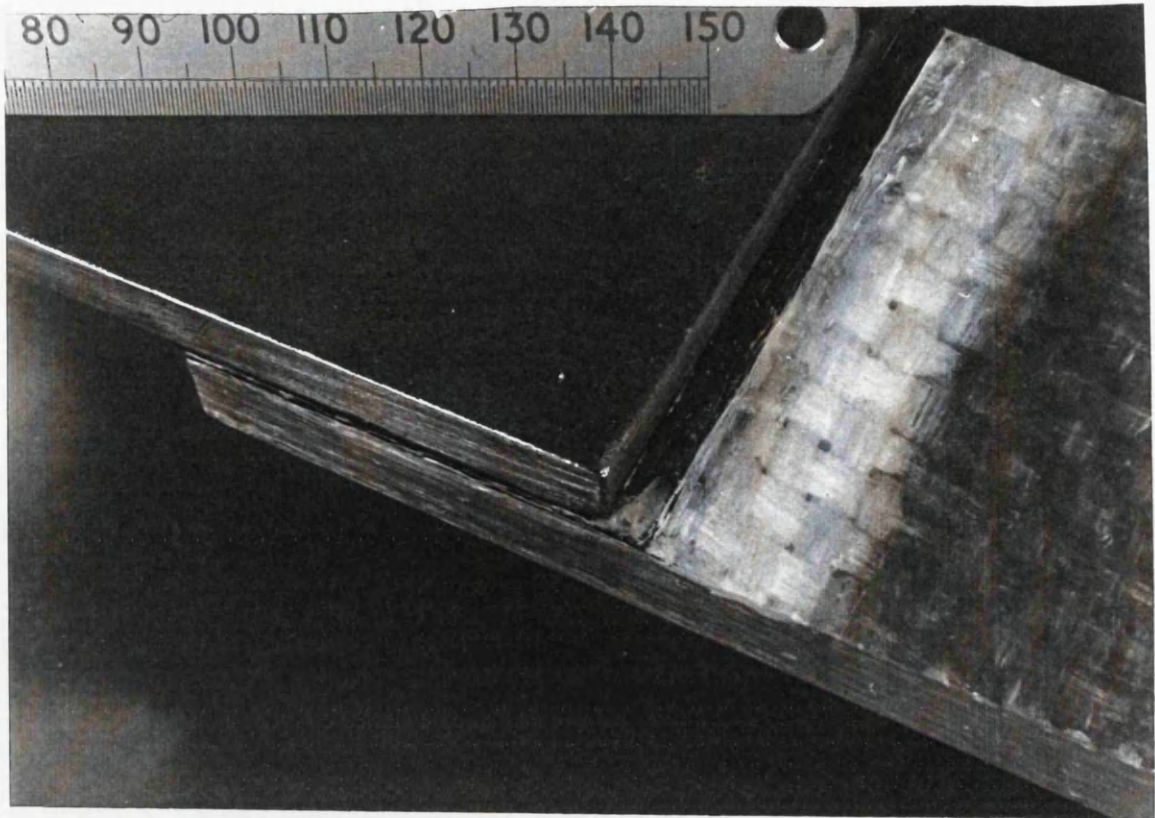


FIGURE 7.15 DELAMINATION OF GRP SKIN IN STEEL/GRP TENSION SPECIMEN PRIOR TO ADHESIVE JOINT FAILURE (TYPE 5-FIGURE 4.22)

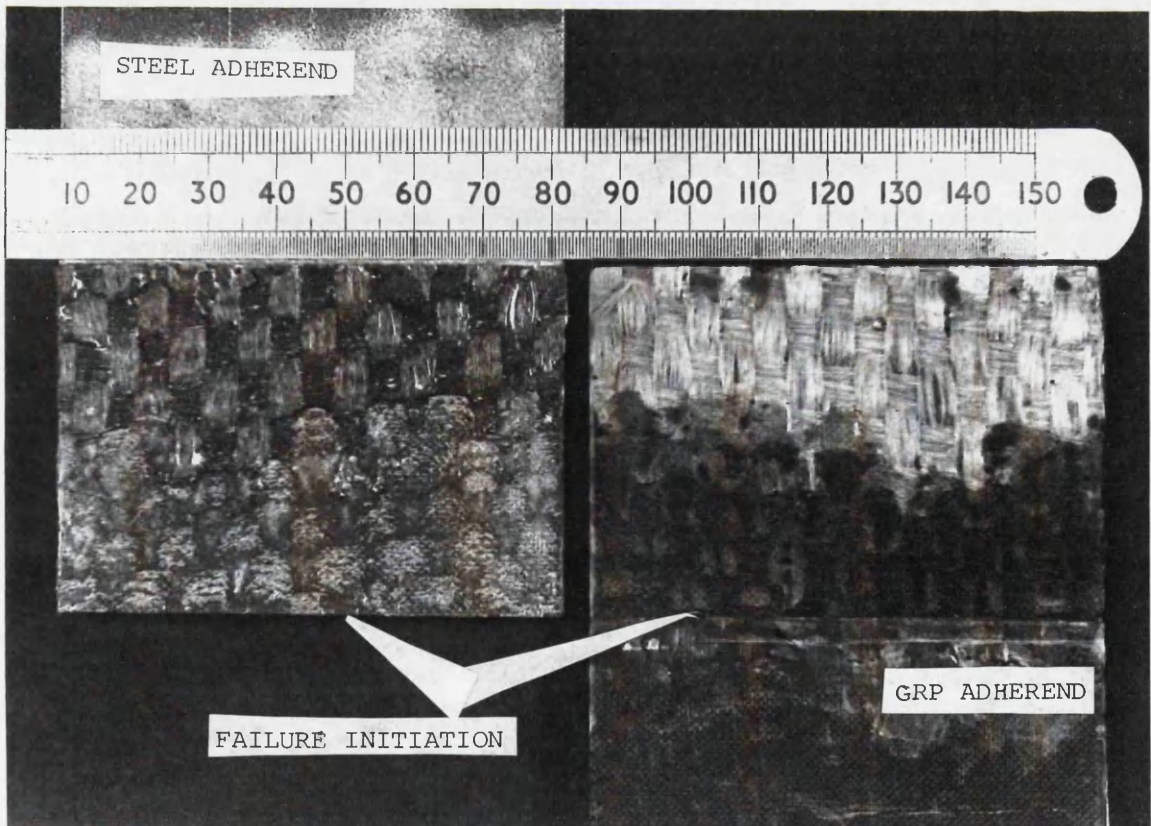


FIGURE 7.16 FRACTURED SURFACE OF STEEL/GRP TENSION SPECIMEN AFTER SEPARATING ADHERENDS (FIGURE 7.15)

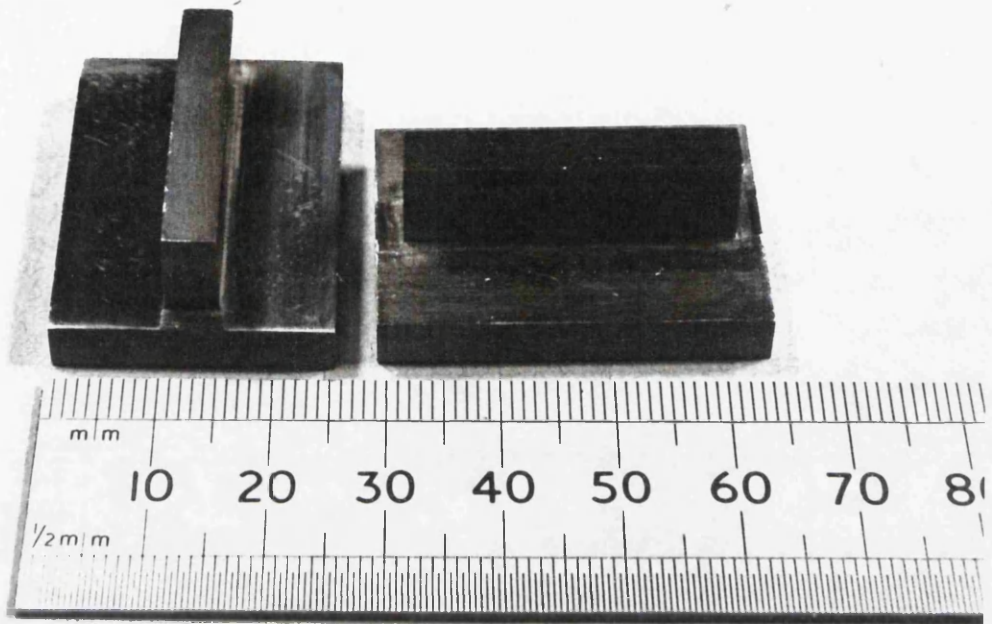


FIGURE 7.17 BEAM SPECIMENS TESTED IN THREE POINT BENDING

8. CONCLUSIONS AND RECOMMENDATIONS

The research work described in the previous chapters leads the author to the following conclusions:

- Single-part heat cured toughened epoxy adhesives offer a viable alternative for the joining of some connections in thick steel plated structures. The performance of adhesive joints in single skin stiffened constructions is such that the joints survive gross plastic deformation of the adherends (discussed in Sections 4.3, 4.4 and 7.3, Tables 4.1, 4.2 and 4.3 and Figures 4.12 to 4.19).
- A lightly toughened two-part structural epoxy adhesive, while substantially weaker than toughened single-part adhesives, can still provide adequate static strength in properly designed steel/GRP bonded joints. Using this adhesive, the local strength of a joint in a prototype fire/blast wall is sufficient to withstand a static overpressure in excess of 2.0 bar, which is well beyond the design requirement (discussed in Sections 3.3, 4.5, 5.2 and 7.1, Tables 3.2 and 3.3 and Figures 4.22 and 4.23).
- A practical bonding process for large plated structures appears to be both feasible and adaptable from current fabrication technology. The advantage of this bonding process is that it does not involve complicated operations and perhaps only semi-skilled personnel will be required (discussed in Sections 4.2 and 7.2 and Figures 4.1 to 4.4).
- Impact strength and elevated temperature (up to 80 °C) resistance of single-part epoxy adhesives, whilst less than the structural metals, are not insubstantial. These adhesives are suitable for many areas of application in marine steel construction where such design criteria are defined (discussed in Sections 3.4 and 6.1 and Tables 3.3, 3.7, 3.8 and 6.1).
- Adhesive bonding can provide a solution to joining composite structures where the fire resistance of such structures is the dominating criterion, provided that adequate thermal insulation is used. It may not be possible to combine the criteria of impact with fire resistance unless the insulating layers are incorporated into the impact absorbing mechanism (discussed in Section 6.2 and Figures 6.14 and 6.16).
- The durability of epoxy adhesives in wet (marine) environments is likely to suffer a reduction in the joint strength. A typical decrease in strength

of about 15% has been measured over three years and is not affected by the application or absence of sustained loading (discussed in Sections 3.4 and 7.4 and Figures 3.15 and 3.16).

- Design of optimum steel/steel bonded load bearing joints must differ from welded design. It has been shown (Section 5.3) that if the design of a welded structure is dominated by strength/stiffness requirements only then the bonded equivalent may incorporate a weight penalty. However not all applications are dominated by a strength/stiffness criterion and if this is so, then the concept of sandwich design may be more suitable than that of single skin design (discussed in Sections 5.3 and 7.7 and Figures 5.20 and 5.21).
- If the adhesive failure criterion is based on maximum stress, the thick tensile lap shear joint can provide a good numerical model and predictive tool for the failure load in load bearing joints for steel/steel and steel/GRP structures where high modulus adhesives are used. Tensile butt and cleavage joints can produce misleading results due to adherend rigidity and sensitivity to loading direction. Results from flexural beam specimens (Figures 5.25 and 5.26) with inherently more uniform stress distributions are likely to be more useful for design guidance (Sections 5.1.3, 5.2.3, 5.3 and 7.4, Table 7.1 and Figures 5.7 to 5.16).
- Determination of the precise failure mode in adhesively bonded steel joints is difficult to assess. However, it has been shown (Section 7.6) that failure can be initiated either adhesively or cohesively, depending on the joint geometry. The adhesive failure mode is more likely to be applicable to structures and such a mode should be regarded as the norm rather than as a direct result of interface defects. Knowledge of failure initiation in a bonded joint can be used to effectively select surface preparation and quality control requirements. In plate/stiffener connections, the surface of the plate at positions of high cleavage forces may require more careful preparation due to the possibility of adhesive mode failure from the plate side. Assessments of bonded steel/GRP failure modes is inconclusive due to the use of the brittle adhesive used in this work (discussed in Section 7.6 and Figures 7.3 to 7.16).
- Significant improvements in steel/GRP joint strength can be achieved through careful surface preparation and controlled mixing and application of the adhesive. The use of peel plies and automatic dispensing

equipment are important aids to this process (discussed in Sections 3.43 and 7.2 and Figure 3.20).

The author recommends the following areas for further research:

- Determination of "in situ" elasto-plastic properties of the adhesives within joints which can then be applied in numerical analyses and failure criteria studies (Sections 2.2.3 and 5.1.3 and Figure 2.13).
- Microscopic modelling of adhesive failure (adhesion) on steel adherend surfaces produced with controlled oxide layers in lap shear or peel joints. This should incorporate topography, analytical, durability and reliability aspects (Sections 7.5 and 7.6)
- Assessment of durability of large structural components in a wet environment subject to different types of loading such as fatigue, creep and impact, correlated with the results of small test specimens.
- Investigation of residual stresses in the bond line as a result of thermal expansions in hot cured adhesively bonded steel structures where the adherends are subject to different expansion rates and boundary conditions (Section 7.2).
- Determination of the interface factor (f_1) with reference to different stiffened and sandwich structure configurations, modes of loading, adherend and adhesive materials (Sections 7.4 and 7.7).
- A feasibility study to examine the requirements for the design of large scale steel bonded structure for a very clearly specified application. The design feasibility study should be carried out from first principles with a view to bonding with single part epoxy adhesive. This study should consider the requirements of durability in wet environments, weight reduction and the cost of the bonding/fabrication process. The assembly of bonded joints in an open site with possible complementary use of welding, bolting or cold curing adhesive should be also incorporated into such a study.

REFERENCES

1. Aitken, D.F. and Blitt, M.A., "Engineers Handbook of Adhesives", The Machinery, 1972.
2. Gillham, J.K., "Cure and Properties of Thermosetting Polymers", Structural Adhesives, Elsevier Applied Science, 1986.
3. Wilson, R G, "Jointing Techniques-Adhesives", Proc., International Conference on Structural Adhesives in Engineering, IMechE, London 1986.
4. Chalmers, D.W., "The Properties and Uses of Marine Structural Materials", Marine Structures, 1988.
5. McGregor, I.J., "Fusion Bonding in Carbon Fibres", Ph.D. Thesis, Department of Aerospace Engineering, University of Glasgow, 1988.
6. Adams, R.D. and Wake, W.C., "Structural Adhesive Joints in Engineering", Elsevier Applied Science, 1984.
7. Lees, W.A., "Adhesive Selection", Proc. of Engineering Applications of Adhesive, RAPRA, Butterworths, 1988.
8. Charnock, R.S., "Toughened Adhesives for Sheet Metal Bonding", IAVD Congress on Vehicle Design, Geneva, 4-6 March 1985.
9. Martin, F.R., "Acrylic Based Adhesives", Structural Adhesives, Elsevier Applied Science, 1988.
10. Powell, J.H., "High Temperature Polymers of Potential for Adhesives", Seminar (unpublished), RAPRA, 1989.
11. Kinloch, A.J., "Rubber Toughened Thermosetting Polymers", Structural Adhesives, Elsevier Applied Science, 1988.
12. Young, R.J., "Rigid Particulate Reinforced Thermosetting Polymers", Structural Adhesives, Elsevier Applied Science, 1988.
13. Kinloch, A.J., Maxwell, D.L. and Young, R.J., J. Mater. Sci., 204, 1985.
14. Good, R.J., "Adhesion Measurements" Journal of Adhesion, Vol. 8, 1976, pp1-9.
15. Mittal, K.L., "Adhesion Measurement of Thin Film, Thick Films and Bulk Coating", ASTM STP640, Mittal, 1978.
16. Bikerman, J.J., "The Science of Adhesive Joints", Academic Press, New York, 1969.
17. Bikerman, J.J., "Problems in Adhesion Measurements", Adhesion Measurement of Thin Film, Thick Films and Bulk Coating, ASTM STP640, K.L. Mittal Ed, ASTM, 1978.

18. Good, R.J., "Locus of Failure and its Implications for Adhesion Measurement", ASTM STP640, 1978.
19. Mattox, D.M., "Thin Film Adhesion and Adhesive Failure - A Perspective", ASTM STP640, 1978.
20. Packham, D.E., "Mechanics of Failure of Adhesive Bonds Between Metals and Polyethylene and Other Polyefins", Development in Adhesives 2, 1986.
22. Vohralik, A "Principales of Adhesion", V140(25), pp1006, 1008, 1018, (1961).
23. Shields, J., Adhesive Handbook, 3rd edition, Butterworths, London, 1984.
24. Minfurod, J.D., "Adhesives", Durability of Structural Adhesives, Ed., Kinloch, A.J, Applied Science Publishers, 1983.
25. Brockmann, W., "Steel Adherends", Durability of Structural Adhesives, Ed., Kinloch, A.J, Applied Science Publishers, 1983.
26. Lees, W A, " Bonding of Composites" , Bonding and Repair of Composites, Proc. RAPRA 1989, Butterworhs 1989.
27. Gilibert, Y. and Vercher, G., "Influence of Surface Roughness on Mechanical Properties of Joints", Adhesive Joints, Mittal, K.L. ed. Plenum Press, New York, 1982.
28. Stein, B.A., Hodges, W.T. and Tyeryar, J.R., "Rapid Adhesive Bonding of Advanced Composites and Titanium", Proc. 26th Structural Dynamics and Materials Conference, Florida, 1985.
29. Fairbairn, G. and Bennett, W.F., "Structural Adhesives in Use", Engineer's Handbook of Adhesive, Ed. Aitken, D.F. and Blitt, M.A., Machinery Publishing Co., 1972.
30. Allan, R.C., Bird, J. and Clark, J.D., "The Use of Adhesives in the Repair of Cracks in Ship Structures", Structural Adhesives in Engineering, I.Mech.E., 1986.
31. Bochkarev, V.P. and Glevitskaya, T.I., "Adhesive Bonded and Welded Joints in Shipbuilding", Welding Production Review, 1970.
32. Bowditch, M.R. and Oliver, R.A., "An Underwater Adhesive Repair Method for teel Offshore Structures", 3rd Intl. Conf. on Polymers and Offshore Engineering, Scotland, 1988.
33. Martin, D.M., "Bonded Shear Stiffeners for Steel Bridges", Ph.D. Thesis, University of Dundee, 1985.

34. Swamy, R.N., Jones, R. and Bloxham, J.W., "Structural Behaviour of Reinforced Concrete Beams Strengthened by Epoxy Bonded Steel Plates", *The Structural Engineer*, V. 65, No. 2, 19.
35. Sadek, M.M., "Critical Assessment of the Cutting Performance of Bonded Horizontal Milling Machine in Engineering". *Proc.. International Conference on Structural Adhesives in Engineering*, IMechE, London 1986
36. Caldwell, J B, "Structural Optimisation: What wrong with it?", *Advances in Marine Structures*, Elsevier Applied Science, 1986.
37. Winkle, I.E. and Baird, D., "Towards More Effective Structural Design Through Synthesis and Optimisation of Relative Fabrication Costs", *The Naval Architect* , Nov. 1986.
38. Lees, W.A., "Adhesives in Engineering Design", The Design Council, 1984
39. Petronio, M., *Handbook of Adhesives*, Chapman & Hall, 1962.
40. Hart-Smith, L.J., "Designing to Minimize Peel Stresses in Adhesive Bonded Joints", ASTM STP876, Johnson, W.S. Ed., Philadelphia, 1985.
41. Tin, W.P. and Sage, G.N., "Fatigue Strength of Bonded Joints in Carbon Reinforced Plastics", *Proc., International Conference on Structural Adhesives in Engineering*, IMechE, London 1986.
42. Semerdjiev, S., "Metal to Metal Adhesive Bonding", Business Book Limited, London, 1970.
43. Ljungstorm, O., "Design Aspect of Bonded Structures 1", *Bonded Aircraft Structures*, Proc. Cambridge 1957, Ciba-Geigy Plastics.
44. Hart-Smith, L.J., "Adhesive Bonded Single Lap Joints", NASA Langley Research Centre, Report NASA CR112236, Hampton Avenue, 1973.
45. Hughes, O.F., "Ship Structural Design", John Willey, Interscience Publication, 1983.
46. McNab, C N, "A new application of structural adhesives", Final year project, Department of Mechanical Engineering, University of Glasgow, 1985.
47. Smith, C S and Chalmers, D W, "Design of Ship Superstructures in Fire-reinforced Plastics", RINA Spring Meetings, London, 1986.
48. Bruce, J.W, "The Integrity of Platform Superstructures", Analysis in acording with APIRP2A, Collins 1985.
49. Wake, W.C., "Structural Applications of Adhesives", *Proc., International Conference on Structural Adhesives in Engineering*, IMechE, London 1986
50. Jordan, M., "The Instrumented Guillotine Impact Testing Apparatus", *Int. J. Adhesion and Adhesives* 8, 1988.

51. Shigley, J.E. and Mitchell, L.D., "Mechanical Engineering Design", McGraw-Hill 1983.
52. Harrier, J.A. and Adames, R.D., "The Impact Strength of Adhesive Lap Joints", Adhesive Joint Formation, Characteristics and Testing, Ed. Mittal, K.L., Plenum Press, New York, 1982.
53. Seamark, M J, "Development in Fire Retardant Composites", Composites in Marine Offshore Engineering, Proc. I Mech E, London 1989.
54. Shipp, M, "Hydrocarbome Fire Standard for Offshore Installations" Report of Fire Research Station to the Dept of Energy 1984.
55. Allen, K.W. and Shanham, M.E.R., "The Creep Behaviour of Structural Adhesive Joints 1", J. of Adhesion, 1976.
56. Allen, K.W. and Shanham, M.E.R., "The Creep Behaviour of Structural Adhesive Joints 2", J. of Adhesion, 1977.
57. Perry, H.A., "Adhesive Bonding of Reinforced Plastics", McGraw-Hill, New York, 1959.
58. Althof, W., Klinger, G. Neumann, G and Scholothaner, J., "Environmental Effects on the Elastic-Plastic Properties of Adhesives in Bonded Metal Joints", RAE Report 1999, Farnborough, 1979.
59. Comyn, J., "Surface Treatment and Analysis for Adhesive Bonding", Structural Adhesives in Engineering II, RAPRA 1989
60. Williams, N.T., "Adhesive Joining of Steel Sheets", Steel Research 10, 1988.
61. Comyn, J., "Kinetics and Mechanism of Environmental Attack", Durability of Structural Adhesives, Ed. Kinloch, A.J., Applied Science Publishers, 1983.
62. Bowditch, M.R. and Oliver, R.A., "An Underwater Adhesive Repair Method for Steel Offshore Structures", 3rd Intl. Conf. on Polymers and Offshore Engineering, Scotland, 1988.
63. Fay, P.A. and Maddison, A., "Durability of Adhesively Bonded Steel under Salt Spray and Hydrothermal Stress Conditions", Proc. Structural Adhesives in Engineering II, Bristol, 1989.
64. Niranjana, V., "Bonded Joints - A Review for Engineers", UTIAS Rev. No. 28, University of Toronto, Sept. 1970.
65. Matsui, K., "Effects of Size on Nominal Ultimate Tensile Stresses of Adhesives, Bonded Circular or Rectangular Joints Under Bending or Peeling Load", Int. J. Adhesion and Adhesives, Vol. 10, No. 2, April 1990.

66. Hart-Smith, L.J., "Design of Adhesively Bonded Joints", Ed. Matthews, F.L., Joining Fibre Reinforced Plastics, Elsevier Applied Science, 1987.
67. BS 5350, 1981 Code for Adhesive Testing
68. ASTM (several codes) including ASTM D3165, 1979 Code for Adhesive Testing.
69. Anderson, G.P., DeVries, K.L. and Sharon, G., "Evaluation of Adhesive Test Methods, Adhesive Joint, Formation, Characteristics and Testing, Ed., Mittal, K.L., Plenum Press, 1982.
70. Anderson, G.P., Bennet, S.J. and DeVries, K.L., "Analysis and Testing of Adhesive Bonds", Academic Press, 1977.
71. Gilvert, Y. and Rigolot, A., "Elastic Theoretical and Experimental Analysis of a Bonded Trans of Two Parallelepipedic Adherends", Structural Adhesive in Engineering, IMechE, London, 1986.
72. Krieger, R.B., "Stress Analysis Concepts for Adhesive Bonding of Aircraft Primary Structure", Adhesive Bonded Joints, Testing Analysis and Design, ASTM STP 981, Johnson, W.S. Ed., ASTM, 1988.
73. Jangblad, D., Gradin, P. and Stenstrom, T., "Determination and Verification of Elastic Parameters for Adhesives, Adhesively Bonded Joint Testing Analysis and Design, ASTM STP 981, Johnson, W.S. Ed., ASTM 1988.
74. Arnold, D.B., "Mechanical Test Methods for Aerospace Bonding", Kinloch, A.J., Ed., Development in Adhesives 2, Applied Science Publisher, 1981.
75. Schliekelmann, R.J., "Quality Control of Adhesive Bonded Joints", Proc., International Conference on Structural Adhesives in Engineering, IMechE, London 1986
76. Adams, R.D. and Cawley, P., "A Review of Defect Types and Non-Destructive Testing Techniques for Composite and Bonded Joints", Bonding and Repair of Composites, Butterworths, 1989.
77. Mackie, R.J. and Vardy, A.E., "A Numerical Study of the Coin Tap Test", Proceedings SAE II, 1989.
78. Adams, R.D., "The Mechanics of Bonded Joints", Proc., International Conference on Structural Adhesives in Engineering, IMechE, London 1986
79. Groth, H.L., "Stress Singularities and Fracture and Interface Corners in Bonded Joints", Int. J. Adhesives and Adhesion, Vol. 8, No. 2, 1988.
80. Crocombe, A.D., Adams, R.D., "Influence of the Spew Fillet and Other Parameters on the Stress Distribution in the Single Lap Joint", J. Adhesion, 1981, Vol. 13, pp141-155.

81. Zhao, X. and Adams, R.C., "Adhesive Joint Predictions for Real Boundary Conditions", Proc. Structural Adhesives in Engineering II, University of Bristol 1989.
82. Ojalvo, I.U. and Eidinoff, H.L., "Bond Thickness Effects Upon Stresses in Single Lap Adhesive Joints", AIAA, J. 16, No. 3, March 1978.
83. Crocombe, A.D., "Global Yielding on a Failure Criteria for Bonded Joints", Int. J. Adhesion and Adhesives, Vol. 9, No. 3, July 1989.
84. Mallick, V. and Adams, R.D., "Strength Prediction of Lap Joints with Elastoplastic Adhesives using Linear Closed Form Methods", Proc. Structural Adhesives in Engineering II, University of Bristol, 1989.
85. Williams, M.L., Calf, Pasadena, "Stress Singularities Resulting From Various Boundary Conditions in Angular Corners of Plates Extension", J. of Applied Mechanics, December 1952, pp526-528.
86. Bogy, D.B., "Two Edge Bonded Elastic Wedges of Different Materials and Wedge Angles Under Surface Traction", J. Applied Mechanics, June 1971.
87. Groth, H.L., "On the Singular Stresses at an Interface Corner", Letter, Int. J. Adhesion and Adhesives, January 1988, pp55-56.
88. Kinloch, A.J., "The Science of Adhesion Part 2: Mechanics and Mechanisms of Failure", J. of Materials Science, Vol. 17, 1982.
89. Baldwin, J.F., "An Experimental Investigation of Mixed Mode Fracture in Adhesively Bonded Joints", AIAA Student Journal, Summer 1986.
90. Russel, A.J. and Street, K.N., "Moisture and Temperature Effect on Mixed Mode Delamination Fracture of Unidirectional Graphite/Epoxy", Delamination and Debonding of Materials, ASTM STP 876, Johnson, W.S., ASTM 1985.
91. MacGregor, D., "An Investigation of Fracture In Adhesive Bonded Joints Containing Large Scale Cracks", Student Project, Department of Mechanical Engineering, University of Glasgow, 1987.
92. Smith, E.M., "Failure in Adhesive Bonds", Final Year Project, Department of Mechanical Engineering, University of Glasgow, 1989.
93. Kinloch, A.J., Kodokian, G.A. and Jamarani, M.B., "Impact Properties of Epoxy Polymers", J. of Material Science, 22 (1987).
94. Luckyram, J. and Vardy, A.E., "Fatigue Performance of Two Structural Adhesives", J. Adhesion, Vol. 26, 1988.

95. Engel, L., Klingele, H., Ehrenstein, G. and Schaper, H., "An Atlas of Polymer Damage", Wolfe Science Book, 1981.
97. Goland, M. and Reissner, E., "The Stress in Cemented Joints", J. Appl. Mech. Trans., ASME 66 (1944).
98. Allman, D.J., "A Theory for the Elastic Stress in Adhesive Bonded Lap Joint", Quart J. of Mech. & Applied Maths 30, 415, 1977.
99. Mallick, V. and Adams, R.D., "The Stress and Strains in Bonded Joints Between Metal and Composite Materials", Proc. Adhesion 87, University of York.
100. Crocomb, A.D., "A General Bonded Joint Peel Analysis", Proc. Structural Adhesive in Engineering, Bristol, 1986 (unpublished).
101. Bydynas, R.G., "Advanced Strength and Applied Stress Analysis", McGraw-Hill, 1977.
103. Evans, J.H., "Ship Structural Design Concepts", Cornell, Maritime Press, 1975.
104. Beevers, A. and Kho, A.C.P., "The Performance of Adhesive Bonded Thin Gauge Sheet Metal Structures with Particular Reference to Box Section Beam", Adhesive Joint Formation, Characteristics and Testing, Edit., Mittal, K.L., Plenum Press, New York, 1982.
105. McDevitt, N.T. and Baun, W.L., "The Three Point Bend Test for Adhesive Joints", Adhesive Joint Formation, Characteristics and Testing, Edit., Mittal, K.L., Plenum Press, New York, 1982.
106. Roche, A.A., Romand, M.J. and Sidoroff, F., "Practical Adhesion Measurement in Adhering Systems: A Phase Boundary Sensitive Test", Adhesive Joint Formation, Characteristics and Testing, Edit., Mittal, K.L., Plenum Press, New York, 1982.
107. Whitney, J.M., "Structural Analysis of Laminated Anisotropic Plates", Technomic Publishing, 1987.
108. Zienkiewicz, O.C., "The Finite Element Methods", McGraw-Hill, London, 1977.
109. Wooley, G.R. and Carrer, D.R., "Stress Concentration Factors for Bonded Lap Joints", J. Aircraft, October 1971, pp817.
110. Adams, R.D. and Peppiatt, N.A., "Stress Analysis of Adhesive Bonded Lap Joint", J. of Strain Analysis, Vol. 9, No. 3, 1974.
111. Matthews, F.L., Kitty, P.F. and Godwin, E.W., A Review of the Strength of Joints in Fibre-Reinforced Plastics, Part 2, Adhesively Bonded Joints, J. of Composites, January 1952.
112. Post, D., Czarnek, R., Wood, J.D. and Joh, D., "Deformation and Strain in Thick Adherend Lap Joint", Adhesively Bonded Joints, Testing Analysis and Design,

- ASTM STP 981, Johnson, W.S., Ed., ASTM 1988.
113. Clark, J.D., "Verification of Finite Element Stress Analysis of Adhesive Bonds", Proc. International Conference on Quality Assurance and Standards in Finite Element Analysis, Brighton, 1987.
 114. Brebbia, C.A., "The Boundary Element Method for Engineers", Pentech Press, London 1980.
 115. Matthews, F.L., "Introduction, Joining Fibre-Reinforced Plastics", Elsevier Applied Science, 1987.
 116. McGregor, I.J. and Nardini, D. , "Modelling and Testing of Aluminium Bonded Structural Components", Alcan International Limited, Banbury.
 117. Nardini, D. and Seeds, A., "Structural Design Consideration for Bonded Aluminium Structural Vehicles", SAE Technical Paper Series, March 1989.
 118. Kemp, P.W, "Some Practical Applications", Proc., International Conference on Structural Adhesives in Engineering, IMechE, London 1986
 119. Begman, M.L and Amstead, B.H., "Manufacturing Processes", John Wiley 1968
 120. Ball, A "Adhesive Bonded Sandwich Constructions", Ciba Giegy Plastics, Seminar- West Point Hotel East Kilbride, Scotland 1991 (Unpublished)
 121. "Quality Control and the Use of Structural Adhesives in Aircraft Manufacture" Unpublished Report, British Aerospace, Military Aircraft Division, Aircraft Laboratories Weybridge, 1986.
 122. Lees, W.A., "Recent Developments in Composite Bonding with Particular Reference to Large Structures and Unprepared Surfaces", Permabond Adhesives Ltd, Report 1991.
 123. Smith, E, Hashim, S, Winkle, I E, Cowling, M J "Adhesively Bonded Steel Sandwich Construction for Marine Structures", Proc. PRI, Structural Adhesives in Engineering 1992
 124. Surface Oxide Modification and Adhesion Promotion, Report, by BP Innovation Centre, The Eurcka magazine 1991
 125. Pialucha, T P, Cawly, P, "The Detection of A weak Adhesive/Adherend Interface in Bonded Joints by Ultrasonic Reflection Measurements", Proc. PRI, Structural Adhesives in Engineering 1992.
 126. Production Bonding with 'Araldite', Proc Bonded Structures Ltd, Bonded Aircraft Structures, Cambridge (Unpublished) 1957.
 127. Cowling M J, Hashim, S A, Smith , E M, Winkle I E, "Adhesive Bonding for Marine

- Structural Applications", Polymers in a Marine Environment, IMarE, 1991.
128. Mortimer, A "Application for Structural adhesives within James Howden and Company Ltd", Unpublished Report, Feb, 1988.
 129. Corbet, D C, "Repair of Composite-an Overview", Proc., RAPRA, Bonding and Repair of Composites, Birmingham 1989.
 130. Fay, P A, Davis, R E, "Bonding of Zinc Coated Steels", Proc, PRI, Structural Adhesives in Engineering III, Bristol 1992.

APPENDIX I: STRESSES IN SOLID RECTANGULAR BEAM SECTIONS
UNDER BENDING

Definition of transverse shear stress: The shear stresses which are developed in elastic beams with solid cross sections due to lateral or transverse shear loads arising from bending^(101,102,103).

Consider a beam element with longitudinal length dx , breadth b , and depth h which is subjected to a bending moment, M and transverse shear force, V as shown in the following diagram:

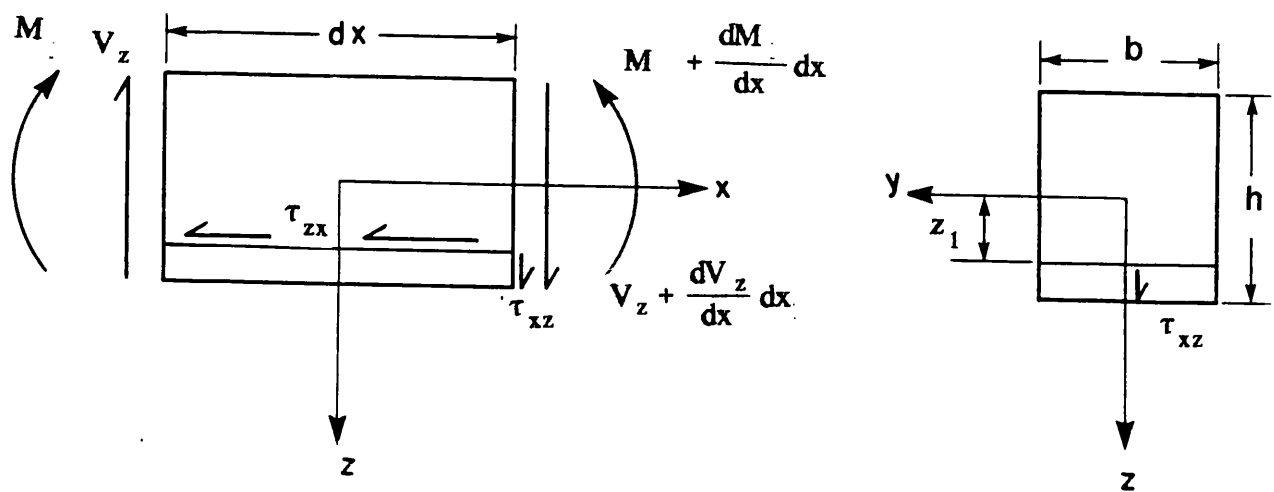


FIGURE I

An expression for shear stress, τ_{xz} , acting on a typical plane at $z=z_1$ may be obtained by examining the longitudinal equilibrium of that portion of the beam which lies in the region

$z_1 \leq z \leq h/2$. Thus:

$$\int_{z_1}^{h/2} \sigma_x b dz + \frac{\partial}{\partial x} \int_{z_1}^{h/2} \sigma_x b dz dx - \int_{z_1}^{h/2} \sigma_x b dz - \tau_{zx} b dx = 0$$

or

$$\tau_{xz} = \int_{z_1}^{h/2} \frac{\partial \sigma_x}{\partial x} dz$$

Where

$$\tau_{xz} = \tau_{zx}$$

Elementary beam bending theory predicts:

$$\sigma_x = z \frac{M}{I}$$

This gives

$$\frac{\partial \sigma_x}{\partial x} = \frac{z}{I} \frac{dM}{dx}$$

Where

I is the second moment of the entire cross-sectional area .

Furthermore, moment equilibrium of the beam shown in the figure above requires:

$$V = \frac{dM}{dx}$$

so that

$$\frac{\partial \sigma_x}{\partial x} = z \frac{V}{I}$$

Finally, the above equations give:

$$\tau_{xz} = \frac{VQ}{bI}$$

where

$$Q = \int_{z_1}^{h/2} z b dz$$

APPENDIX II: CALCULATIONS OF AVERAGE CLEAVAGE STRESS AND JOINT EFFICIENCY (CHAPTER 4)

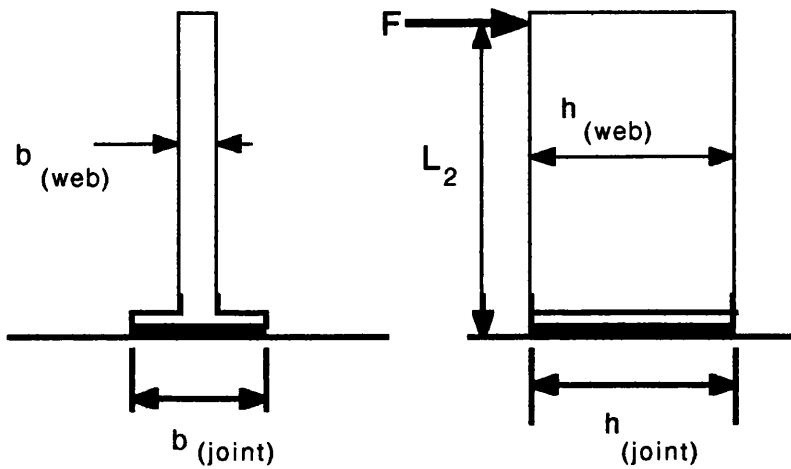


FIGURE II

From Figure II above, bending and average cleavage stresses may be calculated from the following beam equation;

$$\sigma_b = \frac{6FL_2}{bh^2}$$

Assuming

$$\sigma_b = \bar{\sigma}_y$$

Where

$\bar{\sigma}_y$ is the maximum average tensile cleavage stress at the adhesive line

σ_b is tensile bending stress at the web root position.

F is the applied force at the end of the cantilever.

b is the width of the web section or bonded joint

h is the depth of the web section or bonded joint

L_2 is length of cantilever to load point.

A sample calculation for a Type 2 (8mm plate thickness-see Table 4.1) is as follows:

$$b_{(\text{joint})} = w_a = 45\text{mm} \text{ (} w_a \text{ is the width of adhesive joint), } b_{(\text{web})} = 4.3\text{mm} ,$$

$$h_{(\text{joint})} = 75\text{mm}, F = 9.7\text{kN}, L_2 = 80\text{mm}$$

Thus maximum adhesive cleavage stress at bond failure calculated from the above equation is:

$$\sigma_y^- = 18.4 \text{ N/mm}^2$$

In Chapter 5, the stress analysis will show that actual adhesive cleavage stress is several times higher than this average value. The bending stress in the stiffener web was obtained in the same manner as shown above. In case the of Type 3 specimens (with shaped flange end), the depth of the web was assumed to be the same as Type 2 ($h_{(\text{web})} = 75\text{mm}$) for comparison purposes (see Table 4.2).

Joint strength efficiency for the above specimen conditions is calculated as follows;

The maximum bending stress in the web at $L_2 = 8\text{mm}$ (approximately) is

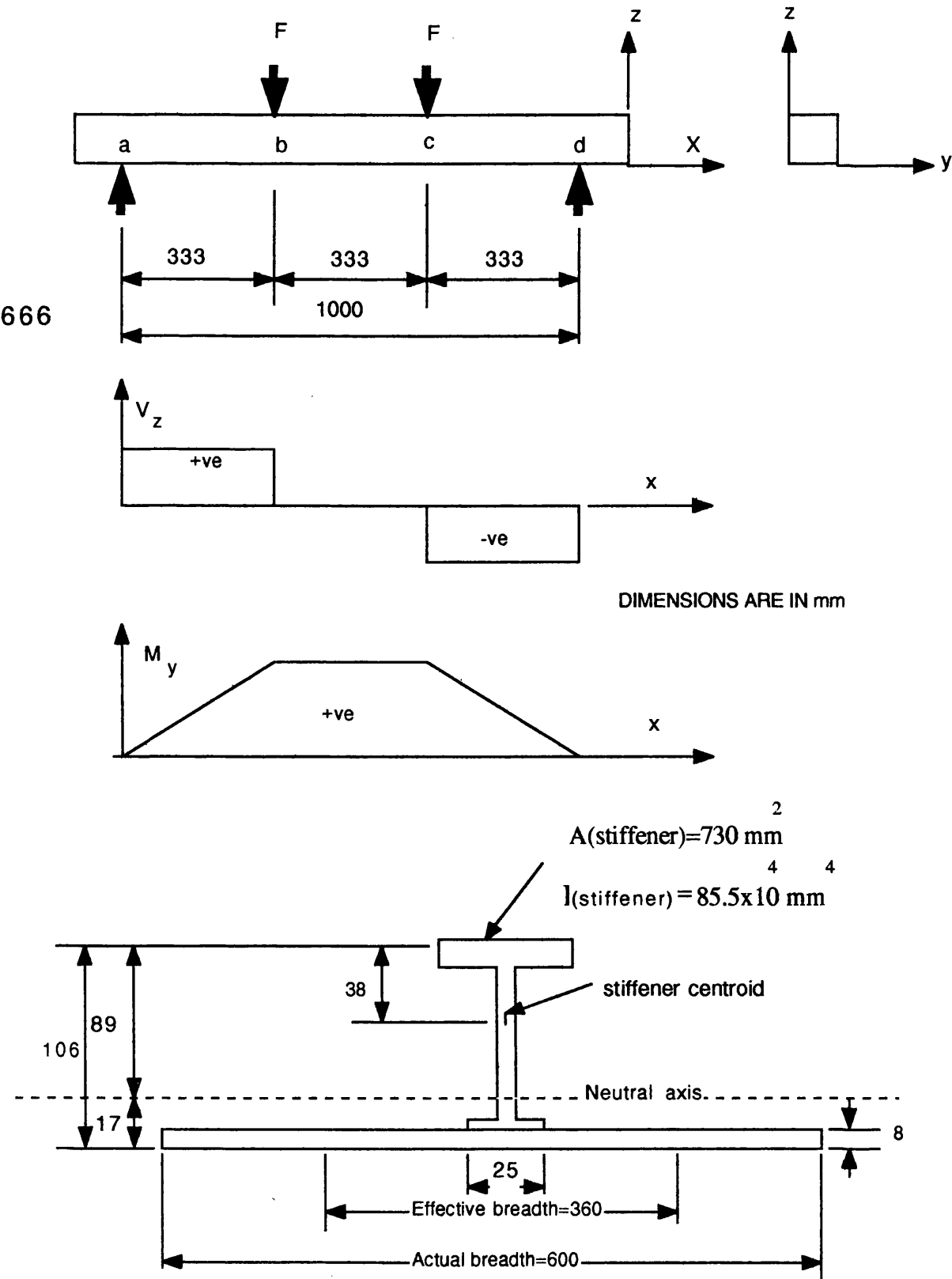
$$\begin{aligned} \sigma_b &= \frac{6 \times 9700 \times 80}{4.3 \times 75^2} \\ &= 192\text{N/mm}^2 \end{aligned}$$

Given that the minimum yield strength for the mild steel = 230N/mm^2

The efficiency = $192/230$

$$= 0.84 \text{ (see Table 4.1)}$$

APPENDIX III: STRESS CALCULATIONS OF BONDED STIFFENED PANEL
IN BENDING



The effective breadth (b_e) of stiffened plate at the maximum bending moment is obtained from the relevant design curves⁴⁵, considering a simply supported beam with uniform loading. The length between the points of zero bending moment (l) is 1000mm and the actual breadth (b) is 600mm. It is found that;

$$\begin{aligned} b_e &= 0.6 b \\ &= 0.6 \times 600 \\ &= 360 \text{ mm} \end{aligned}$$

The position of the neutral axis of the section (z) may be calculated as follows;

$$\begin{aligned} z &= (730 \times 68.4 + 2880 \times 4) / (730 + 288) \\ &= 17 \text{ mm above the lower surface of the plate} \end{aligned}$$

The second moment of area of the section may be calculated as follows;

$$\begin{aligned} I &= 85.52 \times 10^4 + 730 \times 51.4^2 + 1.54 \times 10^4 + 2880 \times 13^2 \\ &= 328.6 \times 10^4 \text{ mm}^4 \end{aligned}$$

The first moment of the area of the plate about the neutral axis may be calculated as follows;

$$\begin{aligned} Q &= 2880 \times 13 \\ &= 3.744 \times 10^4 \text{ mm}^3 \end{aligned}$$

The bending stress at the centre of the beam plate (assuming elastic limit for the beam section) may be obtained from the following equation (Chapter 5)

$$\sigma_x = z f_1 \frac{M_y}{I}$$

Where

σ_x is the bending stress at the outer plate surface

z is the distance between the outer plate surface and the neutral axis

f_1 is the adherend interface coefficient (Chapter 5). The value of f_1 for the bonded steel beam is higher than unity and may be assumed, according to the analysis in Chapter 5, to be 1.3 (engineering assumption).

M is the maximum bending moment (between point b & c along the beam

From experiment the applied force to cause yield stress in each stiffener (double stiffened panel) is;

$$F = 149/4$$

$$= 37.25 \text{ kN}$$

We also have

$$a = 333 \text{ mm}, z = 88 \text{ mm},$$

Thus

$$M = 37.25 \times 333 \times 10^3$$

$$= 1240 \times 10^4 \text{ N.mm}$$

and the maximum bending stress in the adherend will be;

$$\sigma_x = 1.3 \times 1240 \times 10^4 \times 88 / 328.6 \times 10^4$$

$$= 432 \text{ N/mm}^2$$

The shear stress within the adhesive may be calculated from the following composite section formula;

$$\tau_{xz} = f_1 \frac{V_z Q}{I w_a}$$

Where

V_z is the shear force transverse to the section

Q is the first moment of the plate area about the neutral axis

w_a is the width of the adhesive joint

Given

$$V_z = 37250 \text{ N}, w_a = 25 \text{ mm},$$

The shear stress therefore will be;

$$\tau_{xz} = 1.3 \times 37250 \times 3.744 \times 10^4 / 25 \times 328.6 \times 10^4$$

$$= 22 \text{ N/mm}^2$$

APPENDIX IV: INPUT DATA FILES FOR PAFEC FINITE ELEMENTS STATIC STRESS ANALYSES

IV.1. STIFFENED STEEL/STEEL ADHESIVE JOINT (MODEL A-FIGURES 5.1 AND 5.5)

```

1) CONTROL
2) SKIP.CHECK
3) TOLERANCE=10E-5
4) PHASE=1,2,3,4,5,6,7,8,9,10
5) CONTROL.END
6) NODES
7) NODE.NUMBER,X,Y
8) 1,0,0
9) 2,0,005,0
10) 3,0,1325,0
11) 4,0,1775,0
12) 5,0,305,0

13) 6,0,0,004
14) 7,0,005,0,004
15) 8,0,1325,0,004
16) 9,0,1775,0,004
17) 10,0,305,0,004
18) 11,0,0,008
19) 12,0,005,0,008
20) 13,0,1325,0,008
21) 14,0,1775,0,008
22) 15,0,305,0,008
23) 16,0,1325,0,00851
24) 17,0,1775,0,00851
25) 18,0,1325,0,01251
26) 19,0,1775,0,01251
27) 20,0,1325,0,08851
28) 21,0,1775,0,08851
29) MATERIAL
30) MATERIAL.NUMBER,E,NU,RO
31) 20,5E9,0.37,1250
32) PAFBLOCKS
33) BLOCK.NUMBER,TYPE,ELEMENT,TYPE,PROPERTIES,N1,N2,TOPOLOGY
34) 1,1,36210,1,1,2,1,2,6,7
35) 2,1,36210,1,3,2,2,3,7,8
36) 3,1,36210,1,4,2,3,4,8,9
37) 4,1,36210,1,5,2,4,5,9,10
38) 5,1,36210,1,1,2,6,7,11,12
39) 6,1,36210,1,3,2,7,8,12,13
40) 7,1,36210,1,4,2,8,9,13,14
41) 8,1,36210,1,3,2,9,10,14,15
42) 9,1,36210,20,4,5,13,14,16,17
43) 10,1,36210,1,4,6,16,17,18,19
44) 11,1,36210,1,4,7,18,19,20,21
45) MESH

```

```

46) REFERENCE,SPACING,LIST
47) 1,2
48) 2,4
49) 3,30
50) 4,1,1,2,2,2,4,4,8,8,16,16,32,32,16,16,8,8,4
51) 5,2
52) 6,8
53) 7,2,4,8,16,32,64
54) PLATES,AND,SHELLS
55) PLATE,MATERIAL,THICKNESS
56) 1,1,0.075
57) 20,20,0.075
58) LOADS
59) CASE,OF,LOADS,NODE,NUMBER,DIRECTION,OF,LOAD,VALUE,OF,LOAD
60) 1,20,1,10374
61) RESTRAINTS
62) NODE,NUMBER,PLANE,DIRECTION
63) 5,0,2
64) 10,0,1
65) 12,0,2
66) STRESS
67) START,FINISH,STEP
68) 1,1000,2
69) IN,DRAW
70) DRAWING,NUMBER,TYPE,NUMBER,INFORMATION,NUMBER
71) 1,2,9
72) OUT,DRAW
( 73) DRAWING,NUMBER,PLOT,TYPE,SIZE,NUMBER
( 74) 2,3,10
( 75) 3,1,10
( 76) 4,4,10
( 77) END,OF,DATA

```

END OF DATA

D ERRORS

NO ERRORS OR WARNINGS IN VALIDATION

IV.2. STIFFENED STEEL/STEEL ADHESIVE JOINT (MODEL B-FIGURES 5.1 AND 5.5)

```

( 1) CONTROL
( 2) SKIP.CHECK
( 3) TOLERANCE=10E-5
( 4) PHASE=1,2,3,4,5,6,7,8,9,10
( 5) REDUCED.OUTPUT
( 6) CONTROL.END
( 7) NODES
( 8) NODE.NUMBER,X,Y
( 9) 1,0,0
(10) 2,0.005,0
(11) 3,.0775,0
(12) 4,0.1275,0

```

```

(13) 5,0.205,0
(14) 6,0,0.004
(15) 7,0.005,0.004
(16) 8,0.0775,0.004
(17) 9,0.1275,0.004
(18) 10,0.205,0.004
(19) 11,0,0.008
(20) 12,0.005,0.008
(21) 13,0.0775,0.008
(22) 14,0.1275,0.008
(23) 15,0.205,0.008
(24) 16,0.0775,0.00851
(25) 17,0.1275,0.00851
(26) 18,.0775,0.01251
(27) 19,0.1275,0.01251
(28) 20,0.0775,0.08851
(29) 21,0.1275,0.08851
(30) MATERIAL
(31) MATERIAL.NUMBER,E,NU,RO
(32) 20,5E9,0.37,1250
(33) PAFBLOCKS
(34) BLOCK.NUMBER,TYPE,ELEMENT.TYPE,PROPERTIES,N1,N2,TOPOLOGY
(35) 1,1,36210,1,1,2,1,2,6,7
(36) 2,1,36210,1,3,2,2,3,7,8
(37) 3,1,36210,1,4,2,3,4,8,9
(38) 4,1,36210,1,3,2,4,5,9,10
(39) 5,1,36210,1,1,2,6,7,11,12
(40) 6,1,36210,1,3,2,7,8,12,13
(41) 7,1,36210,1,4,2,8,9,13,14
(42) 8,1,36210,1,3,2,9,10,14,15
(43) 9,1,36210,20,4,5,13,14,16,17
(44) 10,1,36210,1,4,6,16,17,18,19
(45) 11,1,36210,1,4,7,18,19,20,21

```

```

( 46) MESH
( 47) REFERENCE,SPACING,LIST
( 48) 1,2
( 49) 2,3
( 50) 3,15
( 51) 4,1,1,2,2,2,4,4,8,8,16,16,32,32,32,16,4
( 52) 5,2
( 53) 6,4
( 54) 7,2,4,8,16,32,64
( 55) PLATES.AND.SHELLS
( 56) PLATE,MATERIAL,THICKNESS
( 57) 1,1,0.075
( 58) 20,20,0.075
( 59) LOADS
( 60) CASE.OF.LOADS,NODE.NUMBER,DIRECTION.OF.LOAD,VALUE.OF.LOAD
( 61) 1,20,1,11630
( 62) RESTRAINTS
( 63) NODE.NUMBER,PLANE,DIRECTION
( 64) 5,0,2
( 65) 10,0,1
( 66) 12,0,2
( 67) STRESS
( 68) START,FINISH,STEP
( 69) 200,500,1
( 70) IN.DRAW
( 71) DRAWING.NUMBER,TYPE.NUMBER,INFORMATION.NUMBER
( 72) 1,2,9
( 73) OUT.DRAW
( 74) DRAWING.NUMBER,PLOT.TYPE,SIZE.NUMBER
( 75) 2,3,10
( 76) 3,1,10
( 77) 4,4,10
( 78) END.OF.DATA

```

END OF DATA 0 ERRORS

NO ERRORS OR WARNINGS IN VALIDATION

IV.3. STEEL/STEEL TENSILE LAP SHEAR ADHESIVE JOINT (FIGURE 5.9)

```

( 1) CONTROL
( 2) PLANE.STRAIN
( 3) SKIP.CHECK
( 4) TOLERANCE=10E-6
( 5) PHASE=1,2,3,4,5,6,7,8,9,10
( 6) FULL.CONTROL
( 7) CONTROL.END
( 8) NODES
( 9) Z=0
(10) NODE,X,Y
(11) 1,0,0
(12) 2,.05,0
(13) 3,.08,0
(14) 4,.085,0
(15) 5,.1,0
(16) 6,.105,0
(17) 9,0,.005
(18) 10,.08,.005
(19) 11,.085,.005
(20) 8,.185,0
(21) 37,.135,.011
(22) 38,.185,.011
(23) 12,.1,.005
(24) 13,.105,.005
(25) 14,.185,.005
(26) 15,0,.0055
(27) 16,.08,.0055
(28) 17,.085,.0055
(29) 19,.105,.0055
(30) 20,.185,.0055
(31) 21,0,.0105
(32) 23,.08,.0105
(33) 24,.085,.0105
(34) 25,.1,.0105
(35) 26,.105,.0105
(36) 27,.135,.0105
(37) 28,.185,.0105
(38) 29,.185,.0025
(39) 30,.135,.008
(40) 32,.05,-.0005
(41) 31,0,-.0005
(42) 18,.1,.0055
(43) PAFBLOCKES
(44) ELEMENT.TYPE=36210
(45) BLOC,TYPE,PROP,N1,N2,TOPO
(46) 1,1,2,3,2,3,4,10,11
(47) 2,1,2,5,2,4,5,11,12
(48) 3,1,6,5,7,11,12,17,18
(49) 4,1,5,5,2,25,24,13,17
(50) 5,1,5,3,2,26,25,19,18
(51) 6,1,2,1,2,1,3,9,10
(52) 7,1,3,1,2,8,6,14,13

```

```

( 53) 8,1,6,1,6,9,10,15,16
( 54) 13,1,5,1,2,28,26,20,19
( 55) 11,1,1,8,9,38,37,28,27
( 56) 9,1,6,1,6,14,13,20,19
( 57) 10,1,4,1,2,21,23,15,16
( 58) 12,1,1,8,9,31,32,1,2
( 59) MESH
( 60) REFE,SPAC
( 61) 1,25,25,10,10,5,5
( 62) 8,25,25
( 63) 2,1,1,1,1
( 64) 3,1,1,1,1,1
( 65) 5,1,1,1,2,2,4,4,10,10,20,20,20,20,10,10,4,4,2,2,1,1,
( 66) 6,2
( 67) 7,5
( 68) 9,1
( 69) MATERIAL
( 70) MATERIAL.NUMBER,E,NU,RO
( 71) 20,5E9,.37,1250
( 72) 30,14E9,.13,2500
( 73) PLATE.AND.SHELLS
( 74) PLAT,MATE,THIC
( 75) 1,1,.025
( 76) 2,1,.025
( 77) 3,1,.025
( 78) 4,1,.025
( 79) 5,1,.025
( 80) 6,20,.025
( 81) LOADS
( 82) CASE,NODE,DIRE,VALU
( 83) 1,28,1,1420
( 84) 1,20,1,1420
( 85) 1,14,1,1420
( 86) 1,8,1,1420
( 87) 1,29,1,5670
( 88) 1,30,1,5670
( 89) RESTRAINTS
( 90) NODE,PLAN,DIRE
( 91) 32,2,2
( 92) 31,1,1
( 93) 37,2,2
( 94) STRESS
( 95) START,FINISH,STEP
( 96) 1,230,1
( 97) IN.DRAW
( 98) DRAW,TYPE,INFO
( 99) 1,2,9
( 100) OUT.DRAW
( 101) DRAWING.NUMBER,PLOT.TYPE,SIZE.NUMBER
( 102) 2,3,10
( 103) 3,1,10
( 104) 4,4,10
( 105) END.OF.DATA

```

END OF DATA

0 ERRORS

IV.4. STEEL/STEEL TENSILE CLEAVAGE ADHESIVE JOINT (FIGURE 5.10)

----- THE TOLERANCE USED IN THIS PHASE IS 1E -6 -----

```

( 1) CONTROL
( 2) SKIP.CHECK
( 3) SKIP.COLLAPSE
( 4) TOLERANCE=10E-6
( 5) PHASE=1,2,3,4,5,6,7,8,9,10
( 6) FULL.CONTROL
( 7) CONTROL.END
( 8) NODES
( 9) NODE,X,Y
(10) 1,0,0
(11) 2,.025,0
(12) 3,0,.01
(13) 4,.025,.01
(14) 5,0,.0105
(15) 6,.025,.0105
(16) 7,0,.0155
(17) 8,.025,.0155
(18) 9,0,.0205
(19) 10,.025,.0205
(20) PAFBLOCKES
(21) ELEMENT.TYPE=36210
(22) TYPE=1
(23) BLOC,PROP,N1,N2,TOPO
(24) 1,1,1,2,1,2,3,4
(25) 2,20,1,3,3,4,5,6
(26) 3,1,1,4,5,6,7,8
(27) 4,1,1,5,7,8,9,10
(28) MESH
(29) REFE,SPAC
(30) 1,5,5,4,3,3,2,1,.5,.5,.2,.2,.2,.1,.1,.05,.05,.05,.05
(31) 2,5
(32) 3,5
(33) 4,3
(34) 5,2
(35) MATERIAL
(36) MATE,E,NU,RO
(37) 20,5E9,.37,1300
(38) PLATES.AND.SHELLS
(39) PLAT,MATE,THIC
(40) 1,1,.025
(41) 20,20,.025
(42) LOADS
(43) CASE,NODE,DIRE,VALU
(44) 1,10,2,12000
(45) RESTRAINTS
(46) NODE,PLAN,DIRE
(47) 2,0,0
(48) STRESS
(49) START,FINI,STEP
(50) 80,300,1
(51) IN.DRAW
(52) DRAW,TYPE,INFO
(53) 1,2,9
(54) OUT.DRAW
(55) DRAW,PLOT,SIZE
(56) 2,3,10
(57) 3,1,10
(58) 4,4,10
(59) END OF DATA

```

END OF DATA

0 ERRORS

IV.5. STIFFENED STEEL/GRP ADHESIVE JOINT (FIGURES 5.13 AND 5.15)

 THE TOLERANCE USED IN THIS PHASE IS 1E -6

```

1) CONTROL
2) PLANE.STRAIN
3) SKIP.COLLAPSE
4) REDUCED.OUTPUT
5) SKIP.CHECK
6) TOLERANCE=10E-6
7) PHASE=1,2,3,4,5,6,7,8,9,10
8) FULL.CONTROL
9) CONTROL.END
10) NODES
11) NODE,X,Y
12) 1,0,0
13) 2,.2235,0
14) 3,.225,0
15) 4,.275,0
16) 5,0,.0145
17) 6,.2235,.0145
18) 15,.224,.015
19) 16,.275,.016
20) 7,.225,.0145
21) 8,.275,.0145
22) 9,.223,.015
23) 10,.225,.016
24) 11,.225,.025
25) 12,.275,.025
26) 13,.275,.015
27) 14,.225,.015
28) MATERIAL
29) MATERIAL.NUMBER,E,NU,RD
30) 20,4E9,.37,1300
31) 21,14E9,.14,1650
32) 22,14E9,.14,1300
33) PAFBLOCKS
34) ELEMENT.TYPE=36210
35) TYPE=1
36) BLOCK.NUMBER,PROPERTIES,N1,N2,TOPOLOGY
37) 1,22,1,2,1,2,5,6
38) 2,21,3,2,2,3,6,7
39) 3,21,4,2,3,4,7,8
40) 5,1,4,5,14,13,10,16
41) 6,1,4,8,10,16,11,12
42) 7,20,3,5,6,7,15,14
43) 8,20,3,5,15,14,9,10
44) 4,20,4,5,7,2,14,13
45) MESH
46) REFE,SPACING,LIST
47) 1,2,4,2,16,32,8,4,4,2,2,1,1,.5,.5
48) 2,9,6,2
49) 3,4
50) 4,1,1,0,2,4,12,24
51) 5,3
52) 3,5
53) PLATED.AND.SHELLS
54) PLATE/MATERIAL/THICKNESS
55) 1,1,0.075
  
```



```

24) 11,,225,,.023
25) 12,,275,,.023
26) 13,,275,,.015
27) 14,,225,,.015
28) MATERIAL
29) MATERIAL.NUMBER,E,NU,RO
30) 20,4E9,,.37,1300
31) 21,14E9,,.14,1650
32) 22,14E9,,.14,1300
33) PAFBLOCKS
34) ELEMENT.TYPE=36210
35) TYPE=1
36) BLOCK.NUMBER,PROPERTIES,N1,N2,TOPOLOGY
37) 1,22,1,2,1,2,5,6
38) 2,21,3,2,2,3,6,7
39) 3,21,4,2,3,4,7,8
40) 5,1,4,5,14,13,10,16
41) 6,1,4,8,10,16,11,12
42) 7,20,3,5,6,7,15,14
43) 8,20,3,5,15,14,9,10
44) 4,20,4,5,7,8,14,13
45) MESH
46) REFE,SPACING,LIST
47) 1,2,4,8,16,32,8,4,4,2,2,1,1,.5,.5
48) 2,9,6,2
49) 3,4
50) 4,1,1,2,2,4,12,24
51) 5,3
52) 8,5
53) PLATES.AND.SHELLS
54) PLATE,MATERIAL,THICKNESS
55) 1,1,0.075
56) 22,22,,.075
57) 20,20,0.075
58) 21,21,0.075
59) PRESSURE
60) PRESSURE.VALUE,LIST.OF.NODE
61) 18E4,5
62) 18E4,6
63) RESTRAINTS
64) NODE,PLANE,AXIS,DIRECTION
65) 5,1,1,1
66) 11,2,1,12
67) STRESS
68) START,FINISH,STEP
69) 1,1000,1
70) IN.DRAW
71) TYPE,INFORMATION
72) 1,3
73) OUT.DRAW
74) DRAWING,PLOT,TYPE
75) 2,32
76) 3,1
77) END.OF.DATA

```

VD OF DATA

O ERRORS

O ERRORS OR WARNINGS IN VALIDATION

IV.6. STEEL/GRP TENSILE LAP SHEAR ADHESIVE JOINT (FIGURE 5.16)

```

( 1) CONTROL
( 2) PLANE.STRAIN
( 3) SKIP.CHECK
( 4) TOLERANCE=10E-6
( 5) PHASE=1,2,3,4,5,6,7,8,9,10
( 6) FULL.CONTROL
( 7) CONTROL.END
( 8) NODES
( 9) Z=0
(10) NODE,X,Y
(11) 1,0,0
(12) 2,.05,0
(13) 3,.05,0
(14) 4,.085,0
(15) 5,.1,0
(16) 6,.105,0
(17) 9,0,.005
(18) 10,.08,.005
(19) 11,.085,.005
(20) 8,.135,0
(21) 37,.135,.011
(22) 38,.135,.011
(23) 12,.1,.005
(24) 13,.105,.005
(25) 14,.125,.005
(26) 15,0,.0055
(27) 16,.08,.0055
(28) 17,.085,.0055
(29) 19,.105,.0055
(30) 20,.135,.0055
(31) 21,0,.0105
(32) 23,.08,.0105
(33) 24,.085,.0105
(34) 25,.1,.0105
(35) 26,.105,.0105
(36) 27,.135,.0105
(37) 23,.135,.0105
(38) 29,.135,.0025
(39) 30,.135,.008
(40) 32,.05,-.0005
(41) 31,0,-.0005
(42) 42,.0835,.005
(43) 41,.0843,.0065
(44) 40,.085,.0065
(45) 45,.1015,.0055
(46) 43,.1,.004
(47) 44,.1002,.004
(48) 18,.1,.0055
(49) PAFBLOCKES
(50) ELEMENT.TYPE=36210
(51) BLOC,TYPE,PROP,N1,N2,TOPO
(52) 1 4 2 7 2 3 4 10 11

```

```

( 52) 1,1,2,3,2,3,4,10,11
( 53) 2,1,2,5,2,4,5,11,12
( 54) 3,1,6,5,7,11,12,17,18
( 55) 4,1,5,5,2,25,24,18,17
( 56) 5,1,5,3,2,26,25,19,18
( 57) 6,1,2,1,2,1,3,9,10
( 58) 7,1,3,1,2,8,6,14,13
( 59) 8,1,6,1,6,9,10,15,16
( 60) 13,1,5,1,2,28,26,20,19
( 61) 11,1,1,8,9,38,37,28,27
( 62) 14,1,6,10,11,11,42,40,41
( 63) 15,1,6,10,11,18,45,43,44
( 64) 9,1,6,1,6,14,13,20,19
( 65) 10,1,4,1,2,21,23,15,16
( 66) 12,1,1,8,9,31,32,1,2
( 67) MESH
( 68) REFE,SPAC
( 69) 1,25,25,10,10,5,5
( 70) 8,25,25
( 71) 2,1,1,1,1,.5,.5
( 72) 3,1,1,1,.5,.1,.1,.2,.4,.4,.2,.1,1

( 73) 5,1,1,1,2,2,4,4,10,10,20,20,20,20,10,10,4,4,2,2,1,1,1
( 74) 6,2
( 75) 7,5
( 76) 10,.1,.1,.2,.4,.4,.2,.1
( 77) 11,.1,.1,.1,.1,.1,.5,.5
( 78) 9,1
( 79) MATERIAL
( 80) MATERIAL.NUMBER,E,NU,RO
( 81) 20,4E9,.37,1250
( 82) 30,14E9,.13,2500
( 83) PLATE.AND.SHELLS
( 84) PLAT,MATE,THIC
( 85) 1,1,.025
( 86) 2,30,.025
( 87) 3,30,.025
( 88) 4,1,.025
( 89) 5,1,.025
( 90) 6,20,.025
( 91) LOADS
( 92) CASE,NODE,DIRE,VALU
( 93) 1,28,1,570
( 94) 1,20,1,570
( 95) 1,14,1,570
( 96) 1,8,1,570
( 97) 1,29,1,2278
( 98) 1,30,1,2278
( 99) RESTRAINTS
( 100) NODE,PLAN,DIRE
( 101) 32,2,2
( 102) 31,1,1
( 103) 37,2,2
( 104) STRESS

```

```
( 105)  START,FINISH,STEP
( 106)  1,1000,1
( 107)  IN.DRAW
( 108)  DRAW,TYPE,INFO
( 109)  1,2,9
( 110)  OUT.DRAW
( 111)  DRAWING.NUMBER,PLOT.TYPE,SIZE.NUMBER
( 112)  2,3,10
( 113)  3,1,10
( 114)  4,4,10
( 115)  END.OF.DATA
```

END OF DATA 0 ERRORS

NO ERRORS OR WARNINGS IN VALIDATION

IV.7. STEEL/STEEL FLEXURAL BEAM ADHESIVE JOINT (FIGURE 5.24)

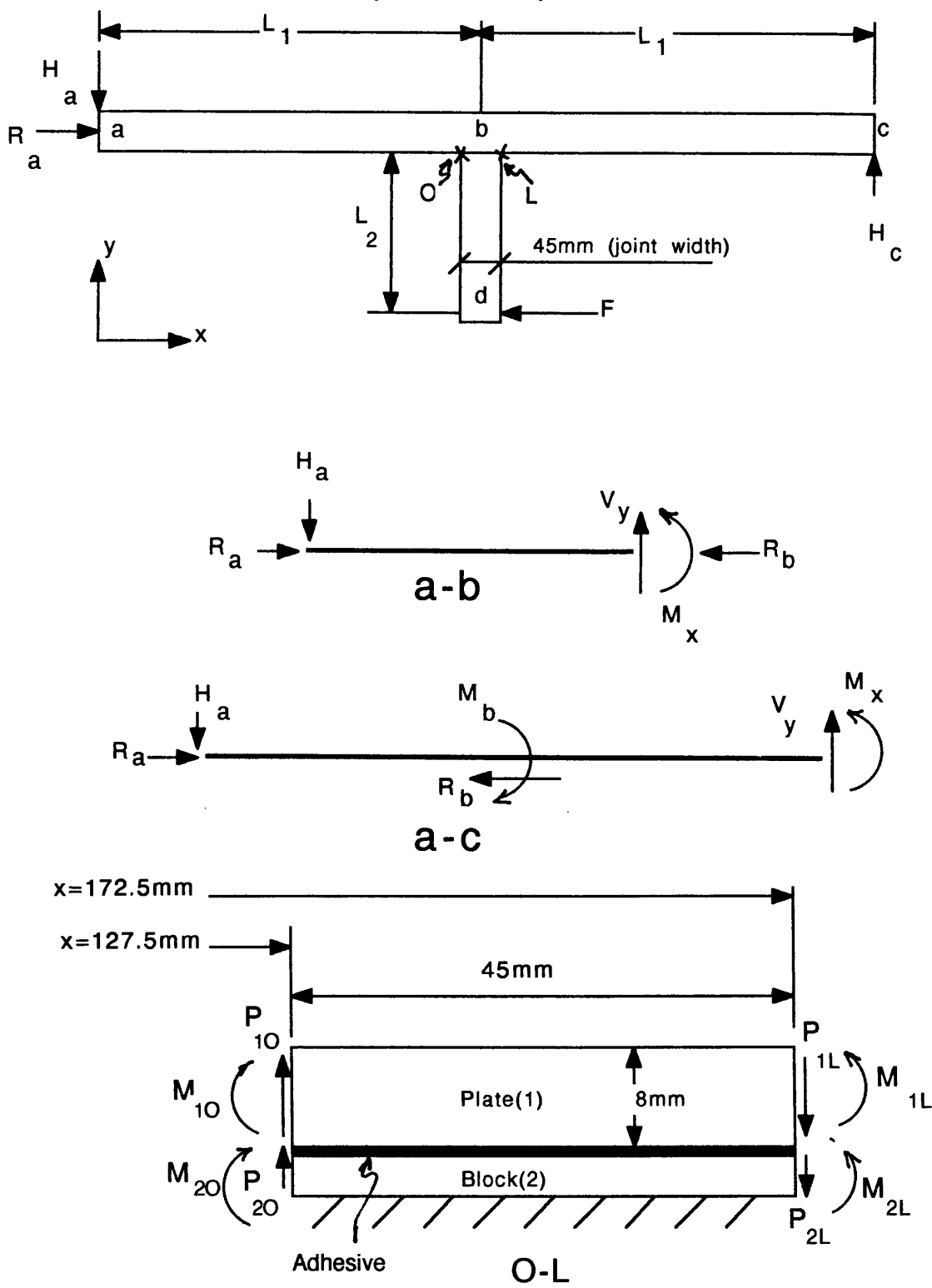
```

( 1) CONTROL
( 2) DOUBLE
( 3) SKIP.CHECK
( 4) TOLERANCE=10E-5
( 5) PHASE=1,2,3,4,5,6,7,8,9,10
( 6) FULL.CONTROL
( 7) CONTROL.END
( 8) NODES
( 9) Z=0
(10) NODE,X,Y
(11) 1,0,0
(12) 2,.0025,0

(13) 3,.0325,0
(14) 4,.035,0
(15) 5,0,.005
(16) 6,.0025,.005
(17) 7,.0325,.005
(18) 8,.035,.005
(19) 9,.0025,.0055
(20) 10,.0325,.0055
(21) 11,.0025,.0105
(22) 12,.0175,.0105
(23) 13,.0325,.0105
(24) PAFBLOCKES
(25) ELEM=36210
(26) TYPE=1
(27) BLOC,PROP,N1,N2,TOPO
(28) 1,1,1,2,1,2,5,6
(29) 2,1,3,2,2,3,6,7
(30) 3,1,1,2,3,4,7,8
(31) 4,20,3,4,6,7,9,10
(32) 5,1,3,5,9,10,11,13
(33) MESH
(34) REFE,SPAC
(35) 1,2
(36) 3,.2,.2,.6,1,1,1,1,1,2,2,5,5,10,10,10,5,5
(37) 4,5
(38) 5,1,1,2,4
(39) 2,4,2,1,1
(40) RESTRAINT
(41) NODE,PLAN,DIRE
(42) 2,0,12
(43) 3,0,2
(44) LOADS
(45) NODE,DIRE,VALU
(46) 12,2,-20000
(47) MATERIAL
(48) MATE,E,NU,RO
(49) 20,5E9,.37,1250
(50) PLATE.AND.SHELLS
(51) PLATE,MATE,THIC
(52) 1,1,.025
(53) 20,20,.025
(54) STRESS
(55) STAR,FINI,STEP
(56) 1,200,1
(57) IN.DRAW
(58) DRAW,TYPE,INFO
(59) 1,2,9
(60) OUT.DRAW
(61) DRAW,PLOT,SIZE
(62) 2,3,10
(63) 3,13,10
(64) 4,4,10
(65) END.OF.DATA

```

APPENDIX V: ANALYTICAL STRESS CALCULATIONS FOR MODELS A & B
(CHAPTER 5)



(Boundary conditions after cutting the block and plate around the adhesive joint)

FIGURE V. DIAGRAM FOR MODEL A (FIGURE 5.1)

Peel stress in the adhesive along the sandwich (steel/adhesive/steel) joint is given by the following equation¹⁰⁰:

$$\frac{\sigma_y}{k_a} = A \cos \alpha x \cosh \alpha x + B \cos \alpha x \sinh \alpha x + C \sin \alpha x \cosh \alpha x + D \sin \alpha x \sinh \alpha x$$

At $x=0$ the equation can be written as follows;

$$\frac{\sigma_y}{k_a} = A \cos \alpha x \cosh \alpha x$$

Where:

σ_y is the normal adhesive stress

k_a is the effective spring stiffness of the adhesive;

$$k_a = w_a E_3 / T_3$$

Where

w_a is the width of the joint

E_3 is the adhesive modulus of elasticity

T_3 is the thickness of the adhesive

A is a constant;

$$A = (K_1 R_6 - 2K_2 \sinh \alpha l \sin \alpha l - K_3 R_3 - K_4 R_4) / R_5$$

Where

$$K_1 = (M_{1O} / D_1 - M_{2O} / D_2) / 2 \alpha^2 w_a$$

$$K_2 = (M_{1L} / D_1 - M_{2L} / D_2) / 2 \alpha^2 w_a$$

$$K_3 = (P_{1O} / D_1 - P_{2O} / D_2) / 2 \alpha^3 w_a$$

$$K_4 = (P_{1L} / D_1 - P_{2L} / D_2) / 2 \alpha^3 w_a$$

Where

M_{1L} , M_{2L} , P_{1O} , P_{2O} , P_{1L} and P_{2L} are the boundary moments and forces as shown in the diagram above (Figure V)

D_1 is the stiffness of the upper adherend

$$D_1 = E_1 I_1 / (1 - \nu_1^2)$$

Where

E_1 is the modulus of elasticity of the upper adherend

I_1 is the second moment of area of the upper adherend

ν_1 is Poisson's ratio of the upper adherend

D_2 is the stiffness of the lower adherend

$$D_2 = E_2 I_2 / (1 - \nu_2^2)$$

Where

E_2 is the modulus of elasticity of the lower adherend

I_2 is the second moment of area of the lower adherend

ν_2 is Poisson's ratio of the lower adherend

α is a constant dependent on the difference between the two adherends stiffnesses

$$\alpha^4 = k_a / 4 (D_1 - D_2)$$

R is function of the compliances and the joint length and;

$$R_3 = \cosh \alpha l \sinh \alpha l - \cos \alpha l \sin \alpha l$$

$$R_4 = \cosh \alpha l \sinh \alpha l + \cos \alpha l \sin \alpha l$$

$$R_6 = \cosh^2 \alpha l - \cos^2 \alpha l$$

When l is large then

$$\cosh \alpha l = \sinh \alpha l \gg \cos \alpha l, \sin \alpha l$$

Therefore

$$A = K_1 - K_3$$

In order to calculate the above constants the forces and moments at the joint boundaries

(Figure V) may to be calculated as follows;

The first stage of the calculation is to consider overall equilibrium of the beam abc (plate) and this is shown below;

Summation of the forces in the x-direction gives;

$$R_a = R_b = F$$

Summation of the forces in the y-direction gives;

$$H_a = H_c$$

Summation of the moments about point a gives;

$$H_c = M_b / 2L_1 = FL_2 / 2L_1 = H_a$$

As it is the internal moments and shear forces which are required for the sandwich analysis, the next stage of the calculation involves considering the beam in two sections/lengths (ab and ac), as shown above;

For a - b

Summation of the forces in the y-directions gives;

$$V_y = H_a = FL_2 / 2L_1$$

Summation of the moments about the longitudinal centre of the beam gives;

$$M_x = -FL_2 x / 2L_1$$

For a - c

$$V_y = FL_2 / 2L_1 = H_a \text{ and}$$

$$M_x = FL_2 - (FL_2 x / 2L_1)$$

Thus for model A the shear forces and bending moments (at $x=172.5\text{mm}$, $F=10370\text{N}$) are;

$$V_y = P_{2O} = -P_{2L} = 27620 \text{ N}$$

$$M_x = M_{2O} = -M_{2L}$$

$$= 352580 \text{ N.mm and}$$

$$M_{1O} = M_{1L} = 0 \text{ also}$$

$$P_{1O} = P_{1L} = 0$$

Thus given $E_1 = E_2 = 210 \times 10^3 \text{ N/mm}^2$,

$$w_a = 75\text{mm},$$

$$T_1 = T_2 = 8\text{mm},$$

$$T_3 = 0.5\text{mm},$$

$$v_2 = v_1 = 0.3,$$

$E_3 = 5000 \text{ N/mm}^2$, the normal stress will be calculated according to the following procedures;

$D_1 = 0$ (the stiffness of part1 (block) has been ignored due to zero moment)

$$D_2 = (210000 \times 3200) / (1 - 0.09)$$

$$= 7.385 \times 10^8 \text{ N.mm}^2$$

$$k_a = 75 \times 5000 / 0.5$$

$$= 75 \times 10^4 \text{ N/mm}^2$$

$$\alpha = (75 \times 10^4 / 4 \times 7.385 \times 10^8)^{1/4} = 0.12623$$

$$A = (352580 / (2 \times 0.12623^2 \times 75 \times 7.385 \times 10^8)) - (27620 / (2 \times 0.12623^3 \times 75 \times 7.385 \times 10^8))$$

$$= 1.984 \times 10^{-4}$$

Thus

$$\sigma_y = k_a \cdot A$$

$$= 75 \times 10^4 \times 1.984 \times 10^{-4}$$

$$= 149 \text{ N/mm}^2 \text{ (normal stress at the adhesive)}$$

Similarly for model B (Figure 5.1) the calculations with reference to the model dimensions ($L_1 = 100 \text{ mm}$) and force (11360 N) will produce;

$$V_y = P_{2O} = P_{2L}$$

$$= 4544 \text{ N}$$

$$M_x = M_{2O} = M_{2L}$$

$$= 352160 \text{ N.mm}$$

Thus the adhesive normal stress is;

$$\sigma_y = 148 \text{ N/mm}^2$$

To calculate the stress in the plate (75mm wide and 8mm thick) at $x = 177.5 \text{ mm}$, this position represents the location of the centre of strain gauge attached to model A (Figure 5.1), the bending moment is ;

$$M_x = M_b = 338753 \text{ N.mm}$$

Thus the tensile bending stress at the plate surface (adherend) is;

$$\sigma_b = 338753 \times 4 / (75 \times 8^3 / 12)$$

$$= 423 \text{ N/mm}^2$$

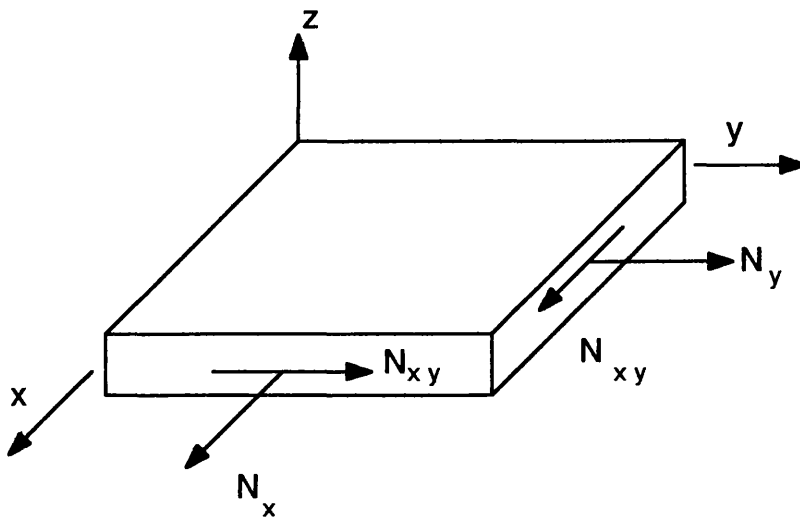
Thus for plane strain state the strain along the plate surface is;

$$\epsilon_x = 423 / 210000$$

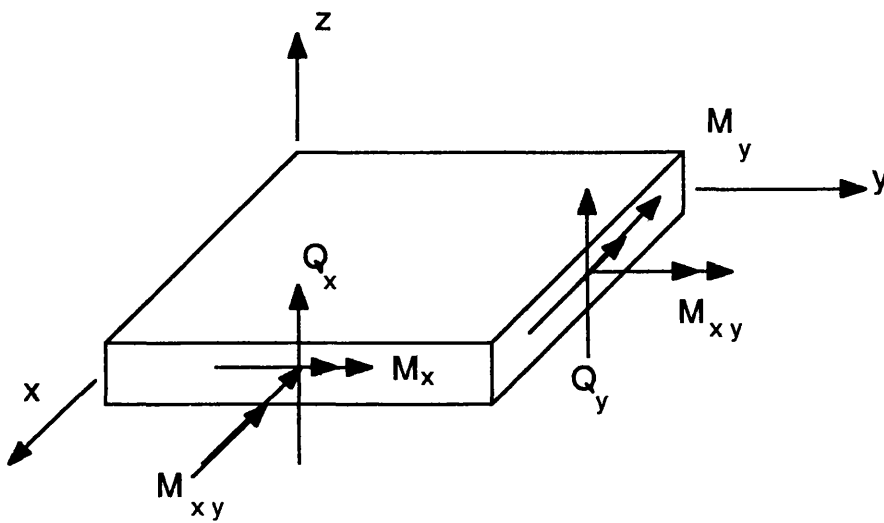
$$= 2014 \times 10^{-6}$$

Similarly, for model B (Figure 5.1) at $x = 127.5 \text{ mm}$, the plate tensile bending stress at the surface is; $\sigma_b = 407 \text{ N/mm}^2$ and $\epsilon_x = 1938 \times 10^{-6}$

APPENDIX VI: BENDING ANALYSIS OF LAMINATED PLATE AND BEAM



Nomenclature for resultant stress



Nomenclature for moment and transverse shear force resultant

FIGURE VI

Assuming an approximate state of plane stress in the plate element shown in Figure VI, the transverse normal strain can be calculated in term of plate stiffnesses through Hook's law (matrix form). Using stiffness terms in conjunction with strain-displacement relations and the stress and moment resultant definitions yields the following constitutive relation for the plate:

$$\begin{bmatrix} N_x \\ N_y \\ N_{xy} \\ M_x \\ M_y \\ M_{xy} \end{bmatrix} = \begin{bmatrix} A_{11} & A_{12} & A_{16} & B_{11} & B_{12} & B_{16} \\ A_{12} & A_{22} & A_{26} & B_{12} & B_{22} & B_{26} \\ A_{16} & A_{26} & A_{66} & B_{16} & B_{26} & B_{66} \\ B_{11} & B_{12} & B_{16} & D_{11} & D_{12} & D_{16} \\ B_{12} & B_{22} & B_{26} & D_{12} & D_{22} & D_{26} \\ B_{16} & B_{26} & B_{66} & D_{16} & D_{26} & D_{66} \end{bmatrix} \begin{bmatrix} \epsilon_x^0 \\ \epsilon_y^0 \\ \epsilon_{xy}^0 \\ \kappa_x \\ \kappa_y \\ \kappa_{xy} \end{bmatrix} \quad (1)$$

Where

$$(A_{ij} \ B_{ij} \ D_{ij}) = \int_{-h/2}^{h/2} Q_{ij}^{(k)}(1, z, z^2) dz \quad (2)$$

Where $A_{ij} \ B_{ij} \ D_{ij}$ represent inverse matrices and $Q_{ij}^{(k)}$ is the reduced stiffness term for k th layer of a laminated plate (function of beam/plate compliance)

For bending of symmetric laminates, the constitutive relations of equation 1 reduce to the form;

$$\begin{bmatrix} M_x \\ M_y \\ M_{xy} \end{bmatrix} = \begin{bmatrix} D_{11} & D_{12} & D_{16} \\ D_{12} & D_{22} & D_{26} \\ D_{16} & D_{26} & D_{66} \end{bmatrix} \begin{bmatrix} \kappa_x \\ \kappa_y \\ \kappa_{xy} \end{bmatrix} \quad (3)$$

For the case of an isotropic material, or a symmetric laminate constructed of layers of isotropic materials, we have

$$\begin{aligned} D_{11} &= D_{22} = D \\ D_{12} &= \nu D \\ D_{66} &= \frac{(1 - \nu)}{2} D \end{aligned} \quad (4)$$

Where

$$\kappa_x = -\frac{\partial^2 w}{\partial x^2}, \quad \kappa_y = -\frac{\partial^2 w}{\partial y^2}, \quad \kappa_{xy} = -2\frac{\partial^2 w}{\partial x \partial y} \quad (5)$$

To write equation (2) in an invertible form,

$$\begin{bmatrix} x_x \\ x_y \\ x_{xy} \end{bmatrix} = \begin{bmatrix} D_{11}^* & D_{12}^* & D_{16}^* \\ D_{12}^* & D_{22}^* & D_{26}^* \\ D_{16}^* & D_{26}^* & D_{66}^* \end{bmatrix} \begin{bmatrix} M_x \\ M_y \\ M_{xy} \end{bmatrix} \quad (6)$$

In order to derive a beam theory the following assumptions are made:

$$M_y = M_{xy} = 0 \quad (7)$$

From equations (3) and (4), the following equation for curvature can be obtained,

$$x_x = - \frac{\partial^2 w}{\partial x^2} = D_{11}^* M_x \quad (8)$$

Neglecting the transverse strain, deflection will be,

$$w = w(x) \quad (9)$$

Where w is deflection in the z direction

Also from equations (5) and (6),

$$x_y = - \frac{\partial^2 w}{\partial y^2} = D_{12}^* M_x \quad x_{xy} = - 2 \frac{\partial^2 w}{\partial x \partial y} = D_{16}^* M_{xy} \quad (10)$$

Thus, the deflection, w , may be identified be independent of y in homogeneous isotropic beam theory (the same may be assumed in a beam with anisotropic materials, provided the beam has large length- to-width ratio)

Combining equations (8) and (9) gives,

$$\frac{d^2 w}{dx^2} = - \frac{M}{E_x^b I} \quad (11)$$

Where,

$$E_x^b I = \frac{12}{h^3 D_{11}^*}, \quad M = b M_x, \quad I = \frac{bh^3}{12}$$

and b is the width of the beam. Equation (11) is the same form as in classical beam theory with homogeneous isotropic modulus E replaced by effective bending modulus E_x^b . For static bending in the absence of body moments and in-plane force effects the following equation of motion may be considered,

$$\frac{\partial^2 M_x}{\partial x^2} + \frac{2 \partial^2 M_{xy}}{2 \partial x \partial y} + \frac{\partial^2 M_y}{\partial y^2} + q = 0 \quad (12)$$

Where q is the shear stress flow in beam and;

$$q = \sigma_z^{(k)}\left(\frac{h}{2}\right) - \sigma_z^{(k)}\left(-\frac{h}{2}\right)$$

Substituting equation (8) into (12) , taking into account equation (9),

$$\frac{d^4 w}{dx^4} = D_{11}^* q \quad (13)$$

Multiplying by the beam width b , equation (13) becomes,

$$\frac{d^4 w}{dx^4} = \frac{P}{E_x^b I} \quad (14)$$

Where

$$P = bq$$

Under static loading equation (12) will be

$$\frac{\partial M_x}{\partial x} + \frac{\partial M_{xy}}{\partial y} - Q_x = 0 \quad (15)$$

From equations (15) and (7) shear force, V acting on beam transverse section will be

$$V_z = \frac{dM}{dx} \quad (16)$$

Where

$$V_z = bQ_x$$

Equation (16) is the same as in homogeneous material. This refers to equilibrium between bending moment and transverse shear resultant. For symmetric laminates under bending loads, strain relations are as follows,

$$\epsilon_x = z\kappa_x, \quad \epsilon_y = z\kappa_y, \quad \epsilon_{xy} = z\kappa_{xy} \quad (17)$$

Thus stresses in the k th layer of the beam given by plane stress condition for the k th layer as follows,

$$\begin{bmatrix} \sigma_x^{(k)} \\ \sigma_y^{(k)} \\ \sigma_{xy}^{(k)} \end{bmatrix} = z \begin{bmatrix} Q_{11}^{(k)} & Q_{12}^{(k)} & Q_{16}^{(k)} \\ Q_{12}^{(k)} & Q_{22}^{(k)} & Q_{26}^{(k)} \\ Q_{16}^{(k)} & Q_{26}^{(k)} & Q_{66}^{(k)} \end{bmatrix} \begin{bmatrix} \epsilon_x \\ \epsilon_y \\ \epsilon_{xy} \end{bmatrix} \quad (18)$$

Combining equations (16) and (4) and multiplying the result by width b we obtain the following plate stresses

$$\sigma_x^{(k)} = z f_1^{(k)} \frac{M}{I} \quad (19)$$

$$\sigma_y^{(k)} = z f_2^{(k)} \frac{M}{I} \quad (20)$$

$$\sigma_{xy}^{(k)} = z f_3^{(k)} \frac{M}{I} \quad (21)$$

Where,

$$f_1^{(k)} = (Q_{11}^{(k)} \cdot D_{11}^{*(k)}) \cdot \frac{h^3}{12}$$

and,

$$f_2^{(k)} = f_3^{(k)} = 0$$

Determination of interlaminar shear stress τ_{xz} can be obtained by substituting equations (19) and (18) into the first equation of motion. For static loading this equation is,

$$\frac{\partial \sigma_x^{(k)}}{\partial x} + \frac{\partial \sigma_{xy}^{(k)}}{\partial y} + \frac{\partial \tau_{xz}^{(k)}}{\partial z} = 0 \quad (22)$$

Thus integrating gives,

$$\tau_{xz}^{(k)} = -\frac{1}{I} \int_{-h/2}^{z^{(k)}} f_1^{(k)} \frac{dM}{dx} \quad (23)$$

Substitute equation (16) gives,

$$\tau_{xz}^{(k)} = - \frac{V_z}{I} \int_{-h/2}^z f_1^{(k)} z dz \quad (24)$$

The maximum interlaminar shear at section centre ($h/2$) is,

$$\tau_{xz}^{(k)} = f_1^{(k)} \frac{h^2 V_z}{8I} \quad (25)$$

APPENDIX VII: CALCULATIONS OF FORCE AND STRESSES DUE TO IMPACT LOADING (CHAPTER 6)

Energy absorbed by test specimen AA1/S may be calculated as follows;

$$E_k = 0.5 m (V_s^2 - V_r^2)$$

Where

E_k is the absorbed kinetic energy

m is the impacting mass

V_s is the striking velocity of the mass

V_r is the return velocity of the mass which may be obtained as follows;

$$V_r = \sqrt{2gh_r}$$

Where

g is the gravity acceleration

h_r is the rebound height

Thus

for $m=6.4\text{kg}$ dropped from 12.5m high

$V_s=14.2 \text{ m/sec}$ (measured by the infra-red switches and timer)

$$V_r = (2 \times 9.81 \times 1.25)^{0.5} \quad (h_r = 1.25\text{m by the rebound observation})$$

$$= 5 \text{ m/sec}$$

Therefore

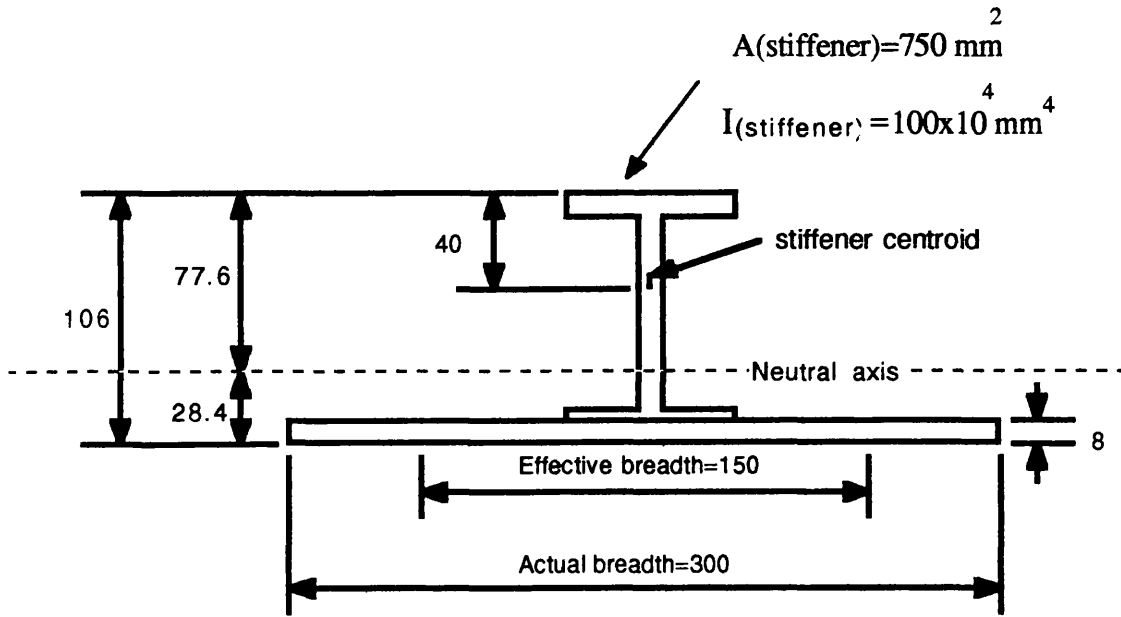
$$E_k = 565 \text{ J}$$

The calculation of the impact force and adhesive shear stress is as follows:

the bending stress at the centre of the beam plate (assuming elastic limit for the beam section) may be obtained using the following equation (Chapter 5)

$$\sigma_x^{(2)} = z f_1^{(2)} \frac{M}{I}$$

The calculation of the second moment of area (I) is as follows:



$$z = (150 \times 8 \times 4 + 750 \times 68) / (300 \times 8 + 750)$$

$$= 28.4 \text{ mm}$$

$$I = (150 \times 8^3 / 12) + 150 \times 8 \times 24.4^2 + 100 \times 10^4 + 750 \times 37.6^2$$

$$= 278 \times 10^4 \text{ mm}^4$$

Given bending stress obtained from the strain measurement at the plate surface

$\sigma_x = 307 \text{ N/mm}^2$, the bending moment will be:

$$M = 278 \times 10^4 \times 307 / 28.4 \times 1.3$$

$$= 23.1 \times 10^6 \text{ N.mm}$$

Thus the impact force is;

$$F = 23.1 \times 10^6 \times 4 / 430$$

$$= 215 \times 10^3$$

The shear stress within the adhesive may be calculated from the following

composite section formula;

$$\tau_{xz}^{(2)} = f_1^{(2)} \frac{V_z Q}{I w_a}$$

Given

$$f_1^{(2)} = 1.3, \quad V_z = 107.5 \times 10^3 \text{ N},$$

$$I = 278 \times 10^4 \text{ mm}^4,$$

$$w_a = 45 \text{ mm and}$$

$$Q = 150 \times 8 \times 24.4$$

$$= 29280 \text{ mm}^3,$$

Therefore the shear stress will be;

$$\tau_{xz} = 1.3 \times 10^7 \times 10^3 \times 29280 / 278 \times 10^4 \times 25$$

$$= \underline{32.6} \text{ N/mm}^2$$

APPENDIX VIII: DETAILS OF A SAMPLE OF FIRE TEST, FOR SMALL SCALE GRP SPECIMEN (100mmx100mm)

NOTES

Parameters measured in the cone calorimeter

Heat Release Rate

is expressed in kiloWatts per square metre of sample. The only measurement is the oxygen consumption and two graphs are provided one with a forced maximum of 500 kW/m² for comparison with other samples.

Effective Heat of Combustion

is expressed in MegaJoules per kilogram combusted. Most materials could not yield more than about 50 MJ/kg and this is made the maximum of the graph. The load cell sensitivity means that very low mass loss rates appear to be zero and thus the effective heat of combustion tends to infinity. Thus this parameter can not be measured reliably at very low mass loss rates.

Rate of Mass Loss

is expressed as grams per second.square metre. A fixed upper limit of 20 g/s.m² is used for this graph. This is often noisy as the load cell is undamped for maximum sensitivity.

Specific Extinction Area

is expressed as square metres per kilogram consumed. This may be thought of as the volume of smoke in cubic metres with unit optical density per metre per kilogram of material combusted. The mass factor in the denominator often produces the same problem as for the effective heat of combustion.

Smoke Yield

is expressed as cubic metres with unit optical density per metre per square metre of original sample area. This parameter is thus strictly unitless and directly related to the extinction coefficient produced by the smoke meter.

Oxides of Carbon

may be expressed as kilograms produced per kilogram combusted or per square metre of original sample area. The former units will produce the same problem as effective heat of combustion in regard to the mass term in the denominator.

Rear Face Temperature

is in degrees Celsius. This measurement is greatly dependent on conduction by the sample and sample holder. It is provided for rough comparison purposes only and cannot give an accurate idea of likely temperatures in real fires.

Page 1 of 3

WARRES No: L20020

TEST REPORT ON HEAT AND VISIBLE SMOKE RELEASE RATES FOR MATERIALSUSING AN OXYGEN CONSUMPTION CALORIMETER ACCORDING TO ISO DIS 5660

WARRES No: L20020
 Test No: C900216
 Material identification: [DB] Glasgow University
 Date of test: 12th February 1990

Specimen thickness: 26 mm
 Specimen initial mass: 301.5 g
 Irradiance: 60 kW/m²
 Exhaust duct flow rate: 0.024±0.002 m³/s
 Orientation: Horizontal
 Time to ignition: 13 s
 Total heat evolved: 14.4 kJ
 Mass loss: 21.9 g

<u>Peak and Average values</u>		Peak	Time (s)	Average
Heat release rate	(kW/m ²):	12.2	15	0.8
Eff. heat of comb.	(MJ/kg):	8.5	1590	0.6
Specific ext. area	(m ² /kg):	153.3	680	9.9
Carbon Monoxide Yield	(kg/kg):	0	0	0
Carbon Dioxide Yield	(kg/kg):	0	0	0

Note: "*" denotes reliable results unobtainable - Mass Loss Rate lower than load cell sensitivity.

Average during period from ignition to ignition plus...

	1 min	2 min	3 min	4 min	5 min	6 min
Heat release rate (kW/m ²):	2.4	1.6	1	0.8	0.6	0.5
Eff. heat of comb. (MJ/kg):	0.8	0.7	0.7	0.4	0.3	0.2
Specific ext. area (m ² /kg):	119.1	79.9	77.9	48	40	31.2
Carbon Monoxide (kg/kg):	0	-	-	-	-	-
Carbon Dioxide (kg/kg):	0	-	-	-	-	-

Signature of Test Engineer

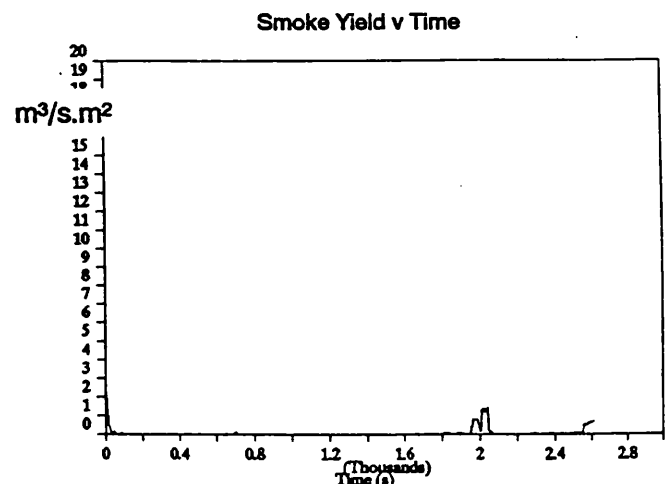
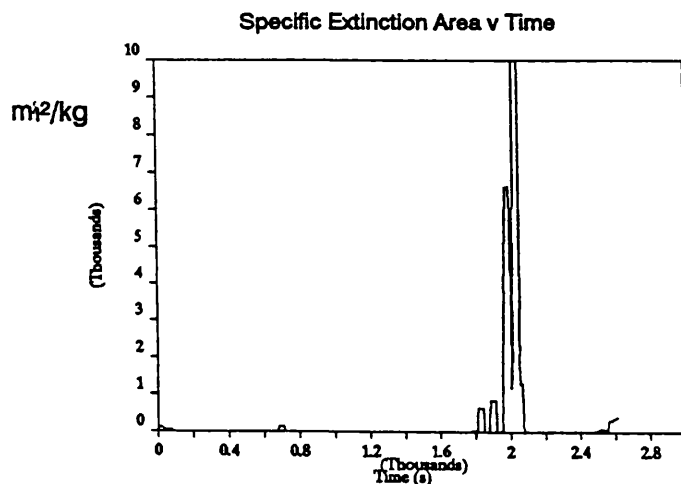
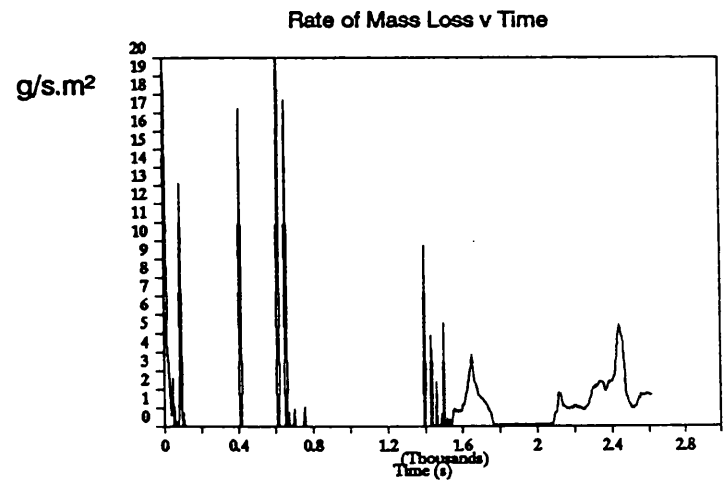
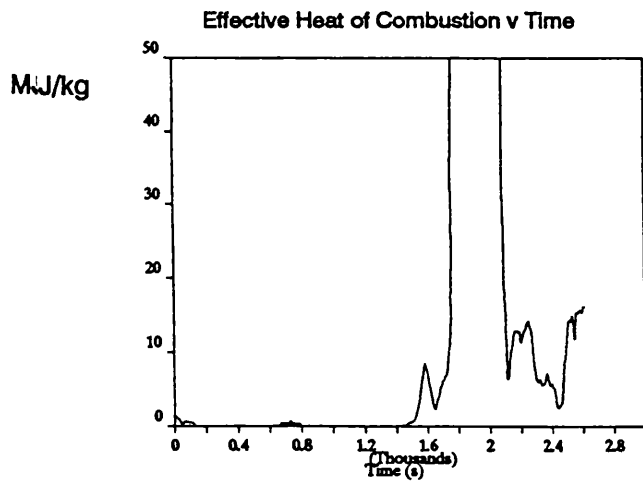
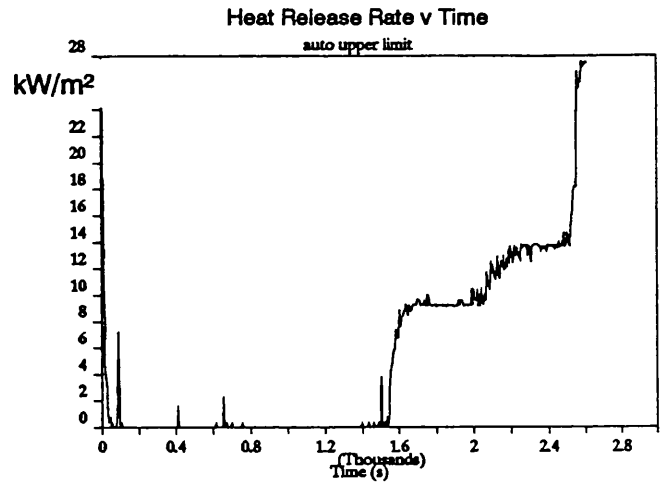
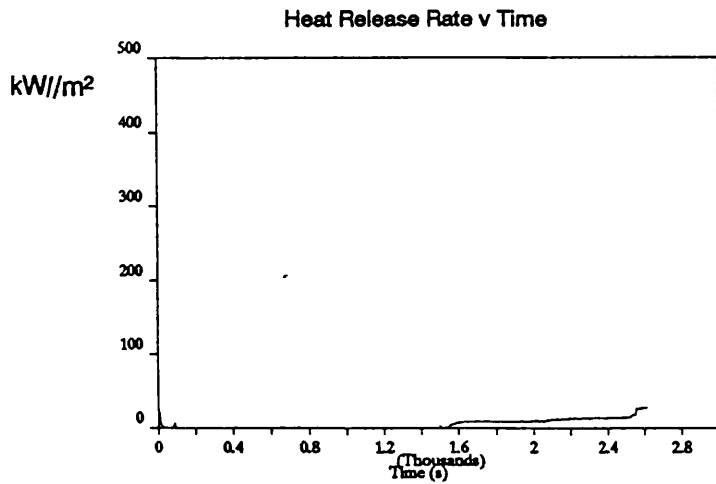
R Trew

MATERIAL:DB

WARRES NO: L10020

HEAT FLUX: 60 kW/m²

ORIENTATION: Horizontal



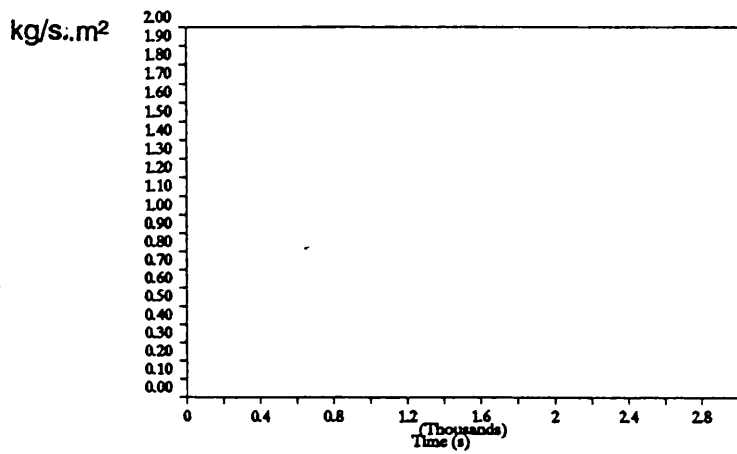
MATERIAL: DB

WARRES NO: L10020

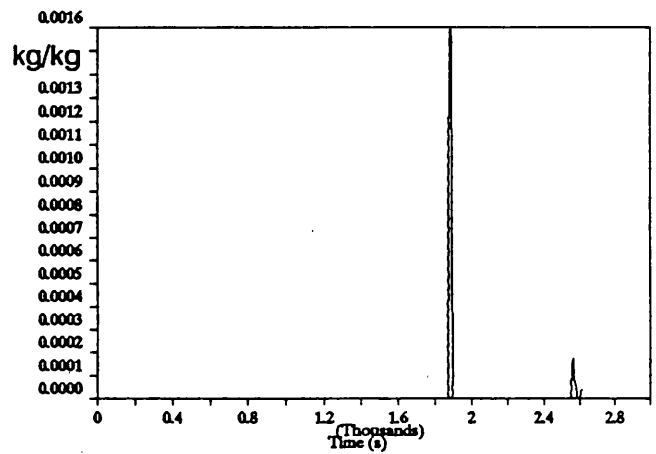
HEAT FLUX: 60 kW/m²

ORIENTATION: Horizontal

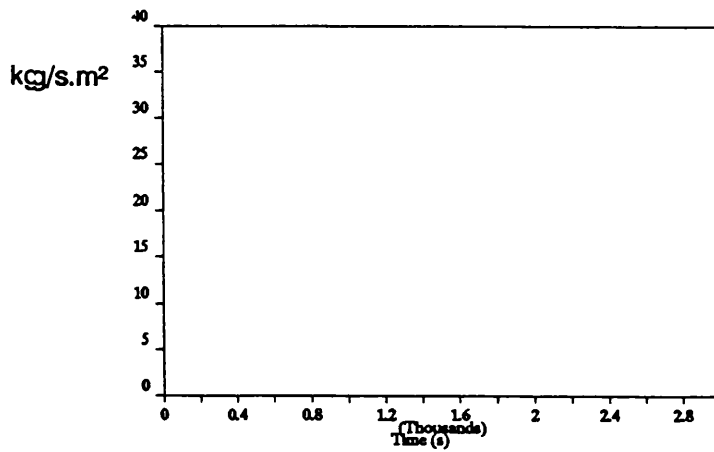
Carbon Monoxide Yield v Time



Carbon Monoxide Yield v Time



Carbon Dioxide Yield v Time



Rear Face Temperature v Time

